

ERDC/CHL TR-05-1

Coastal and Hydraulics Laboratory



**US Army Corps
of Engineers®**
Engineer Research and
Development Center

Monitoring Completed Navigation Projects Program

Monitoring Stone Degradation on Coastal Structures in the Great Lakes – Summary Report

David W. Marcus, Joseph A. Kissane, David A. Lienhart,
Kenneth E. Henn III, and Susan M. Agar

June 2005



Monitoring Stone Degradation on Coastal Structures in the Great Lakes – Summary Report

David W. Marcus

*U.S. Army Engineer District, Buffalo
1776 Niagara Street
Buffalo, NY 14207*

Joseph A. Kissane

*U.S. Army Engineer District, Chicago
111 North Canal Street
Chicago, IL 60606*

David A. Lienhart

*Rock Products Consultants
7229 Longfield Drive
Cincinnati, OH 45243-2209*

Kenneth E. Henn III

*U.S. Army Engineer District, Louisville
P.O. Box 59
Louisville, KY 40201-0059*

Susan M. Agar

*Northwestern University
Department of Geology
Evanston, IL 60201*

Final report

Approved for public release; distribution is unlimited

Prepared for U.S. Army Corps of Engineers
Washington, DC 20314-1000

Under MCNP Work Unit 11M13

Monitored by Coastal and Hydraulics Laboratory
U.S. Army Engineer Research and Development Center
3909 Halls Ferry Road, Vicksburg, MS 39180-6199

ABSTRACT: Stone deterioration on breakwaters and jetties arises from a combination of interactions pertaining to the quality of stone available, operational and handling practices at the quarry, and environmental weathering conditions after placement on the project structure. Four different and distinct investigations were essential to fully comprehend the mechanisms that give rise to chronic premature deterioration of armor stone on breakwaters and jetties around the Great Lakes, including:

a. Quarry field geological observations. Seven different quarries that have historically provided material for Great Lakes breakwater and jetty construction and rehabilitation projects were investigated. The stone produced by these seven quarries included (a) Salem formation limestone from Reed Quarry, Bloomington, IN, (b) Niagaran series dolomite from Valders Quarry, Valders, WI, (c) Waterloo formation quartzite from Dempsey Quarry, Waterloo, WI, (d) Columbus formation limestone from Sandusky Quarry, Parkertown, OH, (e) Columbus formation dolomitic limestone from Marblehead Quarry, Marblehead, OH, (f) Berea formation sandstone from Johnson Quarry, Kipton, OH, and (g) Racine formation dolomite from Thornton Quarry, Thornton, IL. Field geological observations had previously been performed at an eighth quarry (McCook Quarry, McCook, IL). The McCook Quarry produces Niagaran series dolomite.

b. Laboratory durability testing. Laboratory durability testing of stone samples to accelerate weather exposure freeze/thaw and wet/dry effects, and to determine specific gravity and sample petrography, was performed. The laboratory durability testing samples came from the eight quarries where field geological observations had been performed, plus samples from a ninth quarry (Iron Mountain Quarry, Iron Mountain, MI). The Iron Mountain Quarry produces taconite.

c. Quarry sample microstructural analyses. Microstructural analyses of quarry stone samples from seven different quarries to determine microscale features in the rock that affect stability, and their relations to compositional and textural variations, were conducted after laboratory durability testing. These were the same quarries for which quarry field geological observations had also been performed, except stone samples from McCook Quarry were not available for quarry microstructural analyses.

d. Field prototype monitoring. Field monitoring of 10 specific sections of five structures to document progressive deterioration rates among different stone types, different degrees of environmental exposure, and different levels of stone quality control was conducted. The five structures were (a) Chicago Harbor, IL, breakwater, (b) Calumet Harbor, IL and IN, breakwater, (c) Calumet Harbor, IL, confined disposal facility (CDF) revetment, (d) Burns Harbor, IN, breakwater, and (e) Cleveland Harbor, OH, east breakwater. The 10 sections of structures selected for evaluation contained deteriorated stone from the eight quarries previously discussed, plus stone from the Calumet Harbor CDF revetment that originally came from a ninth quarry, the Iron Mountain Quarry, Iron Mountain, MI. The Iron Mountain Quarry produces taconite. Also, stone from a tenth quarry (Cedarville Quarry, Cedarville, MI) was evaluated by this field prototype monitoring study because stone from this quarry has previously been placed on other stone structures around the Great Lakes. The Cedarville Quarry produces Niagaran series dolomite.

Ground inspections by registered professional geologists were made to catalogue, at the monitored sections, all stone fractures and offset measurements in armor stone above the high-water mark, between low water and high water on the harbor side, and between low water and high water on the lake side (annually for 3 years). Broken stones were marked to show in aerial photographs to insure repeatability, and to document progression of deterioration.

DISCLAIMER: The contents of this report are not to be used for advertising, publication, or promotional purposes. Citation of trade names does not constitute an official endorsement or approval of the use of such commercial products. All product names and trademarks cited are the property of their respective owners. The findings of this report are not to be construed as an official Department of the Army position unless so designated by other authorized documents.

Contents

Preface	xix
1—Introduction	1
Monitoring Completed Navigation Projects (MCNP) Program.....	1
Background.....	2
Stone Degradation Investigations	3
MCNP Study Components.....	4
Previous Studies.....	6
1979 Corps-wide survey of stone structures	6
1980-1985 Cleveland Harbor east breakwater monitoring.....	6
1985 Cleveland Harbor east breakwater physical model study.....	6
1989 Cleveland Harbor east breakwater stone survey.....	7
1990 LRD structure stone survey	7
1994 Cleveland Harbor east breakwater study	7
Monitoring Plan	8
Structures and sections monitored.....	8
Monitoring procedure.....	15
2—Quarry Field Geological Observations.....	17
Discontinuities	17
Reed Quarry	19
General geology	19
Method of extraction	19
Stratigraphic section	22
Lithologic description	22
Valders Quarry.....	25
General geology	25
Method of extraction	27
Stratigraphic section	27
Lithologic description	29
Dempsey Quarry	30
General geology	30
Method of extraction	32
Stratigraphic section	33
Lithologic description	36
Sandusky Quarry.....	36
General geology	38
Method of extraction	38
Stratigraphic section	39

Lithologic description	41
Marblehead Quarry	43
General geology	43
Method of extraction	44
Stratigraphic section	45
Lithologic description	45
Johnson Quarry	46
General geology	46
Method of extraction	48
Stratigraphic section	48
Lithologic description	49
Thornton Quarry	51
General geology	51
Method of extraction	51
Stratigraphic section	54
Lithologic description	56
McCook Quarry	57
General geology	58
Method of extraction	58
Stratigraphic section	58
Lithologic descriptions	59
Stability of Freshly Quarried Stone	60
Cut Stone versus Rubble Stone	61
3—Laboratory Durability Testing	63
Reed Quarry Durability Test Results	64
Valders Quarry Durability Test Results	65
Dempsey Quarry Durability Test Results	67
Sandusky Quarry Durability Test Results	69
Marblehead Quarry Durability Test Results	71
Johnson Quarry Durability Test Results	76
Thornton Quarry Durability Test Results	78
Summary of MCNP Durability Testing by ORDL	83
Other Durability Testing by ORDL	83
Conclusions	84
4—Quarry Sample Microstructural Analyses	85
Reed Quarry	85
Test block, samples, and thin sections	85
Composition, grain size, and porosity	88
Texture and diagenesis	88
Fractures, stylolites, and grain fabric	89
Summary	90
Recommendations	90
Valders Quarry	91
Test blocks, samples, and thin sections	91
Composition, grain size, and porosity	95
Texture and diagenesis	97
Fractures, clay seams, stylolites, and grain size layering	98
Summary	99
Recommendations	100

Dempsey Quarry	100
Test blocks, samples, and thin sections	100
Composition, grain size, and porosity	103
Texture and metamorphism	106
Fractures	106
Summary	108
Recommendations	108
Sandusky Quarry	109
Test blocks, samples, and thin sections	109
Composition, grain size, and porosity	115
Texture and diagenesis	115
Fractures and stylolites	116
Summary	117
Recommendations	117
Marblehead Quarry	118
Test blocks, samples, and thin sections	118
Composition, grain size, and porosity	124
Texture and diagenesis	124
Fractures	125
Stylolites	127
Summary	127
Recommendations	127
Johnson Quarry	128
Test blocks, samples, and thin sections	128
Composition, grain size, and porosity	133
Texture and diagenesis	136
Fractures, pressure solution seams, and local grain alignments	137
Summary	138
Recommendations	139
Thornton Quarry	139
Test block, samples, and thin sections	139
Composition, grain size, and porosity	142
Texture and diagenesis	143
Fractures and stylolites	144
Summary	146
Recommendations	146
McCook Quarry	147
Summary of Quarry Sample Microstructural Analyses	147
5—Field Prototype Monitoring	149
Structures and Sections Monitored	150
Inspection of Breakwater Structure Sections	157
Fractures of all magnitudes, orientation, and types	157
Clearly visible evidence	166
Progressive change in each crack	166
Petrographic description of each stone	167
Location of each stone	167
Orientation of each stone	167
Photographic documentation of each stone	167
Breakwater Stone Deterioration	167
Causes of Deterioration	206

Weathering Environment Deterioration.....	206
Method of Extraction Deterioration.....	207
Cutting method.....	207
Blasting method.....	208
Conclusions regarding method of extraction deterioration	209
Placement Techniques Deterioration	220
Depositional Facies Deterioration.....	220
Diagenesis Deterioration.....	228
General observations	228
Influence of gross lithology.....	229
In Situ Stress Deterioration.....	231
Enhanced QC/QA Program.....	232
6—Summary and Conclusions.....	235
Statement of Problem.....	235
Background	235
Stone degradation investigations.....	236
Study components	236
Quarry Field Geological Observations	238
Reed Quarry and Salem Formation limestone.....	238
Valders Quarry and Niagaran series dolomite.....	238
Dempsey Quarry and Waterloo formation quartzite	239
Sandusky Quarry and Columbus formation limestone.....	240
Marblehead Quarry and Columbus formation dolomitic limestone	240
Johnson Quarry and Berea formation sandstone	240
Thornton Quarry and Racine formation dolomite	241
McCook Quarry and Niagaran series dolomite	242
Laboratory Durability Testing	242
Reed Quarry test block durability results.....	242
Valders Quarry test block durability results.....	243
Dempsey Quarry test block durability results	243
Sandusky Quarry test block durability results.....	243
Marblehead Quarry test block durability results	243
Johnson Quarry test block durability results	244
Thornton Quarry test block durability results	244
Conclusions	245
Quarry Sample Microstructural Analyses.....	245
Reed Quarry and Salem formation limestone	245
Valders Quarry and Niagaran series dolomite.....	245
Dempsey Quarry and Waterloo formation quartzite	246
Sandusky Quarry and Columbus formation limestone.....	246
Marblehead Quarry and Columbus formation dolomitic limestone	246
Johnson Quarry and Berea formation sandstone	247
Thornton Quarry and Racine formation dolomite	247
McCook Quarry and Niagaran series dolomite	248
Conclusions	248
Field Prototype Monitoring	249
Causes of deterioration.....	249
Weathering environment deterioration.....	250
Method of extraction deterioration.....	250
Placement technique deterioration	251

Depositional facies deterioration.....	251
Diagenesis deterioration.....	252
In situ stress deterioration.....	253
Enhanced Quality Control/Quality Assurance (QC/QA) program.....	253
Conclusions.....	254
Factors impacting armor stone durability.....	254
Curing time of freshly quarried stone.....	255
Laid-up cut stone versus rubble mound structures.....	256
Service life of armor stone.....	257
Design of armor stone structures.....	258
Stone source selection.....	259
Performance-based specifications.....	261
Stone placement drop height.....	262
Use of lesser quality stone underwater.....	262
Stone bedding plane orientation.....	263
Quality versus cost.....	264
Quality Control and Quality Assurance (QC/QA).....	264
References.....	266
Appendix A: Memorandum for Record.....	A1

SF 298

List of Figures

Figure 1.	Chicago Harbor breakwater, IL, monitored section.....	10
Figure 2.	Calumet Harbor breakwater, IL and IN, monitored section.....	11
Figure 3.	Calumet Harbor CDF revetment, IL, monitored section.....	12
Figure 4.	Burns Harbor breakwater, IN, monitored sections.....	13
Figure 5.	Cleveland Harbor east breakwater, OH, monitored sections.....	14
Figure 6.	Reed Quarry, Bloomington, IN, general view showing amount of rejected architectural stone available for use as armor stone.....	20
Figure 7.	Reed Quarry, Bloomington, IN, overview of operation of new quarry and wire-saw operation.....	21
Figure 8.	Location map, Reed Quarry, Bloomington, IN.....	22
Figure 9.	Reed Quarry, Bloomington, IN, west face.....	23
Figure 10.	Reed Quarry, Bloomington, IN, exploitation of coarse fossiliferous zones by solution.....	24

Figure 11.	Valders Quarry, Valders, WI, overall view showing lower bench, middle bench (being drilled), and upper bench with glacial till drift overburden	26
Figure 12.	Location map, Valders Quarry, Valders, WI.....	26
Figure 13.	Valders Quarry, Valders, WI, splay of spent explosive blown out along joint.....	27
Figure 14.	Valders Quarry, Valders, WI, upper bench with mega-ripples near base	28
Figure 15.	Valders Quarry, Valders, WI, lower bench showing discontinuous horizontal unloading features	29
Figure 16.	Dempsey Quarry, Waterloo, WI, lower bench, north face, with mica schist plunging under quarry floor on left, and rockburst structure on right	31
Figure 17.	Location map, Dempsey Quarry, Waterloo, WI.....	32
Figure 18.	Dempsey Quarry, Waterloo, WI, lower bench, south face.....	34
Figure 19.	Dempsey Quarry, Waterloo, WI, upper bench, east face	35
Figure 20.	Sandusky Quarry, Parkertown, OH, thin-bedded Delaware formation on east side of quarry	37
Figure 21.	Location map, Sandusky Quarry, Parkertown, OH.....	38
Figure 22.	Sandusky Quarry, Parkertown, OH, close-up of contact of Columbus and Delaware formations; also contact of Venice and Marblehead members of Columbus formation	39
Figure 23.	Sandusky Quarry, Parkertown, OH, blasting fractures along blastholes.....	40
Figure 24.	Marblehead Quarry, Marblehead, OH, conjugate system of parallel release fractures opened in a nose or promontory of lower bench as a result of quarrying practices.....	44
Figure 25.	Location map, Marblehead Quarry, Marblehead, OH.....	45
Figure 26.	Marblehead Quarry, Marblehead, OH, 2.9 m (9.6-ft) face on east side of quarry from which armor stone was produced, at or near base of Columbus formation	46
Figure 27.	Marblehead Quarry, Marblehead, OH, sawn block with brown marker bed at 0.8 m (2.7 ft) from left side	47
Figure 28.	Johnson Quarry, Kipton, OH, area where an attempt was made to produce sandstone blocks by blasting.....	47
Figure 29.	Location map, Johnson Quarry, Kipton, OH.....	48

Figure 30.	Johnson Quarry, Kipton, OH, thin-bedded upper unit on north side of quarry	49
Figure 31.	Johnson Quarry, Kipton, OH, close-up of thin-bedded sandstone showing carbonaceous bedding planes.....	50
Figure 32.	Johnson Quarry, Kipton, OH, lower massive sandstone unit.....	50
Figure 33.	Thornton Quarry, Thornton, IL, lower bench.....	52
Figure 34.	Location map, Thornton Quarry, Thornton, IL	53
Figure 35.	Thornton Quarry, Thornton, IL, northwest quarry, middle bench, southeast corner, reef core, and flank beds on either side	53
Figure 36.	Thornton Quarry, Thornton, IL, northwest quarry, middle bench, showing massive flank beds	54
Figure 37.	Thornton Quarry, Thornton, IL, northwest quarry, middle bench, storm block of reef talus	55
Figure 38.	Location map, McCook Quarry, McCook, IL	58
Figure 39.	Reed Quarry Salem formation limestone accelerated weathering durability Test Block R-1-FT	65
Figure 40.	Valders Quarry Niagaran series dolomite accelerated weathering durability Test Block V-1-FT	66
Figure 41.	Valders Quarry Niagaran series dolomite accelerated weathering durability Test Block V-2-FT	67
Figure 42.	Dempsey Quarry Waterloo formation quartzite accelerated weathering durability Test Block D-1-FT	68
Figure 43.	Dempsey Quarry Waterloo formation quartzite accelerated weathering durability Test Block D-3-FT	69
Figure 44.	Sandusky Quarry Columbus formation limestone accelerated weathering durability Test Block S-1-FT/WD	70
Figure 45.	Sandusky Quarry Columbus formation limestone accelerated weathering durability Test Block S-2-FT	72
Figure 46.	Marblehead Quarry Columbus formation dolomitic limestone accelerated weathering durability Test Block M-1-FT	73
Figure 47.	Marblehead Quarry Columbus formation dolomitic limestone accelerated weathering durability Test Block M-2-WD.....	74

Figure 48.	Marblehead Quarry Columbus formation dolomitic limestone accelerated weathering durability Test Block M-3-FT/WD	75
Figure 49.	Johnson Quarry Berea formation sandstone accelerated weathering durability Test Block J-1-WD	76
Figure 50.	Johnson Quarry Berea formation sandstone accelerated weathering durability Test Block J-2-FT	77
Figure 51.	Thornton Quarry Racine formation dolomite accelerated weathering durability Test Block MTC-1-FT/WD.....	78
Figure 52.	Thornton Quarry Racine formation dolomite accelerated weathering durability Test Block MTC-2-FT	79
Figure 53.	Thornton Quarry Racine formation dolomite accelerated weathering durability Test Block MTC-3-FT/WD.....	80
Figure 54.	Thornton Quarry Racine formation dolomite accelerated weathering durability Test Block MTC-4-FT/WD.....	81
Figure 55.	Thornton Quarry Racine formation dolomite accelerated weathering durability Test Block MTC-5-FT/WD.....	82
Figure 56.	Reed Quarry Test Block R-1-FT, front surface and sample locations near open fractures.....	86
Figure 57.	Reed Quarry Sample R-1A-FT, including stylolite seam	87
Figure 58.	Reed Quarry Sample R-1B-FT.....	87
Figure 59.	Valders Quarry Test Block V-1-FT sample locations.....	92
Figure 60.	Valders Quarry Sample V-1A-FT close-up.....	93
Figure 61.	Valders Quarry Sample V-1B-FT close-up.....	94
Figure 62.	Valders Quarry Test Block V-2-FT sample locations.....	95
Figure 63.	Valders Quarry Sample V-2A-FT close-up.....	96
Figure 64.	Valders Quarry Sample V-2B-FT close-up.....	97
Figure 65.	Dempsey Quarry Test Block D-1-FT sample locations	101
Figure 66.	Dempsey Quarry Sample D-1A-FT close-up.....	102
Figure 67.	Dempsey Quarry Sample D-1B-FT close-up	103
Figure 68.	Dempsey Quarry Test Block D-3-FT sample locations	104
Figure 69.	Dempsey Quarry Sample D-3A-FT close-up.....	104
Figure 70.	Dempsey Quarry Sample D-3B-FT close-up	105

Figure 71.	Sandusky Quarry Test Block S-1-FT/WD sample locations	110
Figure 72.	Sandusky Quarry Sample S-1A-FT/WD showing stylolitic seam parallel to bedding, close to edge of block.....	111
Figure 73.	Sandusky Quarry Sample S-1B-FT/WD	111
Figure 74.	Sandusky Quarry Test Block S-2-FT sample locations	112
Figure 75.	Sandusky Quarry Sample S-2A-FT. Seam of dark fine-grained material can be traced across center of sample	113
Figure 76.	Sandusky Quarry Sample S-2B-FT	114
Figure 77.	Marblehead Quarry Test Block M-1-FT sample locations, showing large pretest fractures	119
Figure 78.	Marblehead Quarry Sample M-1A-FT showing pretest fracture tip	120
Figure 79.	Marblehead Quarry Sample M-1B-FT showing open fracture surface	121
Figure 80.	Marblehead Quarry Test Block M-2-WD sample locations with large pretest fracture crossing obliquely across surface	121
Figure 81.	Marblehead Quarry Sample M-2A-WD showing fractures that are perpendicular and parallel to bedding	122
Figure 82.	Marblehead Quarry Sample M-2B-WD containing overlapping pretest fractures that trend approximately 30 deg to bedding	122
Figure 83.	Marblehead Quarry Test Block M-3-FT/WD sample locations, with large pretest fracture	123
Figure 84.	Marblehead Quarry Sample M-3A-FT/WD showing fracture tip region of subvertical fracture in test block	123
Figure 85.	Marblehead Quarry Sample M-3B-FT/WD that includes open surface of same fracture sampled in M-3A-FT/WD.....	124
Figure 86.	Johnson Quarry Test Block J-1-WD sample locations.....	129
Figure 87.	Johnson Quarry Sample J-1A-WD with pretest fractures penetrating from edge of sample	130
Figure 88.	Johnson Quarry Sample J-1B-WD	131
Figure 89.	Johnson Quarry Sample J-1C-WD	132
Figure 90.	Johnson Quarry Test Block J-2 sample location prior to freeze-thaw exposure.....	133

Figure 91.	Johnson Quarry Sample J-2 prior to freeze/thaw exposure	134
Figure 92.	Johnson Quarry Test Block J-2-FT sample location	135
Figure 93.	Johnson Quarry Sample J-2-FT.....	135
Figure 94.	Thornton Quarry Test Block MTC-3-FT/WD sample locations	140
Figure 95.	Thornton Quarry Sample MTC-3A-FT/WD	141
Figure 96.	Thornton Quarry Sample MTC-3B-FT/WD	142
Figure 97.	Chicago Harbor breakwater, Valders Quarry cut dolomite.....	151
Figure 98.	Chicago Harbor breakwater, Reed Quarry cut limestone.....	152
Figure 99.	Calumet Harbor breakwater, Reed Quarry cut limestone	152
Figure 100.	Calumet Harbor breakwater, Dempsey Quarry low energy blasted quartzite.....	153
Figure 101.	Calumet Harbor CDF, McCook Quarry high energy blasted dolomite	153
Figure 102.	Burns Harbor breakwater (Shore Arm section), Dempsey Quarry low energy blasted quartzite	154
Figure 103.	Burns Harbor breakwater (Big Burn section), Reed Quarry cut limestone	154
Figure 104.	Burns Harbor breakwater (Big Burn section), McCook Quarry high energy blasted dolomite	155
Figure 105.	Cleveland Harbor east breakwater, Johnson Quarry cut sandstone	155
Figure 106.	Cleveland Harbor east breakwater, Marblehead Quarry low energy blasted dolomitic limestone.....	156
Figure 107.	Cleveland Harbor east breakwater, Sandusky Quarry high energy blasted limestone	156
Figure 108.	No cracks, Cleveland Harbor east breakwater, Sandusky Quarry high energy blasted limestone, quality rating = 100 percent.....	159
Figure 109.	Minor cracks, Cleveland Harbor east breakwater, Sandusky Quarry high energy blasted limestone, quality rating = 80 percent.....	159

Figure 110.	Multiply minor cracked, Chicago Harbor breakwater, Valders Quarry cut dolomite (low energy blasted, drilled and split, and then surfaces cut), quality rating = 70 percent.....	160
Figure 111.	Significant cracks, Cleveland Harbor east breakwater, Marblehead Quarry low energy blasted dolomitic limestone, quality rating = 60 percent.....	160
Figure 112.	Multiply significant cracked, Cleveland Harbor east breakwater, Marblehead Quarry low energy blasted dolomitic limestone, quality rating = 50 percent.....	161
Figure 113.	Failed, Cleveland Harbor east breakwater, Marblehead Quarry low energy blasted dolomitic limestone, quality rating = 40 percent.....	161
Figure 114.	Multiply failed, Cleveland Harbor east breakwater, Marblehead Quarry low energy blasted dolomitic limestone, quality rating = 30 percent.....	162
Figure 115.	Fragmented, Cleveland Harbor east breakwater, Marblehead Quarry low energy blasted dolomitic limestone, quality rating = 20 percent.....	162
Figure 116.	Multiply fragmented, Cleveland Harbor east breakwater, Marblehead Quarry low energy blasted dolomitic limestone, quality rating = 10 percent.....	163
Figure 117.	Displaced, Cleveland Harbor east breakwater, Marblehead Quarry low energy blasted dolomitic limestone, quality rating = 5 percent.....	163
Figure 118.	Multiply displaced, Cleveland Harbor east breakwater, Marblehead Quarry low energy blasted dolomitic limestone, quality rating = 3 percent.....	164
Figure 119.	Lost1, Cleveland Harbor east breakwater, Marblehead Quarry low energy blasted dolomitic limestone, quality rating = 2 percent.....	164
Figure 120.	Lost2, Cleveland Harbor east breakwater, Sandusky Quarry high energy blasted limestone, quality rating = 1 percent.....	165
Figure 121.	Lost3, Cleveland Harbor east breakwater, Marblehead Quarry low energy blasted dolomitic limestone, quality rating = 0 percent.....	165
Figure 122.	Chicago Harbor breakwater, sta 14+65 to sta 16+00, stone quality classification, end of 1997	168
Figure 123.	Calumet Harbor breakwater, sta 117+55 to sta 118+90, stone quality classification, end of 1997	169

Figure 124.	Calumet Harbor confined disposal facility, sta 33+00 to sta 33+40, stone quality classification, end of 1997.....	170
Figure 125.	Burns Harbor breakwater (Shore Arm section), sta 53+60 to sta 54+55, stone quality classification, end of 1997	171
Figure 126.	Burns Harbor breakwater (Big Burn section), sta 3+30 to sta 4+10, stone quality classification, end of 1997.....	172
Figure 127.	Cleveland Harbor east breakwater, sta 102+00 to sta 103+00, stone quality classification, end of 1997.....	173
Figure 128.	Cleveland Harbor east breakwater, sta 107+40 to sta 108+60, stone quality classification, end of 1997.....	174
Figure 129.	Cleveland Harbor east breakwater, sta 121+90 to sta 123+15, stone quality classification, end of 1997.....	175
Figure 130.	Cleveland Harbor east breakwater, sta 164+00 to sta 165+20, stone quality classification, end of 1997.....	176
Figure 131.	Cleveland Harbor east breakwater, sta 197+50 to sta 198+75, stone quality classification, end of 1997.....	177
Figure 132.	Chicago Harbor breakwater, sta 14+65 to sta 16+00, acceptable versus rejected stone, end of 1997.....	178
Figure 133.	Calumet Harbor breakwater, sta 117+55 to sta 118+90, acceptable versus rejected stone, end of 1997.....	179
Figure 134.	Calumet Harbor confined disposal facility, sta 33+00 to sta 33+40, acceptable versus rejected stone, end of 1997	180
Figure 135.	Burns Harbor breakwater (Shore Arm section), sta 53+60 to sta 54+55, acceptable versus rejected stone, end of 1997.....	181
Figure 136.	Burns Harbor breakwater (Big Burn section), sta 3+30 to sta 4+10, acceptable versus rejected stone, end of 1997	182
Figure 137.	Cleveland Harbor east breakwater, sta 102+00 to sta 103+00, acceptable versus rejected stone, end of 1997.....	183
Figure 138.	Cleveland Harbor east breakwater, sta 107+40 to sta 108+60, acceptable versus rejected stone, end of 1997.....	184
Figure 139.	Cleveland Harbor east breakwater, sta 121+90 to sta 123+15, acceptable versus rejected stone, end of 1997.....	185

Figure 140.	Cleveland Harbor east breakwater, sta 164+00 to sta 165+20, acceptable versus rejected stone, end of 1997.....	186
Figure 141.	Cleveland Harbor east breakwater, sta 197+50 to sta 198+75, acceptable versus rejected stone, end of 1997.....	187
Figure 142.	Percentage of rejected stones at monitored breakwater structure sections by stone type since those stones were originally placed.....	191
Figure 143.	Percentage of rejected stones at monitored breakwater structure sections by stone type, within Chicago District, since those stones were originally placed.....	192
Figure 144.	Percentage of rejected stones at monitored breakwater structure sections by stone type, within Buffalo District (Cleveland Harbor east breakwater), since those stones were originally placed	193
Figure 145.	Stone quality comparison for monitored years at Chicago Harbor breakwater, sta 14+65 to sta 16+00, for total of 131 stones	194
Figure 146.	Stone quality comparison for monitored years at Calumet Harbor breakwater, sta 117+55 to sta 118+90, for total of 153 stones.....	195
Figure 147.	Stone quality comparison for monitored years at Calumet Harbor CDF, sta 33+00 to sta 33+40, for total of 49 stones.....	196
Figure 148.	Stone quality comparison for monitored years at Burns Harbor breakwater (Shore Arm section), sta 53+60 to sta 54+55, for total of 61 stones	197
Figure 149.	Stone quality comparison for monitored years at Burns Harbor breakwater (Big Burn section), sta 3+30 to sta 4+10, for total of 137 stones	198
Figure 150.	Stone quality comparison for monitored years at Cleveland Harbor east breakwater, sta 102+00 to sta 103+00, for total of 94 stones	199
Figure 151.	Stone quality comparison for monitored years at Cleveland Harbor east breakwater, sta 107+40 to sta 108+60, for total of 73 stones	200
Figure 152.	Stone quality comparison for monitored years at Cleveland Harbor east breakwater, sta 121+90 to sta 123+15, for total of 73 stones	201

Figure 153.	Stone quality comparison for monitored years at Cleveland Harbor east breakwater, sta 164+00 to sta 165+20, for total of 127 stones	202
Figure 154.	Stone quality comparison for monitored years at Cleveland Harbor east breakwater, sta 197+50 to sta 198+75, for total of 60 stones	203
Figure 155.	Cleveland Harbor east breakwater stone quality classification for three stone types on the monitored structure sections, for total of 427 stones, and a comparison of their degree of deterioration at end of monitoring period (1997)	205
Figure 156.	Cut versus blasted comparison of rejected sedimentary stones (limestone, sandstone, dolomite, and dolomitic limestone) on monitored structure sections, and weighted average number of years since placement of stone on structure	212
Figure 157.	Percentage of stones rejected on monitored structure sections versus six stone geologies evaluated, and weighted average number of years since placement of stone on structure	215
Figure 158.	Percentage of stones rejected on monitored structure sections versus number of years since placement of stone on structure sections, for five monitored sections with cut and blasted dolomite.....	216
Figure 159.	Percentage of stones rejected on monitored structure sections versus number of years since placement of stone on structure sections, for six monitored sections with cut and blasted limestone	217
Figure 160.	Percentage of stones rejected on monitored structure sections versus stone geologies and production methods (cut and blasted methods of extraction), and weighted average number of years since placement of stone on structure.....	219
Figure 161.	Crack association with quarry facies, 10 years or younger stones, for crack types 0 through 3.....	225
Figure 162.	Crack association with quarry facies, 10 years or younger stones, for crack types 5 through 9.....	226
Figure 163.	Crack association with quarry facies, 10 years or younger stones, for crack types 11 through 17.....	227
Figure 164.	Conventional rehabilitation 1985 QC/QA versus enhanced rehabilitation 1989 QC/QA	233

Figure A1.	Burns Harbor, IN, breakwater looking west.....	A3
Figure A2.	Limestone blocks in place along Chicago shoreline – Belmont to Diversey.....	A6
Figure A3.	Dolomite armorstones showing stylolites in various degrees of separation.....	A7
Figure A4.	Bedding planes in limestone armor stone on Chicago shoreline showing separation	A8
Figure A5.	Granite armor stone during sorting process – note absence of discontinuities.....	A10
Figure A6.	Even with QA/QC practices, this armor stone and others like it appear in Reach 5 breakwater. Note separations occurring at planar weaknesses	A14

List of Tables

Table 1.	Accelerated Weathering Test Results.....	84
Table 2.	Relative Degree of Stone Degradation.....	158
Table 3.	Relative Crack Classification Based on Nature of Crack.....	166
Table 4.	Stone Crack Change Factor Relative Points.....	166
Table 5.	Stone Deterioration, All MCNP Monitored Structure Sections (Continued).....	188
Table 6.	Stone Deterioration, Cleveland Harbor East Breakwater Monitored Sections	204
Table 7.	Freeze and Freeze/Thaw Cycles.....	207
Table 8.	Effect of Extraction Method on Average Quality of Sedimentary Stone.....	210
Table 9.	Rejected Sedimentary Stones, Cut and Blasted Method of Extraction, 1997 Results	211
Table 10.	Rejected Stones for Six Stone Geologies Monitored, Cut and Blasted Methods of Extraction, 1997 Results.....	214
Table 11.	Stone Geology and Production Method, Cut and Blasted Methods of Extraction, 1997 Results	218
Table 12.	Quarry Facies Durability Evaluations	222

Table 13.	Key for Crack Association with Quarry Facies in Figures 161 through 163	224
Table 14.	Summary of Quarry Facies Comparisons	228
Table 15.	Average Durability of Four Lithologic Categories	231
Table A1.	Criteria for Stone Quality	A11
Table A2.	Summary of Issues	A18

Preface

The studies reported herein were conducted as part of the Monitoring Completed Navigation Projects (MCNP) Program (formerly Monitoring Completed Coastal Projects (MCCP) Program). Work was conducted under MCNP Work Unit No. 11M13, “Stone Degradation on Coastal Structures in North Central Division.” Overall program management of the MCNP is provided by Headquarters, U.S. Army Corps of Engineers (HQUSACE). The Coastal and Hydraulics Laboratory (CHL), U.S. Army Engineer Research and Development Center (ERDC), Vicksburg, MS, is responsible for technical and data management, and support for HQUSACE review and technology transfer. Program monitors for the MCNP Program are Messrs. Barry W. Holliday, Charles B. Chesnutt, and David B. Wingerd, HQUSACE. MCNP program managers during the conduct of this MCNP study were Ms. Carolyn M. Holmes and Messrs. E. Clark McNair and Robert R. Bottin, Jr., CHL.

There are 107 coastal projects in the U.S. Army Engineer Great Lakes and Ohio River Division (formerly North Central Division) with breakwaters and/or jetties extending more than 146,304 m (480,000 lin ft). For the greater part of the last century, the Great Lakes and Ohio River Division has experienced chronic and recurring problems with stone durability on these project breakwaters and jetties. The mechanism that is fracturing the stone has not been positively identified. The purposes of these studies are to provide answers to the following specific pertinent concerns: (a) It must be determined if more durable stone types are available, or if the durability of locally produced stone could be increased even if only at a higher cost. (b) It must be determined if it is possible to use stone of a lesser quality on certain specific portions of the structure (i.e., underwater), thus saving the best stone for the most critical and susceptible areas that are subject to large wave conditions. (c) The optimum storage time that a stone needs to lie dormant (age) to allow blast-induced fractures, or fractures from release of tectonic stresses, to become apparent must be determined.

This research was conducted during the time period October 1994 – September 1998 under the general supervision of Dr. James R. Houston, former Director, CHL, and Mr. Thomas W. Richardson, Director, CHL, and under direct supervision of Mr. D. Donald Davidson, former Chief, Wave Research Branch, CHL, and Mr. Dennis G. Markle, former Chief, Coastal Harbors and Structures Branch (CHSB), CHL. Other Corps Division, District, and Laboratory MCNP Team Members who contributed significantly to the development and execution of these studies included: (a) North Central Division, Chicago IL; Mr. Charles N. Johnson; (b) Chicago District, Chicago, IL; Ms. Mary K. Tibbets and Messrs. James G. Mazanec, Mizra M. Baig, Kevin S. Richards,

Joseph A. Kissane, and Olaf Weeks; (c) Buffalo District, Buffalo, NY; Messrs. David W. Marcus, Michael C. Mohr, Shanon Chader, and Thomas J. Bender; (d) Detroit District, Detroit, MI; Mr. Ronald L. Erickson; (e) Ohio River Division Laboratory (ORDL), Cincinnati, OH; Ms. Kathy Loudon and Messrs. Kenneth E. Henn III, and David A. Lienhart (former geologist, ORDL; presently Rock Products Consultants (RPC), Cincinnati, OH); and (f) CHL; Mr. Gordon S. Harkins, CHSB, and Mr. Jon W. Lott, Prototype Measurement and Analysis Branch. Other researchers who contributed significantly to this study included Mr. Albert W. Gerdson, RPC, and Ms. Susan M. Agar, Northwestern University, Evanston, IL. Principal Investigator for this study was Dr. Donald L. Ward, CHL. This report was compiled by Dr. Lyndell Z. Hales and Ms. Donna L. Richey, CHL.

At the time of publication of this report, COL James R. Rowan, EN, was Commander and Executive Director of ERDC. Dr. James R. Houston was Director.

1 Introduction

Monitoring Completed Navigation Projects (MCNP) Program

The goal of the Monitoring Completed Navigation Projects (MCNP) Program (formerly the Monitoring Completed Coastal Projects (MCCP) Program) is the advancement of coastal and hydraulic engineering technology. The program is designed to determine how well projects are accomplishing their purposes and how well they are resisting attacks by their physical environment. These determinations, combined with concepts and understanding already available, will lead to (a) the creation of more accurate and economical engineering solutions to coastal and hydraulic problems, (b) strengthening and improving design criteria and methodology, (c) improving construction practices and cost-effectiveness, and (d) improving operation and maintenance techniques. Additionally, the monitoring program will identify where current technology is inadequate or where additional research is required.

To develop direction for the program, the U.S. Army Corps of Engineers (USACE) established an ad hoc committee of engineers and scientists. The committee formulated the objectives of the program, developed its operation philosophy, recommended funding levels, and established criteria and procedures for project selection. A significant result of their efforts was a prioritized listing of problem areas to be addressed. This is essentially a listing of the areas of interest of the program.

Corps offices are invited to nominate projects for inclusion in the monitoring program as funds become available. The MCNP Program is governed by Engineer Regulation 1110-2-8151 (Headquarters, U.S. Army Corps of Engineers (HQUSACE 1997)). A selection committee reviews and prioritizes the nominated projects based on criteria established in the regulation. The prioritized list is reviewed by the Program Monitors at HQUSACE. Final selection is based on this prioritized list, national priorities, and the availability of funding.

The overall monitoring program is under the management of the Coastal and Hydraulics Laboratory (CHL), U.S. Army Engineer Research and Development Center (ERDC), with guidance from HQUSACE. An individual monitoring project is a cooperative effort between the submitting District and/or Division office and CHL. Development of monitoring plans and conduct of data collection and analyses are dependent upon the combined resources of CHL and the District and/or Division.

Background

There are 107 coastal projects in the U.S. Army Engineer Great Lakes and Ohio River Division (formerly North Central Division) with breakwaters and/or jetties extending more than 146,300 m (480,000 ft) in length. For the greater part of the last century, the Great Lakes and Ohio River Division has experienced chronic and recurring problems with stone durability on these project breakwaters and jetties. Results of a divisionwide deterioration inventory by the Great Lakes and Ohio River Division in 1990 indicated significant premature deterioration of armor stone, most of which was Silurian and Devonian limestones and dolomites. Extensive maintenance and rehabilitation of existing structures is needed due to the premature deterioration, and tens of millions of dollars will be required for these repairs. The seriousness of the situation is reflected in the following examples. At the Cleveland Harbor, OH, east breakwater following a 1988-1990 rehabilitation project, 42 percent of the stones in one reach were cracked after just one season on the structure, and 76 percent of the stones were cracked after just 4 years following a 1985-1986 repair. At Calumet Harbor, IL, armor stone on a dredged material confined disposal facility (CDF) is highly deteriorated, although less than 10 years old.

The mechanism that is fracturing the stone has not been positively identified. There indeed may be several contributors to susceptibility of stones to weathering and degradation. Each of several physical factors may result in fractures in the armor stone; however, and more importantly, they make it more likely that the environment present at the sites can more readily degrade the stone. So, it is a matter of conditions prior to the stone being placed at the structure (from its formation as a rock mass through its geologic history and, ultimately, its being transformed from a natural rock mass to a construction material transported and placed onsite) that determine how durable it is when faced with the stresses to which it is subjected in the structure.

One hypothesis regarding stone degradation concerns quarrying techniques. Most quarries in the Great Lakes region operate primarily for the production of construction aggregate, and blasting procedures used in these quarries are designed to maximize fracture in the rock lift. These blast effects may produce stresses in the stone that, over time, create fractures and break the stone into smaller pieces that may be below design specifications. Using different quarrying techniques may reduce the blast effects but at a higher cost for the stone production.

Another mechanism that may be responsible for the observed stone degradation is the removal of overburden. In situ stresses are present in some rock units as a consequence of thousands of feet of ice overburden during the Pleistocene ice age (12,000 years before present). Removal of that ice has resulted in isostatic rebound and uplift stresses, with fracturing in some rock masses. Regional uplift in the geologic past may also have resulted in stress in the rock fabric. When stone is blasted free, the overburden pressures of the surrounding stone are removed. In some cases, it is believed that these overburden stress releases can produce fractures that occur for some time after the rock is excavated.

With either of these fracture mechanisms, hairline cracks will become apparent over time. Aging the stone, or storing the quarried stone for a prescribed period before placement on the breakwater, will allow the cracks to develop to the point where they can be seen and the stone can be rejected. However, storing the large quantities of stone required for a breakwater is expensive.

Intensive Quality Control and Quality Assurance (QC/QA) measures have been shown to substantially decrease the degradation of stone placed in construction. Again, costs may be a major factor. Not only are intensive QC/QA measures expensive to perform, the cost of the rock will increase substantially if a high percentage of the stone is being rejected.

The problem of stone degradation is not limited to the Great Lakes region or the Great Lakes and Ohio River Division. A 1993 survey of the breakwater extension at St. Paul Harbor, AK, conducted just four years after construction reported that hairline cracks were too numerous to document, with 73 stones cracked all the way through or separated (Bottin 1993), and 131 stones cracked all the way through just one year later (Bottin 1994). Broken armor stones have also been observed on jetties in Oregon and Washington. Although the problem with stone degradation was most recently identified with the Great Lakes and Ohio River Division, it is likely that the extent of the problem has simply not been documented in other areas at this time.

Stone Degradation Investigations

The purposes of the present MCNP investigation of stone degradation on Great Lakes coastal structures were to provide answers to the following specific pertinent concerns.

- a.* It must be determined if more durable stone types are available, or if the durability of locally produced stone could be increased even if only at a higher cost. It may be more cost-effective in terms of life-cycle costs to use the better quality stone at a higher initial construction cost than using lower quality stone with a higher maintenance cost. Answers to these questions will require information on deterioration rates for different stone types available from different quarries that use different quarrying procedures. This information can then be incorporated with the effects of more stringent QC/QA practices during construction or rehabilitation.
- b.* It may be possible to use stone of a lesser quality on portions of the structure, thus saving the best stone for the most critical and susceptible areas. Armor stone placed below the wave splash zone may deteriorate at a slower rate than armor stone placed above this zone. The savings potential would be readily apparent if it could be shown that a less expensive stone could be used on the underwater portion of a breakwater or jetty. There may be significant differences in deterioration rates between stones exposed to wave action on the lakeside versus the harbor side of a structure, and between stones above and below the splash zone. Answers to these questions may be obtained by comparing damage levels on stone placed above the splash zone, in the surf zone, and below water

on existing structures. The worst degradation will be seen in regions where wet/dry and freeze/thaw cycles are at a maximum. Sections of existing structures containing a range of stone types and quarry sources will be examined.

- c. The length of time that stones should be stored (aged) before placement on a structure is critically important. This storage factor concerns the length of time that a stone needs to lie dormant to allow blast-induced fractures or fractures from release of tectonic stresses to become apparent. Waiting periods of 30 to 90 days are typically specified, but it is commonly believed that a longer waiting period would be beneficial. However, storage of the large amount of armor stone required for a breakwater or jetty is expensive, and is not practical without documentation data to prove the benefits, if any, of longer storage. This concern should be addressed by monitoring degradation of freshly placed stone on a new repair of a breakwater, or by instrumenting freshly quarried stone to monitor stress relief. Curing requirements will vary by stone type, porosity, and in situ percent water; therefore, the waiting period is not a standard number of days.

MCNP Study Components

Stone deterioration on breakwaters and jetties arise from a combination of interactions pertaining to the quality of stone available, operational and handling practices at the quarry, and environmental weathering conditions after placement on the project structure (Livingston 1975). Four different and distinct components of the stone degradation investigation are essential to fully comprehend the mechanisms that give rise to chronic premature deterioration of armor stone on breakwaters and jetties around the Great Lakes. These four investigation components include:

- a. *Quarry field geological observations.* Seven different quarries that have historically provided material for Great Lakes breakwater and jetty construction and rehabilitation projects were investigated. These seven quarries were selected for evaluation because stone from these quarries has been used on sections of prototype structures to be monitored due to premature deterioration. Evaluations of these quarries, and evaluations of their operational techniques, were performed by Rock Products Consultants (1995). The stone produced by these seven quarries included:
 - (1) Salem formation limestone--Reed Quarry, Bloomington, IN.
 - (2) Niagaran series dolomite--Valders Quarry, Valders, WI.
 - (3) Waterloo formation quartzite--Dempsey Quarry (now Michels Quarry), Waterloo, WI.
 - (4) Columbus formation limestone--Sandusky Quarry, Parkertown, OH.
 - (5) Columbus formation dolomitic limestone--Marblehead Quarry, Marblehead, OH.

- (6) Berea formation sandstone--Johnson Quarry, Kipton, OH.
- (7) Racine formation dolomite--Thornton Quarry, Thornton, IL.

Field geological observations had previously been performed at an eighth quarry (McCook Quarry, McCook, IL) by STS Consultants Ltd. (1992). The McCook Quarry produces Niagaran series dolomite.

- b. *Laboratory durability testing.* Laboratory durability testing of stone samples to accelerate weather exposure freeze/thaw and wet/dry effects, and to determine specific gravity and sample petrography, were performed by the U.S. Army Engineer Ohio River Division. The laboratory durability testing samples came from the eight quarries where field geological observations had been performed, plus samples from a ninth quarry (Iron Mountain Quarry, Iron Mountain, MI). The Iron Mountain Quarry produces taconite. Samples of taconite from the Iron Mountain Quarry also were evaluated by laboratory tests because prototype stones from this quarry had been specifically placed on the Calumet Harbor Confined Disposal Facility (CDF) in 1995 for durability evaluation by the field prototype monitoring part of this MCNP investigation.
- c. *Quarry sample microstructural analyses.* Microstructural analyses of quarystone samples from seven different quarries to determine micro-scale features in the rock that affect stability, and their relations to compositional and textural variations, were conducted by Agar (1998) after these samples had undergone laboratory durability testing. These were the same quarries for which quarry field geological observations had also been performed, except stone samples from McCook Quarry were not available for quarry microstructural analyses.
- d. *Field prototype monitoring.* Field monitoring of 10 specific sections of five prototype structures to document progressive deterioration rates among different stone types, different degrees of environmental exposure, and different levels of stone quality control, was conducted by ERDC and U.S. Army Engineer Districts, Buffalo and Chicago. The structures which were selected for monitoring were Chicago Harbor, IL, breakwater; Calumet Harbor, IL and IN, breakwater; Calumet Harbor, IL, CDF; Burns Harbor, IN, breakwater; and Cleveland Harbor, OH, east breakwater. The 10 sections of prototype structures selected for evaluation contained deteriorated stone from the eight quarries previously discussed, plus stone from the Calumet Harbor CDF revetment that originally came for a ninth quarry, the Iron Mountain Quarry, Iron Mountain, MI. Also, stone from a 10th quarry (Cedarville Quarry, Cedarville, MI) was evaluated by this field prototype monitoring study because stone from this quarry has previously been placed on other stone structures around the Great Lakes. The Cedarville Quarry produces Niagaran series dolomite.

A total of six different stone types were evaluated by the field prototype monitoring, including (a) dolomite, (b) limestone, (c) quartzite, (d) sandstone, (e) taconite, and (f) dolomitic limestone.

Previous Studies

Guidance from previous Corps-wide and regional Great Lakes breakwater and jetty studies significantly assisted the development of the monitoring plan for investigating premature critical stone deterioration in this region. Knowledge gained from these previous studies was incorporated into this present MCNP monitoring program.

1979 Corps-wide survey of stone structures

A 1979 Corps-wide survey of breakwaters and jetties (Lutton et al. 1981; Lutton 1982) reported that deterioration or cracking of riprap, armor stone, jetty stone, etc. constituted a problem for Districts and Divisions during the previous 10 years at least occasionally in 24 of 38 responses. Although questionnaire responses did not include detailed surveys of rubble-mound structures, analyses of the responses clearly revealed the potential importance of several factors influencing stone quality and performance, including (a) rock type, (b) geologic structure, (c) scale effect, (d) quarry yield, (e) quarry method, and (f) operational compatibility.

1980-1985 Cleveland Harbor east breakwater monitoring

Cleveland Harbor was the site of a previous MCCP study (Pope et al. 1993). A major rehabilitation of 1,340 m (4,400 ft) of the east end of the east breakwater was constructed in 1979-1980 using 1,815-kg (2-ton) dolos concrete armor units. The dolos-repaired section was selected for monitoring to (a) determine the stability of a dolos armor unit cover, (b) determine wave transmission by overtopping, (c) qualitatively evaluate wave runup, and (d) document the effects of ice on stability of dolos units.

The Cleveland Harbor east breakwater monitoring was originally scheduled to cover the period November 1980 to September 1983 but was extended under a reduced monitoring program for an additional 2 years (until September 1985) after a severe storm damaged the head and trunk of the length being monitored. The damaged head section was repaired in October 1982. The program included aerial photography, wave and water level data, survey data, inventory of broken dolos units, time lapse photography, and underwater inspections utilizing both side-scan sonar and diver inspections.

1985 Cleveland Harbor east breakwater physical model study

A two-dimensional (2-D) physical model investigation of a typical cross section of the Cleveland Harbor east breakwater trunk was conducted in 1985 after a 1984 proposal to rehabilitate an additional 1,000 m (3,300 ft) of the east breakwater with dolos armor units (Markle and Dubose 1985). The purposes of the model study were to (a) evaluate the stability of 3,630-kg (4-ton) dolosse when exposed to design wave and still-water level conditions, (b) determine the degree of breakwater damage that could occur on the 3,630-kg (4-ton) dolos

design for a storm condition that exceeds the design wave condition, and (c) determine the maximum nonbreaking wave heights that the existing 1,815-kg (2-ton) dolos design and the proposed 3,630-kg (4-ton) dolos and 8,165- to 18,145-kg (9- to 20-ton) armor stone designs could withstand.

The study found that the 8,165- to 18,145-kg (9- to 20-ton) stone exhibited the greatest stability of the plans tested under design conditions, and the 3,630-kg (4-ton) dolosse were found to be marginally acceptable under design conditions. Following storms and high-water levels in 1986-1987 and a massive failure of the breakwater head, 3,630 kg (4-ton) dolosse were placed around the head of the east jetty and in low areas along the trunk to bring it back to design elevation.

1989 Cleveland Harbor east breakwater stone survey

After significant stone fracturing of newly placed stone was found on the Cleveland Harbor east breakwater during a rehabilitation project in 1988-1990, a study was conducted of another reach of the breakwater that had been rehabilitated in 1985-1986. The survey found 76 percent of the stone on the 5-year-old repair was significantly fractured, and half of those were believed to be due to blast-induced damage (Marcus 1992). The U.S. Army Engineer District, Buffalo, commissioned Blasting Analysis International, Inc., in August 1989 to (a) assess causes for stone fractures on the Cleveland Harbor east breakwater, and if possible correlate causes of fractures to quarrying operations that produced the stone, and (b) assess significance of cracked stone on structure stability, and recommend a quarrying operation that would reduce the occurrence of significant cracking.

The blasting consultants opinion was that the main cause of the significant and undesirable fracture patterns were a direct result of blasting (Chiapetta 1989).

1990 LRD structure stone survey

In 1990, the Great Lakes and Ohio River Division initiated a detailed survey of breakwaters and jetties within the Division using ground surveys to document breakage and deterioration of stone on the structures. Included in the survey was percent breakage, description of cracking, and classification of observed cracks (i.e., delamination, random cracking, etc.). This present MCNP study provided further data on rates of degradation and comparisons of quarry sources and quarrying techniques.

1994 Cleveland Harbor east breakwater study

Stone deterioration on the Cleveland Harbor east breakwater was studied by Marcus (1994) who mapped, measured, classified, and photographed cracks and deterioration for several reaches of the breakwater for the previous 5 years, including the reaches selected for monitoring in this present MCNP study. This present MCNP study provided a continuation of part of the study conducted by Marcus (1994), and thus provided an extended monitoring of progressive

deterioration. Data were obtained by Marcus (1994) (and for the present MCNP study) by directly walking over the structure and conducting surveys by measuring from baselines and offsets to locate individual stones, and by annual boat inspections. Those data include:

- a. Surveyed location of cracked or deteriorated stones.
- b. Number of significant cracks. (Significant was defined as a crack opening no less than 0.3 m (1 ft) in length penetrating through at least two adjacent sides of the stone, and projected to separate at least 20 percent of the stone mass.)
- c. Crack damage type. (Crack damage was categorized into one of four types, depending on the severity of the crack; (a) no cracked stone, (b) minor cracked stone, (c) significant cracked stone, and (d) reject stone.)
- d. Location of crack relative to the geology of the stone.
- e. Apparent mechanism for cracking, based on stone stress characteristics.

Photographs document the year-to-year progression of individual cracks. Results of that study by Marcus (1994) showed that about 80 percent of the stones from the 1985-1986 repair had cracked after 4 years, while stones from the same quarry placed after stringent QC/QA measures were implemented during the 1988-1990 repair showed 1 percent cracked after 1 year, 11 percent cracked after 2 years, and 18 percent cracked after 3 years. Marcus (1994) focuses on the large stone durability of the Cleveland Harbor east breakwater, with additional information from other projects on the Great Lakes.

Monitoring Plan

Monitoring of construction and repairs that have already been completed provides answers to key questions that offer potential for tremendous savings in operation and maintenance (O&M) expenditures for both repairs to existing structures and new construction projects. Ten different sections of five different structures were monitored over the 3-year period 1996-1998. In the Chicago District, four sections (Chicago Harbor breakwater, Calumet Harbor breakwater, Calumet Harbor CDF revetment, Burns Harbor breakwater (Big Burn section)) were monitored annually, and one section (Burns Harbor breakwater (Shore Arm section)) was monitored quarterly. In the Buffalo District, five sections of the Cleveland Harbor east breakwater were monitored annually, and some of these sections had previously been monitored annually prior to this MCNP study.

Structures and sections monitored¹

Ten different sections of five Great Lakes harbor structures were selected for field prototype monitoring because these sections had experienced premature stone deterioration, and because these sections provided a maximum variety of

¹ This section is extracted essentially verbatim from Rock Products Consultants (1995).

produced stone on the structures from local quarries. During a preliminary base condition inspection in early 1995, all stones within the selected sections were numbered and photographed for precise location, and for determination of displacement and progression of degradation during later monitoring. The 10 sections are located as follows:

- a. *Chicago Harbor breakwater, IL*
Section 1 – sta 14+65 to sta 16+00
- b. *Calumet Harbor breakwater, IL and IN.*
Section 2 – sta 117+55 to sta 118+90
- c. *Calumet Harbor CDF revetment, IL and IN.*
Section 3 – sta 33+00 to sta 33+40
- d. *Burns Harbor breakwater, IN.*
Section 4 – Shore Arm section sta 53+60 to sta 54+55
Section 5 – Big Burn section sta 03+30 to sta 04+10
- e. *Cleveland Harbor east breakwater, OH.*
Section 6 – sta 102+00 to sta 103+00
Section 7 – sta 107+40 to sta 108+60
Section 8 – sta 121+90 to sta 123+15
Section 9 – sta 164+00 to sta 165+20
Section 10 – sta 197+50 to sta 198+75

Chicago Harbor breakwater, IL. Valdars Quarry Niagaran series cut dolomite (low energy blasted, drilled and split, and then surfaces cut; see editor's note, p. 149) is concentrated mostly on the north half of this reach of the Chicago Harbor breakwater, IL (Figure 1), in holes created by weathering of the Reed Quarry Salem formation Indiana limestone blocks, and over badly weathered sections of the limestone blocks. The Valdars Quarry dolomite in the monitored section was placed in 1994. Fractures observed in the Valdars Quarry dolomite are of four types: (a) blasting, (b) unloading and stress relief, (c) vugular weathering, and (d) contact parting. Fractured stone is not limited to either lakeside or harbor side of the breakwater.

The Reed Quarry Salem formation cut limestone blocks had been placed in a somewhat random manner, with some stones placed horizontally, some vertically, and some diagonally with respect to bedding planes. The vertical orientation may possibly allow water to permeate the stone along the more permeable bedding direction. However, there is no conclusive relationship between orientation and durability independent of other factors (e.g., clay minerals present along the bedding). The fractures in these limestone blocks are mostly zones of exfoliation or delamination associated with highly porous, fossiliferous grain stone zones adjacent to large stylolites. This stone might have performed better if it had been placed such that the bedding planes were oriented horizontally, although horizontally placed stones have also shown separation along bedding planes in



Figure 1. Chicago Harbor breakwater, IL, monitored section

other structures in the Chicago District. Furthermore, aligning stone with bedding planes horizontal has serious problems in execution. Stone other than cut rectangular blocks does not make such placement a simple matter. Even with cut rectangular blocks, it is sometimes difficult to determine the orientation of bedding planes in some rock types that do not have conspicuous bedding planes in the first place (and are therefore more desirable since the contrasting bedding planes are often visible because of the clay content). The Reed Quarry cut limestone had been placed in the monitored section in 1966.

Calumet Harbor breakwater, IL and IN. The Reed Quarry Salem formation cut limestone is located on both the lakeside and harbor side of the double row of steel sheet pile forming the interior walls of the breakwater structure at Calumet Harbor breakwater, IL and IN (Figure 2). The Reed Quarry limestone in the monitored section had been placed in 1988. Just as in the Chicago Harbor breakwater, some of the Reed Quarry cut limestone blocks had been placed with bedding oriented vertical. The fractures in the Calumet Harbor breakwater stone are of three types; (a) mechanical fractures due to waves pounding against the flexible steel sheet pile immediately adjacent to the armor blocks; (b) parting along a stylolite, and (c) exfoliation or delamination zones associated with highly porous fossiliferous grain stone zones adjacent to large stylolites. The combination of the high-porosity zone with the fact that a stylolite is a permeability discontinuity, together with the placement of the blocks such that the bedding is oriented vertically, insures weathering susceptibility. The vertical orientation of the bedding allows the stone to become fully saturated. Freezing is then initiated. With the fully saturated high-porosity zone trapped between the stylolite and a less porous zone, ice forms within the high-porosity zone. Hydraulic pressure due to volumetric expansion of the ice increases as



Figure 2. Calumet Harbor breakwater, IL and IN, monitored section

temperatures drop below freezing, and reaches a maximum of 2,110 kg per sq cm (30,000 lb per sq in.) at a temperature of -22 deg C. This pressure is sufficiently adequate to fracture the rock parallel to the stylolite.

The Dempsey Quarry Waterloo formation blasted quartzite had been placed on top of the Indiana limestone capstone in those areas of the breakwater where the Indiana limestone had weathered, leaving holes in the capstone. The Dempsey Quarry blasted quartzite in the monitored section had been placed in 1994. Stone fracturing appeared to be strictly a mechanical fracture that occurred either during placement or during a storm event.

Calumet Harbor CDF revetment, IL. The McCook Quarry Niagaran series blasted dolomite armor stone consists of various facies from a reef environment. These various lithologies are evenly distributed over the Calumet Harbor CDF revetment, IL (Figure 3). All of the lithologies contain thin seams and/or disseminated glauconite, and have a chalky, argillaceous appearance. This is generally a poor quality stone. In a random survey of a 30.48-m (100-ft) section of this facility, the following percentages of rock types were encountered; (a) reef dolomite, 16 percent, (b) forereef, 10 percent, (c) backreef, 22 percent, (d) inter-reef, 13 percent, and (e) reef breccia, 39 percent. 80 percent of all blocks were fractured, with the fracture development by rock type as follows; (a) reef dolomite, 0 percent, (b) forereef, 33 percent, (c) backreef, 71 percent, (d) inter-reef, 100 percent, and (e) reef breccia, 100 percent. Fractures were almost totally due to argillaceous (glauconitic) nature of this particular stone source and resulting weathering effects. No blasting fractures were detected. The McCook Quarry blasted dolomite in the monitored section had been placed in 1982.



Figure 3. Calumet Harbor CDF revetment, IL, monitored section

Burns Harbor breakwater, IN. Burns Harbor, IN (Figure 4), is a deepwater harbor at the southern end of Lake Michigan that receives significantly greater wave heights than other navigation harbors around Lake Michigan. The breakwater, completed in 1968, consists of an east-west section (Big Burn section) connected to the shore by a north-south section (Shore Arm section), which is semiprotected from severe Great Lakes storms. The breakwater is a multilayer rubble-mound structure with two layers of randomly-placed Reed Quarry Salem formation cut limestone. The parallelepiped cut stone armor units, which range from 9,070 to 14,515 kg (10 to 16 tons) on the trunk and from 13,605 to 18,145 kg (15 to 20 tons) on the head, are typical for coastal structures in the Great Lakes, but the two-layer random placement is unusual. Numerous repairs have been necessary since about 1975 as the structure was unable to withstand the severe storm waves that it would experience. There exists uncertainty as to whether there is a single cause for the problems or whether there are multiple factors contributing to the need for repairs (e.g., foundation issues, material suitability, greater wave climate than originally believed, etc.) Over the years, repair stone has consisted of Reed Quarry cut limestone, McCook Quarry Niagaran series blasted dolomite, and Dempsey Quarry Waterloo formation blasted quartzite. For the monitored Big Burn section, Reed Quarry cut limestone was placed in 1970, and McCook Quarry blasted dolomite was placed in 1988. For the monitored Shore Arm section, Reed Quarry cut limestone and Dempsey Quarry blasted quartzite were placed in 1995.



Figure 4. Burns Harbor breakwater, IN, monitored sections

Cleveland Harbor east breakwater, OH. The original east breakwater at Cleveland, OH (Figure 5), was built between 1903 and 1905 as a laid-up structure from cut stone from one or more of the quarries now owned or formerly owned by Cleveland Quarries. One of these is the Johnson Quarry, Kipton, OH. The Johnson Quarry Berea formation cut sandstone blocks are still present in the structure, and form the base of the breakwater structure. In recent years, as the cut stone became more expensive, the U.S. Army Engineer District, Buffalo, has been maintaining the structure with rubble armor stone. This has created a somewhat less stable structure with the blocks of rubble rocking back and forth on the somewhat flat surface created by the laid-up cut stone. Additionally, the much larger blocks of rubble on top of the laid-up cut stone are destroying the stability of the laid-up structure. The Johnson Quarry cut sandstone in the monitored section had been placed over 30 years ago. The only fractures noted in the Berea sandstone are those created by movement of the structure as a result of placement of the less stable and larger rubble blocks.



Figure 5. Cleveland Harbor east breakwater, OH, monitored sections

The Marblehead Quarry Columbus formation blasted dolomitic limestone was placed on the crest and lakeside of the structure. This armor stone is extensively fractured in spite of what appears to be an excellent QC/QA program. Although it is not possible to determine the cause of the fracturing, it is suspected that most of the fracturing may be attributed to a combination of several factors, including; (a) extremely low bench height blasting, (b) explosive agent in column adjacent to armor stone zone of interest, (c) high in situ stress field and glacial rebound effects, both triggered by blasting (Toksoz et al.1971), and (d) inadequate set-aside (seasoning or curing) period prior to acceptance. It is also believed that some fracturing may simply be mechanical due to instability of rubble blocks and lack of support of the blocks (Livingston 1975). Often these 8,165- to 18,145-kg (9- to 20-ton) blocks are supported only by a few small contact points where the blocks touch other blocks. The Marblehead Quarry blasted dolomitic limestone in the monitored sections was placed between 1985 and 1989.

The Sandusky Quarry Columbus formation blasted limestone was placed on the crest and lakeside of the structure in 1992. This blasted limestone has experienced significant cracking and deterioration.

Monitoring procedure

The monitoring procedures for each of the reaches included:

- a.* Ground inspections by registered professional geologists would be made to catalogue, at the monitored sections, all stone fractures and offset measurements in armor stone above the high-water mark, between low water and high water on the harbor side, and between low water and high water on the lakeside annually for 3 years. Broken stones would be marked to show in aerial photographs to insure repeatability and to document progression of deterioration.
- b.* High-resolution, low-altitude aerial photography would be obtained to document location and movement of deteriorating stones, and to provide a reference for subsequent years.
- c.* Underwater inspection would be conducted to measure, mark, and classify cracks in armor stone for comparison to above-water results, for both lakeside and harbor side. Underwater inspection would be conducted by a diver with video equipment, directed by a geologist on the support boat who would be observing the video.
- d.* Laboratory analyses of samples from different rock types on the breakwaters to provide details on rock composition and structural characteristics would be conducted. Details to be determined included (a) specific gravity, (b) adsorption/absorption rates, (c) tensile strength and modulus of elasticity, (d) total porosity and pore size distribution, (e) sonic velocity, (f) point load index, (g) Schmidt hammer index, and (h) petrographic (thin-section) examination.

- e. Climatological and meteorological information would be collected from nearby weather stations. Wave information would be obtained from existing sources (wave gages, U.S. Coast Guard stations, harbormasters) or by wave hindcasts.

2 Quarry Field Geological Observations¹

Rock Products Consultants (1995) performed one part of the quarry investigations of this MCNP study to ascertain if relationships exist among depositional facies, rock fabric, extraction methods, and durability of stone for coastal breakwater and jetty projects from seven specific quarries. These seven quarries had previously provided stone for prototype structure sections that were selected for field prototype monitoring because these sections had experienced premature deterioration. Field geological observations had previously been performed at an eighth quarry (McCook Quarry) by U.S. Army Engineer District, Chicago, and are reported herein. The methodology employed in this part of the investigations is well established and recognized throughout North America and Europe, and has been described by Fookes and Poole (1981), Latham et al. (1990), Latham et al. (1994), Lienhart and Stransky (1981), and Lienhart (1998). This study was performed by onsite field inspections and geological observations of the quarries. Discontinuities were found to be a persistent problem in attempting to produce any large-size stone block from any of the quarries, regardless of the type of stone or the method of extraction.

Discontinuities

Discontinuities are inherent features that take many forms and result from conditions at the time of deposition, diagenesis, metamorphism, tectonism, production, and environmental exposure. There are bedding planes, joints, stylolites (with accompanying tension gashes), intrinsic fractures due to grain alignment (because of recrystallization either during diagenesis or metamorphism), faults, blasting fractures, fractures due to handling, fractures due to unloading (stress relief), and fractures due to weathering. Faults, bedding planes, joints, and stylolites are easy to identify, as are most blasting fractures. The intrinsic fractures due to grain realignment usually show up as a result of blasting or stress relief or both, and always occur as discontinuous parallel sets. According to Nichols (1980), stress relief (also known as rebound or relaxation or strain recovery) fracturing is particularly common in carbonate quarries and is not uncommon in igneous and metamorphic terrains, particularly among highly anisotropic rocks. Lienhart and Stransky (1981) found stress relief fractures still developed in cores from a dolomite quarry 90 days after the core was taken from

¹ This section is extracted essentially verbatim from Rock Products Consultants (1995).

the quarry face. Toksoz et al. (1971) found that overblasting appears to activate the development of release fractures.

Geologic terms used in the stone investigations are defined by Bates and Jackson (1987) as:

- a. *Facies*. The term facies (or depositional facies) is defined as the combination of lithologic, textural, and compositional makeup of the stone produced by the specific depositional environment in which the rock was originally deposited. Generally, one facies is represented by a working lift in most quarries; however, a single facies often contains a number of significant lateral variations that can influence stone durability. Depending on the depositional environment and geologic history, facies can pinch out laterally within a working bench. Hence, a single bench may sometimes contain more than one facies.
- b. *Diagenetic features*. Superimposed upon the facies are the diagenetic characteristics of the stone. Diagenesis occurs after the materials that make up a particular facies have been deposited and buried. Diagenesis occurs when the sediments are indurated into the rock fabric. Several episodes of diagenesis can occur after a rock has formed. Diagenetic history is dependent on depth of burial, tectonic history, history of the chemistry of fluids that pass through the formation, and history of temperature/pressure fluctuations of the rock. Primary diagenetic features include degree of dolomitization and dissolution of carbonate minerals that results in forming vugs.
- c. *Vugs*. Vugs are defined as voids in rock that may be either due to moldic (remains of fossil molds) porosity, dissolution of carbonate cements, dissolution of framework grains, or primary porosity. Vugs can vary from large (up to 30 cm (12 in.)) to pinpoint size.
- d. *Stylolites*. Stylolites are discontinuities commonly found in carbonate rocks such as a limestone, dolomite, or sandstone. These features are commonly jagged in cross section and, when viewed in plan view, appear as a surface covered with incised and protruding cones, in micro- and well-developed dimensions (generally less than 2.5 cm (1 in.) diam with up to 7.6 cm (3 in.) of relief). Stylolites form in carbonate rocks due to pressure dissolution of the carbonate grains. Stylolites generally have insoluble residues coating the discontinuity. Large amplitude (2.5 to 7.6 cm (1 to 3 in.)) from top of cone to trough) stylolites are common to the Salem formation and Silurian dolomite. Incipient stylolites are stylolites that have just begun to form, as evidenced by the presence of insoluble residues, but do not have a large amplitude. Some incipient stylolites appear as an undulating plane.
- e. *Favosites*. Favosites are specific types of coral common to the Silurian series, especially from the Cedarville, MI, and the Valders, WI, quarries. They are roughly spherical or oblate in three dimensions, 10 to 30 cm (4 to 12 in.) in size, and are found either as widely scattered (i.e., not many in one stone) or in concentrations separated by at least 30 cm (1 ft) (i.e., many in one stone). Favosites were preferentially dissolved during

diagenesis in many stones, with most of the organism gone and a large vug remaining.

- f. Depositional surface.* Depositional surfaces are thin breaks in lithology that may be overlaid and underlaid by identical rock. Depositional surfaces can be tight in a fresh rock but, with weathering, open up to reveal themselves. Depositional surfaces are identified by the presence of characteristic carbonate mud or clay which is very different than its host rock, and by the presence of ripple marks, flute casts, desiccation cracks, or planosites. These are commonly found in the Columbus formation and occasionally in the Silurian series.
- g. Planosites.* Planosites are horizontal burrows approximately 1.3 cm (0.5 in.) in diameter, common in marine bottom sediments and in the Columbus formation.
- h. Brachiopod beds.* Brachiopods are bivalve marine organisms. Large concentrations of brachiopod shells are indicative of a shallow marine environment. Brachiopod beds form on the marine bottom and in large concentrations, as observed in the Columbus formation, can form a continuous thin discontinuity within an otherwise competent stone. The shells generally settle on the bottom with the concave side facing up.

Reed Quarry

Reed Quarry (Figures 6 and 7) is located slightly northwest of Bloomington, IN (Figure 8), and excavates limestone from Mississippian age Salem formation.

General geology

Salem formation limestone is primarily mined for architectural purposes and is relatively lithologically homogeneous, as evidenced by the small variation in lithology and physical properties throughout the area. These rocks evolved during the Paleozoic on the eastern edge of the Illinois Basin, just west of the Cincinnati Arch (Collinson et al. 1988). Previous studies identified different lagoonal facies (e.g., restrictive/open lagoonal facies, sand flat facies, and shoal facies) within a marine platform environment (Swann 1963).

Method of extraction

Reed Quarry is one of the last wire cut or cable saw quarry operations left in the Indiana limestone region. Most of the other operations have gone to a chain saw device. Production at Reed Quarry involves wire sawing four sides of each block and then line drilling and wedging out each block. Production averages about 8 blocks per day. Each block is about 2.7 m (9 ft) high, 1.2 m (4 ft) wide, and 2.1 m (7 ft) long. At a specific gravity of 2.48, this amounts to 17,700 kg (19.5 tons) per block, and a production rate of approximately 141,500 kg (156 tons) per day. The stone is only produced during nonfreezing months.

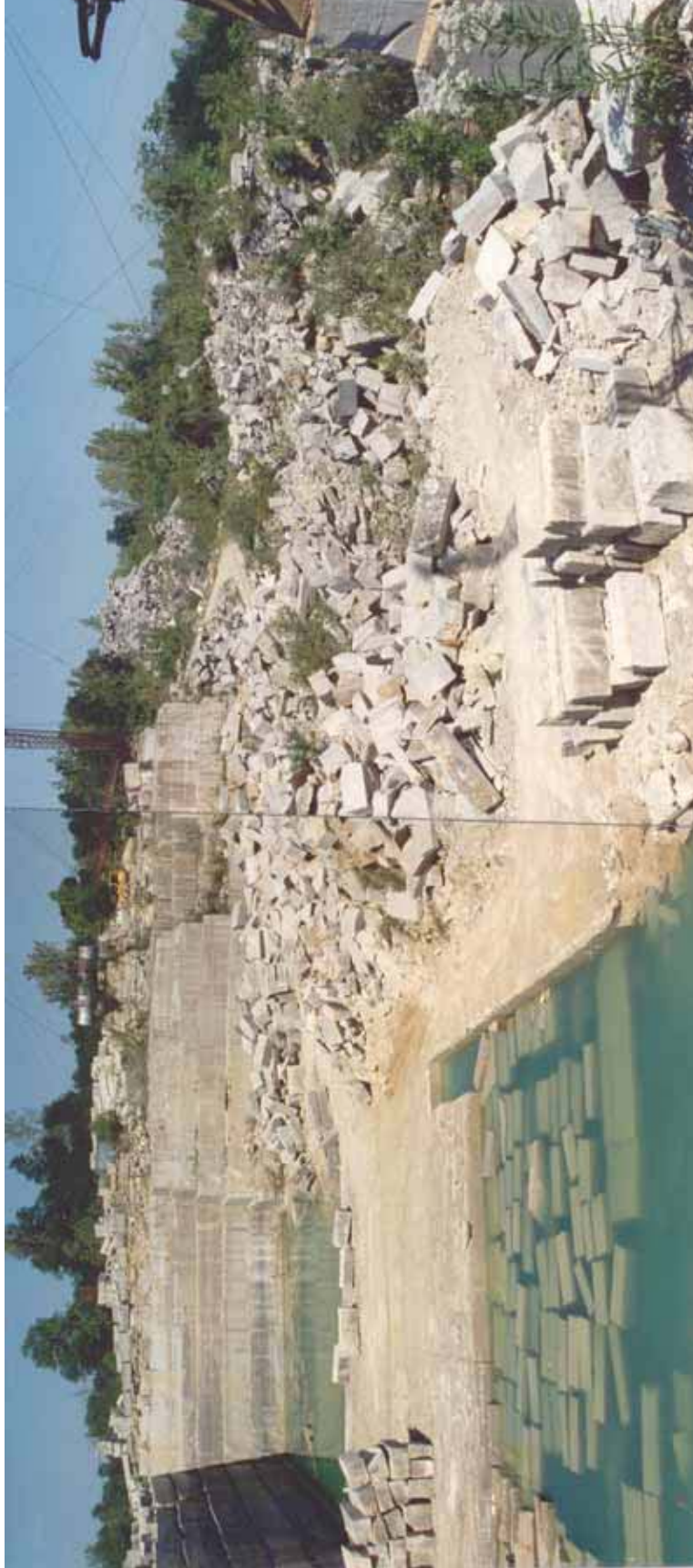


Figure 6. Reed Quarry, Bloomington, IN, general view showing amount of rejected architectural stone available for use as armor stone (after Rock Products Consultants 1995)



Figure 7. Reed Quarry, Bloomington, IN, overview of operation of new quarry and wire-saw operation (after Rock Products Consultants 1995)

The stone is handled with stone tongs and a crane since it is very soft rock which must be handled carefully to prevent breakage. A clamshell bucket (with either two or four leaves) will destroy or permanently damage stone cut from the soft Salem limestone. All quarried stone is set aside and cured for a minimum period of 60 days. Stone that is unevenly colored cannot be used for architectural purposes and is cast aside in muck piles. The majority of stone in the muck piles has been cured for more than 2 years. Stone from the muck piles is available for use as armor stone. Transportation is by truck only.



Figure 8. Location map, Reed Quarry, Bloomington, IN

Stratigraphic section

The Salem formation limestone is a bryozoan and crinoid-rich oolitic foraminiferal limestone indicative of a shallow marine environment. The dip of cross bedding is toward the northwest. The stratigraphic section is broken into 13 units (Figure 9). This figure shows the entire face with the various lithologic units delineated. Unit 13 and the top portion of Unit 12 are representative of a restrictive lagoonal facies that thickens toward the south. The bottom portion of Unit 12 is representative of an open lagoonal facies and also thickens toward the south. Units 11, 10, and 9 represent a sand flat facies that again thickens toward the south. Several large solution fissures (Figure 10) striking N 80 deg W and dipping 86 deg S were noted in the face of the quarry. These solution fissures seem to follow the more soluble, permeable coarse-grained fossil layers (Units 10, 7 and portions of Units 13, 12 and 11). Hence, the principal regressive facies are (from top to bottom) (a) restricted lagoonal facies, (b) open lagoonal facies, (c) tabular cross-bedded intertidal sand flat facies, (d) massive to trough cross-bedded ebb flow delta facies, and (e) bioturbated distal subtidal facies.

Lithologic description

The Salem formation limestone (exclusive of the restricted lagoonal facies waste rock) varies from a very coarse-grained bioclastic trough tabular cross-bedded grainstone to medium-grained massive bioclastic oolitic grainstone over a 14-m- (45-ft-) thickness. Occasional localized channels, bioturbation, and stylolites are also present. Stylolites are loosely confined to beds just below cross-bedded units, and in the lagoonal facies.

The west face of the quarry consists of 4.9 m (16 ft) of overburden of which 3.7 m (12 ft) are St. Louis Limestone, and the top 1.2 m (4 ft) of the Salem formation are stripped. The working face consists of the following limestone rock units:

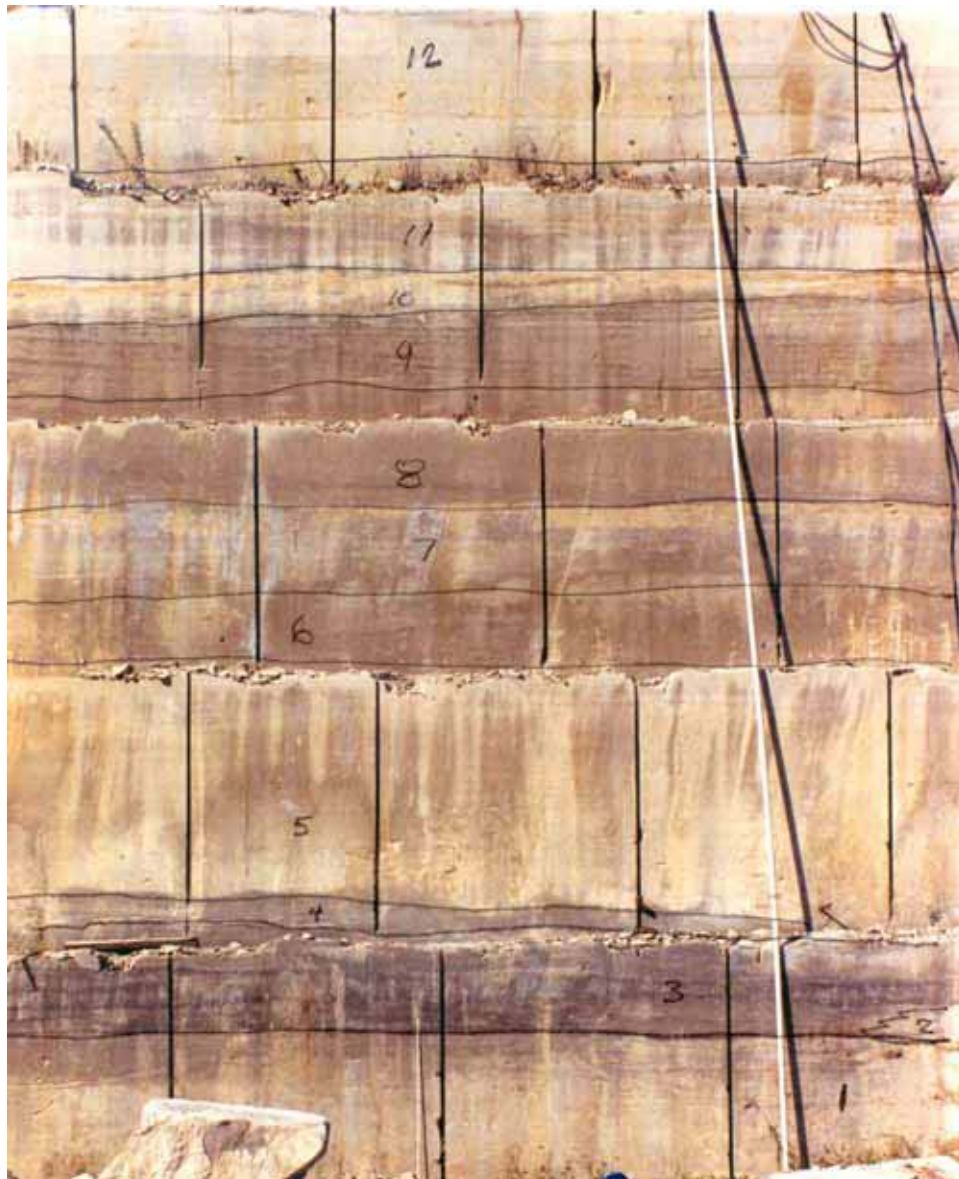


Figure 9. Reed Quarry, Bloomington, IN, west face (after Rock Products Consultants 1995)

- a. Unit 13: Wackestone--micritic, medium-to-coarse-grained fossil debris, calcite-filled vertical seams ending at base; lower portion shows solution activity; 0.4 m (1.4 ft) thick.
- b. Unit 12: Grainstone--medium-to-coarse-grained fossil debris, pale yellow brown; contains three stylolites (one about 0.6 m (2 ft) from the top, one about 0.6 m (2 ft) from the bottom, and one about 0.3 m (1 ft) from the bottom); 1.9 m (6.1 ft) thick.



Figure 10. Reed Quarry, Bloomington, IN, exploitation of coarse fossiliferous zones by solution (after Rock Products Consultants 1995)

- c.* Unit 11: Grainstone--medium-grained, well-sorted fossil debris, pale yellowish brown; some cross-bedding evident; bottom portion becoming very coarse-grained with large stylolite at base; 0.5 m (1.7 ft) thick.
- d.* Unit 10: Grainstone--very-coarse-grained fossil debris, pale yellowish brown; some slight cross-bedding; definite contact with Unit 11; 0.3 m (0.9 ft) thick.
- e.* Unit 9: Grainstone--medium-grained fossil debris, very pale yellowish brown; cross-bedded but with horizontal planar cut-off laminations; stylolite about 0.8 m (2.6 ft) from bottom; 2.1 m (7.0 ft) thick.
- f.* Unit 8: Grainstone--medium-to-very-coarse-grained fossil debris and contains numerous foraminifers; cross-beds lined with very coarse fossil fragments; definite contact with Unit 7; 1.3 m (4.4 ft) thick.
- g.* Unit 7: Grainstone--very-coarse-grained fossil debris, pale gray brown to pale yellow brown; contains whole and large fragments of corals, gastropods, brachiopods, and crinoid calyxes. A channel deposit pinches in and out along the center portion of this unit with the channel deposit being finer-grained and stylolites forming the upper and lower limits. This unit is 0.8 m (2.7 ft) thick.

- h.* Unit 6: Grainstone--pale yellowish brown, coarse-grained fossil debris plus forams; cross-bedded; 1.1 m (3.5 ft) thick.
- i.* Unit 5: Grainstone--medium-to-very-coarse-grained fossil debris and contains some foraminifers; very-coarse-grained, fossiliferous zone about 0.6 m (2 ft) from the bottom of this unit; 2.8 m (9.1 ft) thick.
- j.* Unit 4: Grainstone--medium-grained fossil debris, light yellowish brown; 0.3 m (1 ft) thick.
- k.* Unit 3: Grainstone to Micrite--medium yellowish brown; consists of alternating fossil debris and organic-rich zones; fossil debris zones are coarse-grained but grade into extensively bioturbated, black, wavy, lace-like, fine-grained organic-rich zones where fossil debris is absent; 1.0 m (3.4 ft) thick.
- l.* Unit 2: Grainstone--very-coarse-grained fossil debris, medium yellow brown; pinches out laterally to merge with Unit 3; 0.3 m (1.0 ft) maximum thickness.
- m.* Unit 1: Grainstone--medium-grained fossil debris, pale yellowish brown; 1.2 m (4.0 ft) thick.

All rock units dip slightly to the northwest, but can be traced from one side of the quarry to another with just slight vertical adjustments. All of these units can be traced to other quarries on this property, but again with some vertical adjustments in alignment. Almost all cross-bedding also dips to the northwest with the exceptions being limited to a few thin channel-type beds where the dip of the cross-beds is toward the south.

Valders Quarry

Valders Quarry (Figure 11) is located off U.S. Highway 151 just north of the town of Valders, WI (Figure 12), about 16 km (10 miles) west of a stone dock in Manitowoc, WI. Transportation from the stone dock is by barge.

General geology

The Niagaran series dolomite quarried near Valders, WI, is one of numerous reef complexes that formed around the fringes of the Michigan Basin and northeast of the Wisconsin arch. Several lithological units are identified, including dolomitic mudstone interpreted as a supratidal, backreef environment and reef dolomite. The dolomitic mudstone intertongues with reef-like dolomite. Reef accumulations are more discontinuous, allocthonous, and thinner, as compared to the large pinnacle Niagaran reef structures found in Illinois. Early descriptions of the lithologies and paleoenvironments can be found in Shrock (1939) and Lowenstam (1950).



Figure 11. Valders Quarry, Valders, WI, overall view showing lower bench, middle bench (being drilled), and upper bench with glacial till drift overburden (after Rock Products Consultants 1995)



Figure 12. Location map, Valders Quarry, Valders, WI

Method of extraction

Production is through a single line of 7.6-cm- (3-in.-) diam drill holes with a burden of 0.9 to 1.2 m (3 to 4 ft) and a spacing of 0.9 m (3 ft), from a maximum bench height of approximately 6.4 m (21 ft). The blast program is designed to parallel the principal joint orientation. This blast pattern is specifically designed to minimize overbreak and maximize the production of large armor stone and architectural stone. Stone with excessive vugs or discoloration is considered unsuitable for architectural stone and is readily available for armor stone. Since the architectural stone is taken from the lowermost bench, there is a significant amount of overburden that is wasted. Figure 13 shows waste rock resulting from explosive fracturing.



Figure 13. Valders Quarry, Valders, WI, splay of spent explosive blown out along joint (after Rock Products Consultants 1995)

Stratigraphic section

There are approximately 18 m (60 ft) of glacial drift resting on the top bench. The present floor of the quarry is the top of an aborted reef. This unit is occasionally seen as a thin reef rock layer adhering to the bottom of the dolomitic mudstone on the breakwaters. The lower bench is a dolomitic mudstone representing the regression of the sea and resulting in a supratidal, backreef environment, and the common presence of bird's-eye structures. The lower bench is a dense,

homogeneous unit of fairly consistent texture and color and is the primary source for Valder's architectural stone products. The upper bench (Figure 14) contains mega-ripples near the base. The middle bench is a reef-like dolomite that may represent a generation-4 reef development as defined by Droste and Shaver (1977). This correlates well with other generation-4 buildups in other parts of the Michigan Basin. The lower bench (Figure 15) indicates discontinuous horizontal unloading fractures.

In different parts of the quarry, additional beds of dolomitic mudstone appear intertonguing with the reef like dolomite. The middle bench is vuggy, contains depositional hiatal surfaces, allocthonous carbonate clasts and discontinuous argillaceous seams. The top bench is another dolomitic mudstone indicating another regression of the sea. Shrock (1939) believed a generation-3 reef may have existed with continuous buildup at this location, and that what is visible today is merely the backreef facies intertonguing with the edge of the organic reef facies and the rest of the reef being eroded away. The top bench contains numerous scattered large Favosites casts with secondary euhedral dolomite mineralization linings, all in a fine-grained dolomitic matrix. The extensive remineralization and abundant fossil casts result in a friable and porous rock from the top bench. Hence, the principal facies are (from top to bottom) (a) restricted lagoon argillaceous Favosites facies, (b) interreef, patch reef, reef talus wackestone facies, and (c) supratidal mudflat, backreef bird's eye mudstone facies.



Figure 14. Valders Quarry, Valders, WI, upper bench with mega-ripples near base (after Rock Products Consultants 1995)



Figure 15. Valders Quarry, Valders, WI, lower bench showing discontinuous horizontal unloading features (after Rock Products Consultants 1995)

Lithologic description

The dolomitic mudstone is highly variable. It varies from dense massive micrite bird's eye mudstone in the lower bench, to vuggy brecciated reef talus packstone/boundstone in the middle bench, to thin bedded very vuggy moderately argillaceous mudstone/wackestone in the upper bench.

The lower bench of the west wall is a source of architectural stone from 3.0 m (10 ft) to 4.6 m (15 ft) above the floor. It consists of very pale yellowish gray, very finely crystalline dolomite. Dense and vug-free, this stone is massive and appears to darken in color toward the east, becoming light brown to light reddish brown. Within the massive units there appears to be discontinuous bedding planes. These are actually unloading fractures due to rebound from both the quarrying operation and due to past continental glacial activity as evidenced by glacial polishing of the top of the upper bench. Joints are evident at (a) N 14 deg W (vertical), (b) N 80 deg E (vertical), and (c) N 25 deg W (N 85.5 deg E). Because of the practice of blasting along existing joints (an excellent practice), splays of spent explosive are evident on the joint surfaces. The top of lower bench is the floor of the middle bench.

From 4.5 m (14.9 ft) to 5.9 m (19.4 ft) above the floor of the middle bench on the east side of the north wall, there appears to be an inter-reef on the west side, grading into reef talus on the east with numerous 2.5 cm (1 in.) to 7.6 cm (3 in.) green clay seams in a braided pattern around fist- to head-size reef-rock particles. These particles are often coated with drusy pyrite.

From 2.5 m (8.2 ft) to 5.9 m (19.4 ft) above the floor of the middle bench, there exists a light gray reef flank deposit, completely dolomitized, fine-grained and vuggy. The vugs range up to fist-size and are lined with drusy quartz or pyrite, or both. This region contains numerous paper-thin, discontinuous, lace-like argillaceous seams with a lateral extent not exceeding 0.6 to 0.9 m (2 to 3 ft). At 2.5 m (8.2 ft) above floor of middle bench is a weathered bedding surface (depositional/erosional hiatus).

From the floor to 2.5 m (8.2 ft) above the floor of the middle bench the rock is the same as the rock immediately above but with fewer and smaller vugs. The top of the middle bench is the floor of the upper bench.

At the upper bench of the north wall, there is an overburden of glacial drift/till of approximately 60 ft (18 m). From the top of the upper bench 3.4 m (11.2 ft) above the floor down to 1.9 m (6.2 ft) above the floor of the bench, the material is pale brownish gray, extremely fine-grained, dense dolomite. The upper part is very vuggy and weathered with paper-thin argillaceous seams that appear tight while the lower part is vug-free and massive. The bottom 0.3 m (1 ft) is darker in color with a layer of 0.6 cm (0.25 in.) vugs spaced well apart at about 1.9 m (6.2 ft) above the floor.

From 1.9 m (6.2 ft) above the floor of the upper bench down to 1.5 m (4.9 ft) above the floor of the upper bench, the material is micrite grading imperceptibly into the dolomite above with no break in bedding. The Micrite is medium yellow brown, dense, and breaks with a conchoidal fracture. Clay seams of 0.6 cm (1/4 in.) are present at 1.8 m (5.8 ft) above the floor, and at the bottom of the micrite at 1.3 m (4.4 ft) above the floor.

From 1.3 m (4.4 ft) above the floor of the middle bench down to the floor, the material is pale olive gray or pale yellow brown, massive, fine-grained dolomite with a vuggy zone about 0.2 m (0.8 ft) below the top of this unit (1.1 m (3.6 ft) above floor). A mega-ripple exists at 0.5 m (1.5 ft) above the floor. Below this mega-ripple, this lithologic unit tends to fracture into thin beds.

Dempsey Quarry

Dempsey Quarry (now Michels Quarry) (Figure 16) is located about 4 km (2.5 miles) northeast of Waterloo, WI (Figure 17), northwest of the intersection of Wisconsin Highway 19 and Hubbleton Road. The quarry is 97 km (60 miles) from the stone dock in Milwaukee. Stone must be trucked from the quarry to the stone dock, where it is loaded onto Lake Michigan barges for shipping.

General geology

Waterloo formation quartzite is mined from shallow inliers of Precambrian crystalline bedrock at Dempsey Quarry near Portland, WI. This formation is believed to be equivalent to the late Early Proterozoic Baraboo quartzite (Haimson 1978). The Waterloo formation quartzite is a metaquartzite composed



Figure 16. Dempsey Quarry, Waterloo, WI, lower bench, north face, with mica schist plunging under quarry floor on left, and rockburst structure on right (after Rock Products Consultants 1995)



Figure 17. Location map, Dempsey Quarry, Waterloo, WI

of well-sorted coarse sand with low angle tabular cross-bedding, to poorly sorted gravel breccia. The gravels are well rounded and predominantly composed of siliclastic materials. The quartz mica assemblage supports a greenschist facies metamorphism. The age of the rock is estimated to be 1.63 billion years (Smith 1978). The unit was mildly folded along with Precambrian basement rocks during the early Paleozoic.

Method of extraction

The Dempsey Quarry is an open-pit operation working out of two benches. The upper bench is 3 to 6 m (10 to 20 ft) in height and the lower bench is 4.5 to 9.1 m (15 to 30 ft) in height. Because the stone is a quartzite with dipping beds, the quarry must make an extra effort to produce a flat floor. Production costs are much higher than for dolomite or limestone. Drills, loaders, tires, crushers, etc. wear out at a much faster rate. Due to the lack of parting planes and dominance of separation along joint surfaces, a horizontal row of holes are necessary to maintain a level floor in the quarry.

Stone is blasted using a single row of 7.0-cm- (2.75-in.-) diam holes drilled to 7.6-m (25-ft) depth drilled horizontally from the quarry floor. After the blast, the rock tumbles into the quarry separating along joint surfaces and micaceous seams. Using this method, some blocks may weigh as much as 36,285 kg (40 tons) after the blast. Large stones are further broken down by diamond drilling 5.0-cm- (2-in.-) diam holes and splitting with hydraulic splitters. Finished stone is separated and stockpiled using stone tongs with special carbide teeth to facilitate gripping this very hard rock. Stockpiled stone is cured for 30 to 90 days.

Stratigraphic section

The Waterloo quartzite was once a sandstone/sandstone-conglomerate formation but metamorphism has fused the individual sand grains and pebbles into a large quartzitic dense mass. Relict features and structures such as pebble gravel beds, ripples, and cross-bedding may still be seen within this quartzite. Two basalt dikes metamorphosed to amphibolite are running north/south through the quarry. A thick layer of muscovite quartz schist appears on the north side of the quarry, plunging southward beneath the floor of the quarry. Relict bedding dips toward the southeast at approximately 20 to 25 deg.

The lower bench (Figure 18) consists of a basal metaconglomerate overlaid by 1.2 m (4 ft) of metaquartzite. Above this is a coarse-grained quartzite with an overlying sharp contact with thinly bedded quartzite. A micaceous seam runs along the sharp contact.

The middle units grade from a coarse-grained quartzite up to quartzite that in turn is overlaid by a cross-bedded quartzite. The overall sequence is grading from coarse material to finer material at the top, with depositional breaks highlighted by micaceous seams. The well rounded moderately sorted gravel sized clasts in the lower unit and finer cross bedded unit on top indicate the material could be fluvial deltaic; however, an alternative depositional environment could be a glacial outwash sequence from a retreating glacier.

The upper bench (Figure 19) contains alternating beds of pebble gravel layers and coarse quartzite layers with two ripple marked discontinuities. There is also a bed of coarse-grained quartzite with pockets of gravel-sized material. Again, micaceous seams are found at depositional breaks in the sequence. This fabric is indicative of cyclic depositional energy levels, which also could be due to fluvial deltaic processes or alternatively glacial outwash plain from glacial advance and retreat.

The beds on the north end of the quarry are much more poorly sorted, which may support a glacial depositional environment due to their similarity to till. All of these remnant-bedding features are in the upper greenschist metamorphic facies. The principal depositional facies are all highly fused (with the exception of Schist), and include (a) banded gravel/pebble/coarse quartzite, (b) cross-bedded quartzite, (c) channel quartzite, (d) micaceous quartzite, (e) massive quartzite, (f) poorly sorted pebbly quartzite, (g) thin-seam quartzite, (h) basalt dike, and (i) Schist.



Figure 18. Dempsey Quarry, Waterloo, WI, lower bench, south face (after Rock Products Consultants 1995)



Figure 19. Dempsey Quarry, Waterloo, WI, upper bench, east face (after Rock Products Consultants 1995)

Lithologic description

The quartzite contains seams of mica (muscovite) quartz schist, and traces of hornblende, feldspar, apatite, and reportedly andalusite. Lithic fragments are pelite, quartz with varying amounts of iron, and possible jasper. Feldspars are highly altered with clay rinds, hornblends are weathered with hematite rinds.

There is little variability in the lithology of the Waterloo quartzite that would be of significance to the quality of armor stone produced from this quarry. Based on the mineral assemblage found here, this quartzite may be classified as being within the upper greenschist metamorphic facies. This is a relatively low grade of metamorphism and assumes a burial pressure of between 35,600 and 71,200 kg per sq cm (60,000 and 120,000 lb per sq in.) and exposure to temperatures of between 400 and 500 °C. Considering the extent of metamorphism, although relatively low, it is quite amazing to find relict structures within this quartzite like pebble beds, ripples and cross-bedding.

The thin clay layers that were occasionally deposited as interbeds or bedding planes have all been metamorphosed to mica schist. These layers are occasionally termed phyllites, but the grain-size of a phyllite is microscopic while for a schist, it is megascopic. At the Dempsey Quarry these interbeds are schists. These schistose layers are the main control on the size of quartzite blocks quarried from this source.

Because of the depositional/burial/metamorphic history of the Waterloo quartzite (estimated to be approximately 1.63 billion years old) numerous joint sets have developed within the stone. Haimson (1978) found 1,317 joints in 350 m (1,150 ft) of rock core drilled into the Waterloo quartzite. This amounts to one joint per 25 cm (10 in.) of core. Numerous joints were observed in the quarry face, but were not that closely spaced. Three major sets were noted: (a) N 60 °E (vertical), (b) N 75 °W (vertical), and (c) N 17 °W (65 °W). Four additional sets were noted: (a) N 22 °W (88 °W), (b) N 25 °W (82 °E), (c) N 55 °E (71 °W), and (d) N 70 °E (88 °N).

Examination of the stockpile shows that the stone being quarried is of high quality with few blocks actually containing fractures or planes of weakness. There are thin micaceous schist seams along almost every break. The micaceous seams act as glide-planes along which the stone moves out from the face during the snake-hole blasting. Almost every block on the quarry floor exhibits a thin micaceous schist seam along at least one face of the block and often along more than one face, but these seams do not affect the quality of the block. The presence of these seams merely indicates that the quarry is using the right techniques to produce fracture free blocks.

Sandusky Quarry

Sandusky Quarry (Figure 20) is located at Parkertown, OH (Figure 21), on the border of Sandusky and Seneca counties, OH, in the northeast quadrant of



Figure 20. Sandusky Quarry, Parkertown, OH, thin-bedded Delaware formation on east side of quarry (after Rock Products Consultants 1995)

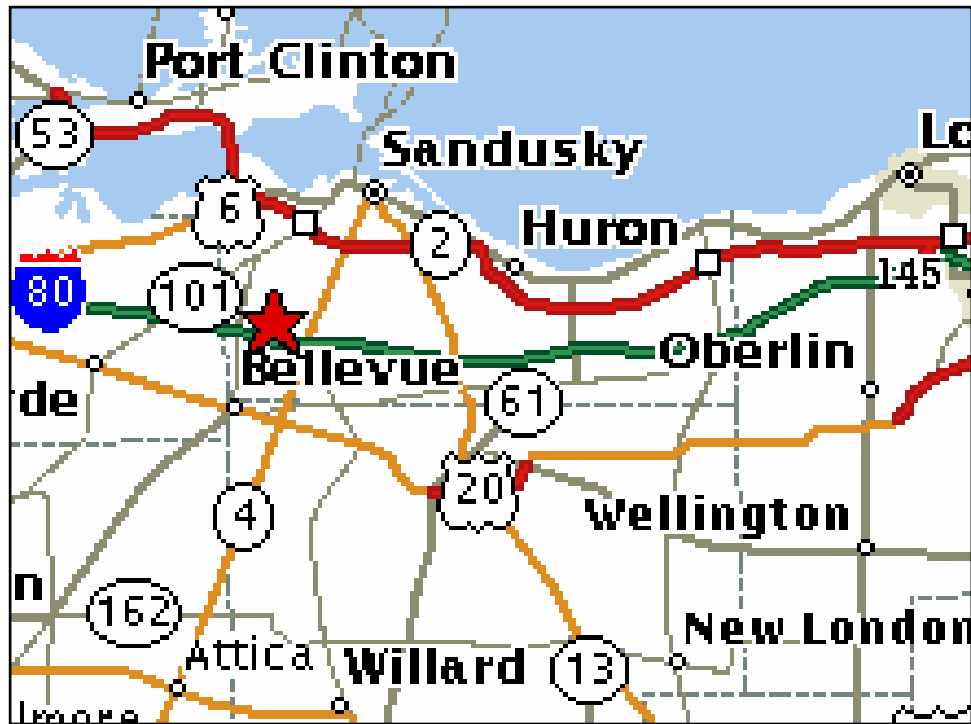


Figure 21. Location map, Sandusky Quarry, Parkertown, OH

the intersection of Billing and Strecker Roads, and on the southeast flank of the Findlay Arch. Stone is trucked approximately 16 km (10 miles) to Lake Erie, where it is transported by barge.

General geology

Sandusky Quarry is located on the southeast flanks of the Findlay Arch. The Sandusky Quarry extracts material through middle Devonian age Delaware and Columbus formations (Droste and Shaver 1977). Within the quarry are sequences of fine-grained clastics, limestones, and dolomites. The primary breakwater unit is the limestone Marblehead member of the Columbus formation. The Marblehead has been interpreted as a transgressive trend from intershoal to shoal to outershoal conditions. The overlying basal Delaware formation has been interpreted as a sudden submergence below wave base followed by continued transgression and deeper water sedimentation (Feldmann and Bjerstedt 1987).

Method of extraction

Sandusky Quarry primarily produces Columbus formation limestone aggregates with a production capacity of up to 1,800,000 kg (2,000 tons) per hour. Armor stone is currently taken from the west side top bench of the quarry. The spacing of blast holes as measured in the quarry face ranges from 2.1 to 2.7 m (7 to 9 ft), and the blast holes are 17 cm (6.75 in.) in diameter (Figure 22). The bench height is approximately 15 m (50 ft). As evidenced by the blasting fractures within the blast holes (Figure 23) and the large block of the Venice



Figure 22. Sandusky Quarry, Parkertown, OH, close-up of contact of Columbus and Delaware formations; also contact of Venice and Marblehead members of Columbus formation (after Rock Products Consultants 1995)

member, the blasting agent must be high energy leading to possible overbreakage. The quarry operator would not reveal the specifics of blasting operations, however, due to the large bench height, large diameter holes, and apparent overbreak, it would appear that aggregate production methods may be utilized. The groundwater table is thought to be 4.6 m (15 ft) below the floor of the west face.

Stratigraphic section

The glacial ground moraine at this location is thin, no more than about 4.6 m (15 ft) thick to the top of rock. The quarry has been excavated through the Middle Devonian age Delaware and Columbus formations. Because of the quarry's location relative to the Findlay arch, the bedrock dips slightly to the southeast; therefore, in the southeastern section of the quarry, the basal Plum Brook shale is exposed as well as the underlying Delaware formation. The Delaware formation is about 14.3 m (47 ft) thick at this location. In the northwest



Figure 23. Sandusky Quarry, Parkertown, OH, blasting fractures along blastholes (after Rock Products Consultants 1995)

section of the quarry, however, only the basal 7.6 m (25 ft) of the Delaware is present, the remainder being removed by glaciation. Below the Delaware is the Columbus formation. The Columbus formation is about 18.6 m (61 ft) thick at this location. All formation thicknesses are approximate as individual beds within the formations thin and thicken laterally. The floor of the present operation is founded at the top of the Lucas formation. The quarry is probably between 0.8 to 1.2 km (0.5 and 0.75 mile) across in an east-west direction, and probably exceeds that dimension in a north-south direction.

Because of extensive quarrying activity on the east side of the quarry, only the west face of the quarry was logged. The west side, however, is where all armor stone has thus far been produced and therefore, is more applicable to this study. The bedding on the east side of the quarry is much thinner but individual beds identified on the west side were traced and identified on the east.

Although the floor of the quarry was quite moist, no obvious seeps were identified in the west face of the quarry, which could lead one to identify the probable water table. Further observations in other parts of the quarry lead to the conclusion that the water table was perhaps 4.6 to 6.1 m (15 to 20 ft) below the floor of the west face. Two joint sets were observed. One joint set strikes N-S with a dip of 80.5 °E. The other joint set is vertical with a strike of N 60 °E. The N-S joint system coincides with the Maximum Principal Stress (i.e., the horizontal compressional tectonic stress) an in situ stress measurement reported by Sbar and Sykes (1973) for north-central Ohio (450 kg per sq cm (6,383 lb per sq in.) striking N 90 deg W). This high horizontal in situ stress, when combined with the effects of unloading due to both glaciation and quarrying, often leads to

rockbursts in the quarry floor. Such an event did occur at this quarry as confirmed by Marcus (1994).

The first bench of the west face consists of approximately 4.6 m (15 ft) of the Delaware formation that is extremely thin-bedded due to glacial unloading (Figure 20). This material is sold as flagstone.

Armor stone from this quarry was reportedly produced from the second bench of the west face. The second bench consists of about 3.7 m (12 ft) of basal Delaware formation over about 10.9 m (36 ft) of Columbus formation (about 5.2 m (17 ft) of Venice member over about 5.8 m (19 ft) of Marblehead member) (Figure 22). Beginning at the floor of the second bench, the Marblehead member consists of 1.6 m (5.1 ft) of cherty mudstone and wackestone overlaid by 3 cm (0.1 ft) of black shale, 2.8 m (9.3 ft) of fossiliferous, bioturbated packstone and grainstone, 1.3 m (4.3 ft) of moderately fossiliferous packstone and grainstone, and 12 cm (0.4 ft) of nodular limestone (interpreted as above wave base). This entire portion of the Marblehead member is interpreted as reflecting a transgressive trend from intershoal to shoal to outershoal conditions. The black shale may represent a brief period of regression.

The Venice member consists of a 5 cm (0.3 ft) of bioclastic grainstone overlaid by 1.6 m (5.4 ft) of fossiliferous crinoidal wackestone and mudstone, 1.9 m (6.15 ft) of moderately argillaceous crinoidal wackestone, and 1.6 m (5.1 ft) of fossiliferous dolomitic wackestone and packstone. All of these units are separated by and contain thin carbonaceous-pyritic seams and disseminated pyrite. The Venice member is interpreted as representative of a low-energy environment below wave base. The combination of black carbonaceous seams and pyrite suggest euxinic depositional conditions, but the top of the Venice reflects a return to wave-base conditions with an erosional hiatus.

The basal Delaware formation constituting the top 3.6 m (12 ft) of the second bench consists of 1.8 m (5.9 ft) of argillaceous crinoidal wackestone and mudstone with a thin black shale layer about 5 to 8 cm (2 to 3 in.) above the base. This thin black shale unit has been identified as Tioga Bentonite. Overlying the 1.8 m (5.9 ft) unit is 1.9 m (6.0 ft) of cherty, argillaceous lime mudstone. The top of this unit forms the top of the second bench. The basal Delaware formation reflects a sudden submergence below wave-base followed by continued transgression and deeper water sedimentation.

Blasting data were not made available for this study; however, the spacing of blastholes as measured in the quarry face ranges from 2.1 to 2.7 m (7 to 9 ft), and the blastholes are 17 cm (6.75 in.) in diameter (Figure 23). As evidenced by the blasting fractures within the blastholes (Figure 23), the blasting agent must be high energy.

Lithologic description

The lower bench of the west face consists of 11 m (36 ft) (11 units, six of which are primary) of Columbus formation overlaid by 3.7 m (12 ft) (2 units) of Delaware formation. The Columbus formation consists of (from bottom to top):

- a. *Unit 11.* 1.6-m- (5.1-ft-) thick nodular cherty mudstone-to-wackestone limestone starting at the bottom of the Columbus formation, overlaid by a thin carbonaceous shale; pale yellowish brown, massive, very fine-grained; contains scattered 2.5 to 10.2 cm (1 to 4 in.) white, porous, chalky chert nodules within the lower 0.5 m (1.8 ft) of the unit.
- b. *Unit 10.* 3-cm- (0.1-ft-) thick black carbonaceous shale.
- c. *Unit 9.* 2.8-m- (9.3-ft-) thick fossiliferous, bioturbated packstone, grainstone, and mudstone limestone with medium massive bedded units 0.6 to 0.9 m (2 to 3 ft) thick, interbedded with thin layers of brachiopod beds; pale yellowish brown with occasional cream mottling, massive bedded but with zones of bioturbation, bioclastics, and thin layers of whole brachiopods and corals; bioturbated at top with tubes filled with light gray micrite; wave-base disturbed zones at 1.3 m (4.4 ft) and 2.5 m (8.3 ft) from top; bioclastic zones at 24 cm (0.8 ft); three zones between 0.6 and 1.0 m (2.1 and 3.3 ft); and another zone at 1.8 m (5.8 ft) from top.
- d. *Unit 8.* 1.2-m- (4-ft-) thick moderately fossiliferous packstone and grainstone dolomitic limestone overlaid by a 12-cm- (0.4-ft-) thick nodular limestone (top of Marblehead member); pale yellowish brown, medium-to-coarse-grained; contains scattered, very thin layers of whole fossils and a 24 cm (0.8-ft) bioclastic zone at top; bedding planes are not present.
- e. *Unit 7.* 12-cm- (0.4-ft-) thick nodular limestone.
- f. *Unit 6.* 9-cm- (0.3-ft-) thick bioclastic grainstone.
- g. *Unit 5.* 1.6-m- (5.4-ft-) thick fossiliferous crinoidal wackestone and mudstone limestone which varies from nodular to dense and bioclastic, with very thin shaley seams; dark grey at top becoming light brown, fine and medium grained; top 6 cm (0.2 ft) is dark gray carbonaceous, very dense and hard, and bioclastic; below this bed is a 30-cm- (1.0-ft-) thick nodular limestone, indicative of a wave-base depositional environment; 1.2 m (4 ft) from top of unit is another 6-cm- (0.2-ft-) thick bioclastic zone with several paper-thin, wavy, shaley seams.
- h. *Unit 4.* 1.9-m- (6.1-ft-) thick moderately argillaceous crinoidal dolomitic wackestone, dolomitic; medium gray to grayish tan, becoming more tan toward base; fine-to-medium grained; top 12 cm (0.4 ft) somewhat laminated with a few paper-thin carbonaceous seams; beds 0.4- to 0.9-m (1.4- to 3.0-ft) thick with carbonaceous/pyretic seams separating each bed (euxinic depositional conditions).
- i. *Unit 3.* 1.6-m- (5.1-ft-) thick dolomitic fossiliferous wackestone and packstone, dolomitic, fossiliferous to very fossiliferous, with predominantly brachiopods and carbonaceous/pyritic seams separating bed 0.3- to 0.6-m (1- to 2-ft) thick, indicating euxinic conditions at the time of deposition; medium gray to grayish tan, coarse-grained; top of Columbus formation.

The Delaware formation consists of two units (from bottom to top of bench):

- a. *Unit 2.* 1.8-m- (5.9-ft-) thick dolomitic argillaceous crinoidal wackestone and mudstone with 0.6-m- (2-ft-) thick beds starting at the bottom of the Delaware formation, separated by carbonaceous seams and several thin shaley bentonitic seams at bottom of unit (Tioga Bentonite).
- b. *Unit 1.* 1.8-m- (6-ft-) thick dolomitic cherty argillaceous mudstone limestone, dolomitic, with prominent 1.3-cm- (0.5-in.-) thick black shale seams, and scattered allocthonous packstone zones throughout the unit; fossil hash zones throughout the unit; medium gray, fine to medium grained; beds vary from a few inches to 0.6 m (2 ft); top of Delaware formation and top of bench.

The entire Marblehead member is interpreted as reflecting a transgressive trend from intershoal-to-shoal-to-outershoal conditions. The Venice member is offshore shallow marine. Hence, the principle facies are Marblehead member (a) intershoal (Unit 10), (b) shoal (Unit 9), and (c) outershoal (Unit 8); and Venice member shallow marine (below wave base).

Facies a is a cherty mudstone and wackestone, massive, very-fine-grained with scattered 2.5 to 10.2 cm (1 to 4 in.) white, porous, chalky chert nodules within the lower 0.5 m (1.8 ft) of the unit. Facies b is a fossiliferous, bioturbated packstone, grainstone, and mudstone, massive bedded but with zones of bioturbation, bioclastics and thin layers of whole brachiopods and corals. Bioturbated at top with tubes filled with light gray micrite. Wave base disturbed zones, and bioclastic zones at intervals. Facies c is moderately fossiliferous packstone and grainstone, dolomitic, medium-to-coarse-grained, with scattered very thin layers of whole fossils and a bioclastic zone at top, overlaid by nodular limestone. Facies d is dolomitic moderately argillaceous crinoidal wackestone, fine to medium-grained, top laminated with very thin carbonaceous seams, bedding 0.5- to 0.9-m (1.5- to 3-ft) thick with carbonaceous/pyritic seams.

Marblehead Quarry

Marblehead Quarry (Figure 24) is located at Marblehead, OH (Figure 25), on the eastern end of Marblehead Peninsula in northern Ohio, near Sandusky.

General geology

Coastal structure armor stone from Marblehead Quarry comes from medium bedded dolomitic limestone in the basal Columbus formation of Middle Devonian age. Units of fossiliferous packstone/mudstone, a dark brown bioclastic zone, and a dolomitic burrowed limestone have been interpreted as indicative of near normal marine lagoonal depositional conditions (Lilienthal 1974; 1978; Feldmann and Bjerstedt 1987).



Figure 24. Marblehead Quarry, Marblehead, OH, conjugate system of parallel release fractures opened in a nose or promontory of lower bench as a result of quarrying practices. By allowing nose of lower bench to exist, confining stress was reduced on three sides of rock mass. Over-blasting helped to activate development of these release fractures (after Rock Products Consultants 1995)

Method of extraction

Excavation is performed by open-pit quarry utilizing three benches. Only the middle bench is currently used for breakwater stone. The bench height of the middle bench is approximately 3 m (10 ft). Blast holes are 7 cm (2.75 in.) in diameter, and spacing between blast holes is 0.9 m (3 ft). Powder factors are not available.

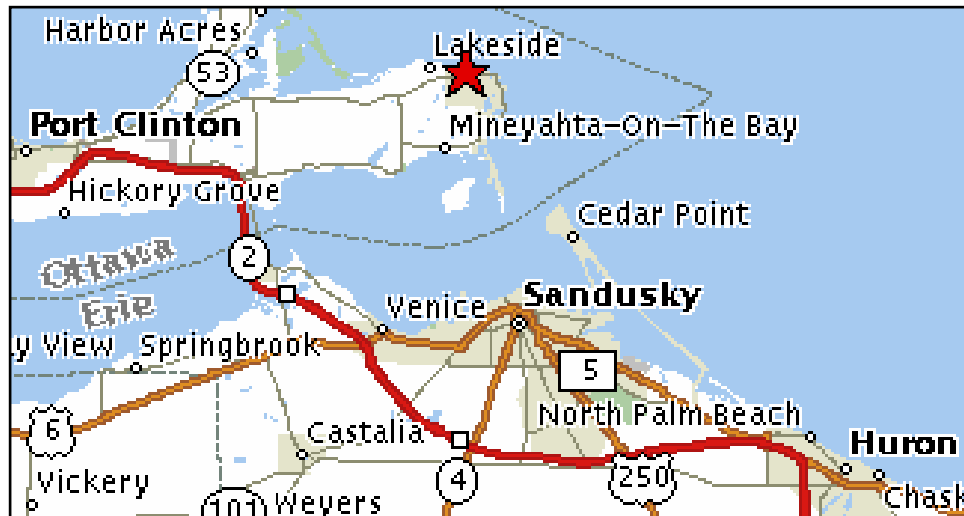


Figure 25. Location map, Marblehead Quarry, Marblehead, OH

Stratigraphic section

Only the middle bench was investigated (Figure 26). The floor of this bench is the contact between the Lucas and Columbus formations. The bench consists of only two units. The material is fine to medium-grained fossiliferous, bioturbated dolomitic mudstone, and contains numerous thin fossiliferous zones alternating with thicker burrowed mud zones. There are occasional thin, black, wavy shaley seams. Prominent shaley carbonaceous marker bed separates a lower lithologic unit.

Lithologic description

The lower lithologic unit is a 0.9-m- (2.9-ft-) thick dolomitic fossiliferous packstone/mudstone. It is pale yellowish brown, fine to medium-grained, very porous (up to 0.3 cm (0.1 in.) in diameter) with widely scattered vugs averaging about 0.3 cm (1 in.) in diameter, and is massive bedded. The lower unit is the base of the Marblehead member of the Columbus formation. A thin (less than 3-cm (0.1-ft) thick), persistent, dark brown bioclastic zone delineates this unit from the unit above.

The upper lithologic unit is a 2.0-m- (6.5-ft-) thick dolomitic burrowed lime mudstone. This unit exhibits extensive bioturbation. Both the lower and upper units are interpreted as lagoonal depositional environment. Hence, the primary facies are (a) massive dolomitic mudstone, (b) bioturbated dolomitic mudstone, and (c) fossiliferous dolomitic mudstone. This unit is pale yellow brown with medium yellowish brown mottling, fine to medium-grained, fossiliferous, massively bedded, but with intensively bioturbated zones. The top surface of the bench is a bioturbated, burrowed shoresurface, with branching corals attached. This unit contains numerous thin (3 to 6 cm (0.1 to 0.2 ft thick)), fossiliferous zones alternating with thicker (12 to 20 cm (0.4 to 0.65 ft thick)) burrowed mud zone. A prominent 4.6-cm- (0.15-ft-) thick fossiliferous zone with thin, black,



Figure 26. Marblehead Quarry, Marblehead, OH, 2.9 m (9.6-ft) face on east side of quarry from which armor stone was produced, at or near base of Columbus formation (after Rock Products Consultants 1995)

wavy shaley seams is located at 1.2 m (3.85 ft) from the top. Another prominent marker bed is present at the base of the unit. This marker bed is sometimes distinctively shaley and sometimes just carbonaceous. This marker bed was identified by Hill and Lienhart (1975),¹ and may be traced to other quarries throughout the Sandusky area. Figure 27 shows a sawn block from Marblehead Quarry.

Johnson Quarry

Johnson Quarry (Figure 28) is located about one-half mile east of Ohio Highway 511, about one-half mile north of Kipton, OH (Figure 29).

General geology

Johnson Quarry excavates rock from the Berea formation sandstone. This rock unit is well documented in the literature as a homogeneous material well suited for experimental rock deformation studies. The Berea sandstone was deposited in a large deltaic complex that was expanding in a southwest direction as part of the Ontario paleofluvial system during Upper Devonian time. Sediment geometry includes large, linear sand bodies indicative of a constructive bird's foot-type delta similar to the Mississippi delta (Harrell et al. 1991).

¹ Hill, M. L., and Lienhart, D. A. (1975). "Quarry investigation report and stratigraphic correlation chart for Kellstone Quarry, Marblehead Quarry, and Johnson Quarry," unpublished report.



Figure 27. Marblehead Quarry, Marblehead, OH, sawn block with brown marker bed at 0.8 m (2.7 ft) from left side (after Rock Products Consultants 1995)



Figure 28. Johnson Quarry, Kipton, OH, area where an attempt was made to produce sandstone blocks by blasting (after Rock Products Consultants 1995)

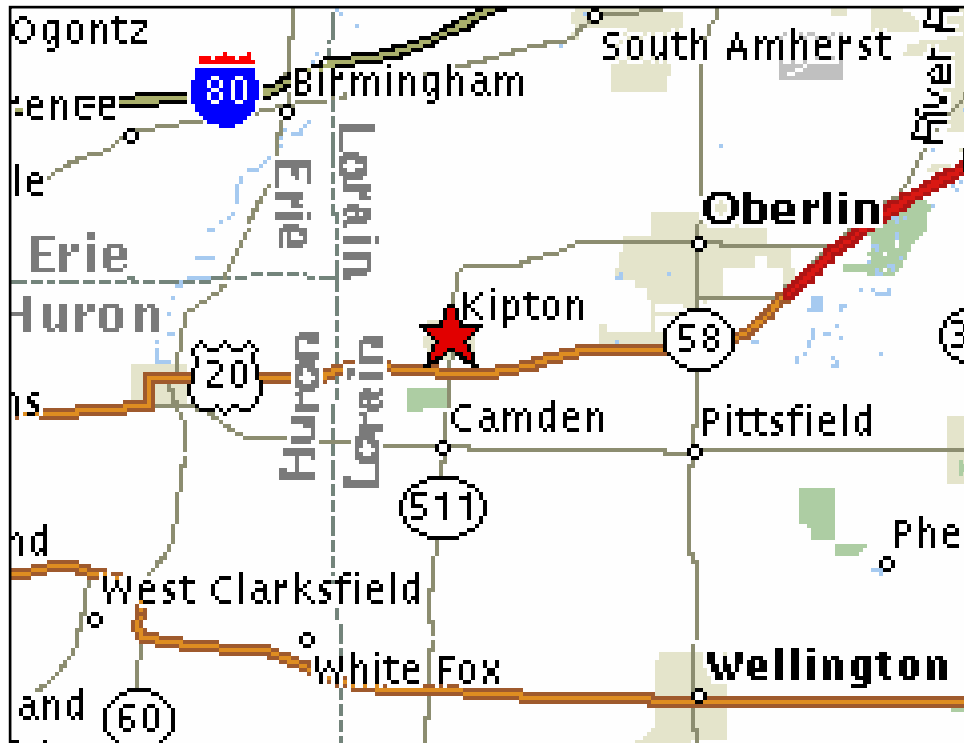


Figure 29. Location map, Johnson Quarry, Kipton, OH

It is reported that the Johnson Quarry comprises several fault-bound blocks that formed thick growth fault deposits of the Berea sandstone (Pashin and Ettensohn 1987). The complex contains shale units (Bedford shale) that have generated natural gas in some locations. The Berea sandstone forms economically viable hydrocarbon reservoirs that produced 222,600 kL (1.4 million barrels) of oil between 1980 and 1986 (Gunn 1986).

Method of extraction

The quarry has been worked for over 100 years. The quarry is filled with water and with previously sawn blocks of stone available. Production has been by wire saw. Blasting is currently being tried on this sandstone.

Stratigraphic section

Although the Berea has always been assigned an age of Lower Mississippian, Pashin and Ettensohn (1987) have found that the Bedford shale/Berea sandstone sequence actually occurs as a thin lens between the Pocono and Catskill delta wedges, and the Bedford shale actually forms a tongue within the Berea. They have assigned the Bedford/Berea an age of upper Devonian. They have recognized nine lithofacies within the Berea but only three types of sandstone. All of the quarries in northern Ohio fall within the Pashin and Ettensohn (1987) quarry-stone lithofacies. The three types of sandstone are (a) pebbly sandstone, (b) pure sandstone, and (c) silty sandstone.

The quarystone lithofacies forms a blanket that contains isolated elongate bodies of pure sandstone. These bodies appear as topographic highs, and it is one of these elongate bodies in which the Johnson Quarry is situated. The uppermost unit in the Johnson Quarry is a thin-bedded, laminated sandstone (Figure 30), about 5.5-m (18-ft) thick, with a lag deposit of clay siderite cobbles along a disconformable contact with a more massive unit below. Figure 31 is a close-up of the thin-bedded sandstone. This more massive unit is about 1.5 m (5 ft) thick but pinches out toward the western portion of this face. Below this is about a 30-cm- (1-ft-) thick carbonaceous somewhat argillaceous sandstone, and then a massive coarse-grained sandstone down to the waterline (Figure 32). The primary facies is deltaic with subfacies of delta front and channel (Units 1, 2, and 4) and overbank (Unit 3).



Figure 30. Johnson Quarry, Kipton, OH, thin-bedded upper unit on north side of quarry (after Rock Products Consultants 1995)

Lithologic description

The quarry section is broken into units (from top to bottom):

- a. *Unit 1.* 5.5-m- (18-ft-) thick quartz Arenite but with occasional subarkose and sublitharenite facies; bottom of Unit 1 is bounded with clay ironstone conglomeratic layer forming an irregular surface; uppermost bed of Unit 1 is approximately 15 ft (4.6 m) thick with localized cross bedding; bedding dips slightly to the southwest; bottom of this unit bounded by a clay ironstone conglomeratic layer which forms an irregular surface dipping to southwest; this unit would not be acceptable for use as riprap or armor stone.



Figure 31. Johnson Quarry, Kipton, OH, close-up of thin-bedded sandstone showing carbonaceous bedding planes (after Rock Products Consultants 1995)



Figure 32. Johnson Quarry, Kipton, OH, lower massive sandstone unit (after Rock Products Consultants 1995)

- b. *Unit 2.* 1.5-m- (5-ft-) thick quartz Arenite, homogeneous and more massive than Unit 1.
- c. *Unit 3.* 30-cm- (1-ft-) thick Carbonaceous quartz Arenite; dark gray carbonaceous layer with salts efflorescing into Units 2 and 4; this is a highly evident marker bed throughout the quarry.
- d. *Unit 4.* 3.4-m- (11-ft-) thick quartz Arenite, massive similar to Unit 2; this unit extends to the waterline throughout most of the quarry, but occasional erosional surface remnants from a unit below may extend above the waterline; quarry is filled with water to the 4.0 m (13 ft) level.

Thornton Quarry

Thornton Quarry (Figure 33), located in Thornton, IL (Figure 34), is situated in a monadnock of resistant Silurian (Niagaran) series dolomitized reef (the Thornton reef) that rimmed the Illinois and Michigan basins. This is an old quarry, having been opened in 1887, with Materials Service Corporation purchasing the property in 1938.

General geology

Thornton reef complex is probably the best exposed and most widely known Silurian (Niagaran) series dolomite reef in the world (Mikulic and Kluessendorf 1985; Mikulic 1987). It has been used as a key analog to develop models of Paleozoic reef development, and has significant economic importance as the largest source of high quality aggregate in the Chicago metropolitan area. The reef is one of numerous exposures of Silurian reefs that developed in mid-to-late Silurian time on a broad platform surrounding shallow seas in the Great Lakes/ Upper Mississippi River Valley area. Classic papers on the Thornton reef include Bretz (1939), Lowenstam (1950, 1957), Ingels (1963), Pray and Mikulic (1976) and Shaver (1978). More recent summaries of the Thornton Quarry in Cook County, IL, can be found in Mikulic (1987).

Method of extraction

Thornton Quarry operation has grown over the years into a complex, open-pit operation consisting of four pits divided by roadways but interconnected by tunnels. The four pits are termed the north, the south, the middle, and the north-west quarries. Each quarry consists of two benches, the uppermost bench being approximately 50.3 m (165 ft) high and the middle bench being about 33.5 m (110 ft) high. The current operation is in a newly developed lower bench, approximately 24.4 m (80 ft) high in the middle quarry.

The south face of the middle bench (Figure 35) would be the source of any large stone purchased from this quarry. The reef flank deposit (Figure 36) is massive enough to produce large-size stone but, because bench height is so high, there is very little likelihood that a fracture free stone could be produced. The

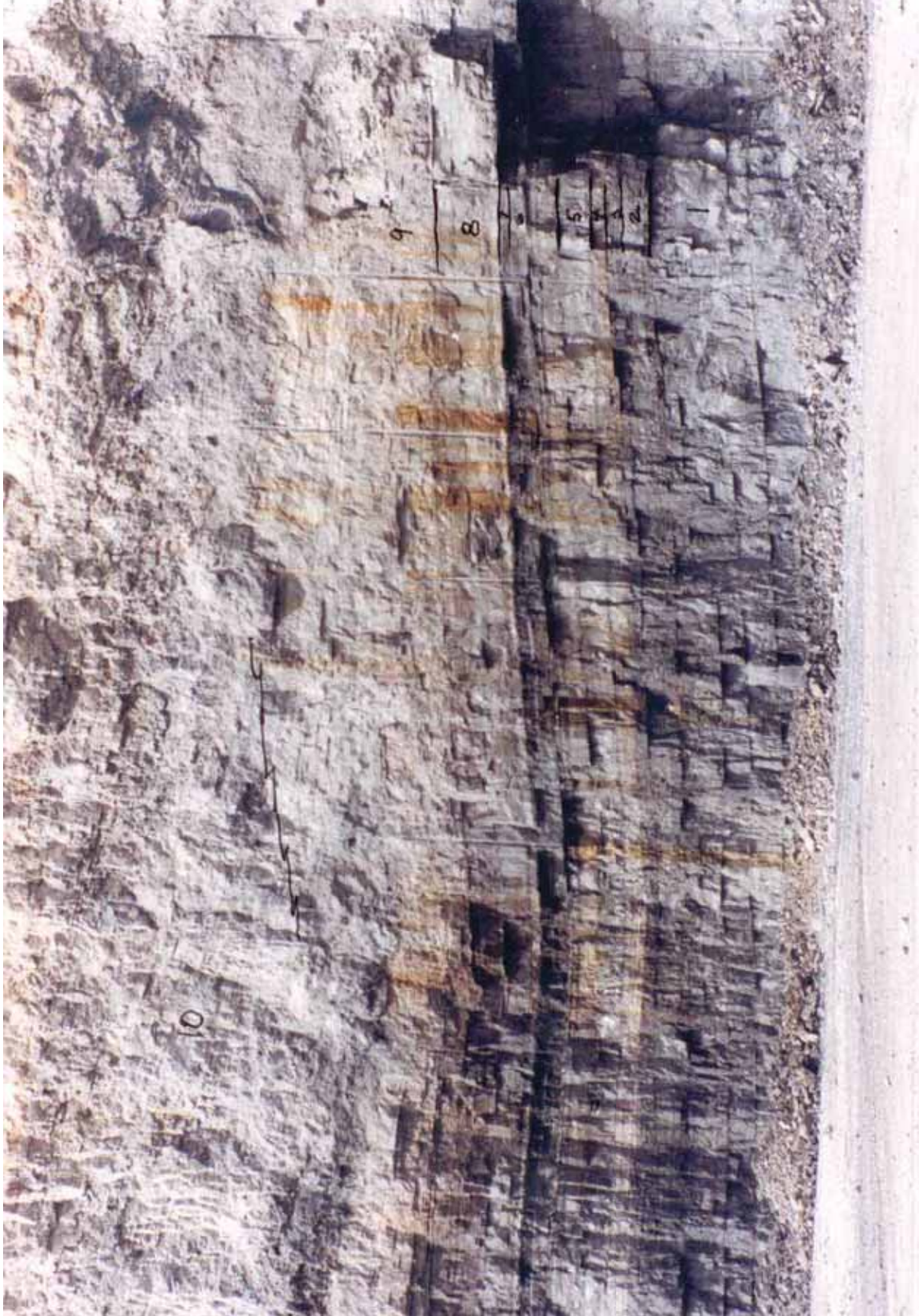


Figure 33. Thornton Quarry, Thornton, IL, lower bench (after Rock Products Consultants 1995)



Figure 34. Location map, Thornton Quarry, Thornton, IL

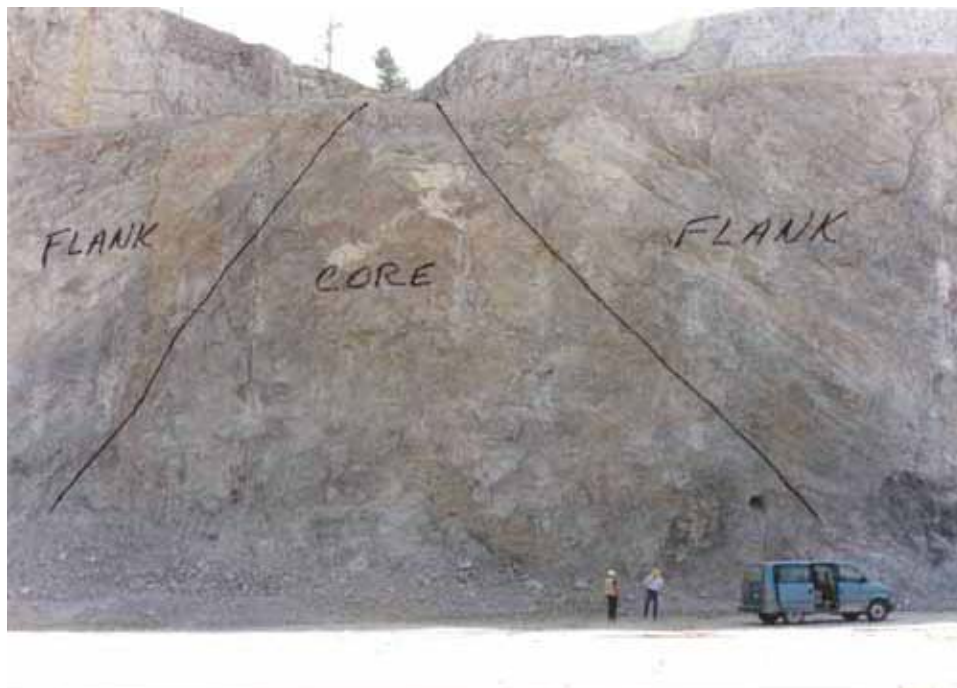


Figure 35. Thornton Quarry, Thornton, IL, northwest quarry, middle bench, southeast corner, reef core, and flank beds on either side (after Rock Products Consultants 1995)



Figure 36. Thornton Quarry, Thornton, IL, northwest quarry, middle bench, showing massive flank beds (after Rock Products Consultants 1995)

bench height would have to be reduced to no more than 90.1 m (30 ft) and the blasting methods would have to be modified. Considering that the current production of aggregate at this quarry is 8 billion kg per year (9 million tons), there is no incentive for the quarry operators to go through such a change in production methodology in order to produce 9 to 18 million kg (10 to 20 thousand tons) of armor stone.

Another problem with this bench is the considerable lateral variation in stone quality because of the rapidly changing facies from reef flank to proximal fore-reef where large, poorly cemented, reef talus blocks up to 15 m (50 ft) across constantly appear (Figure 37). Also present are extensive glauconitic zones and seams. Toward the west end of the south middle bench the quality of the rock decreases significantly as blocks of reef talus become more frequent and the thin interreef beds appear.

Stratigraphic section

Because of the sheer vertical height of this quarry face (31 m (103 ft) on the east end, and 34 m (112 ft) on the west end), the face of the middle bench could not be examined in detail; therefore, only a general description of the entire length of this face, approximately 0.8 km (0.5 mile) is available.

The east end of this face exposes the reef core and accompanying reef flank rock. The reef core is a dark brown, almost black, dense to slightly vuggy dolomite. It is massive and free of bedding. The reef flank rock is a massive,



Figure 37. Thornton Quarry, Thornton, IL, northwest quarry, middle bench, storm block of reef talus (after Rock Products Consultants 1995)

banded, pale yellowish gray and light medium gray dolomite. It is dense with scattered macropores and some vugs. The vugs are mostly small, 0.6 to 1.3 cm (0.25 to 0.5 in.) in diameter, but some may get as large as 46 cm (18 in.) in diameter or even larger. There are no distinct bedding partings in the reef flank facies.

The reef flank facies is prominent throughout most of the length of this face, but about midway a large storm block of reef talus is evident. These storm blocks or slumps of reef talus become more frequent toward the west end of this face. The blocks or slumps of reef talus consist of loosely cemented chunks of reef debris, and are rubbly and easily fragmented.

Also toward the west end, the interreef facies begins to appear just above the floor of the quarry, and becomes the dominant facies in the west face of the Northwest Quarry. The interreef facies is thin bedded with distinct bedding plane partings.

About 510 to 550 m (550 to 600 yd) west of the east end of the south face is a glauconitic zone with two distinct seams of glauconite dipping toward the west at an angle of about 55 deg. These two seams are about 15 cm (6 in.) thick. A third less distinct seam parallels the first two just a few feet to the right. This glauconitic zone appears to be a storm roller or slump. It is large and can be traced from about 10 m (35 ft) above the floor up into and near the top of the upper bench, a vertical distance of about 60 m (200 ft) or more.

Near the west end of the south face, iron stained seeps appear in the interreef facies about 1.5 to 1.8 m (5 to 6 ft) above the floor. An examination of the rock surrounding these seeps shows that this is a vuggy zone with drusy pyrite or marcasite lining the surface of the vugs.

Lithologic description

The Thornton Quarry is situated in a monadnock or klint of resistant Silurian (Niagaran) dolomitized reef that lies within the Glacial Lake Plains subsection of the Great Lakes section of Fenneman's Central Lowland Province. The Thornton reef began during late Wenlockian time (late Joliet or late early Niagaran) that continued to grow without interruption probably to the end of the Silurian. The depositional setting of the reef was along the northern edge of a low clastic belt on an extensive shelf. Widespread submergence had begun in early Silurian time with an interruption in sedimentation at the end of Alexandrian time, resulting in a slight disconformity at the top of the Alexandrian. The Niagaran brought widespread carbonate deposition of grainstones, oolitic carbonates and reefs with accompanying flank beds. In early Niagaran time reefs became widespread with substantial development along the western and southern perimeter of the Michigan Basin.

The formations exposed in the lower bench are thought to be the Joliet formation making up the bottom 9 to 12 m (30 to 40 ft), and the Racine formation making up the balance of this bench. The base of the Racine formation is also the base of the Thornton reef, and therefore the base of the reef is exposed in this lower bench. Even at this early stage of development, reef talus blocks are present. The upper portion of what is believed to be the Joliet is cherty and therefore, could be proximal forereef facies. Shaver (1977) proposed that the base of the reef is founded upon the Sugar Run formation. Droste and Shaver (1983) note that the Thornton reef exhibits severe gravity effects with a depression of the reef substrate amounting to 15 to 21 m (50 to 70 ft), an effect which has also been noted at several other large reefs in the Illinois, Indiana, Ohio, and Wisconsin Silurian.

The lower bench is about 24.4 m (80 ft) high and consists of 10 units. Descriptions are general in nature because of the sheer height of the bench and inaccessibility because of extensive quarrying activity.

- a. *Unit 10.* Reef flank--dolomite, porous, vuggy, and massive with imperceptible bedding planes; what appears to be bedding is only color banding; about 50 ft (15 m) thick.
- b. *Unit 9.* Interreef/reef talus--light gray to medium gray, porous dolomite with numerous stylolites and dark carbonaceous, fossiliferous layers about 1.9 cm (0.75 in.) thick; within this facies is a slump-type deposit of reef talus which can be traced from the west side of the of the lower pit to the east side; however, on the east side of the pit the slump is much smaller; slump consists of a mixture of reef rock and reef flank debris plus some glauconite and is loosely cemented; about 2.4 m (8 ft) thick.

- c. *Unit 8.* Dolomite--thin-bedded, light medium gray to medium gray, fine-grained, dense, microporous, with carbonaceous/argillaceous seams spaced about 5 cm (2 in.) apart forming bedding planes; top of this unit is the ocean floor on which the reef formed; bottom of this unit is lined with a thin layer (slightly more than paper-thin) of a mixture of drusy marcasite and glauconite ooids; about 30 cm (1 ft) thick.
- d. *Unit 7.* Chert--about 35 cm (14 in.) thick on the west side of the pit but only about 7.5 cm (3 in.) thick on the east side; this chert is black with some light gray bands, very dense but with the texture of unglazed porcelain; banding makes it appear to be varved; about 30 cm (1 ft) thick.
- e. *Unit 6.* Fenestral Dolomite--extremely fine-grained, micritic, light gray with bird's eyes or fenestrae of dark carbonaceous matter; unit contains many small, 0.3 to 1.9 cm (0.1 to 0.75 in.), vugs lined with clear quartz crystals; some of the larger vugs are oozing asphalt; about 0.9 m (3 ft) thick.
- f. *Unit 5.* Dolomite--fine-grained with scattered macropores, light gray with slight medium gray mottling; contains a few scattered fenestrae; about 0.9 m (3 ft) thick.
- g. *Unit 4.* Argillaceous Dolomite--greenish brown gray in color, fine-grained, micritic; dense with a subconchoidal fracture across bedding but a somewhat lamellar fracture parallel to bedding; appears to be variably argillaceous with some zones which appear to be only slightly argillaceous; about 0.9 m (3 ft) thick.
- h. *Unit 3.* Argillaceous Dolomite--pale greenish gray, dense with a conchoidal fracture; appears to be slightly more argillaceous than Unit 4; about 0.9 m (3 ft) thick.
- i. *Unit 2.* Cherty Dolomite--light yellowish gray with medium gray mottling, fenestral fabric, thin-bedded containing thin cherty, nodular layers; a 2.5-cm- (1-in.-) thick black chert seam is along the contact with Unit 1; about 0.6 m (2 ft) thick.
- j. *Unit 1.* Dolomite--mottled light to medium olive gray, dense but with scattered macropores; contains several stylolites that control parting; about 1.8 m (6 ft) thick.

McCook Quarry

McCook Quarry is located near the town of McCook, IL (Figure 38), near La Grange Road and Interstate 55.

A request for permission to investigate the McCook Quarry for this MCNP study was rejected by the quarry owners. Samples for durability testing and quarry description were taken from a previous quarry investigation by STS Consultants Ltd. (1992). Stones from the McCook Quarry that had been placed on prototype breakwater structures were evaluated for deterioration by the field prototype monitoring phase of this MCNP study.



Figure 38. Location map, McCook Quarry, McCook, IL

General geology

McCook Quarry is located on Silurian (Niagaran) dolomite bedrock high where there is little glacial overburden. The quarry has been in operation for approximately 70 years, and is a primary source of aggregate for the Chicago region. The Niagaran series formations exposed in the quarry consist of the Racine, the Sugar Run, and the Joliet formations. The Alexandrian is also exposed in the lowermost part of the quarry, but since the primary production is from the Niagaran, this discussion will not focus on the Alexandrian. The 60 m (200 ft) of exposed Niagaran is a shoaling upward sequence of dolomites that were deposited in a shallow marine environment. There is a pronounced disconformity at the top of the Alexandrian.

Method of extraction

Stone is mined for construction aggregate or as feed for the onsite lime plant. Blasting is from large diameter holes with high (24-m (80-ft)) benches. The blasting is designed for high fragmentation. Large blocks of stone are set aside to sell as armor stone. There also was previously a riprap plant in the quarry that has been decommissioned.

Stratigraphic section

The Niagaran series rests on a disconformity at the top of the Alexandrian. Starting from this disconformity and working upwards lies the Joliet, the Sugar Run and the Racine formations.

The Joliet formation is broken into three members (from bottom to top); (a) Brandon Bridge, (b) Markgraf, and (c) the Romeo member. The Brandon Bridge member forms a distinctive marker bed that can be traced throughout the quarry. It ranges from dark gray to light gray to a distinctive brownish red in color. The rock consists of thin, shaley dolomite beds that exhibit partings along thin seams of greenish gray silt. Above the Brandon Bridge member is the

Markgraf member. The Markgraf member is a gray to greenish gray slightly argillaceous dolomite with beds ranging from 0.2 to 0.9 m (0.5 to 3 ft) in thickness. The uppermost member of the Joliet formation is the Romeo member. This member consists of light gray to dark gray massive 6-m- (20-ft-) thick dolomite with pervasive pinpoint vugs. This is the best unit from which armor stone is obtained.

The Sugar Run formation, which lies directly above the Joliet formation, is a slightly argillaceous dolomite and is approximately 7.6 m (25 ft) thick. It contains zones of chert, local small patch reefs and is relatively thin bedded near the top.

Finally, the Racine formation rests at the top of the exposed rock sequence. The Racine formation is approximately 15 to 24 m (50 to 80 ft) thick. An unconformity bounds the upper surface, and the lowermost Racine rests conformably on the Sugar Run.

Several prominent chert horizons have been mapped in the quarry. In general, the formation consists of interreef horizontal bedded dolomites periodically interrupted by biohermal masses of dolomite. The interreef dolomites are a greenish gray, locally cherty dolomite with less vuggy porosity than the reef rock, and contain numerous partings along the medium to thin bedded rock. Localized zones of moderately argillaceous material are present.

The reef core is primarily in the northern lobe of the quarry, and is used as flux due to its pure chemical nature. The reef core is vuggy, generally does not contain chert or argillaceous material, and is massive. Towards the southeast of the main reef core is another smaller reef that is easily identified by its flat base and convex top. The reef cores are highly fossiliferous as determined from vug geometry, with secondary pyrite and drusy calcite lining some pores. The reef core also makes suitable armor stone. The primary facies are (a) reef core, (b) interreef, (c) carbonate bank (carbonate-rich), and (d) carbonate bank (clastic-rich).

Lithologic descriptions

The Niagaran series in the McCook Quarry consists of three formations.

- a. *Racine formation:* This formation consists of (a) pure dolomite that is gray and vuggy in reefs, and (b) cherty dolomite that is argillaceous, silty, brownish and greenish gray, with local beds of relatively pure dolomite between well developed reefs.
- b. *Sugar Run formation:* This formation consists of dolomite that is slightly argillaceous, silty, light greenish gray with brown weathering, in smooth surfaced medium and flagstone beds.
- c. *Joliet formation:* This formation consists of three members: (a) Romeo member (pure dolomite that is light gray to white, mottled gray, and pink, with stylolitic beds); (b) Markgraf member (dolomite that is silty at the base to slightly argillaceous at the top, and is light gray, cherty, and

medium bedded); and (c) Brandon Bridge member (dolomite that is argillaceous to shaley, gray, red to green, and contains a few thin pure beds with siliceous foraminifera abundant).

Stability of Freshly Quarried Stone

Quarried stone, like any construction material, must reach a state of equilibrium with its new environment prior to being utilized in any construction project. Once a block of stone is quarried, it is released from a state of equilibrium within the rock formation and placed in another environment within which it must reach stability prior to being used in construction. This was recognized almost 20 centuries ago by the Roman architect Vitruvius who required that stone be seasoned or cured for two years before being used in any construction (Morgan 1960).

Richey (1951) stated that stone freshly quarried and placed in a structure without proper seasoning may develop cracks months after being placed in the masonry. He recommended that blocks taken from a quarry should be permitted to season for several months before cutting to finished size. Richey (1951) also advised that because most sandstones are more or less soft when first quarried, such stone should not be placed until it has seasoned and hardened after being taken from the quarry. The civil engineering profession is only just beginning to acknowledge the advisability of allowing quarried stone to stabilize prior to use.

The need for curing is based on two conditions that coexist and are inter-related in freshly quarried stone. The first condition is the existence of connate water within the freshly quarried stone. The presence of connate or pore water within porous stone results in reduced strength and durability. Krynine and Judd (1957) recommend that freshly quarried stone, particularly limestones, dolomites, and sandstones be seasoned (i.e., reasonably dried) before being placed into structures. Lamar (1967), Legget (1973), and Patton (1974) discuss the advisability of allowing the stone to dry to both improve durability and to allow carbonates and sandstones to case-harden. Case-hardening is described by Lamar (1967) as a process occurring in porous stone in which calcium carbonate is moved from the interior of a rock particle or block to the exterior by the wicking movement of pore water or rain water as the particle air-dries.

The effect of pore water on the strength of rock is well known among practitioners of the field of rock engineering or rock mechanics. Jumikis (1983) states that water in the rock affects the strength and elastic properties of rock, and notes that strength decreases with increasing degree of saturation. Vutukuri et al. (1974) found a 50 percent reduction in compressive strength of saturated sandstones when compared to air-dried specimens from the same formations. For limestones and dolomites, the reduction in strength ranged from 15 to 50 percent, and for quartzite, the reduction amounted to almost 25 percent.

The second condition that suggests a need for seasoning is stress release or unloading. Both terms refer to the loss of confining pressure as a block of stone is removed from the quarry face. Stress release results from the removal of horizontal stresses (i.e., removal of a thick section of stone from the quarry wall resulting

in vertical release fractures normal to the maximum principal stress direction and often also normal to the medium stress direction). Unloading is the removal of vertical stresses (i.e., denudation or removal of upper layers of rock or retreat of continental glaciers). Unloading or rebound fractures are illustrated by sheeting or extensional fractures generally parallel to the local topography and increasing in density toward the surface (Nichols 1980). Rockbursts in quarry floors such as that experienced at the Sandusky Quarry as described by Adams (1982) are a result of the presence of both high horizontal tectonic compressional forces and unloading (Nichols 1980). Nichols (1980) also relates that carbonates are particularly susceptible to rebound and stress relaxation effects because of the high degree of anisotropy associated with these particular rock types. Sbar and Sykes (1973) report that the Maximum Principal Stress (i.e., the horizontal compressional tectonic stress) in situ measurement for north-central Ohio is 450 kg per sq cm (6,383 lb per sq in.) striking N 90 deg W. Flint (1957) provides a discussion of crustal warping and unloading in the Great Lakes area as a result of continental glaciation.

A third condition exists which also recommends a need for seasoning. This condition is the result of the interrelationship of the first two conditions. If the stone is quarried during or just prior to the onset of freezing weather and a sufficient amount of connate water is present, the unconfined stone now released from the confining pressure of the rock formation will react much like opening a frozen soda-pop bottle. Release of confining pressure results in relatively rapid freezing of the pore water, and consequently, causes the rock to pop. An event in which 50 to 75 percent of a barge load of freshly quarried stone popped and fractured with an audible creaking noise was reported by Hill (1992).

The time required for seasoning by air-drying of freshly quarried armor stone blocks will vary depending on porosity and pore size distribution, and on the degree of saturation. Recommendations of the Indiana Limestone Institute of America (undated) range from 60 to 90 days for stone quarried above the water table to at least 6 months for stone quarried from below the water table. Lienhart (1975) found that the Berea sandstone stabilizes after about 90 days. For seasoning related to stress release and unloading, the time required will depend on the intensity of the stress field and on the rate of unloading, or to some combination of both. The duration will also depend on the degree of anisotropy of the geologic formation under consideration. Lienhart and Stransky (1981) were able to detect the development of rebound fractures as long as 90 days after removal of a limestone sample from the quarry face. A reasonable approximation of required seasoning time, therefore, appears to be approximately 90 days minimum. Some stone may require more time.

Cut Stone versus Rubble Stone

The use of large cut stone blocks in massed stone masonry construction may be seen in railroad trestles, bridge piers, retaining walls, foundations, and breakwaters built prior to 1920. These structures use both large and small stone in load bearing walls, as was done in ancient city fortifications and medieval cathedrals. Stone with the integrity to bear significant compressive loads was laid in bonded patterns to assure structural integrity. This method of construction persisted into

the early twentieth century, as evidenced by the breakwater at Cleveland Harbor. Much of the knowledge and technique involved in this type of construction was transmitted through apprentice-type learning and, usually, no written record was kept. Stone as a structural element, as well as the knowledge and technique associated with such work, has disappeared with the advent of reinforced concrete and structural steel construction. The repair or partial replacement of cut stone laid-up type breakwater with rubble armor stone units presents an interesting juxtaposition of the old and the new. A number of elements have changed, including:

- a.* Blasted stone has replaced cut (sawn) stone.
- b.* Rubble masonry has replaced bonded masonry.
- c.* Compressively loaded cut stone has been augmented by or replaced with larger irregularly shaped, supposedly interlocking angular stone.
- d.* Gravity has largely become a negative element in stone construction, replacing the positive role it plays in the construction of unmortared masonry walls.

In a quest to control costs and minimize problems of wave overtopping, the rubblemound breakwater has become today's structure of choice. Nevertheless, many of the principles that were used in building the older cut stone laid-up breakwaters still have great value in the maintenance and restoration of the old structures. These principles may provide valuable insight into problems arising in the newer rubble-mound structures, and are listed as follows:

- a.* Stone with the integrity to bear significant compressive loads is indispensable.
- b.* Stone placed with its natural bedding horizontal is superior to stone placed in any other manner.
- c.* Bonding of masonry units adds dramatically to the integrity of a masonry structure.
- d.* Rectilinear units are usually preferable to irregular, angular masonry units in a structure.
- e.* Stone used as cladding benefits greatly from a batter that allows gravity to stabilize units, and moves the center of gravity inward.
- f.* Any placement that subjects stone to forces other than compression has an adverse effect.
- g.* Stone fractured from movement (gentle rocking and rolling due to wave action) may be a significantly unrecognized and unreported problem.
- h.* Water in stone exposed to variable climate and weathering detracts from strength and lowers durability.
- i.* The more the elements of the design and construction process are used to maximize a stone's positive qualities and minimize its negative qualities, the longer will be the durability and service life of the resulting stone structure.

3 Laboratory Durability Testing¹

Seventeen stone test blocks were subjected to accelerated environmental weathering freeze/thaw and wet/dry conditions in the U.S. Army Corps of Engineers, Ohio River Division Laboratory (ORDL), Cincinnati, OH, as one part of this MCNP study. (Not all 17 test blocks were subjected to both freeze/thaw (FT) and wet/dry (WD) testing cycles.) The 17 test blocks were obtained from seven different quarries that have historically provided material for Great Lakes breakwater and jetty construction and rehabilitation. Analyses of five test blocks from the McCook Quarry had been performed by ORDL during a previous quarry investigation by STS Consultants Ltd. (1992) under contract to U.S. Army Engineer District, Chicago, and these results were included in this present MCNP study. All samples were evaluated according to nationally accepted scientific testing standards, including:

- a. Freeze/thaw: U.S. Army Corps of Engineers (1992), Rock Standard CRD C144 (50 cycles).
- b. Wet/dry: American Society for Testing and Materials (1992), International Standard ASTM D5313 (80 cycles).
- c. Specific gravity: American Society for Testing and Materials (1988), International Standard ASTM C127.
- d. Petrography: American Society for Testing and Materials (1994), International Standard ASTM D4992.

The minimum dimensions for the test slab sizes cut parallel and perpendicular to the bedding to be tested with Standards CRD C144 and ASTM D5313 were not less than 38 cm (15 in.) long by 33 cm (13 in.) wide by 5 cm (2 in.) thick.

The stone test blocks came from seven quarries from which stone had been used on the prototype structure sections that were selected for field prototype monitoring due to premature deterioration, and include:

- a. Reed Quarry, Bloomington, IN: One (1) limestone sample weighing 454 to 907 kg (1,000 to 2,000 lb) (Test Block R-1-FT).

¹ This section was written by Kenneth E. Henn, III, former, geologist, U.S. Army Corps of Engineers, Ohio River Division Laboratory, Cincinnati, OH; presently, geologist, U.S. Army Engineer District, Louisville.

- b. Valders Quarry, Valders, WI: Two (2) dolomite samples weighing 680 to 907 kg (1,500 to 2,000 lb) each (Test Block V-1-FT, and Test Block V-2-FT).
- c. Dempsey Quarry, Waterloo, WI: Two (2) quartzite samples weighing 454 to 907 kg (1,000 to 2,000 lb) each (Test Block D-1-FT, and Test Block D-3-FT).
- d. Sandusky Quarry, Parkertown, OH: Two (2) limestone samples weighing 680 to 907 kg (1,500 to 2,000 lb) each (Test Block S-1-FT/WD, and Test Block S-2-FT).
- e. Marblehead Quarry, Marblehead, OH: Three (3) limestone samples weighing 680 to 907 kg (1,500 to 2,000 lb) each (Test Block M-1-FT, Test Block M-2-WD, and Test Block M-3-FT/WD).
- f. Johnson Quarry, Kipton, OH: Two (2) sandstone samples weighing 680 to 907 kg (1,500 to 2,000 lb) each (Test Block J-1-WD, and Test Block J-2-FT).
- g. Thornton Quarry, Thornton, IL: Five (5) dolomite stone samples weighing 454 to 907 kg (1,000 to 2,000 lb) each (Test Block MTC-1-FT/WD, Test Block MTC-2-FT, Test Block MTC-3-FT/WD, Test Block MTC-4-FT/WD, and Test Block MTC-5-FT/WD).

Reed Quarry Durability Test Results

Test Block R-1-FT. This test block (Figure 39) was subjected to freeze/thaw (FT) testing only (where FT indicates after freeze/thaw exposure). Samples R-1A-FT and R-1B-FT were extracted from this test block. Subsequently, Thin Section Samples TS-R-1A-1FT, TS-R-1A-2FT, and TS-R-1A-3FT were extracted from Sample R-1A-FT. Thin Section Samples TS-R-1B-1FT and TS-R-1B-2FT were extracted from Sample R-1B-FT.

The test block is light yellowish-gray to medium gray oolitic limestone. Lithologically, the sample is comprised of an oolitic grainstone with occasional fossil fragments. The sample lacks intergranular cement except for small deposits of rimming cements that bind grains at granular point contacts. The low density of the sample is readily observed by its heft.

Macroscopically, the material appears porous and rough. Microscopically, the lack of carbonate cement is predominant. Microscopic analysis revealed approximately 10 percent porosity associated with calcitic cement at grain contacts. These contacts also show some interesting dripstone morphologies of the cement on the underside of grains, formed during lithofication, and can be used to ascertain direction of bedding.

The bedding exhibits irregular, interbedded, and cross-bedded structures. Elongated grains are oriented parallel to the bedding planes, but no planes of weakness appear in the sample. One large, high frequency and moderate amplitude, highly ferrous, stylolitic seam exists parallel to bedding in the middle of the sample. The stylolite has partially parted along one surficial boundary, but was



Figure 39. Reed Quarry Salem formation limestone accelerated weathering durability Test Block R-1-FT

intact in the area where the tests were taken. The iron-rich character of the stylolite increases the specific gravity slightly in this area, but the general porous quality is still prevalent.

Overall, the test block is sound, with no visible fracturing; however, the stylolitic seam can be deleterious to the soundness. The stylolite did part during freeze/thaw testing and a 41 percent loss was the result. The sample is fairly tough, fairly hard, and porous. The freeze/thaw percent loss was 41.8 percent, due to parting of the stylolitic seam. The specific gravity was 2.43. Absorption was 3.80, and adsorption was 0.11, resulting in an adsorption/absorption ratio of 0.03.

Valders Quarry Durability Test Results

Test Block V-1-FT. This test block (Figure 40) was subjected to freeze/thaw testing only. Samples V-1A-FT and V-1B-FT were extracted from this test block. Subsequently, Thin Section Samples TS-V-1A-1FT, TS-V-1A-2FT, and TS-V-1A-3FT were extracted from Sample V-1A-FT. Thin Section Samples TS-V-1B-1FT and TS-V-1B-2FT were extracted from Sample V-1B-FT.

The test block is light brownish-gray, fine to medium grained micritic dolomite with a massive, even structure. The matrix of the test block is mostly fine-grained micritic dolomite with a small component of argillaceous clays locked in the structure. The samples are dense due to the fine-grained, well packed, interlocked dolomitic micrite. Rare, tight, noncontinuous fractures occur near the surficial boundaries of the samples.

Overall, the test block is dense, tough, and hard. The freeze/thaw percent loss was 0.28 percent, due to surficial spalling. The specific gravity was 2.78. Absorption was 1.00, and adsorption was 0.08, resulting in an adsorption/absorption ratio of 0.08.

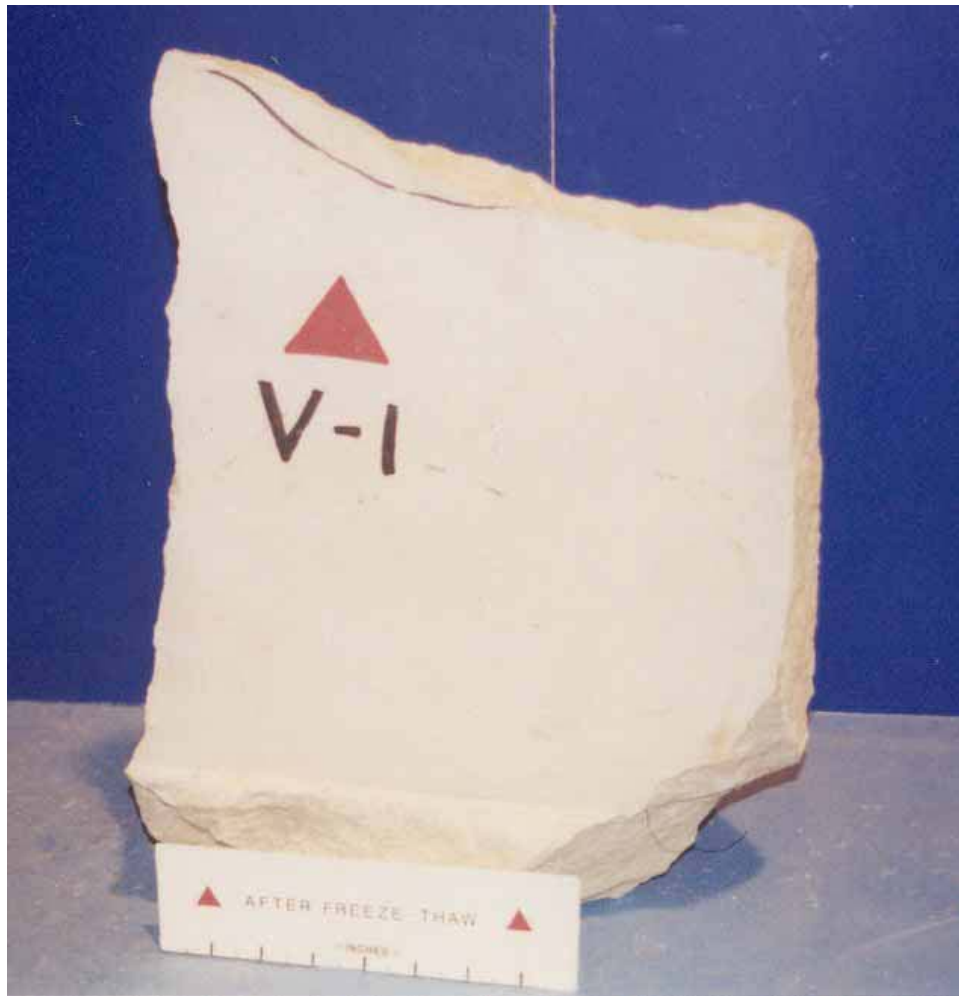


Figure 40. Valders Quarry Niagaran series dolomite accelerated weathering durability Test Block V-1-FT

Test Block V-2-FT. This test block (Figure 41) was subjected to freeze/thaw testing only. Samples V-2A-FT and V-2B-FT were extracted from this test block. Subsequently, Thin Section Samples TS-V-2A-1FT, TS-V-2A-2FT, and TS-V-2A-3FT were extracted from Sample V-2A-FT. Thin Section Samples TS-V-2B-1FT and TS-V-2B-2FT were extracted from Sample V-2B-FT.

The test block is light to medium brownish-gray, medium to coarse-grained micritic dolomite with a mottled texture and relatively massive structure. The ground matrix of the sample is mostly fine-grained micritic dolomite with extremely common dissolution voids of fossil fragments, mostly crinoid fragments. The areas are porous but rarely permeable on the macroscopic range. Occasional dolomitized fossil fragments are observable as ghostly white bryozoan, brachiopod, and crinoid fragments with no distinct boundaries. Common, tight, noncontinuous, fractures and shrinkage cracks occur perpendicular to bedding. These run sinuously, approximately 4 cm (1.6 in.) before dissipating into the groundmass and dissolution voids. These are not major weaknesses and are not overly deleterious to the overall strength of the sample.

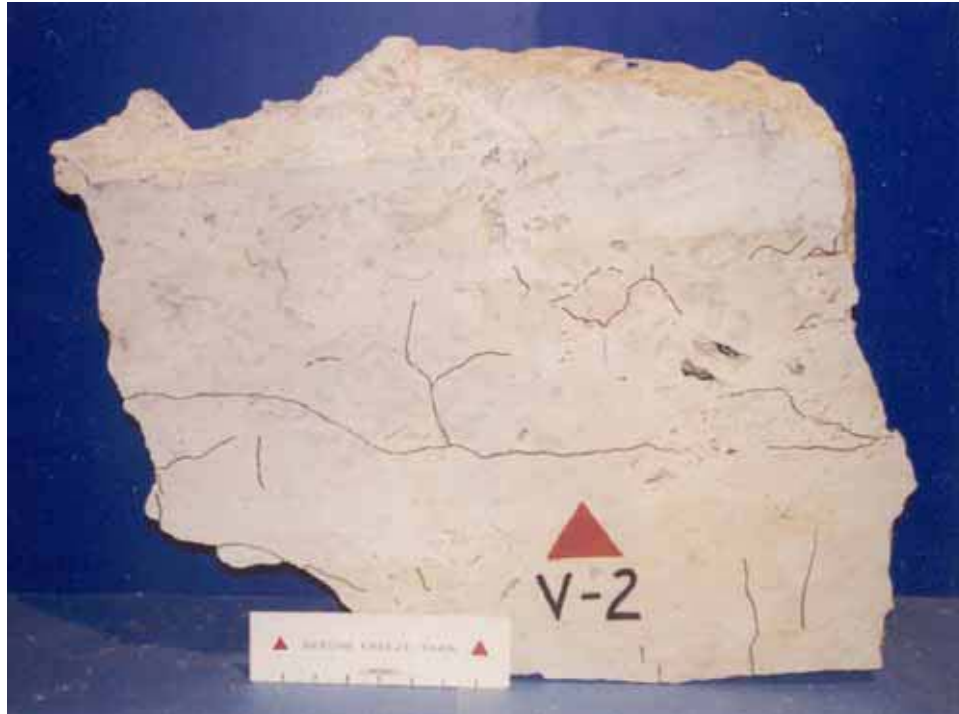


Figure 41. Valders Quarry Niagaran series dolomite accelerated weathering durability Test Block V-2-FT

Overall, the test block is fairly dense, tough, and hard. The freeze/thaw percent loss was 0.25 percent, due to surficial spalling. The specific gravity was 2.76. Absorption was 1.04, and adsorption was 0.05, resulting in an adsorption/absorption ratio of 0.05.

Dempsey Quarry Durability Test Results

Test Block D-1-FT. This test block (Figure 42) was subjected to freeze/thaw testing only. Samples D-1A-FT and D-1B-FT were extracted from this test block. Subsequently, Thin Section Samples TS-D-1A-1FT and TS-D-1A-2FT were extracted from Sample D-1A-FT. Thin Section Sample TS-D-1B-1FT was extracted from Sample D-1B-FT.

The test block is pale red to dark dusky red, coarse grained, cross-bedded, high-grade meta-quartzite. Grains are well sutured with no to little void space. Original iron-rich sand grains can be observed within the ground matrix. Freshly fractured surfaces exhibit a fine, sugary texture. Bedding can be determined by vertical color changes, vertical grain size distribution changes, and thin laminations of black iron-oxide mineralization. These iron-rich minerals are formed in small rosettes, probably during metamorphism, and are not associated with any open fracturing.



Figure 42. Dempsey Quarry Waterloo formation quartzite accelerated weathering durability Test Block D-1-FT

Short, tight, noncontinuous, stress relief fractures are common and occur perpendicular to bedding or intergranularly. These fractures average 1 cm (0.4 in.) in length, and begin and dissipate in the ground mass. These fractures do not appear to affect the integrity of the sample, but they do have the potential to connect, forming larger continuous fractures. Open fractures do exist, but are predominantly short and are close to the surficial boundaries of the sample. These also dissipate into the groundmass.

Overall, the test block is tough, dense, and hard. The freeze/thaw percent loss was 0.83 percent, due to spalling of thin edges. The specific gravity was 2.69. Absorption was 0.08, and adsorption was 0.01, resulting in an adsorption/absorption ratio of 0.12.

Test Block D-3-FT. This test block (Figure 43) was subjected to freeze/thaw testing only. Samples D-3A-FT and D-3B-FT were extracted from this test block. Subsequently, Thin Section Samples TS-D-3A-1FT and TS-D-3A-2FT were extracted from Sample D-3A-FT. Thin section Samples TS-D-3B-1FT and TS-D-3B-2FT were extracted from Sample D-3B-FT.

The test block is pale red to dark dusky red, coarse grained, cross-bedded, high-grade meta-quartzite. Grains are well sutured with no to little void space. Original iron-rich sand grains can be observed within the ground matrix. Freshly fractured surfaces exhibit a fine, sugary texture. Bedding can be determined by vertical color changes, vertical grain size distribution changes, and thin laminations of black iron-oxide mineralization. The noticeability of the cross-bedded nature of this sample is much better than Test Block D-1. This is a result of the sharp truncation of medium- to coarse-grained beds with coarse-grained deposits. Some of these coarse grains are up to 3 cm (1.18 in.) in diameter.



Figure 43. Dempsey Quarry Waterloo formation quartzite accelerated weathering durability Test Block D-3-FT

Short, tight, noncontinuous, stress relief fractures are common and occur perpendicular to bedding or intergranularly. These fractures average 1 cm (0.4 in.) in length, and begin and dissipate in the groundmass. These fractures do not appear to affect the integrity of the sample, but they do have the potential to connect, forming larger continuous fractures. These also dissipate into the groundmass. Open fractures do exist, predominantly short and close to the surficial boundaries of the sample. However, there are joint sets (with apparent angles of approximately 55 and 125 deg) that permeate the sample fairly deep and, in some cases, run the width of the sample. Upon parting, secondary micaceous mineralization can be readily noticed partially infilling these joint sets.

Overall, the test block is tough, dense, and hard. The freeze/thaw percent loss was 0.25 percent, due to spalling of thin edges. The specific gravity was 2.68. Absorption was 0.10, and adsorption was 0.01, resulting in an adsorption/absorption ratio of 0.10.

Sandusky Quarry Durability Test Results

Test Block S-1-FT/WD. This test block (Figure 44) was subjected to both freeze/thaw and wet/dry (WD) testing (where FT/WD indicates after both freeze/thaw and wet/dry exposure). Samples S-1A-FT/WD and S-1B-FT/WD were extracted from this test block. Subsequently, Thin Section Samples TS-S-1A-1FT/WD and TS-S-1A-2FT/WD were extracted from Sample S-1A-FT/WD. Thin Section Samples TS-S-1B-1FT/WD and TS-S-1B-2FT/WD were extracted from Sample S-1B-FT/WD.



Figure 44. Sandusky Quarry Columbus formation limestone accelerated weathering durability Test Block S-1-FT/WD

The test block is light gray to olive-gray, coarse-grained limestone, poorly sorted, well-packed, well lithofied, fossiliferous wackestone to packstone (30 percent fossils; 70 percent calcitic and micritic matrix). The matrix consists of intergranular argillaceous micrite with crystalline calcium carbonate grains. Fossils consist of mostly medium grained crinoid fragments and other fossil hash.

Interbedded with these fossil-rich limestone layers are dark brown, argillaceous laminations, which are wavy, continuous, and potentially fissile. The relatively high percentage of loss during freeze/thaw is a direct result of failure of one of these laminations. Also present are fine, continuous, wavy, high frequency, low to medium amplitude stylolites. The fracture patterns present are irregular and random in orientation. These mostly occur as surficial fractures and spalls.

Overall, the test block is dense, hard, and fairly tough, although the sample is prone to parting due to the high content of argillaceous laminations. The freeze/thaw percent loss was 4.10 percent, due to surficial spalling and parting of argillaceous laminations. The wet/dry percent loss was 0.17 percent, due to surficial spalling. The specific gravity was 2.63. Absorption was 2.87, and adsorption was 0.20, resulting in an adsorption/absorption ratio of 0.07.

Test Block S-2-FT. This test block (Figure 45) was subjected to freeze/thaw testing only. Samples S-2A-FT and S-2B-FT were extracted from this test block. Subsequently, Thin Section Samples TS-S-2A-1FT and TS-S-2A-2FT were extracted from Sample S-2A-FT. Thin Section Samples TS-S-2B-1FT and TS-S-2B-2FT were extracted from Sample S-2B-FT.

The test block is light gray to olive-gray, coarse-grained limestone, poorly sorted, well-packed, well lithofied, fossiliferous wackestone to packstone (40 percent fossils; 60 percent calcitic and micritic matrix). The matrix consists of intergranular argillaceous micrite with crystalline calcium carbonate grains. Fossils consist of mostly coarse-grained crinoid fragments. Interbedded with these fossil-rich limestone layers are a high amount of dark brown, argillaceous laminations, which are wavy, continuous, and potentially fissile. Some of these laminae are up to 1 mm (0.04 in.) thick. A high percentage of loss during sawing of the freeze/thaw sample was a direct result of failure of one of these laminations. The fracture patterns present, are irregular and random in orientation. These mostly occur as surficial fractures and spalls.

Overall, the test block is dense, hard, and fairly tough, although the sample is prone to parting, due to the high content of argillaceous laminations. The freeze/thaw percent loss was 0.51 percent, due to surficial spalling. (23.60 percent loss was attained during sawing.) The specific gravity was 2.55. Absorption was 3.27, and adsorption was 0.07, resulting in an adsorption/absorption ratio of 0.02.

Marblehead Quarry Durability Test Results

Test Block M-1-FT. This test block (Figure 46) was subjected to freeze/thaw testing only. Samples M-1A-FT and M-1B-FT were extracted from this test block. Subsequently, Thin Section Sample TS-M-1A-1FT was extracted from Sample M-1A-FT. Thin Section Samples TS-M-1B-1FT and TS-M-1B-2FT were extracted from Sample M-1B-FT.



Figure 45. Sandusky Quarry Columbus formation limestone accelerated weathering durability Test Block S-2-FT

The test block is medium to dark brownish-gray, fine to medium grained dolomite, with mottled texture. Common dissolution voids of fossil fragments ranging from moderately large voids up to 1 cm (0.4 in.) to microscopic voids exist. Most voids do not exceed 2 mm (0.08 in.) in diameter. Dolomitized fossil fragments consist mostly of bryozoan and crinoid remnants. Bedding is very difficult to determine, with no prominent planes or orientation to elongated grains. An overall bedding can be weakly seen due to vertical color changes. The sample is porous but not permeable in the macroscopic scale. All major, open fractures run parallel to each other, and perpendicular to the weakly observable bedding planes. Minor, tight fractures occur randomly, wavy, and noncontinuously between or branching from the major open fractures. Most of the fractures begin and dissipate into the groundmass or voids. Freshly broken surfaces exhibit a sugary texture.



Figure 46. Marblehead Quarry Columbus formation dolomitic limestone accelerated weathering durability Test Block M-1-FT

Overall, the test block is hard, tough, and fairly porous. The freeze/thaw percent loss was 0.31 percent, due to surficial spalling. The specific gravity was 2.58. Absorption was 3.21, and adsorption was 0.05, resulting in an adsorption/absorption ratio of 0.02.

Test Block M-2-WD. This test block (Figure 47) was subjected to wet/dry testing only. Samples M-2A-WD and M-2B-WD were extracted from this test block. Subsequently, Thin Section Samples TS-M-2A-1WD and TS-M-2A-2WD were extracted from Sample M-2A-WD. Thin Section Sample TS-M-2B-1WD was extracted from Sample M-2B-WD.

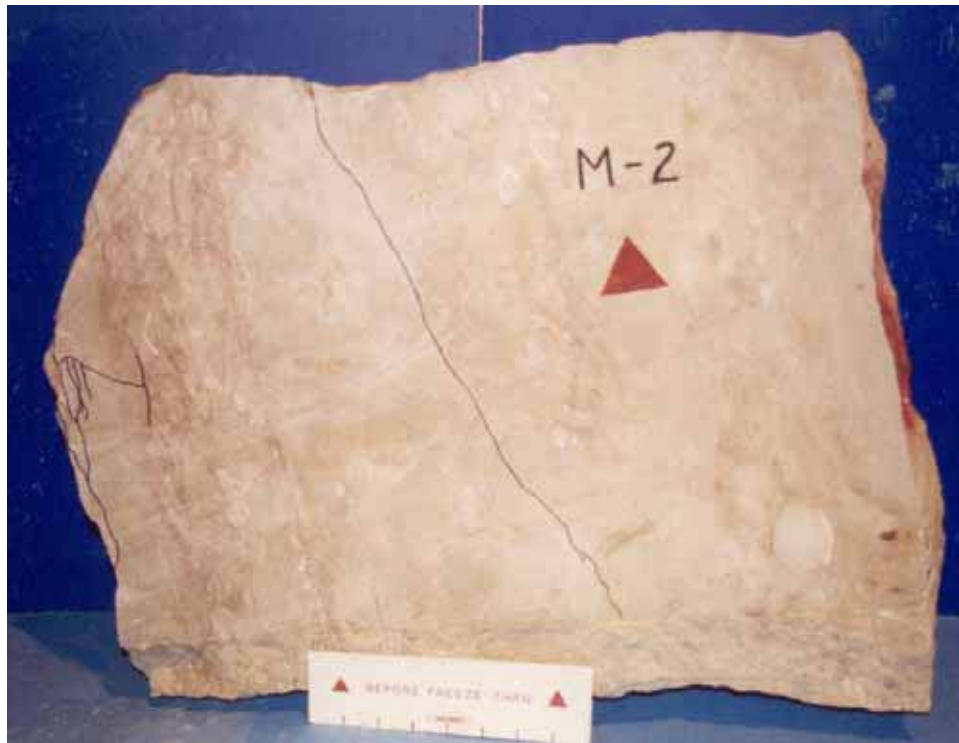


Figure 47. Marblehead Quarry Columbus formation dolomitic limestone accelerated weathering durability Test Block M-2-WD

The test block is medium to dark brownish-gray, fine to medium grained dolomite, with mottled texture. Dolomitized fossil fragments consist mostly of bryozoan and brachiopod remnants with occasional crinoid fragments. Large bryozoan (up to 4 cm (1.6 in.)) are common and are often lapped over by argillaceous laminations. Bedding is pronounced as alternating layers of dark brown, highly argillaceous laminations with dense, medium brownish-gray, mottled dolomite. Elongated grains are oriented lengthwise parallel with the bedding planes. The sample is dense, but some small voids 1 to 2 mm (0.04 to 0.08 in.) in diameter are present. All major, open fractures run parallel to each other, and to the bedding planes. Minor, tight fractures occur randomly, wavy, and noncontinuously between or branching from the major open fractures. Most of the fractures begin and dissipate into the groundmass or voids. Freshly broken surfaces exhibit a sugary texture.

Overall, the test block is hard, tough, and porous. The wet/dry percent loss was 0.25 percent, due to surficial spalling. (48.5 percent loss was attained during sawing.) The specific gravity was 2.63. Absorption was 2.11, and adsorption was 0.06, resulting in an adsorption/absorption ratio of 0.03.

Test Block M-3-FT/WD. This test block (Figure 48) was subjected to both freeze/thaw and wet/dry testing. Samples M-3A-FT/WD and M-3B-FT/WD were extracted from this test block. Subsequently, Thin Section Sample TS-M-3A-1FT/WD was extracted from Sample M-3A-FT/WD. Thin Section Samples TS-M-3B-1FT/WD and TS-M-3B-2FT/WD were extracted from Sample M-3B-FT/WD.



Figure 48. Marblehead Quarry Columbus formation dolomitic limestone accelerated weathering durability Test Block M-3-FT/WD

The test block is medium to dark brownish-gray, fine to medium grained dolomite, with mottled texture. Dolomitized fossil fragments consist mostly of bryozoan and brachiopod remnants with occasional crinoid fragments. Large bryozoan (up to 3 cm (1.2 in.)) are common and are often lapped over by argillaceous laminations. Bedding is pronounced as alternating layers of dark brown, highly argillaceous laminations with dense, medium brownish-gray, mottled dolomite. Elongated grains are oriented lengthwise parallel with the bedding planes. The sample is dense, but some small voids 1 to 2 mm (0.04 to 0.08 in.) in diameter are present. All major, open fractures run parallel to each other, and perpendicular to the bedding planes. Minor, tight fractures occur randomly, wavy, and noncontinuously between or branching from the major open fractures. Most of the fractures begin and dissipate into the ground mass or voids. Freshly broken surfaces exhibit a sugary texture.

Overall, the test block is hard, tough, and porous. The freeze/thaw percent loss was 0.12 percent, due to surficial spalling. The wet/dry percent loss was 0.52 percent, due to surficial spalling. (50.0 percent loss was attained during sawing.) The specific gravity was 2.52. Absorption was 4.46, and adsorption was 0.06, resulting in an adsorption/absorption ratio of 0.01.

Johnson Quarry Durability Test Results

Test Block J-1-WD. This test block (Figure 49) was subjected to wet/dry testing only. Samples J-1A-WD, J-1B-WD, and J-1C-WD were extracted from this test block. Subsequently, Thin Section Samples TS-J-1A-1WD and TS-J-1A-2WD were extracted from Sample J-1A-WD. Thin Section Samples TS-J-1B-1WD and TS-J-1B-2WD were extracted from Sample J-1B-WD. Thin Section Sample TS-J-1C-1WD was extracted from Sample J-1C-WD.

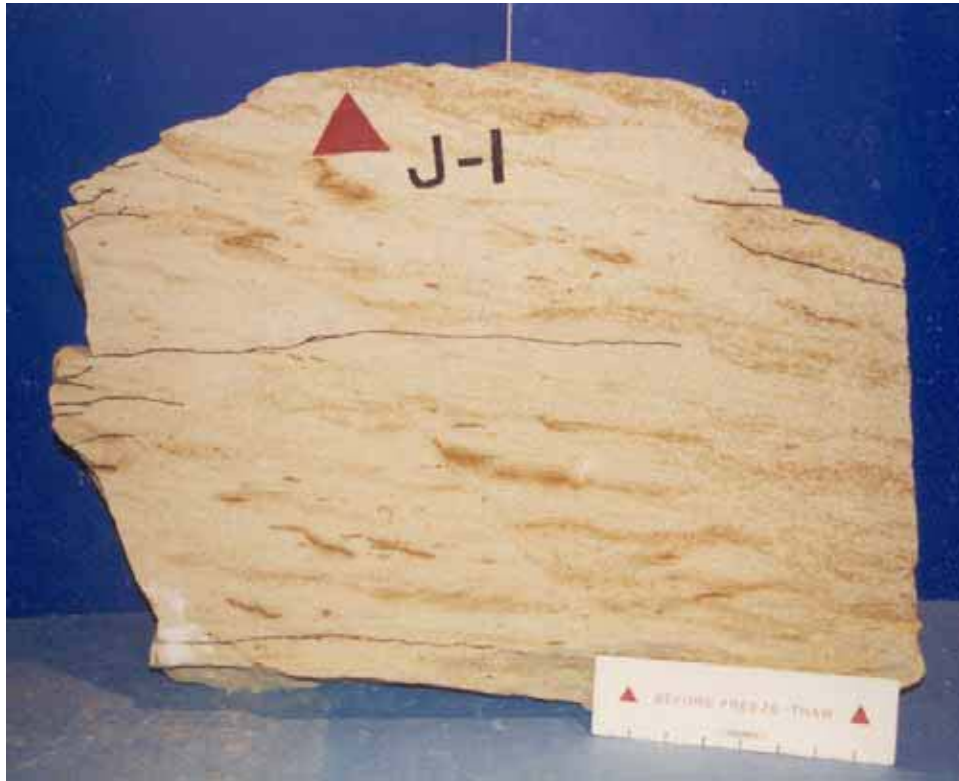


Figure 49. Johnson Quarry Berea formation sandstone accelerated weathering durability Test Block J-1-WD

The test block is light yellowish-gray, fine to medium grained, poorly cemented, thinly cross-bedded, porous sandstone. Grains consist of mostly quartz with occasional rock fragments, feldspar, calcite, iron minerals, and micaceous minerals. Grains are mostly well rounded to sub-angular. Grains are well packed, but poorly cemented, resulting in a porous and permeable quality. Cross-bedding is readily observable due to iron-rich grains and oxidized ferruginous cements, which are deposited in horizons. These distinct deposits also make climbing ripples easy to observe. A fracture permeates into the sample approximately 45 cm (18 in.) from the surface into the middle of the sample. This fracture is at an apparent angle of 6 deg from the average cross bedding. Other small fractures penetrate the sample approximately 7 cm (2.75 in.). These fractures are open, meander between grains, and dissipate into the groundmass. On fresh surfaces, the sample has a tendency to be susceptible to grain disaggregation when rubbed by a finger.

Overall, the test block is porous, hard, and tough. The wet/dry percent loss was 0.17 percent, due to surficial spalling and disaggregation of surficial grains. The specific gravity was 2.23. Absorption was 8.86, and adsorption was 0.07, resulting in an adsorption/absorption ratio of 0.01.

Test Blocks J-2 and J-2-FT. Test Block J-2 (Figure 50) was the pretest (prior to freeze/thaw exposure) equivalent of Test Block J-2-FT that was subjected to freeze/thaw testing only. Sample J-2 was extracted from Test Block J-2. Subsequently, Thin Section Samples TS-J-2-1 and TS-J-2-2 were extracted from Test Block J-2. Sample J-2-FT was also extracted from Test Block J-2. Subsequently, Thin Section Samples TS-J-2-1FT and TS-J-2-2FT were extracted from Sample J-2-FT.

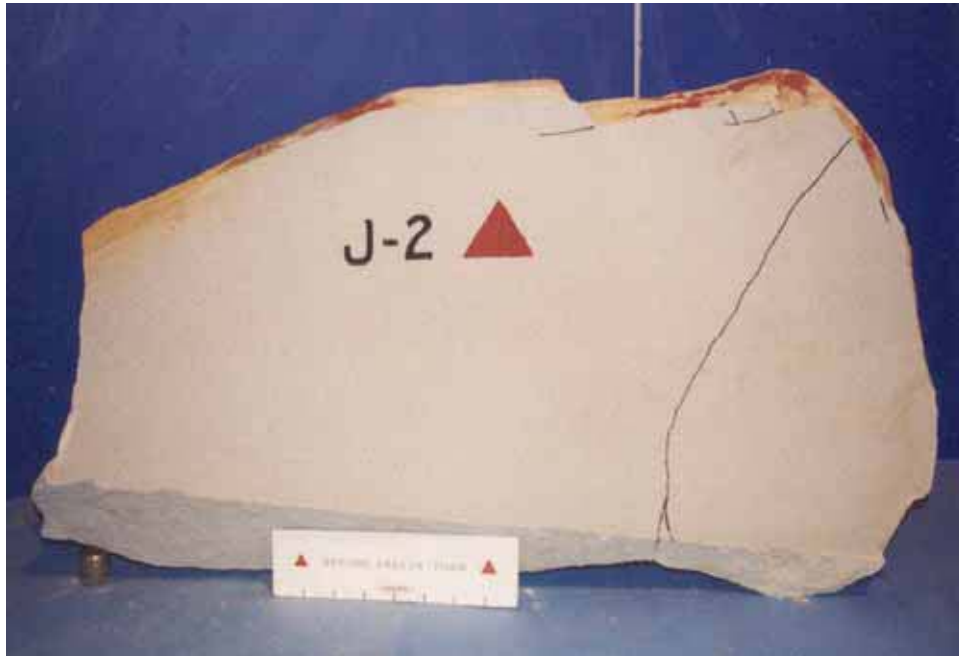


Figure 50. Johnson Quarry Berea formation sandstone accelerated weathering durability Test Block J-2-FT (Test Block J-2 after freeze/thaw testing)

The test block is light gray, fine to medium grained, well-rounded to subangular grains, well packed, poorly cemented sandstone. Grains consist of mostly quartz with iron-minerals and occasional feldspar and rock fragments. Fringing and meniscus cement bonds the grains at their contacts, but results in a porous rock property. The test block is of massive structure with no bedding or grain orientation. Oxidation of intergranular ferruginous cement exists near the surface of one surficial boundary and permeates the sample about 13 cm (5 in.). This is indicative of a readily permeable material. On fresh surfaces, the sample has a tendency to be susceptible to grain disaggregation when rubbed by a finger.

Overall, the test block is porous, hard, and tough. The freeze/thaw percent loss was 0.56 percent, due to surficial spalling and disaggregation of surficial grains. The specific gravity was 2.22. Absorption was 7.36, and adsorption was 0.18, resulting in an adsorption/absorption ratio of 0.02.

Thornton Quarry Durability Test Results

Test Block MTC-1-FT/WD. This test block (Figure 51) was subjected to both freeze/thaw and wet/dry testing. No samples were extracted from this test block for microstructural analyses.



Figure 51. Thornton Quarry Racine formation dolomite accelerated weathering durability Test Block MTC-1-FT/WD

The test block is light to medium bluish-gray, fine-grained, micritic dolomite with a highly mottled texture. Bedding is determined by algal mat remnant structures oriented elongate to the horizontal length of the samples. These algal structures are fine grained, ranging from white to a dark bluish-gray color and often are quite dense. These structures are rarely more than 2.0 cm (0.8 in.) thick and are continuous across the entire length of the sample. They are mostly sinuous to wavy, and do not affect the parting of the sample.

The ground matrix of the sample is mostly fine-grained micritic dolomite with common, small, dissolution voids of fossil fragments, mostly crinoid fragments. The areas are porous but rarely permeable on the macroscopic range. Occasional dolomitized fossil fragments are observable as ghostly white fossil fragments with no distinct boundaries.

Two major open fractures are present. One runs perpendicular to the bedding planes, the other runs parallel to the bedding. They both are sinuous and continuous before dissipating into the groundmass. These are not major weaknesses, but could be deleterious to the overall strength of the sample. In fact, the slab fractured along the bedding planes during sawing.

Overall, the test block is dense, tough, and hard. The freeze/thaw percent loss was 0.37 percent, due to surficial spalling. The wet/dry percent loss was 0.28 percent, due to surficial spalling. The specific gravity was 2.70. Absorption was 1.56, and adsorption was 0.21, resulting in an adsorption/absorption ratio of 0.13.

Test Block MTC-2-FT. This test block (Figure 52) was subjected to freeze/thaw testing only. No samples were extracted from this test block for micro-structural analyses.



Figure 52. Thornton Quarry Racine formation dolomite accelerated weathering durability Test Block MTC-2-FT

The test block is light to medium bluish-gray, fine-grained, micritic dolomite with a highly mottled texture. Bedding is determined by algal mat remnant structures oriented elongate to the horizontal length of the samples. These algal structures are fine grained, ranging from white to a dark bluish-gray color and often are quite dense. These structures are rarely more than 3 cm (1.2 in.) thick and are continuous across the entire length of the sample. They are mostly sinuous to wavy, and do not affect the parting of the sample.

The ground matrix of the sample is mostly fine-grained micritic dolomite with rare, small, dissolution voids of fossil fragments. Occasional dolomitized fossil fragments are observable as ghostly white fossil fragments with no distinct boundaries. One, major, open fracture is present. It traverses parallel to the bedding, sinuously and continuous before dissipating into the groundmass.

Overall, the test block is dense, tough, and hard. The freeze/thaw percent loss was 0.11 percent, due to minor surficial spalling. The specific gravity was 2.73. Absorption was 0.67, and adsorption was 0.25, resulting in an adsorption/absorption ratio of 0.37.

Test Block MTC-3-FT/WD. This test block (Figure 53) was subjected to both freeze/thaw and wet/dry testing. Samples MTC-3A-FT/WD and MTC-3B-FT/WD were extracted from this test block. Subsequently, Thin Section Samples TS-MTC-3A-1FT/WD and TS-MTC-3A-2FT/WD were extracted from Sample MTC-3A-FT/WD. Thin Section Samples TS-MTC-3B-1FT/WD and TS-MTC-3B-2FT/WD were extracted from Sample MTC-3B-FT/WD.

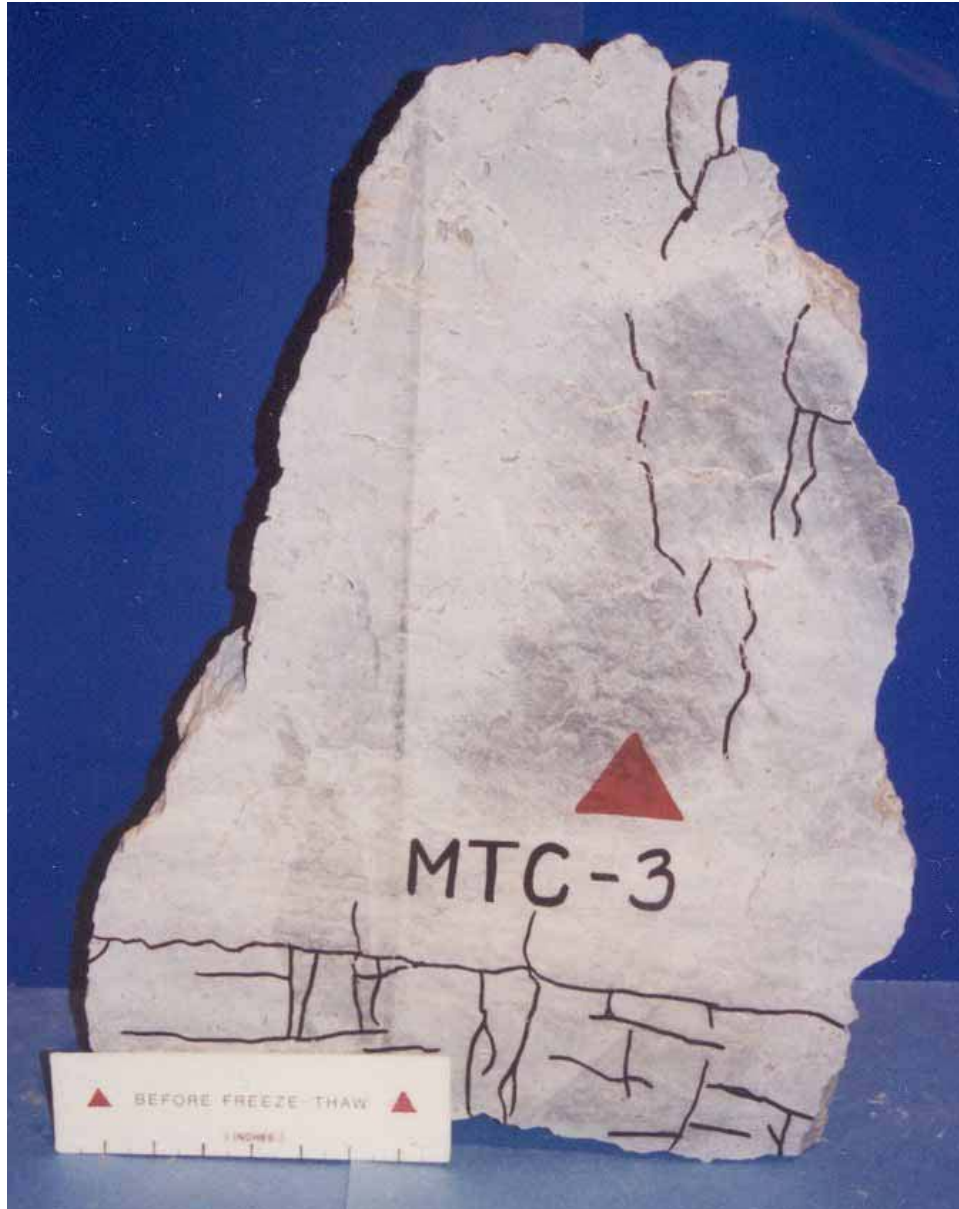


Figure 53. Thornton Quarry Racine formation dolomite accelerated weathering durability Test Block MTC-3-FT/WD

The test block is light to medium bluish-gray, fine-grained, micritic dolomite with a highly mottled texture. Bedding is determined by algal mat remnant structures oriented elongate to the horizontal length of the samples. These algal structures are fine grained, ranging from white to a dark bluish-gray color and

often are quite dense. These structures are rarely more than 2.0 cm (0.8 in.) thick and are continuous across the entire length of the sample. They are mostly sinuous to wavy, and do not affect the parting of the sample.

The ground matrix of the sample is mostly fine-grained micritic dolomite with common, small, dissolution voids of fossil fragments, mostly crinoid fragments. The areas are porous but rarely permeable on the macroscopic range. Occasional dolomitized fossil fragments are observable as ghostly white fossil fragments with no distinct boundaries.

The sample is highly fractured, with fractures running mostly parallel and perpendicular to the bedding planes. Most of the fractures are sinuous and continuous before dissipating into the groundmass. Some are present for only short distances. These fractures have the potential of becoming prominent weaknesses and many small fractures could join to form a major parting.

Overall, the test block is dense, tough, and hard, but highly fractured. The freeze/thaw percent loss was 0.38 percent, due to surficial spalling. The wet/dry percent loss was 0.51 percent, due to surficial spalling. The specific gravity was 2.69. Absorption was 0.82, and adsorption was 0.07, resulting in an adsorption/absorption ratio of 0.09.

Test Block MTC-4-FT/WD. This test block (Figure 54) was subjected to both freeze/thaw and wet/dry testing. No samples were extracted from this test block for microstructural analyses.

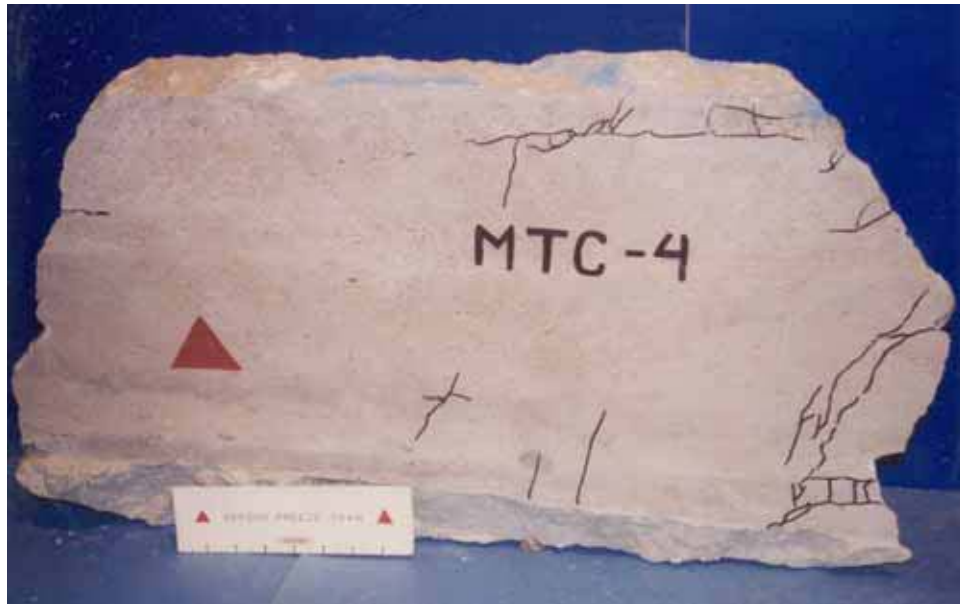


Figure 54. Thornton Quarry Racine formation dolomite accelerated weathering durability Test Block MTC-4-FT/WD

The test block is light to medium bluish-gray, fine-grained, micritic dolomite with a highly mottled texture. Bedding is determined by algal mat remnant structures oriented elongate to the horizontal length of the samples. These algal

structures are fine grained, ranging from white to a dark bluish-gray color and often are quite dense. These structures are thick, approximately 11.0 cm (4.3 in.), and are continuous across the entire length of the sample. They are mostly sinuous to wavy, and do not affect the parting of the sample.

The ground matrix of the sample is mostly fine-grained micritic dolomite with common, small, dissolution voids of fossil fragments, mostly crinoid fragments. These areas are porous but rarely permeable on the macroscopic range. Occasional dolomitized fossil fragments are observable as ghostly white fossil fragments with no distinct boundaries.

A multitude of small, open fractures are present near the surfaces of the samples. Also, occasional, noncontinuous, fractures, running perpendicular and parallel to the bedding planes are present. These traverse sinuously before dissipating into the groundmass.

Overall, the test block is porous, tough, and hard. The freeze/thaw percent loss was 1.41 percent, due to small surficial fracture partings. The wet/dry percent loss was 0.26 percent, due to surficial spalling. The specific gravity was 2.70. Absorption was 0.97, and adsorption was 0.06, resulting in an adsorption/absorption ratio of 0.06.

Test Block MTC-5-FT/WD. This test block (Figure 55) was subjected to both freeze/thaw and wet/dry testing. No samples were extracted from this test block for microstructural analyses.



Figure 55. Thornton Quarry Racine formation dolomite accelerated weathering durability Test Block MTC-5-FT/WD

The test block is light to medium bluish-gray, fine-grained, micritic dolomite with a highly mottled texture. Bedding is determined by algal mat remnant structures oriented elongate to the horizontal width of the samples. These algal

structures are fine grained, ranging from white to a dark bluish-gray color and often are quite dense. These structures are rarely more than 5.0 cm (2 in.) thick and are continuous across the entire width of the sample. They are mostly sinuous to wavy, and can affect the parting of the sample.

The ground matrix of the sample is mostly fine-grained micritic dolomite with common, small, dissolution voids of fossil fragments, mostly crinoid fragments. The areas are porous but rarely permeable on the macroscopic range. Occasional dolomitized fossil fragments are observable as ghostly white fossil fragments with no distinct boundaries. Occasional thin, black, continuous, low amplitude, high frequency stylolites are present.

Several major open fractures are present. Most run parallel to the bedding planes, some run perpendicular to the bedding. They are mostly sinuous and continuous before dissipating into the groundmass. Some are major weaknesses, and could be deleterious to the overall strength of the sample. In fact, the freeze/thaw sample attained much loss because the slab fractured along a bedding plane and a stylolite during testing.

Overall, the test block is dense, tough, and hard. The freeze/thaw percent loss was 36.52 percent, due to open fracturing of bedding planes and of stylolitic seams. The wet/dry percent loss was 0.78 percent, due to surficial spalling. (53.2 percent loss was attained during sawing.) The specific gravity was 2.67. Absorption was 1.05, and adsorption was 0.18, resulting in an adsorption/absorption ratio of 0.17.

Summary of MCNP Durability Testing by ORDL

Accelerated weathering test results for the 17 stone test blocks evaluated by ORDL for this MCNP study are presented in Table 1.

Other Durability Testing by ORDL

The five samples from the McCook Quarry, McCook, IL, that had previously been analyzed by ORDL during a study by STS Consultants Ltd. (1992) were dolomite samples weighing 680 to 907 kg (1,500 to 2,000 lb) each. Results from these sample analyses were incorporated into the field prototype monitoring conclusions.

Additionally, six other quarry samples had been analyzed by ORDL under another ongoing annual quarry inspection program in 1994. These quarry samples were placed on the Calumet Harbor CDF revetment structures in 1995 as part of this present MCNP study. Results from these sample analyses also were incorporated into the field prototype monitoring conclusions. The six samples analyzed by ORDL and placed on the Calumet Harbor CDF include:

Table 1 Accelerated Weathering Test Results						
Quarry and Sample No.	Percent Loss			Specific Gravity	Absorption	Adsorption
	Sawing	Freeze/Thaw	Wet/Dry			
Reed						
R-1-FT	0.00	41.80	0.00	2.43	3.80	0.11
Valders						
V-1-FT	0.00	0.28	0.00	2.78	1.00	0.08
V-2-FT	31.60	0.25	0.00	2.76	1.04	0.05
Dempsey						
D-1-FT	0.00	0.83	0.00	2.69	0.08	0.01
D-3-FT	0.00	0.25	0.00	2.68	0.10	0.01
Sandusky						
S-1-FT/WD	23.60	0.51	0.00	2.55	3.27	0.07
S-2-FT	0.00	4.10	0.17	2.63	2.87	0.20
Marblehead						
M-1-FT	0.00	0.31	0.00	2.58	3.21	0.05
M-2-WD	48.50	0.00	0.25	2.63	2.11	0.06
M-3-FT/WD	50.00	0.12	0.52	2.52	4.46	0.06
Johnson						
J-1-WD	0.00	0.00	0.17	2.23	8.86	0.07
J-2-FT	0.00	0.56	0.00	2.22	7.36	0.18
Thornton						
MTC-1-FT/WD	0.00	0.37	0.28	2.70	1.56	0.21
MTC-2-FT	0.00	0.11	0.00	2.73	0.67	0.25
MTC-3-FT/WD	0.00	0.38	0.51	2.69	0.82	0.07
MTC-4-FT/WD	0.00	1.41	0.26	2.70	0.97	0.06
MTC-5-FT/WD	53.20	36.50	0.78	2.67	1.05	0.18

- a. Valders Quarry, Valders, WI: Three dolomite samples weighing 680 to 907 kg (1,500 to 2,000 lb) each, and were obtained from the upper, middle, and lower lifts.
- b. Reed Quarry, Bloomington, IN: One limestone sample weighing 680 to 907 kg (1,000 to 1,500 lb).
- c. Iron Mountain Quarry, Iron Mountain, MI: Two taconite stone samples weighing 907 to 1,360 kg (2,000 to 3,000 lb) each.

Thus, a sum total of 28 stone samples were subjected to accelerated environmental freeze/thaw and wet/dry weather conditions by ORDL for analyses and incorporation into the field prototype monitoring conclusions.

Conclusions

The number of freeze/thaw cycles a stone in the Cleveland and Chicago areas experiences each year can be much greater than the 30 to 50 cycles conducted during these accelerated weathering durability tests. Therefore, results drawn from these lab tests may not be sufficient to accurately predict the performance under the harsh effects of the Great Lakes.

4 Quarry Sample Microstructural Analyses¹

Agar (1998) performed one part of the quarry investigations of this MCNP study regarding microscale structural features in rock that affect stability. The investigations also determined the relationships of the microscale structural features to compositional and textural variations. Agar (1998) analyzed 27 samples taken from 14 of 18 test blocks obtained from seven different quarries. Seventeen of the 18 test blocks had previously undergone accelerated weather exposure testing (freeze/thaw and/or wet/dry) at the U.S. Army Corps of Engineers, Ohio River Division Laboratory, Cincinnati, OH. One test block was evaluated prior to any freeze/thaw and/or wet/dry exposure. These 14 test blocks evaluated by Agar (1998) had come from quarries from which stone had been used on prototype structures selected for field monitoring due to premature stone deterioration. This microstructural study included (a) sample cutting, photography, and preparation of thin sections, (b) optical microscopy for basic petrographic description and photomicrographs, (c) secondary and backscatter electron microscopy, (d) electron microprobe analysis, and (e) image scattering and digital image processing for data compilation, and for evaluation of grain sizes and porosity.

Reed Quarry

Test block, samples, and thin sections

Test Block R-1-FT. Test Block R-1-FT (Figure 56) from the Reed Quarry was subjected to freeze/thaw testing. The test block lithology is classified as a grainstone under Dunham's modified classification of limestones (Dunham 1962; Embry and Klovan 1971). In hand specimens, the rock is gray buff color with greater than 80 percent bioclastic grains. The most prominent feature in the block is a stylolite along which the block split into two parts before sampling. The surface of the block has a pitted texture with fine gray brown powder in the stylolitic seam and in some of the pits. Bedding can be clearly identified by the alignment of shell fragments concentrated in some laminations but the way-up could not be ascertained. Two samples (Samples R-1A-FT and R-1B-FT) were taken from the block.

¹ This section is extracted essentially verbatim from Agar (1998).

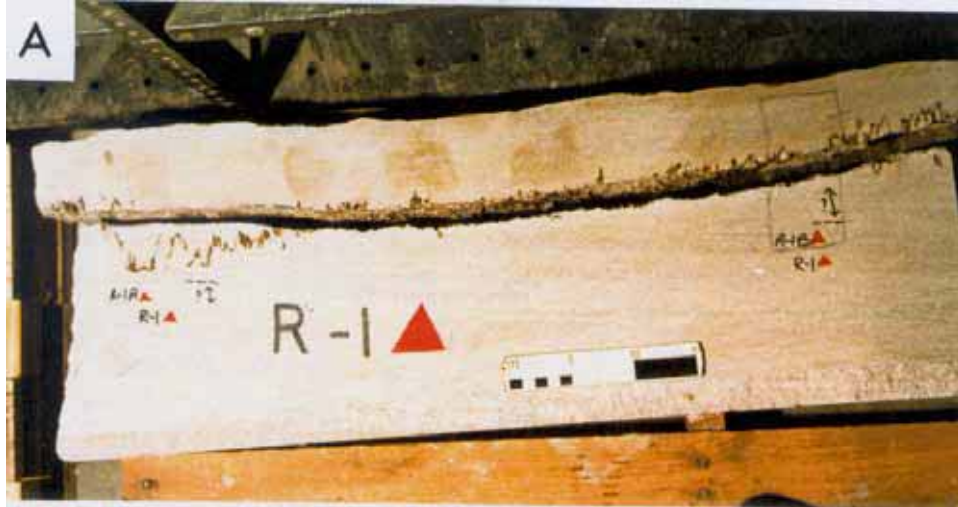


Figure 56. Reed Quarry Test Block R-1-FT, front surface and sample locations near open fractures. Way-up is unknown, but stylolitic seams are known to be approximately parallel to bedding. Double-headed arrows show directions perpendicular to bedding (after Agar 1998)

- a. *Sample R-1A-FT.* This sample (Figure 57) was located in one half of the test block to include a portion of the stylolite seam that did not coincide with the main throughgoing fracture. The stylolite has an undulation amplitude of up to 5 cm (2 in.) and is delineated by dark brown/black staining that varies in thickness from less than 1 mm (0.04 in.) to 0.5 cm (0.2 in.). Thin Section Sample TS-R-1A-1FT was located on the original marked surface of the block with the stylolite centrally located in the section. Thin Section Sample TS-R-1A-2FT was placed on a vertical plane perpendicular to the original marked surface to sample the stylolite. Thin Section Sample TS-R-1A-3FT was located away from the stylolite seam to examine the undisrupted fabric (not shown). Thin Section Sample TS-R-1A-3FT was stained with K-ferricyanide (ferrous carbonate).
- b. *Sample R-1B-FT.* This sample (Figure 58) was located to include an open surface of the stylolite that controlled the main throughgoing fracture. Part of the stylolite seam surface was exposed on the marked side of the test block as well as along the open fracture surfaces. Thin Section Sample TS-R-1B-1FT was placed on the marked side of the test block to include the open stylolite surface and the region within 1.5 cm (0.6 in.) of it. Thin Section Sample TS-R-1B-2FT was cut parallel to the seam surface so that the thin section would provide a view down onto the stylolite seam to compare grain shape fabrics.



Figure 57. Reed Quarry Sample R-1A-FT, including stylolite seam (after Agar 1998)

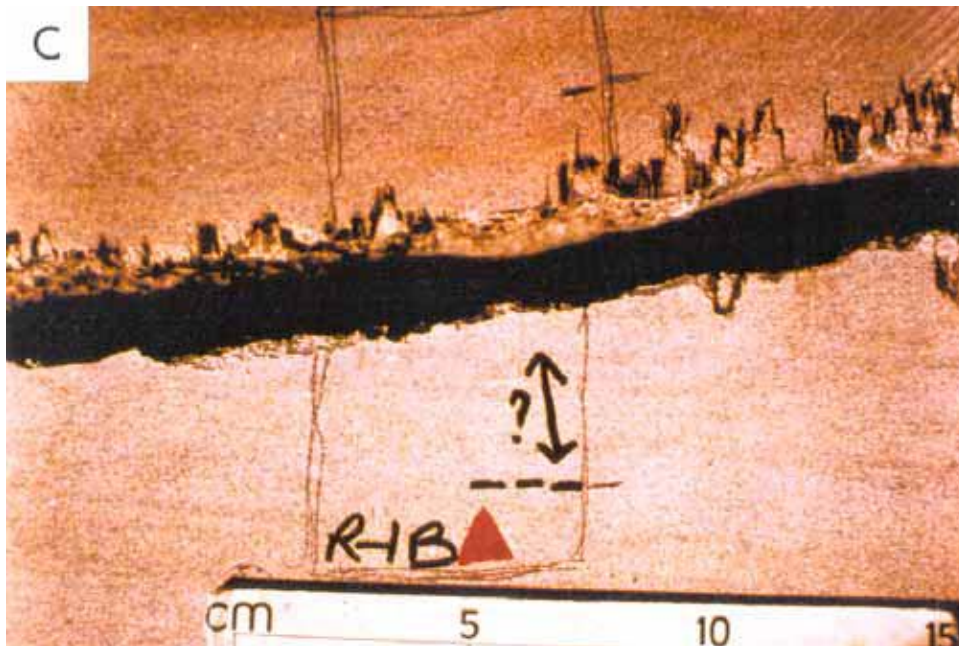


Figure 58. Reed Quarry Sample R-1B-FT (after Agar 1998)

Composition, grain size, and porosity

The Reed Quarry thin sections show the rock is predominantly supported by bioclastic grains (80 to 90 percent of the rock). Identified clasts include bivalve shell fragments with micritic envelopes, echinoderm fragments, crinoid stems and gastropods. Bivalve fragments commonly align with their long axes parallel to bedding planes as evenly distributed clasts and as concentrations within laminations. The bulk of the rock is calcite (both cement and bioclasts), but the stylolites contain clastic material comprising potassium feldspar, quartz, and Fe-sulfides in a potassium bearing clay matrix. No dolomite was detected either by staining or under backscatter imaging, but the calcite grains have slight variations in iron content.

The grain sizes of bioclasts range from 0.05 mm (0.002 in.) to greater than 0.08 in. (2 mm) (e.g., elongate shell fragments). The calcite cement grains generally fall in the range of 0.01 to 0.5 mm (0.0004 to 0.02 in.). The average estimate of the mean cement grain size from digital images is 0.11 mm. Clasts within the stylolite seams range from less than 1 micron (0.00004 in.) to 100 microns (0.004 in.). The mean porosity on thin section scale is estimated from digital images to be 20 percent. Porosity is controlled by different elements, including the body cavities of bioclasts, the body structure of bioclasts and the intergranular porosity. Some pore space exhibits ragged edges that may represent local dissolution. Although some grains may have been plucked during sample preparation, some of the remaining pore space could represent relict primary porosity that was never filled.

Texture and diagenesis

The original depositional texture of the rock has been modified by pressure solution. Grains are abruptly truncated by pressure solution seams and, in places, more than 50 percent of the original grain has probably been removed. The distribution of pressure solution is heterogeneous. In places, grains are only slightly affected by pressure solution and the primary depositional character is preserved. In sections that are cut perpendicular to bedding planes there is a clear preferred orientation of elongate clasts parallel to bedding. However, in the thin section that parallels bedding, the preferred alignment is less well developed and the cross-sectional areas of grains tend to be more circular than elliptical. Thus, there appears to be a grain-shape preferred orientation of clasts introducing a weak anisotropy into the rock.

Although the thin sections contain regions of strong pressure solution associated with stylolites, other parts of the sample preserve only minor amounts of pressure solution. The rock is grain supported, but the undeformed sparry calcite cement filling relatively large pore spaces preserved locally suggests that cementation probably occurred before significant compaction. The heterogeneous nature of pressure solution preserves some of this early texture.

The bioclastic grains are replaced and filled by calcite with fibrous, micritic, and sparry textures. Brachiopod shells are commonly fibrous in appearance and in places micritized. Echinoderm fragments and crinoid platelets that have been

completely micritized are also evident. The primary structure has been obliterated in many crinoid fragments although their uniform extinction indicates that they are still single crystals. Late, cavity infilling calcite has large crystals with smooth, well-polished surfaces. Where calcite has replaced bioclast body structures the cement has a pitted appearance. Some regions have relatively high proportions of calcite cement (up to 50 percent) that has grown as coarse sparry grains between bioclasts.

Under backscatter imaging, subtle variations in the composition of the calcite are evident. Narrow zones within crystals have higher proportions of iron in them. They appear to represent growth zones formed during influxes of more iron-rich fluids as the calcite grain was expanding to fill remaining pore space. Some zoning patterns are more or less concentric whereas others have a strong asymmetry that may indicate the growth direction of calcite into cavities. The consistent backscatter-contrasts of the calcite in the cement and that filling the cavities in the bioclasts indicate that their compositions are similar. Calcite cementation clearly preceded the generation of stylolite seams as calcite cement grains are truncated by the seams. Minor fractures across bioclasts that were probably formed during compaction are also sealed by calcite cement suggesting that the cement formed relatively early in the rock's formation. Straight, even thickness twins in the sparry cement indicate that differential stresses were not high during burial. There is no indication of static recrystallization during metamorphism, and so the maximum burial depths are inferred to be relatively shallow.

Fractures, stylolites, and grain fabric

The microstructures in the two Reed Quarry samples are similar and are therefore summarized together. Fractures are relatively sparse in the Reed samples apart from those localized by stylolite seams. Irregular intragranular microcracks dismember some of the calcite grains. Intergranular fracturing in calcite cement also forms micro arrays of en-echelon fractures and splays, but these fractures do not penetrate the bioclasts. Crystallographic cleavage planes have also opened in places but represent only very minor damage. The fractures in the calcite cement are open with no evidence of secondary mineral fill within them. Where fractures have opened along the stylolite seams the fracture surface is coated with clays that envelope bioclast grains protruding from the fracture surface. No striations or kinematic indicators were evident on the fracture surface, nor was any major increase in fracture damage approaching the surface. Straight, even thickness twins in the sparry cement indicate that differential stresses were not high during burial. There is no indication of static recrystallization during metamorphism and so the maximum burial depths are inferred to be relatively shallow.

Stylolites represent the major structures in the Reed samples that will localize breakup. The unstable nature of these structures is indicated by the extensive plucking of material from the stylolite seams during thin section preparation. The stylolites have a fractal character in which the short limbs of the stylolites are effectively formed by short wavelength stylolites. The pressure solution that generated these structures has dissolved substantial proportions of bioclasts

(greater than 50 percent in some cases) and calcite cement that forms an apparent offset across the seam. Minor rotations caused by the dissolution of material are the most likely cause of abrupt changes in extinction across stylolite seams. The homogeneous backscatter contrast in the surrounding limestone indicates that the pressure solution has had minimal effect on the calcite composition.

The stylolites contain clasts of quartz, feldspar, minor Fe-Ti oxides (bright phases) as well as a clay matrix. They appear to have localized along silty layers within the limestone. The presence of clays may have promoted dissolution within adjacent bioclastic grains and calcite cement although new clay growth may have occurred within the seams. As dissolution proceeded, clasts that could not be readily dissolved from the silty layers and residual material from the surrounding clasts were left in the seams as contorted layers. More of the detrital material tends to be preserved along the short ends of the stylolites versus the sides that are perpendicular to bedding. They are also dissected by numerous microcracks that follow irregular traces within the seam as well as along the seam margin. These cracks may be caused by desiccation of clay minerals prior to epoxy impregnation but may also be related to stress release during the exhumation of quarry blocks. There are domains of weak shape preferred orientation where clasts of quartz are aligned parallel to the seam margins. The irregular, wavy margins of the quartz grains indicated extensive dissolution of the clasts that probably controlled the shape preferred orientation. Opaque phases have been concentrated by their resistance to dissolution relative to other phases.

Summary

The dominant features that affect failure in the Reed Quarry samples are clearly the stylolite seams. The stylolites are oriented subparallel to bedding; thus, any blocks used in breakwater construction would be better oriented with the bedding horizontal rather than vertical to avoid axial splitting. Of all the carbonate rocks examined in this study, the Reed samples have by far the most continuous and the highest amplitude stylolites. Although the process of pressure solution can help to cement the rock, the relatively high proportion of clay material left in the pressure solution seams can make the stylolites vulnerable to surface weathering and relatively weak.

Regions away from stylolite seams appear to be stable. Once a block has separated along a stylolite seam it may be relatively stable within a breakwater construction. Other features such as microcracks and grain shape fabric appear to be relatively insignificant compared to the potential impact of any stylolite seam. Neither cementation nor weathering away from the stylolite seams appear to influence the location of weaknesses within the rock.

Recommendations

- a. Further studies of the Reed Quarry should quantify the distribution of the major stylolite seams similar to those in the block examined here. It is important to understand their spatial distribution on the scales of blocks used in armor stone as well as their distribution through the entire quarry.

- b. Examine other potential sources of breakup in the quarry and breakwater settings such as fractures at a high angle to bedding generated during unloading.
- c. Examine the possible role of grain size and shape preferred orientations in breakwater blocks in localizing mesoscale fractures.
- d. It is critical to map out the development of fractures in the breakwaters over multiyear periods to constrain the timing of possible breakup along stylolite seams and in other areas such as at point contacts between blocks or at different levels within the breakwater.

Valders Quarry

Test blocks, samples, and thin sections

Test Block V-1-FT. Test Block V-1-FT (Figure 59) is an extremely homogeneous fine-grained dolomite, and was subjected to freeze/thaw testing only. Samples V-1A-FT and V-1B-FT are gray-buff fine-grained dolomite. In hand sample, fine-grained light brown gray clay/organic seams can be traced through the specimen, but the rock is otherwise extremely homogeneous with sparse, small vugs (generally less than 1 mm (0.04 in.)). The fractured surfaces of both samples are irregular and preserve fine overlapping layers controlled by microfractures that form subparallel to the main fracture surface. A fine white powder has formed in irregular patches over the fracture surface. No absolute orientation could be determined from the samples but double-headed arrows were marked perpendicular to interpreted bedding planes, as delineated both by clay seams and subtle changes in grain size indicated by color changes. The test block was relatively free of damage, containing only fine cracks within the blocks. The Thin Section Samples V-1A-FT and V-1B-FT contain examples of the primary damage areas, even though these are minimal.

- a. *Sample V-1A-FT.* This sample (Figure 60) was selected to include a pretest (black line) fracture located close to one margin of the test block. The fracture follows a curvilinear trace, branching away from the fractured edge of the test block and then veering towards it again. Thin Section Sample TS-V-1A-1FT was cut on the original marked surface of the test block whereas Thin Section Sample TS-V-1A-2FT was taken from a vertical surface perpendicular to that original surface. The two sections were positioned to include the same fracture plane so that possible textural anisotropies would be detected. On the second surface the fracture divides into two fractures with traces subparallel to light brown clay seams. Thin Section Sample TS-V-1A-1FT was stained for calcite using Alizarin red. Thin Section Sample TS-V-1A-2FT was stained for ferrous carbonate using K-ferricyanide.
- b. *Sample V-1B-FT.* This sample (Figure 61) was selected to include the fractured edge of the test block. As previously described, the fracture has an irregular trace. Thin Section Sample TS-V-1B-1FT was cut parallel to the original marked surface of the sample to include the fractured edge

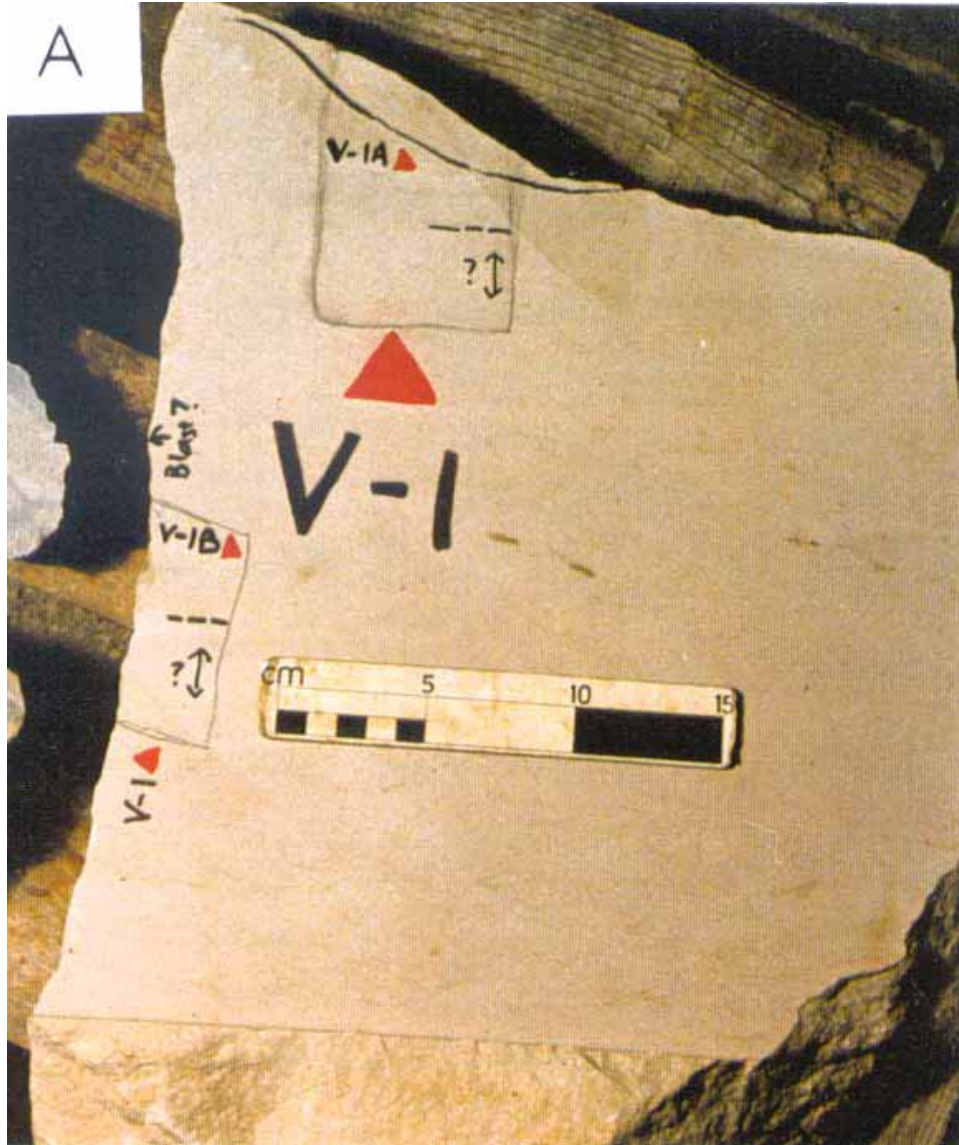


Figure 59. Valders Quarry Test Block V-1-FT sample locations. Arrows show direction perpendicular to interpreted bedding plane based on fine color banding and clay seams (after Agar 1998)

and as much of the sample adjacent to it as a single thin section could contain. This section was placed to evaluate the possible maximum lateral extent of damage associated with the fracture although no subsidiary fractures were evident in the hand sample. Thin Section Sample TS-V-1B-2FT was cut on the opposite, parallel face of the block but was placed lengthwise to examine variations in damage intensity along the fracture surface. This section contained a subsidiary fracture that splayed into the section, subparallel to the main fracture surface. The second thin section was stained for ferrous carbonate.

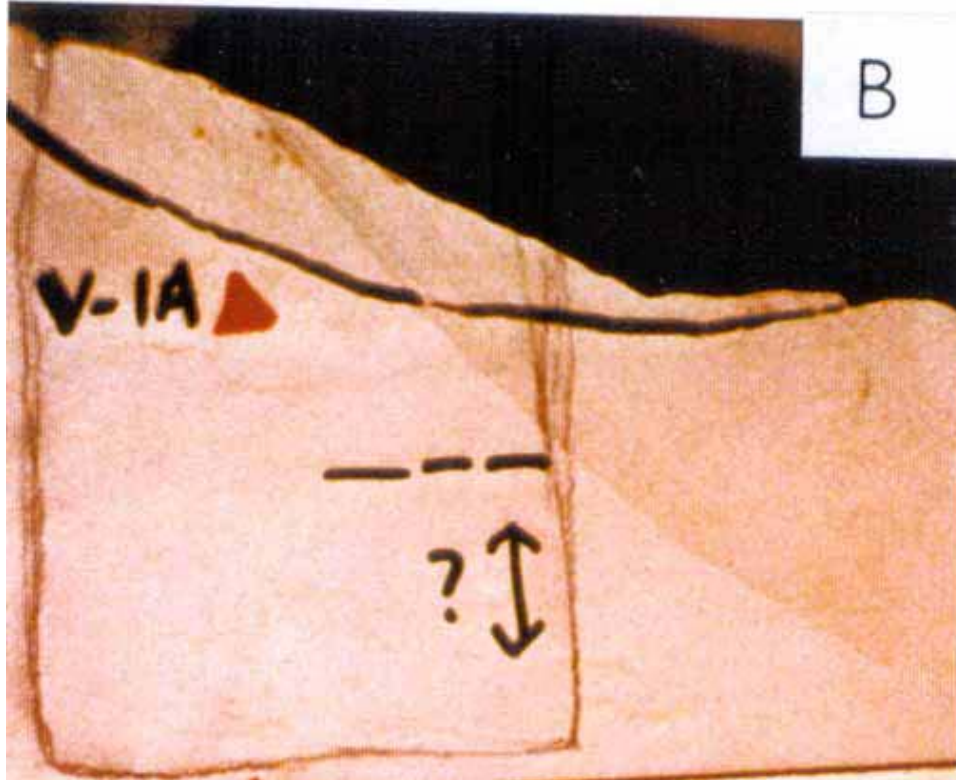


Figure 60. Valders Quarry Sample V-1A-FT close-up (after Agar 1998)

Test Block V-2-FT. Test Block V-2-FT (Figure 62) is a vuggy, fractured sample, and was subjected to freeze/thaw testing only. Samples V-2A-FT and V-2B-FT contrast with the Test Block V-1-FT samples, being a buff gray fine to medium-grained dolomite with numerous irregular vugs, some exceeding 2 cm (0.8 in.) in length. The samples have a mottled appearance with dark gray and light brown patches distributed through the rock. The gray patches are commonly, but not always associated with vuggy areas or relict coral fragments. The light brown areas generally represent fine clay seams, some of which have stylolitic traces with undulation amplitudes of up to 2 cm (0.8 in.). As in the Test Block V-1-FT samples, the clay seams are interpreted to be approximately parallel to bedding. Grain size variations occur in irregular patches with drusy fabrics around the vugs. Both of these samples exhibit more fracture damage than the Test Block V-1-FT samples. Irregular fracture traces tend to be deflected along vuggy regions. Both steeply dipping and shallow dipping fractures are evident. Sample V-2A-FT contains a subvertical hairline fracture (post-test) that cuts across the whole sample. Sample V-2B-FT contains an irregular open fracture (pretest) dipping at about 60 deg that divides the sample into two parts.

- a. *Sample V-2A-FT.* This sample (Figure 63) was selected to include several irregular pretest fractures and one post-test fracture. Overall this sample has fewer vugs than Sample V-2B-FT, but they are otherwise similar. Thin Section Sample TS-V-2A-1FT includes the fractured edge of the surface block and a zone of irregular pretest fractures. Thin Section Sample TS-V-2A-2FT contains the steeply dipping post-test

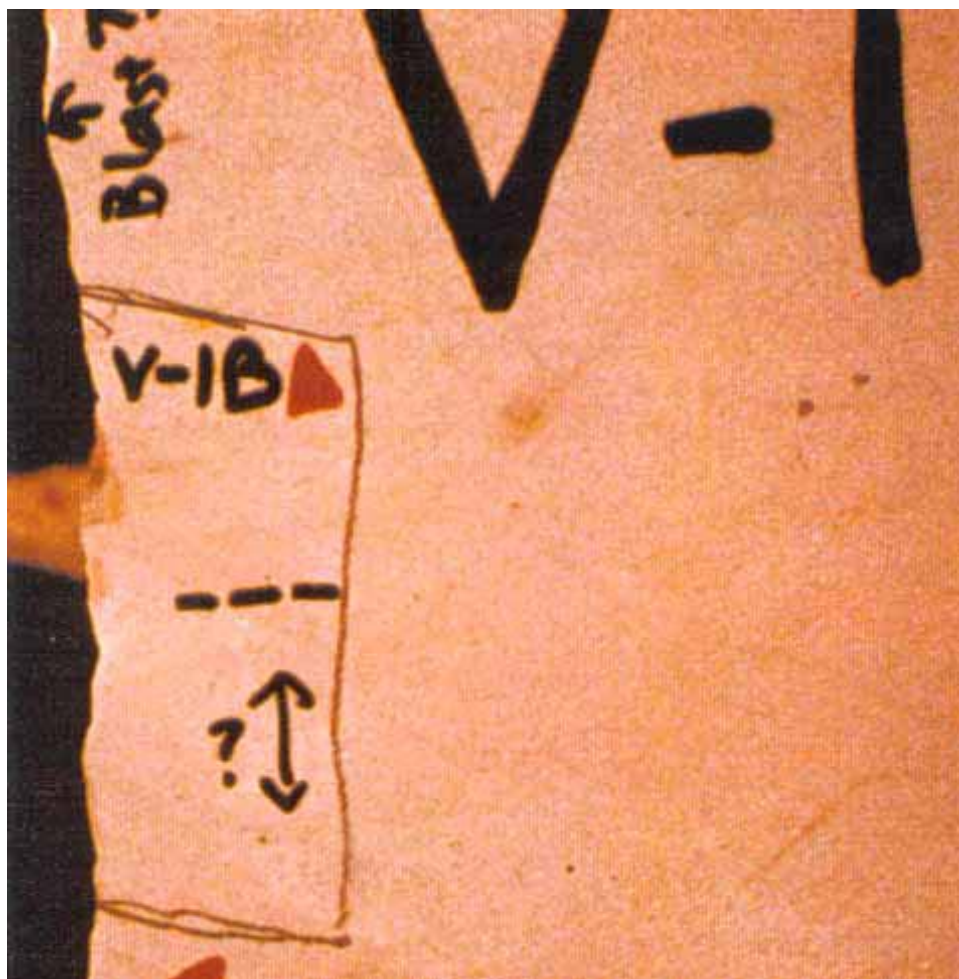


Figure 61. Valders Quarry Sample V-1B-FT close-up (after Agar 1998)

fracture and the edge of the surface block. Thin Section Sample TS-V-2A-3FT is on an orthogonal surface and contains another section of the post-test fracture where its orientation parallels a vuggy region. This thin section also includes a microstylolite seam and the fractured edge of the test block. Both Thin Section Samples TS-V-2A-2FT and TS-V-2A-3FT contain overlapping fracture segments. All three sections were cut parallel to the original marked surface of the block. Thin Section Sample TS-V-2A-3FT was stained for calcite with Alizarin Red.

- b. *Sample V-2B-FT.* This sample (Figure 64) includes the open pretest fracture surface previously described. Brown clay minerals are exposed on the fracture surface where stylolitic seams intersect it. Thin Section Sample TS-V-2B-1FT was cut to include the open fracture surface and the pretest fracture branching from it. A second pretest fracture also crosses the section at a low (approximately 10 deg) angle. The second pretest fracture links to the open fracture surface on the right hand side of the sample. The second Thin Section Sample TS-V-2B-2FT contains a microstylolitic seam and several vugs, as well as the open pretest fracture surface. Both sections were cut parallel to the original marked surface of the test block.



Figure 62. Valders Quarry Test Block V-2-FT sample locations. Arrows show direction perpendicular to interpreted bedding planes based on clay seams and associated stylolites (after Agar 1998)

Composition, grain size, and porosity

The test blocks from the Valders Quarry used in this study compose predominantly fine-grained dolomite. Authigenic feldspar grains are dispersed through the dolomite and generally have a finer grain size. Within fine, proto-stylolite seams, grains of potassium feldspar, quartz, dolomite, opaques, and clay minerals are present. Dolomite represents between 80 and 90 percent of the rock with varying proportions of authigenic feldspar (orthoclase) making up most of the rest. Quartz, clays, and opaques represent less than 2 percent of the rock volume.

The average grain size ranges from 20 to 40 microns (0.0008 to 0.0016 in.) based on estimates from digital images. The authigenic feldspar grains generally represent the smaller grains in the grain size spectrum. Changes in grain size occur across curvilinear boundaries in both Test Blocks V-1-FT and V-2-FT. Given the extensive dolomitization of all the Valders samples, it is difficult to determine whether changes in grain size reflect primary grain size laminations or whether they are related to subsequent replacement processes. The changes in grain size commonly coincide with compositional variations. Finer-grained



Figure 63. Valders Quarry Sample V-2A-FT close-up (after Agar 1998)

regions have more authigenic feldspar whereas the coarser grain size regions compose dolomite with scattered, fine crystals of authigenic feldspar. Very-fine-grained dolomite may have replaced earlier micritic horizons.

The porosity is spatially variable in character and quantity. Intergranular porosity is typically low, but vugs up to 20 mm (0.8 in.) in length cause local elevations in porosity. Overall the porosity in Test Block V-2-FT is higher than that in the finer grained relatively vug-free Test Block V-1-FT. The vugs resemble fenestrae formed as secondary porosity resulting from gas pockets that form in supratidal environments.

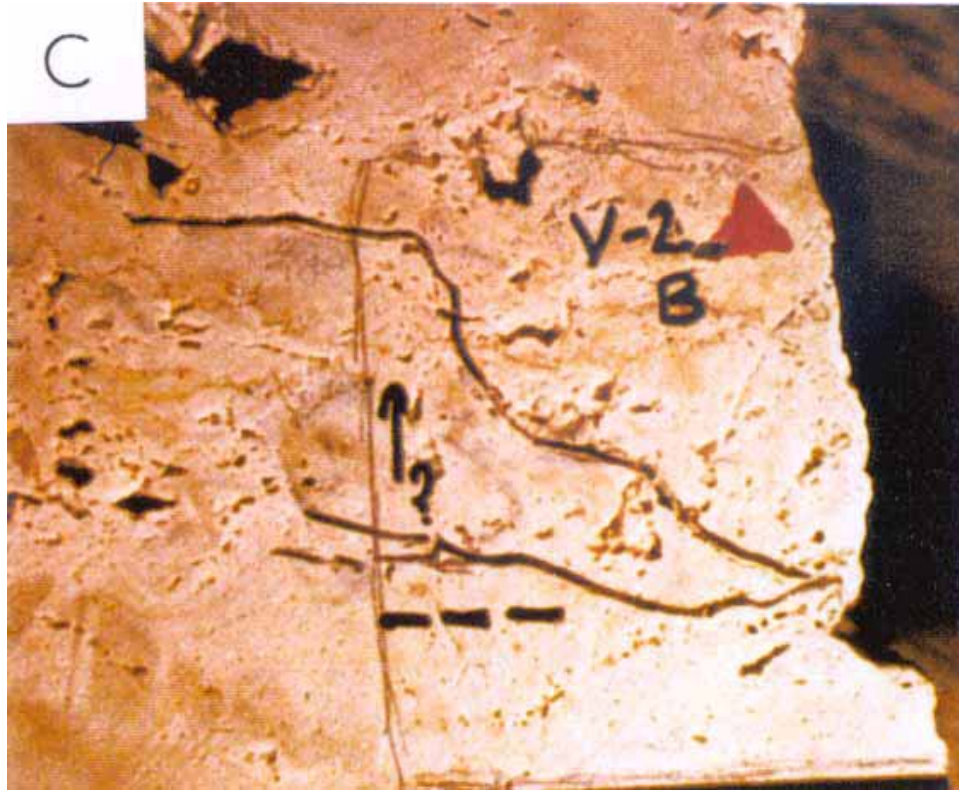


Figure 64. Valdres Quarry Sample V-2B-FT close-up (after Agar 1998)

Texture and diagenesis

The Valdres Quarry test blocks have a distinctly sugary texture under secondary imaging in which grains with well-formed, striated faces are pitted by local dissolution. Overall the grains are equant and well defined. Some grain coarsening and straightening of the grain edges may have been enhanced by a local heating event although there are no metamorphic phases to support high temperatures. Potassium feldspar grows in cavities within the dolomite or clearly grows across dolomite grain boundaries suggesting that the feldspar formed later.

Test Block V-1-FT. Backscatter electron imaging and x-ray dot maps of Test Block V-1-FT reveal a dolomitic cement with higher magnesium content than the dolomitic grains it envelopes. The subtle boundary between an early generation of rounded, lower magnesium dolomite grains and a dolomite cement that grows around them shows up distinctly under luminescence imaging. The early phase of dolomite has bright luminescence whereas the later phase of dolomite has much lower luminescence. Overgrowths of feldspar on feldspar are also identifiable in a few places under backscatter imaging.

Test Block V-2-FT. Fenestrae in Test Block V-2-FT are rimmed by large drusy crystals of dolomite that jut out in the vug cavities. Narrow, late rims of calcite can be detected on some of these crystals. The dolomite grains commonly contain arrays of fluid inclusions but these do not have a preferred orientation.

The sequence of cementation and dolomitization is interpreted as an early phase magnesium calcite-dolomite overgrown by a late stage of dolomite, followed by precipitation of feldspar and a later generation of feldspar overgrowth. Any early calcite/ aragonite cements have been largely obliterated although there is some late stage calcite on the margins of vugs. The precipitation of authigenic feldspar in later stages was probably caused by a change in the fluid composition percolating through the rock.

Virtually no crystallographic preferred orientation is evident. A few regions have a weak shape and crystallographic preferred orientation, but these do not represent significant anisotropies in the rock. Fine silt horizons localize minor stylolites but these are relatively rare and do not represent significant weaknesses in the rock.

Fractures, clay seams, stylolites, and grain size layering

Sample V-1A-FT. The pretest fracture in Sample V-1A-FT is less than 100 microns (0.004 in.) wide and follows a slightly irregular trace through the specimen. The margins of the fracture match directly with each other indicating no lateral offset. There is only minimal damage surrounding the main fracture. Intragranular microfractures have formed subparallel to the fracture surface and some grain boundaries close to the fracture margins have opened slightly.

There is no evidence of alteration or variations in dolomite composition along the fracture surfaces. The latter indicates that the fracture was a relatively recent feature and may have been induced during quarrying. On the perpendicular surface, the fracture has a similar appearance with a constant aperture of about 100 microns (0.004 in.). The fracture in the perpendicular section cuts across boundaries. Several overlapping segments of hairline fractures are located between the main fracture and the edge of the thin section.

Sample V-1B-FT. The pretest fracture surface of this sample showed minimal damage close to the edge of the thin section. Microfractures that are barely discernible can be seen crossing grain boundaries, but they do not extend for more than two or three grains. None of the grains have disaggregated, and there is no detectable chemical alteration along the fracture surface.

On the other sectioned face of the sample, a vertical hairline fracture with several overlapping segments cuts across grain size layering (similar to that in Sample V-1A-FT). This fractured surface appears to be extremely stable and unlikely to nucleate zones of disaggregation.

Sample V-2A-FT. The post-test fracture in Sample V-2A-FT has a similar form to the open pretest fracture in Sample V-1A-FT. The fracture is less than 50 microns (0.002 in.) wide and its margins can be directly matched with each other, indicating no lateral displacement. The path of the crack also has a slightly irregular trace, but in this case, there is a sharp deflection where the fracture intersects a silty horizon. The fracture is deflected along the horizon for less than 1 mm (0.04 in.). A vug adjacent to the silty horizon appears to be undisrupted by the fracture.

No damage surrounding the main fracture walls is evident. The deflection of the fracture indicates that the clay-rich horizons can influence the fracture orientations and may promote fracture localization in quarried blocks even though in this case the effects are minor. The same fracture is segmented with overlapping tip regions between each of the segments. The fracture tips either terminate in vugs or split into numerous ultrafine fractures that trace fluid inclusion trails or grain boundaries.

- a. *Thin Section Sample TS-V-2A-2FT.* The pretest fracture in Thin Section Sample TS-V-2A-2FT traces the path of a series of vugs dividing into several hairline fractures that cut the vugs. In most ways, the pretest fracture does not appear much different from the post-test fracture except that it has a slightly more irregular margin and is in a different orientation. The segmented character of the vugs cut by the pretest fracture may have been determined by the structure of a reef building organism.
- b. *Thin Section Sample TS-V-2A-3FT.* In Thin Section Sample TS-V-2A-3FT the steeply dipping pretest fracture cuts across a boundary in which a fine-grained region exhibits a moderate crystallographic preferred orientation. A splay from the curvilinear trace of the main pretest fracture connects into adjacent vugs with minor damage along the edge of the specimen.

Sample V-2B-FT. Some of the strongest microfracture development in Sample V-2B-FT arises in vug walls, but it is still fairly limited. Drusy dolomite crystals that have grown into a small vug are fractured by intragranular fractures follow crystallographic cleavage planes. A set of intergranular fractures also forms closely spaced concentric rings around the vug.

Seams of clays and feldspar, about 100 microns (0.004 in.) thick, can be traced through the sample. In general the seams are subparallel to bedding but microfolds have formed locally. The horizons represent fine silt layers in the protolith where the proportion of authigenic feldspar is much higher in the seam than in the surrounding dolomite. These features are probably the beginning stages of stylolite formation.

Summary

The two Valdres test blocks are markedly different in their textural characteristics (primarily due to presence or absence of vugs) although both are pervasively dolomitized. Relict sedimentary layers and some fossils, such as corals, can still be observed in both test blocks but predolomite cements cannot be distinguished. Both samples preserve evidence for two phases of dolomitization with subtle changes in the dolomite composition. Authigenic feldspar is the most abundant phase after dolomite and grew after dolomitization. Fractures examined from Test Block V-I-FT appear to be stable and cause minimal damage in the surrounding rock except towards the edge of the specimen. Silty horizons in Test Block V-2-FT have locally deflected fractures but the fracture characteristics are otherwise similar to those of the Test Block V-I-FT samples.

Even though Test Block V-2-FT appeared much more unstable during sampling, the microstructures do not indicate extensive internal damage. All the fractures are fresh with unaltered surfaces, indicating that they are recent. Minor stylolite seams and local domains of crystallographic preferred orientation represent minor anisotropies in the samples but are unlikely to represent major sources of weakness.

Recommendations

- a. Map out the geometries and orientations of fractures in the quarry to determine how they relate to the distribution of vugs, stylolites, grain size variations and bedding.
- b. Make detailed observations of Valdres samples in breakwaters and compare their fracture patterns with those on a similar scale in the quarry.
- c. Compare the mechanical behavior of samples with and without vugs. Although there are more fractures in the vuggy regions they do not appear to be contributing significantly to the breakup of the sample.
- d. Further examination of the stability of block edges is warranted given the indications in this study that these regions are more prone to develop segmented hairline fractures.
- e. Compare the microstructures described in this study with samples from breakwater blocks that have been exposed for more than a decade.

Dempsey Quarry

Test blocks, samples, and thin sections

Test Blocks D-1-FT and D-3-FT from the Dempsey Quarry were acquired from two quartzite blocks that had been subjected to freeze/thaw testing only.

Test Block D-1-FT. Samples D-1A-FT and D-1B-FT were selected From Test Block D-1-FT (Figure 65). In hand specimen, small red/pink and gray pebbles are evident in the quartzite. The pebble size ranges from less than 2 mm (0.08 in.) to more than 2 cm (0.8 in.). Within the test block, horizons could be identified by variations in the percentage of quartz rich clasts versus the quartzite matrix. These horizons were interpreted to represent relict bedding planes and trends in grain size were used to orient the samples for way-up. The samples have a slightly schistose appearance due to fine seams of white mica that anastomose around individual quartz grains and pebbles. The micas do not form a penetrative foliation, but on some open surfaces, the sheen of a micaceous layer indicated that some seams of micas were well connected, more or less on one plane. Two pretest fractures were identified but the block has not disaggregated. Both fractures were oriented at a low angle to interpreted bedding plane orientations.

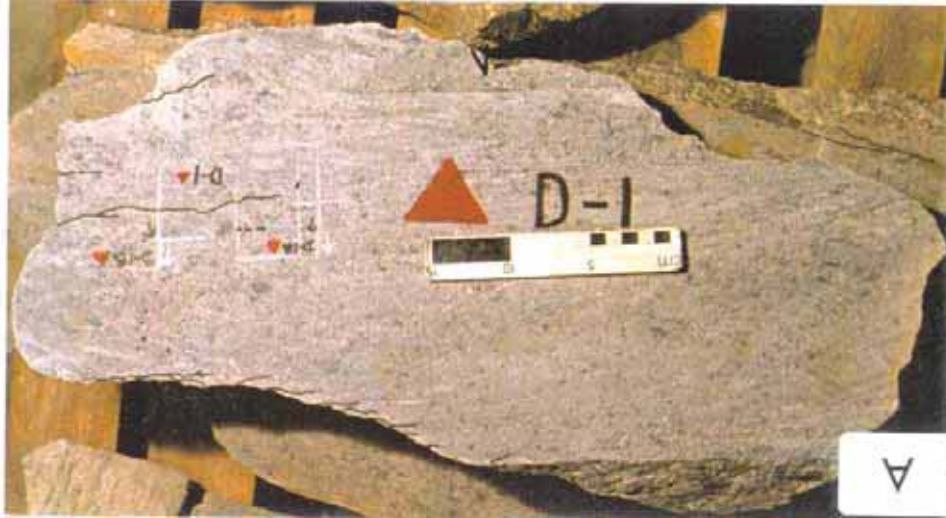


Figure 65. Dempsey Quarry Test Block D-1-FT sample locations. Arrows for way-up are based on interpreted relic grain size grading (after Agar 1998)

- a. *Sample D-1A-FT.* This sample (Figure 66) was positioned to include the tip of the longest pretest fracture in the block. Thin Section Sample TS-D-1A-1FT was positioned on the original marked surface of the block and included the tip of the fracture that extended to the edge of the block. Thin Section Sample TS-D-1A-1FT was impregnated with blue epoxy in order to examine porosity. Thin Section Sample TS-D-1A-2FT was positioned to include the same fracture that dips at about 50 deg on the plane that is perpendicular to the original marked surface, and was stained for potassium feldspar. This thin section also includes the open fractured edge of the sample. Both thin sections were oriented with a single headed arrow to show the way-up.
- b. *Sample D-1B-FT.* This sample (Figure 67) included the intersection of the same fracture whose tip was sampled in Sample D-1A-FT with the edge of the test block where the fracture splays. Thin Section Sample TS-D-1B-1FT was positioned to include the open fracture surface on one edge of the section at a fracture splay. The rest of the width of the thin section was positioned to examine the distribution of subsidiary fractures relative to the main fracture. The thin section was impregnated with blue epoxy and way-up delineated by a single-headed arrow. A fragment of the fracture surface was mounted for secondary electron imaging.

Test Block D-3-FT. Test Block D-3-FT (Figure 68) was similar in character to Test Block D-1-FT but overall had a much higher pebble content. A distinct pebble fill horizon that resembled a graded channel fill was evident at the top of the block. As in Test Block D-1-FT, only pretest fractures were identified. Two samples were taken to examine these fractures.



Figure 66. Dempsey Quarry Sample D-1A-FT close-up (after Agar 1998)

- a. *Sample D-3A-FT.* This sample (Figure 69) was located to include the tip of a pretest fracture oriented subparallel to bedding. Thin Section Sample TS-D-3A-1FT included the lower surface of the pretest fracture that had opened during sample cutting. Thin Section Sample TS-D-3A-2FT was taken from the upper surface of the open fracture on a plane that was vertical and perpendicular to the original marked surface of the test block. This thin section was also stained for potassium feldspar.



Figure 67. Dempsey Quarry Sample D-1B-FT close-up (after Agar 1998)

- b. *Sample D-3B-FT.* This sample (Figure 70) included the tip region of a fracture that cuts relict bedding at an angle of approximately 60 deg. Thin Section Sample TS-D-3B-1FT was placed to include the tip region of the fracture. Thin Section Sample TS-D-3B-2FT was oriented on a bedding parallel plane, perpendicular to the original marked surface of the block. This thin section included the same fracture plane as that examined in Thin Section Sample TS-D-3B-1FT. A combination feldspar stain was used on this second section.

Composition, grain size, and porosity

The Dempsey samples comprise predominantly quartz (80 to 90 percent), muscovite (5 to 10 percent) and feldspar (5 percent) with proportions varying on a thin section scale. Detrital feldspar grains with numerous mica and quartz inclusions are present, with small amounts of Fe-Ti oxide and phosphate. Quartz inclusions tend to be concentrated along cleavage planes of the feldspars.

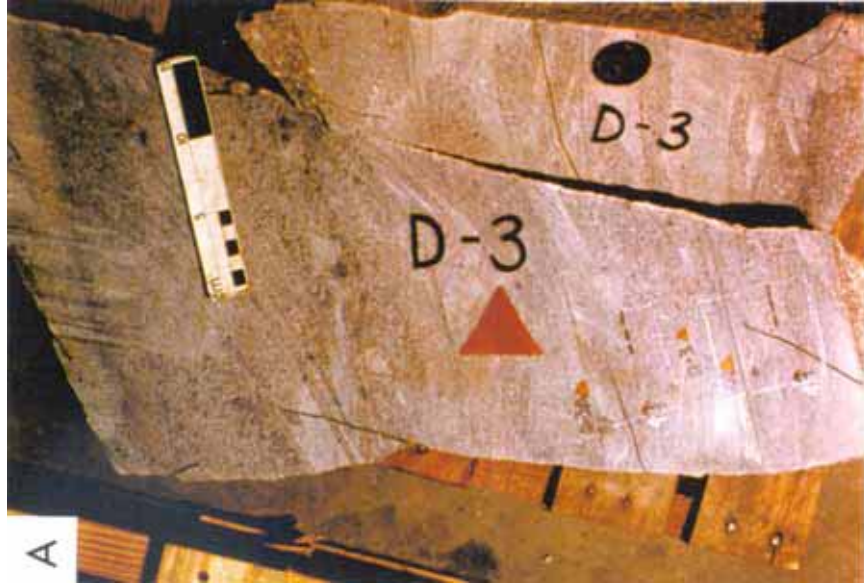


Figure 68. Dempsey Quarry Test Block D-3-FT sample locations. Arrows for way-up are based on interpreted relict grain size grading (after Agar 1998)

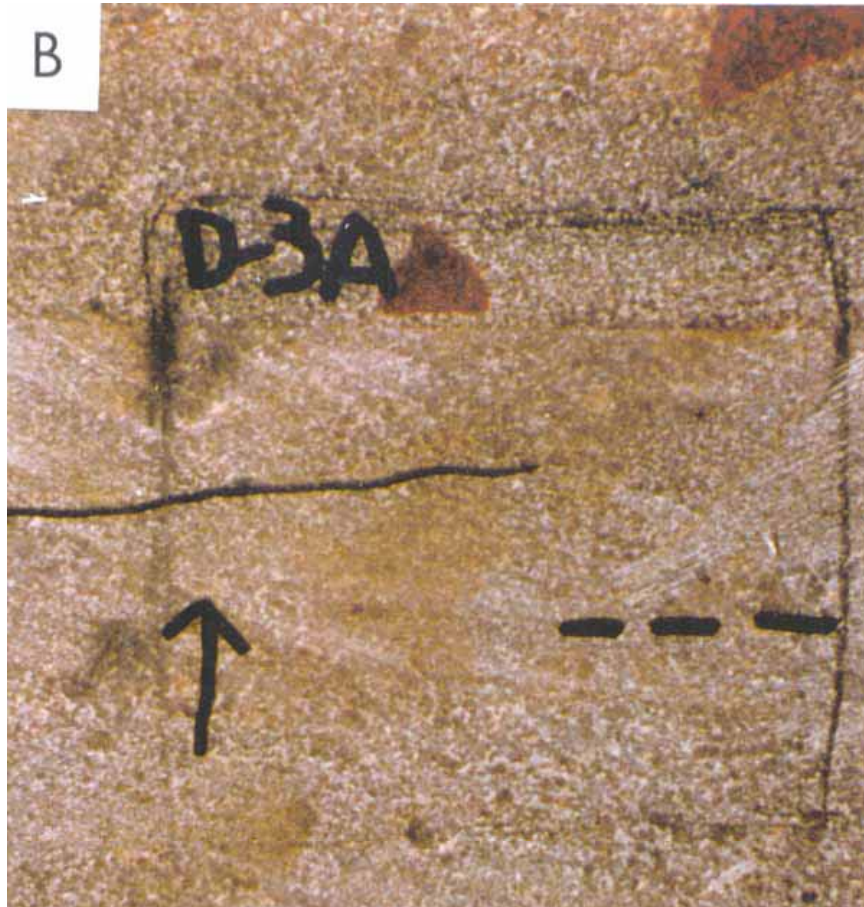


Figure 69. Dempsey Quarry Sample D-3A-FT close-up (after Agar 1998)



Figure 70. Dempsey Quarry Sample D-3B-FT close-up (after Agar 1998)

In Sample D-3A-FT, small feldspar grains are interspersed with muscovite grains within micaceous domains. These feldspar grains have corroded edges and are relatively inclusion free compared to the larger detrital feldspars. The second most abundant phase is muscovite. Electron microprobe analyses of muscovites show no compositional variation between muscovite grains in fractures, pressure fringes, or isolated grains. Opaque phases of Fe-Ti oxides are concentrated in pressure shadow and mica seam regions but are not pervasively distributed through the specimens. Lanthanum bearing apatite grains were also found in one area of Sample D-3A-FT.

Although the range of grain sizes within a thin section varies, optical examination shows the grain size of individual quartz grains to be relatively homogeneous within domains of variable shapes and sizes. These domains may represent the boundaries of lithic fragments in the original sandstone with the finer grained domains representing the surrounding matrix of sand grains. Estimates of mean quartz grain size from digital images range from 22 to 55 microns (0.0009 to 0.002 in.) although clearly there are much larger metamorphosed detrital clasts composed mainly of quartz in the rock.

Blue epoxy impregnation shows the porosity in this rock to be very low (generally lower than 5 percent estimated from selected areas of digital images). Most occurrences of blue epoxy are locations where grains have been plucked from the specimen during thin section preparation or open microcracks.

Texture and metamorphism

The overall textural and compositional characteristics in each thin section are similar. Most of the quartz grains have sutured boundaries where small, irregular protrusions invade neighboring grains. Grain boundary triple junctions, indicative of static recrystallization (Vernon 1970) are also common. Even though the grain boundary textures are typical of recrystallization, the quartz grains are relatively strain free, exhibiting only weak undulatory extinction. No microstructures indicative of dynamic recrystallization were found (such as subgrains or grain boundary migration features (Tullis et al. 1973)). The lack of dynamic recrystallization in the quartz is also supported by the general absence of a preferred crystallographic orientation (as indicated by the insertion of the gypsum plate in optical microscopy). In some places small domains of fine-grained quartz show a consistent color under crossed-polarized light with the gypsum plate inserted.

Feldspars, muscovite and Fe-Ti oxide crystals form interstitial phases between quartz grains. Some of this filling may represent an original detrital component of the sandstone, but there also may be some residuals from pressure solution in quartz along foliation planes. Fluid inclusions of quartz in feldspar grains also may be a relict volcanic texture formed prior to sandstone deposition.

The muscovite flakes have a general shape-preferred orientation that is subparallel to variations in recrystallized quartz grain sizes. Seams about 100 microns (0.004 in.) wide of muscovite with minor chlorite can be traced across thin sections but the seams are rarely straight or continuous. In places they have an anastomosing character, branching around quartz grains. Solitary mica flakes grow across the sutured quartz grain boundaries and are often associated with domains of finer quartz grain size. The presence of clays (subsequently metamorphosed to muscovite and chlorite) in these domains may have inhibited quartz growth (Hobbs et al. 1976). Muscovite grains are also found as pressure fringes growing from the edges of quartz porphyroclasts. The pressure shadows suggest synkinematic growth subparallel to layering and the weak, shape-preferred orientation of some porphyroclasts. The flattened margins of quartz grains adjacent to the mica seams may be due to pressure solution, although the micas may have also controlled quartz grain shapes during recrystallization. Closer examination of mica seams under backscattered electron microscopy shows that small fragments of quartz are included in the seams. These fragments tend to have a shape-preferred orientation parallel to the mica seam. Textural relations where muscovite grains grow across the quartz grain boundaries indicate that at least some mica growth post-dates quartz recrystallization.

Fractures

Sample D-1A-FT. This sample encloses the fracture tip region of a pretest crack. In this case the marked fracture trace can be directly related to a seam of muscovite grains that can be traced inwards from the edge of the specimen. The mica seam is more or less intact with no separation at the level at which the thin section was cut. Towards the center of the thin section the seam thins and can be traced, discontinuously, through the quartzite.

Intragranular and transgranular microcracks that parallel the mica seam have developed in quartz grains along its boundaries. Quartz grains close to the muscovite seam have higher fracture densities than those further away. Shattered quartz grains adjacent to the muscovite seam show preferred crack alignment.

Flattened edges of quartz grains adjacent to the muscovite seam support the role of pressure solution during metamorphism. These arrays are most intense where muscovite grains have been plucked out during thin section preparation. Their development may thus have been influenced by stress release during specimen preparation or during excavation. The same fracture was examined in a perpendicular thin section (Thin Section Sample TS-D-1A-2FT) section. This view reveals similar characteristics, but the preferred orientation of muscovite grains is diminished, indicating an overall fabric anisotropy.

Sample D-1B-FT. Optical microscopy shows zones about 2 mm (0.08 in.) wide of open transgranular microcracks pervading quartz grains along the boundary of the open pretest fracture surface. In places the microcracks have no strong preferred orientation but in other locations they form an array that parallels the fracture surface. The sample displays dense intragranular fracturing in quartz surrounding muscovite seams. There are also dislodged regions of fine-grained aggregates of potassium feldspar, muscovite, and quartz. The splay fracture propagates into the specimen along a mica seam that forms a clear plane of weakness controlling the fracture.

Not all micas, however, are oriented parallel to the fracture surface and in places fractures cut across micas. Mica seams are not continuous even on the thin section scale. At the fracture tip the single fracture aperture decreases and splays into irregular cracks in the surrounding quartz grains. Different displacements between muscovite, feldspar, and quartz may have dissipated the main fracture displacement in this region.

Sample D-3A-FT. This sample contains an open fracture surface along the long side of the thin section. Under backscatter imaging the surface has an irregular trace, but no chemical variations are evident in the rock adjacent to the surface. The damage associated with this crack is minimal, being restricted to a zone less than 1 mm (0.04 in.) wide. Some of the most extensive microfracturing is near a fracture tip as in Sample D-1B-FT. In contrast to part of the crack in Sample D-1A-FT, this crack surface is not controlled by a mica seam although it trends roughly parallel to neighboring seams. The fracture surface follows micaceous layers for short intervals but also cuts across them.

Quartz grains along the crack surface contain numerous microcracks, but do not display the regular alignment of those in Sample D-1A-FT. In one location a narrow zone of microfractures have shattered the quartzite into irregular slivers along the fracture surface. The damage along the crack surface side of the thin section is slightly higher than that observed on other cut surfaces. It should be recognized, however, that many of these microcracks could have been induced during specimen preparation. None of the fractures have any mineral fill. Disaggregation of quartz, potassium feldspar, and muscovite is evident in the fracture damage zone. The strongest fracturing tends to occur in finer-grained regions where potassium feldspar, quartz, and muscovite are present. The open

fracture surface investigated in Thin Section Sample TS-D-3A-2FT shows that the edge of the sample is stable and free of damage beyond the microrelief along the fracture surface.

Sample D-3B-FT. A fracture in this sample trends about 60 deg to the layering and foliation in the rock. Backscattered electron images show that this part of the test block has a much weaker foliation than other sections from Samples D-3A-FT, D-1A-FT, and D-1B-FT. The crack cuts across mica with relatively little deflection by the grain shape anisotropies. Although approximately planar in hand sample, the fracture has a slightly irregular trace that was deflected by quartz grain boundary locations. The termination of the crack is located at a quartz/mica junction where the grain boundaries have opened up slightly more than other grain boundaries away from the crack tip. Disaggregation occurs along grain boundaries in the region adjacent to the fracture.

A second fracture can be traced along the lower edge of the specimen on the right hand side. The backscatter images show no discernible chemical changes around the fracture. This suggests that the fracture is a recent feature that has not been subjected to weathering. The fracture ends in zone of microcracks with different orientations controlled by grain boundaries. In the perpendicular section (Thin Section Sample TS-D-3B-2FT), the fracture exhibits similar characteristics with intergranular hairline cracks running parallel to the main fracture margins.

Summary

The Dempsey quartzite fabric is dominated by muscovite seams that form an anastomosing spaced cleavage, and that are locally schistosity. Pressure solution along these cleavage planes has locally modified quartz grain shapes and redistributed chemical elements during metamorphism. Greenschist facies metamorphism has generated a mosaic texture within quartz with tight grain boundaries. Stress release in quartz grains surrounding fractures that have opened along the muscovite seams contributes to grain scale instabilities that promote disaggregation. A secondary anisotropy is controlled by changes in grain size, but this does not appear to localize significant weaknesses in the samples used in this study. Quartz crystallographic preferred orientation is localized and is unlikely to generate planes of weakness. The samples appear chemically stable except where open fracture surfaces coated with muscovite have been partly illitized.

Recommendations

- a. The stability of the Dempsey quartzite as an armor stone will be strongly influenced by the proportions of muscovite. It is therefore important to establish the spatial variations in muscovite seams within the quarry and within existing breakwaters composed of this material.
- b. Changes in grain size may promote layer parallel fracturing. It is important to establish at outcrop scale whether grain size variations play an important role in nucleating fractures.

- c. Some fractures clearly propagate in from irregularities on the block edges. These features should be identified in breakwaters to see if these are a significant source of failure or if other mechanisms promote breakup.
- d. The orientations of fractures should be mapped out relative to block surfaces in breakwaters and the quarry. The fracture orientations should be examined to see whether they can be simply related to stress release as a result of unloading, the metamorphic fabric, or loading configurations within the breakwater (e.g., point-point contacts).

Sandusky Quarry

Test blocks, samples, and thin sections

Two test blocks were selected from the Sandusky Quarry for this study. Test Block S-1-FT/WD was subjected to both freeze/thaw and wet/dry testing. Test Block S-2-FT was subjected to freeze/thaw testing only. Because the test blocks were being tested when samples were initially delineated, it was not possible to examine the test blocks in detail. Bedding could be identified, but the way-up could not be determined. Both test blocks have similar characteristics. They have a mottled surface coloring that is caused by partial dolomitization. They both contain fragments of fossils, some of which are randomly distributed and others have a weak, preferred orientation in accumulations parallel to bedding planes. Some of the clasts may be calcified bioturbation structures. Stylolite seams were identified in both test blocks and locally represent relatively strong anisotropies. These stylolites have relatively low amplitudes but can be seen to truncate bioclasts in hand specimen. No markings were placed on these samples to identify pre- and post-test fractures during sample selection, but the disintegration of stylolite seams during cutting makes them post-test fractures.

Test Block S-1-FT/WD. This test block is shown in Figure 71.

- a. *Sample S-1A-FT/WD.* This sample (Figure 72) was located in one corner of the test block close to a fractured edge. A stylolitic seam, oriented parallel to bedding, could be identified during sampling. This seam fell apart during sample cutting, dividing the sample into two parts. Thin Section Sample TS-S-1A-1FT/WD samples the region above a fracture surface that formed during cutting of the test block. Dark gray seams form closely spaced laminations near the edge of the opened stylolite seam/fracture. Thin Section Sample TS-S-1A-2FT/WD samples the region below the fracture surface and includes a discrete stylolitic seam. The fractured edge of the sample trends obliquely (10 to 20 deg) to the stylolite in the center of the section.
- b. *Sample S-1B-FT/WD.* This sample (Figure 73) was just visible from the edge of the test unit, being located further into the center of the test block. No lithological features could be identified at the time of sampling. Thin Section Sample TS-S-1B-1FT/WD samples a zone of discrete, spaced stylolitic seams close to the edge of the block. Thin Section Sample TS-S-1B-2FT/WD is oriented with the long axis of the section



Figure 71. Sandusky Quarry Test Block S-1-FT/WD sample locations. Bedding is identifiable in block, but way-up could not be determined (after Agar 1998)

perpendicular to bedding and includes a zone of color banding where bands of white/gray/green colors are interlaminated.

Test Block S-2-FT. This test block is shown in Figure 74.



Figure 72. Sandusky Quarry Sample S-1A-FT/WD showing stylolitic seam parallel to bedding, close to edge of block (after Agar 1998)



Figure 73. Sandusky Quarry Sample S-1B-FT/WD (just visible from edge of test unit) (after Agar 1998)



Figure 74. Sandusky Quarry Test Block S-2-FT sample locations. Bedding is identifiable in block, but way-up could not be determined (after Agar 1998)

- a. *Sample S-2A-FT.* This sample (Figure 75) contains a seam of dark fine-grained material that can be traced across the center of the sample. The sample surface displays irregular discoloration. Thin Section Sample TS-S-2A-1FT samples an opened surface of a stylolitic seam in the center of the sample. The edge is included in the thin section and the long axis of thin section is oriented parallel to bedding. Thin Section Sample TS-S-2A-2FT samples the same surface and structure as the first thin section but cuts a vertical section at 90 deg to the first section.

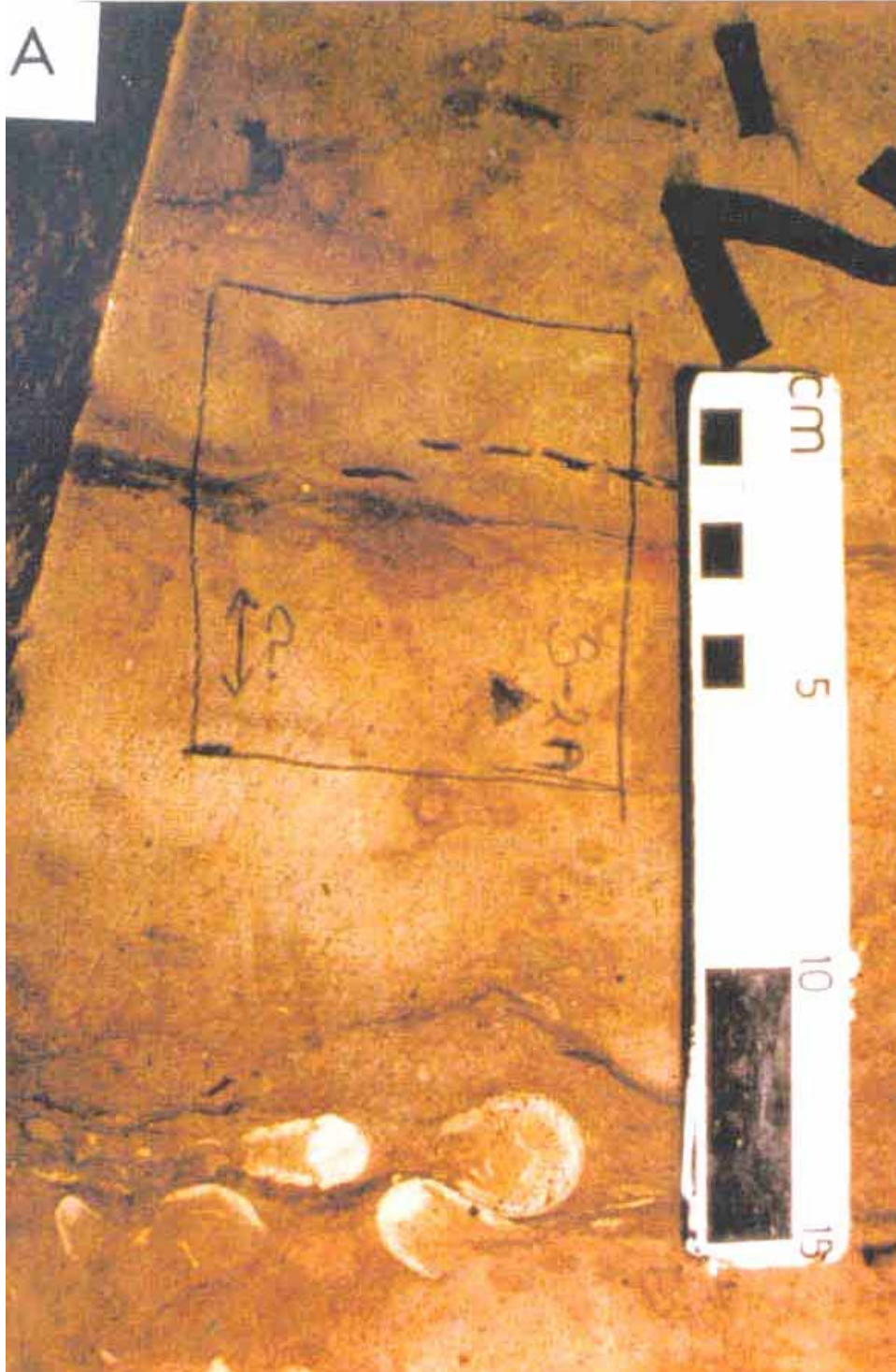


Figure 75. Sandusky Quarry Sample S-2A-FT. Seam of dark fine-grained material can be traced across center of sample. Black dashed lines show inferred trace of bedding planes. Surface of sample exhibits some irregular discoloration (after Agar 1998)

- b. *Sample S-2B-FT*. This section (Figure 76) exhibits dark discoloration in irregular patches on its exposed surface. Thin Section Sample TS-S-2B-1FT samples dark gray streaks that trend parallel to bedding. Thin Section Sample TS-S-2B-2FT includes a region of patchy discoloration evident on the original marked surface of the block that reflects the incomplete dolomitization of the sample. When the block is dry, the discoloration appears yellow brown.



Figure 76. Sandusky Quarry Sample S-2B-FT. Sample shows dark discoloration in irregular patches on exposed surface (after Agar 1998)

Composition, grain size, and porosity

Both samples are incompletely dolomitized as indicated by the presence of red staining for calcite. Estimates of modal composition based on digital image analysis of the stain distribution indicate that calcite forms approximately 21 percent of the rock. The distribution, however, is irregular and the modal estimates are dependent on the scale of observation. Overall, dolomite grains tend to be larger than the calcite grains giving the rock a locally bimodal grain size character. Larger dolomite grains are surrounded by a sugary matrix of fine-grained calcite and dolomite. Variations in calcite and dolomite proportions occur over distances less than a millimeter. The cores of many dolomite grains are inclusion-rich, giving them a darker appearance. Body cavities in bioclasts are commonly preserved in calcite and filled with a mixture of calcite and dolomite cement. Pyrite and iron oxide grains are sparsely distributed through the rock and concentrated in stylolitic seams and veins. Estimates of the mean grain size for the Sandusky samples from each test block range from 40 to 50 microns (0.0016 to 0.0020 in.) for the dolomite and calcite matrix, but the overall grain sizes are wide ranging due to the fragmentation of bioclasts.

Both sample sets display a high proportion of bioclasts (e.g., brachiopods, echinoderm spines), and various shell fragments are among the clasts, locally greater than 50 percent on thin section scale, most of which have been replaced by calcite. Many of the clasts are unidentifiable due to extensive calcite replacement and partial dolomitization. Some may represent bioturbation structures that have been replaced by calcite but the original porosity structure is still preserved in some clasts.

Porosity in the Sandusky samples is moderate, with average estimates from digital images indicating between 10 and 12 percent porosity, but varies with the composition. Some porosity is contributed by the original structure of bioclasts, some regions of calcite that have not been replaced by dolomite also have elevated porosity. In places elongate pores resemble fenestrae aligned parallel to bedding.

Texture and diagenesis

The overall texture of the samples consists of relatively large rhombs of dolomite grains growing in a matrix comprising mainly finer-grained calcite. The dolomite grains (darker) have relatively well-defined crystal faces whereas the calcite grains have more irregular margins. Some of the calcite grains appear to infill pore space between the dolomite, but in other places the dolomite appears to be replacing the calcite. Spatial variations in textures are caused by local concentrations in dolomite-only, coarse-grained, calcite-only, or bioclast-rich regions. Euhedral calcite filling cavities in bioclasts and small veins have smooth surfaces whereas the pitted texture of calcite replacing the structural parts of the bioclast.

The overall cementation sequence is interpreted to be a primary aragonite cement replaced by calcite, calcite partly replaced by dolomite, secondary porosity generated by dolomitization filled with later calcite crystals. Zoning

within the dolomite grains is formed by clusters of inclusions that were trapped early in their growth history.

Pressure solution along stylolite seams post-dates the dolomitization and truncates some of the replacement textures in bioclasts. Residual concentrations of iron oxide grains concentrated along the seams although some iron oxides and pyrite grains may have been introduced by external fluid sources into veins. There is an alignment of detrital micas parallel to parts of the open stylolite seam surface.

Fragments of brachiopods are locally aligned parallel to bedding amongst various coral and shell fragments. Some local pressure solution may have also enhanced to shape preferred orientation of clasts. Some alignment of calcite fragments may represent calcite filled fenestrae or possibly compacted bioturbation structures.

Fractures and stylolites

Sample S-1A-FT/WD. This sample displays the features surrounding an open pretest fracture surface and specimen edge damage. Fragments of stylolitic seams are evident along the specimen edge, but otherwise there is minimal damage. Other sections of the same feature show a similar lack of damage.

Sample S-1B-FT/WD. The dominant features in thin section from Sample S-1B-FT/WD were stylolite seams. The stylolites are generally subparallel to bedding but locally form more complex intersecting geometry. Dissolution along the stylolites develops a preferred shape orientation in bioclasts adjacent to them.

Aligned, elongate calcite fragments form a weak preferred orientation, subparallel to bedding. These may represent calcite filled fenestrae or possibly compacted bioturbation structures.

Sample S-2A-FT. The open pretest fracture in Sample S-2A-FT has locally straight edges where the fracture cuts across bioclasts. Many of the surrounding dolomite grain boundaries have been opened close to the fracture and could be easily dislodged. The fracture has an aperture of about 100 microns (0.004 in.), and is intersected by steeply dipping fractures with more variable apertures. Fractures elsewhere within the sample intersect at varying angles generally between 40 and 90 deg. In places, these microfractures cut across compositional boundaries between calcite and dolomite with no evidence for deflection. In other spaces the compositional boundaries have clearly localized fractures and are a likely source of major instability in the Sandusky samples. Several microfractures trend subparallel to bedding and may be related to stress release.

Arrays of stylolite seams are also abundant in the thin sections from this sample and exhibit similar characteristics to those previously described. In Thin Section Sample TS-S-2A-2FT there is a gradational boundary from the edge of the thin section where dolomite is the dominant phase to a horizon of bioclastic material. Elongate vugs and fractures are oriented parallel to the margin of the sample in this section. A vein of pyrite is also oriented parallel to the margin of

the thin section and appears to be locally buckled around grains possibly as a result of compaction. Calcite veins were also located in this sample, both as shallow and steeply dipping veins that cut the dolomite texture and therefore postdate it.

Sample S-2B-FT. In this sample, minor damage occurs along the grain boundaries of coarse calcite grains where they have been opened, and fragments of calcite have been dislodged.

Other microfracture damage occurs around cavity margins. Stylolite seams have locally deformed calcite fragments and concentrate trails of iron oxides through the sample. Part of the trace of some stylolites appears to be guided by compositional boundaries between calcite and dolomite.

Summary

The Sandusky samples are compositionally and texturally heterogeneous. There is considerable evidence from microstructures that compositional boundaries within the samples are regions that can promote fracturing because of the mismatch of elastic properties between calcite and dolomite. Stylolite seams appear to have low cohesion, falling apart during sampling. However, there is minimal fracture damage around this type of parting. Grain boundaries around discrete open fractures are prone to opening and promote disaggregation. Local anisotropies are generated by clustering of stylolite seams parallel to bedding with some preferred alignment of bioclasts. A fissility develops along the edge of some samples, controlled by a combination of open fractures that may be generated through stress release, stylolite seams, and veins. Porosity is spatially variable, changing with compositional variations.

Recommendations

- a.* The degree of compositional heterogeneity within the quarry (percent calcite versus percent dolomite) needs to be established together with observations of fracture development in relation to compositional variations.
- b.* Structures in breakwater stone need to be compared with those in the test blocks. For example, are the blocks disaggregating at point contacts or are they splitting along stylolites?
- c.* The abundance of stylolites and their spatial variations need to be established, together with an evaluation of whether or not the stylolites are an important factor in the breakup of this material.
- d.* Oriented samples are needed to check how the fissility observed in this study compares with orientations of joint sets and other features in the quarry.

Marblehead Quarry

Test blocks, samples, and thin sections

Three test blocks were selected from the Marblehead Quarry. Test Block M-1-FT was subjected to freeze/thaw testing only. Test Block M-2-WD was subjected to wet/dry testing only. Test Block M-3-FT/WD was Test Block M-1-FT after being subjected to wet/dry testing.

Test Block M-1-FT. Test Block M-1-FT (Figure 77) has a light brown gray mottled appearance and contains two pretest fractures oriented perpendicular to the interpreted bedding orientation.

- a. *Sample M-1A-FT.* This sample (Figure 78) includes the tip of one of these fractures. Sample M-1A-FT fractured during sampling to one side of the fracture tip leaving an open fracture surface along one edge of Thin Section Sample TS-M-1A-1FT. The marked pretest fracture can be traced to the edge of the block through a zone of overlapping segments.
- b. *Sample M-1B-FT.* This sample (Figure 79) included the edge of the block where fragments have broken away from the fracture leaving part of the fracture surface open. Thin Section Sample TS-M-1B-1FT sampled the fracture surface and stylolitic layering perpendicular to it. Thin Section Sample TS-M-1B-2FT sampled another fracture surface of the same structure in a section perpendicular to that of Thin Section Sample TS-M-1B-1FT.

Test Block M-2-WD. Test Block M-2-WD (Figure 80) has a similar coloring and texture to that of Test Block M-1-FT. Some shell fragments and burrows are evident on the surface of the block as well as numerous stylolites. The block contains a fracture that trends at an angle of approximately 35 deg to stylolitic seams. The fracture is locally segmented but has a fairly consistent orientation and trace. Close to one edge of the test block, there are several layer parallel and layer perpendicular fractures. Two samples were taken of the test block, focusing on the pretest fracture that had propagated into the block and a mesh of fractures at the edge of the block.

- a. *Sample M-2A-WD.* This sample (Figure 81) was located at the upper edge of the block where there were numerous layer parallel and layer perpendicular fractures. Thin Section Sample TS-M-2A-1WD sampled the intersections between subhorizontal and steeply dipping fractures. Thin Section Sample TS-M-2A-2WD sampled a steeply dipping fracture on a section perpendicular to that in Thin Section Sample TS-M-2A-1WD.
- b. *Sample M-2B-WD.* This sample (Figure 82) was located over the overlapping fracture segments of the longest pretest fracture in the block. Thin Section Sample TS-M-2B-1WD samples an open surface of this fracture in the region of overlapping segments.

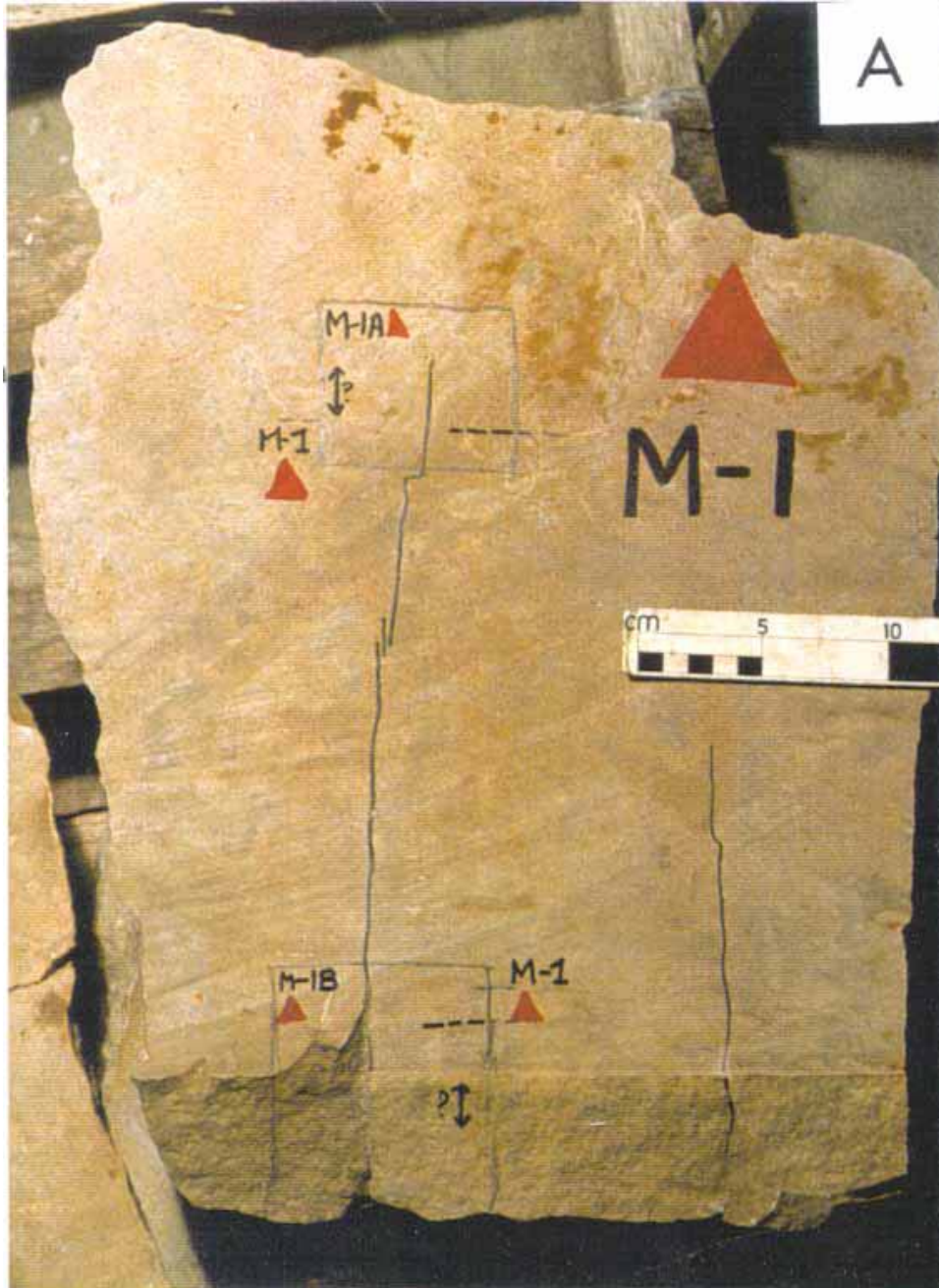


Figure 77. Marblehead Quarry Test Block M-1-FT sample locations, showing large pretest fractures (after Agar 1998)

Test Block M-3-FT/WD. Test Block M-3-FT/WD (Figure 83) was subjected to wet/dry cycles, but otherwise it was similar in composition to Test Block M-1-FT. A large pretest fracture crosses the block. Samples were taken where this fracture intersects the block margin and near the center of the block where the fracture dies out. The whole block broke apart along this fracture during sample cutting.

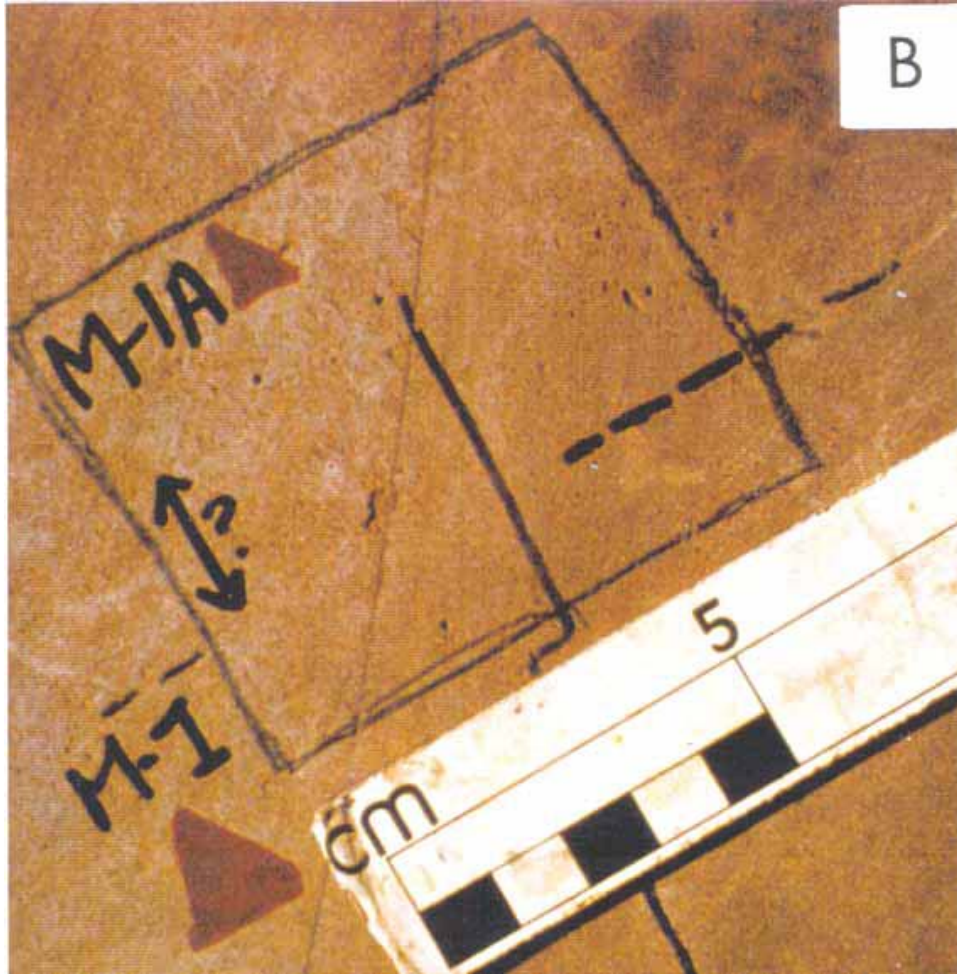


Figure 78. Marblehead Quarry Sample M-1A-FT showing pretest fracture tip. Dashed line indicates inferred orientation of bedding (after Agar 1998)

- a. *Sample M-3A-FT/WD*. This sample (Figure 84) was taken from the center of the test block where the pretest fracture tip is located. Thin Section Sample TS-M-3A-1FT/WD includes this fracture tip.
- b. *Sample M-3B-FT/WD*. This sample (Figure 85) was taken from the edge of the block where it is intersected by the large pretest fracture. Thin Section Sample TS-M-3B-1FT/WD covers this fracture and the block edge. Thin Section Sample TS-M-3B-2FT/WD is located over a vertical hairline fracture that cuts fine, dark stylolitic seams that parallel bedding. It is on the surface orthogonal to Thin Section Sample TS-M-3B-1FT/WD.

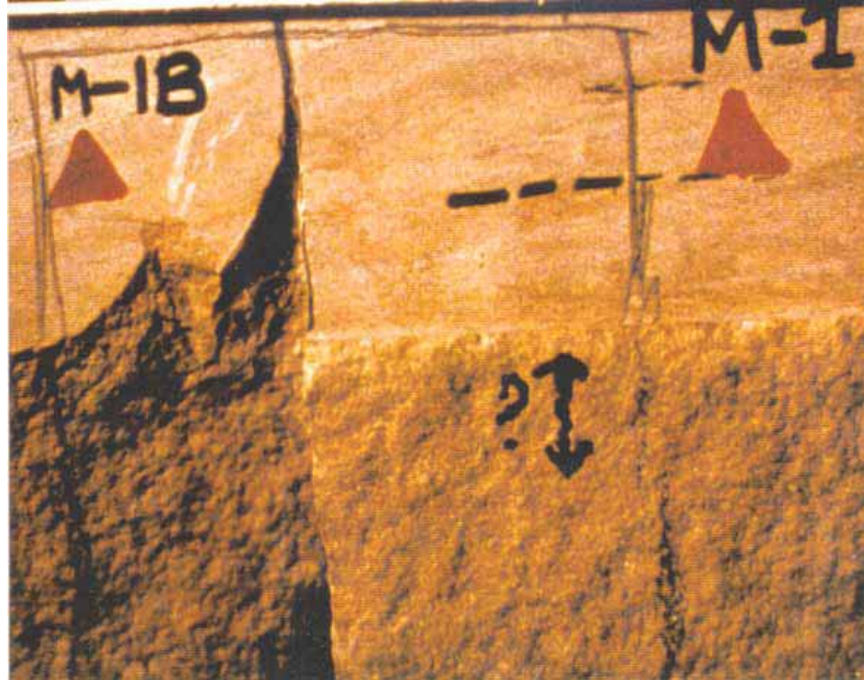


Figure 79. Marblehead Quarry Sample M-1B-FT showing open fracture surface (after Agar 1998)

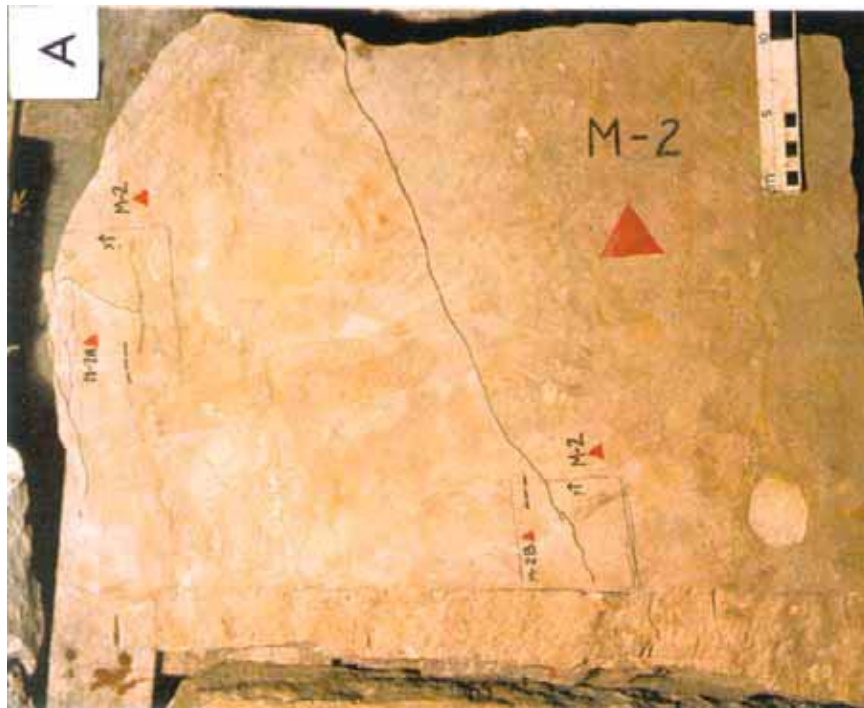


Figure 80. Marblehead Quarry Test Block M-2-WD sample locations with large pretest fracture crossing obliquely across surface (after Agar 1998)

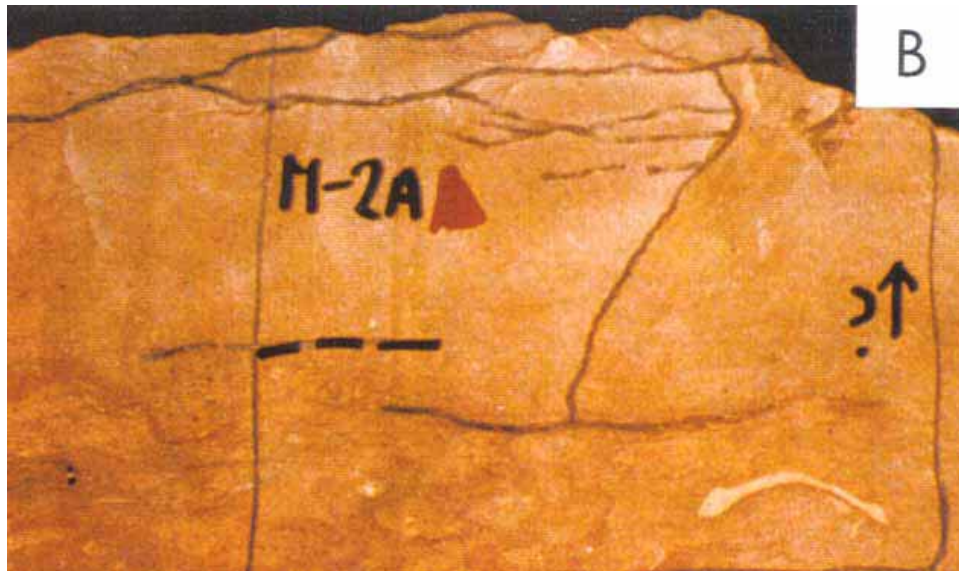


Figure 81. Marblehead Quarry Sample M-2A-WD showing fractures that are perpendicular and parallel to bedding. Dashed line indicates inferred orientation of bedding (after Agar)



Figure 82. Marblehead Quarry Sample M-2B-WD containing overlapping pretest fractures that trend approximately 30 deg to bedding (after Agar 1988)



Figure 83. Marblehead Quarry Test Block M-3-FT/WD sample locations, with large pretest fracture (Test Block M-1-FT after being subjected to wet/dry testing) (after Agar 1998)

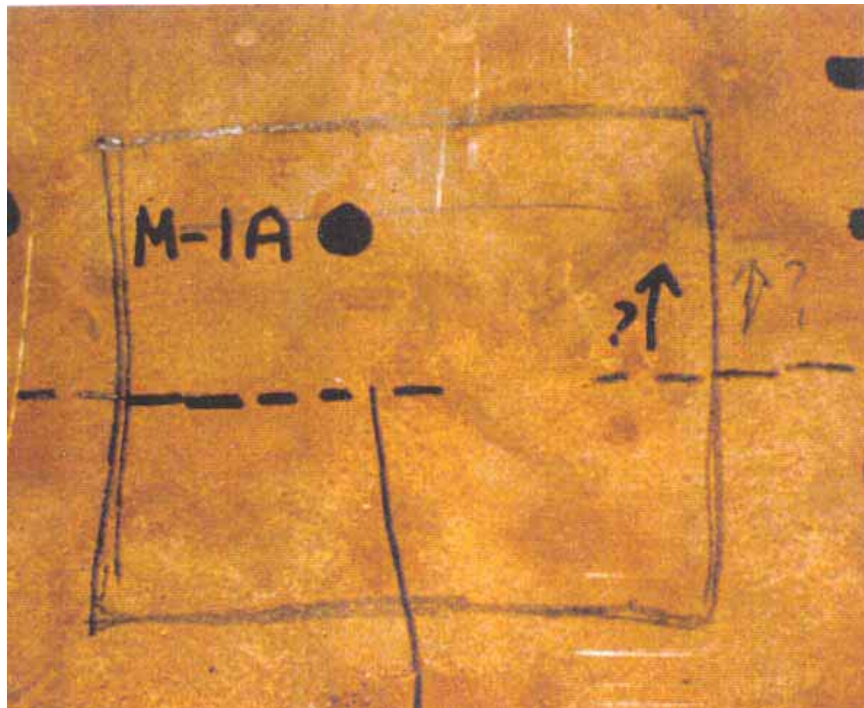


Figure 84. Marblehead Quarry Sample M-3A-FT/WD showing fracture tip region of subvertical fracture in test block (from Test Block M-1-FT after being subjected to wet/dry testing) (after Agar 1998)



Figure 85. Marblehead Quarry Sample M-3B-FT/WD that includes open surface of same fracture sampled in M-3A-FT/WD (Figure 67) (from Test Block M-1-FT after being subjected to wet/dry testing) (after Agar 1998)

Composition, grain size, and porosity

The Marblehead samples are predominantly dolomite but the dolomitization was incomplete. The composition of all three test blocks appears similar from the selected samples and are therefore summarized together. The dolomite has a bimodal distribution in which fine-grained dolomite fills the interstices between subhedral rhombs of dolomite. The cores of larger dolomite crystals are commonly darkened by rings of inclusions where an earlier generation of magnesium calcite is preserved. Secondary images show well formed dolomite rhomb crystal faces, generally tightly cemented but locally separated by vugs. Mean estimates for the dolomite are about 35 microns (0.0014 in.).

The percentage of calcite and dolomite is variable on a thin section scale ranging from less than 10 percent to 50 percent calcite (up to 70 percent calcite in one case). Overall more calcite is present in Sample M-2A-WD than in Sample M-1A-FT. Calcite grains interspersed with the dolomite both as a replacement phase in bioclasts, as a relict cement and as a late pore filling phase. Later calcite grains are generally inclusion free. Small grains of pyrite are also present (less than 1 percent).

The uneven distribution of porosity on thin section scale gives estimates of mean porosity ranging between 9 and 19 percent. Representative images of the typical dolomite texture in Sample M-1A-FT show the relatively high porosity, unevenly distributed through the sample and a few sparse grains of calcite.

Texture and diagenesis

Finer-grained dolomite is not evenly distributed through the rock but tends to cluster in patches. Coarse-grained dolomite crystals have more fluid inclusion-rich cores that finer-grained dolomite. All three Marblehead samples preserve the

same diagenetic sequence. Bioclasts comprise predominantly calcite that probably replaced an original aragonite structure. The original structure of the bioclasts forms pitting in the calcite. In some sections, the calcite is unevenly distributed due to the abundance of fossil fragments and possibly replacement in burrows. Within the cores of dolomite grains an earlier generation of magnesium and iron-bearing calcite with abundant fluid inclusions is preserved. This may represent the earliest stages of dolomitization with more magnesium-rich fluids precipitating dolomite later. Relict calcite grains or cores tend to have rounded and/ or corroded margins. Dolomitization was incomplete, leaving identifiable bioclasts and a secondary porosity in the form of small pores at grains' interstices and numerous vugs. A later generation of euhedral calcite grains with smooth surfaces partly infills the secondary porosity.

Fractures

Sample M-1A-FT. The sampled region is where pretest fracture slivers of the dolomite have been dislodged from the fracture walls by parallel subsidiary fractures. The fracture aperture broadens towards the edge of the thin section. Even though the slivers have been dismembered, the rest of the fracture walls appear stable with the secondary porosity related to dolomitization undisturbed. Brighter phases in the dolomite are relict grains of calcite.

In a post-test fracture at a high angle to the pretest fracture, the wall of the fracture has been partly removed along the edge of the thin section with some scoops plucked out of the edge of the section. There is only minor microfracturing along the edge of the main fracture and the surrounding dolomite although relief under secondary imaging shows numerous inclusion pits.

Some grains have disaggregated along the edge of the thin section as well as fragments that have dislodged from the fracture walls. The fracture surfaces match directly across the fracture indicating no lateral displacement. The open fracture cuts a stylolitic seam that trend subparallel to bedding. Damage at the edge of the thin section is minimal. In this case the fracture aperture stays constant to the edge of the section. The same fracture further away from the edge of the thin section shows more ragged fracture margins and some subsidiary fracturing around them.

Sample M-2A-WD. One of the fractures that cross the sample exhibits an irregular, wavy trace with variable aperture. Bright grain clusters are fossil fragments replaced by calcite. Solitary calcite grains are still preserved in the dolomite matrix. This region contains a high proportion of fine-grained dolomite. The fracture walls have disaggregated in numerous locations and the grain boundaries in the surrounding dolomite are less cohesive than in other fractures observed in freeze/thaw test blocks from Marblehead Quarry.

Subhorizontal microfractures intersect an open pretest fracture dipping at approximately 50 deg in a calcite-rich region of Sample M-2A-WD. It is not possible to assess which fractures formed first. Although the microfractures appear to be offset by the larger open fracture, they could have been refracted by the open fracture if it existed prior to their formation. Fracture propagation in this

region may be promoted by the relatively high and interconnected porosity. At the end of open fracture in Sample M-2A-WD, the fracture turns as it intersects the edge of the thin section and splays into two fractures that isolate a triangular fragment of dolomite.

Fragments of fossils are evident in a calcite-rich matrix that is highly birefringent. In places, microfractures propagate through the calcite-rich matrix. As in previous examples, the calcite-rich matrix appears to be more prone to developing damage around fractures than the dolomite-rich matrix.

Sample M-1B -FT. Sample M-1B-FT has many of the same fracture characteristics as Samples M-1A-FT and M-2A-WD. These include branching and intersecting microfractures dissecting a stylolitic seam. Some microfractures intersect the major open fracture in this sample at a high angle. In one case a subsidiary fracture trends parallel to the main fracture surface partially dislodging a fragment from the fracture wall.

Sample M-3A-FT/WD. The open pretest fracture surfaces in this sample are slightly irregular but appear stable with little evidence for grain disaggregation. The fracture aperture broadens at the edge of the thin section, but the intensity of fracturing in the fracture walls remains relatively low. The fracture aperture changes abruptly along its trace with fine-scale roughness controlled by grain boundaries.

Changes in the character of porosity coincide with variations in the grain size distribution and do not appear to be related to the open fracture surface. Coarse-grained dolomite grain boundaries appear cohesive but the finer-grained dolomite may be prone to plucking during thin section preparation. The porosity, shown by black epoxy under backscatter imaging is high, but the dolomite surrounding the fracture at this location appears relatively stable. Although the porosity is relatively high, subsidiary fractures in the main fracture wall are rare.

Some microfractures cut through dolomite grains approximately parallel to the fracture surface. There is no evidence for chemical variations around the fracture surface, indicating that is a relatively recent feature.

Vertical hairline fractures in this sample have slightly irregular traces, influenced by grain boundaries in the dolomite. One fracture splays into several branches that penetrate the surrounding matrix. There is no evidence of weathering or mineral fill along the fractures. Minor grain-scale disaggregation and slight opening of grain boundaries causes local porosity enhancements close to fractures, but the damage is limited. In some places microfractures connect through vugs.

Sample M-3B-FT/WD. The sampled fracture comprises several branches of anastomosing hairline fractures less than 5 mm (0.2 in.) wide. Numerous grains of partially replaced calcite (brighter phase) are present in the matrix. The flat margins of the pore space suggest that it is primarily controlled by the growth of dolomite although some may be due to plucking of calcite grains. The fracture cuts across and around grain boundaries and does not appear to be influenced by any other textural or chemical features in the rock.

At the tip of the hairline fracture approaching edge of thin section, the fracture links into regions of porosity that have become interconnected to form a throughgoing fracture perpendicular to the hairline fracture (vertical). There is some opening of grain boundaries along the edge of the thin section but no significant increase in damage around the hairline fracture.

At the opposite end of the same fracture, the aperture is wider and remains constant to the edge of the thin section. The trace of the fracture follows sharp angular turns controlled by dolomite rhombs. Transgranular microfractures deform the walls of the fractures, locally controlled by crystallographic cleavage planes in dolomite.

Stylolites

Fractures are not the only heterogeneity in the Marblehead samples. Some fine-grained regions follow roughly linear traces through the dolomite ranging from 0.1 to 0.3 mm (0.004 to 0.01 in.) in width. They are commonly darker (under plane polarized light) with a red brown stain. Fe-oxides and some Fe-sulfides were detected by Energy Dispersive Spectrometry (EDS) in these zones. Close examination of the grains in these regions indicates that the porosity is reduced and the finer-grained material tends to have more rounded grains than those commonly found in the interstices of coarser dolomite grains. Grain size reduction along these linear traces in Samples M-1A-FT and M-1B-FT may represent zones of enhanced dissolution caused by fluid flow along these planes. They are oriented at low and high angles to bedding and could be the precursors of stylolitic seams.

Summary

The Marblehead samples are characterized by incomplete dolomitization that may play an important role in weakening blocks. The calcite-rich matrix appears to be less mechanically stable than the dolomite-rich matrix, but more extensive observations, testing, and studies would be needed to test this hypothesis. The uneven distribution of porosity resulting from different fluid compositions permeating the rock and localized pressure solution may also influence the location of fractures. There do not appear to be any substantial differences in the fracture behavior of the wet/dry test samples to those of the freeze/thaw test samples. Nor does there appear to be any major chemical influence on the fracturing beyond that of the basic modal composition. The fractures in these samples represent some of the more complex fracture arrays examined in this study, with ambiguous crosscutting relationships and numerous intersecting and splay fractures. There were, however, no indications of slip along the fractures.

Recommendations

- a. Further investigation is needed of the role of compositional and grain size heterogeneities in localizing fractures in these samples via an expanded structure/textural database and more mechanical testing.

- b. Detailed mapping of microfracture networks relative to mesoscopic features would help to understand the effects of boundary discontinuities and lithological variations on the fracture network origin. Such detailed studies are beyond the scope of this report.
- c. It is important to understand how the fissility reported from the quarry is related to the features observed in the samples. For example, is the fissility localized along stylolite seams, or does it cut across them?
- d. Examination and comparison of structures in the same material in a breakwater with those in a quarry is important to isolate features induced by loading within the breakwater, as opposed to those inherent to the rock's fabric.

Johnson Quarry

Test blocks, samples, and thin sections

Three test blocks were sampled for this study. Test Block J-1-WD was subjected to wet/dry testing only. Test Block J-2 was the pretest (prior to freeze/thaw exposure) equivalent of Test Block J-2-FT that was subjected to freeze/thaw testing only.

Test Block J-1-WD. Test Block J-1-WD is shown in Figure 86. Only pretest fractures were identified in Test Block J-1-WD. One of these fractures extends from a right angle on the edge of the block across more than two-thirds of the width of the block subparallel to the laminations. The pretest fractures have clearly nucleated from relief on the edge of the test block. The way-up was not recorded on the original test block. Samples were marked with a double-headed arrow to show the direction perpendicular to bedding. Although way-up could not be confirmed from preliminary observations of the test block during sampling, it is possible that careful mapping of the fault curvature on the block surface would give better clues to the way-up.

Samples J-1A-WD, J-1B-WD and J-1C-WD were acquired from a freeze/thaw test block of medium-grained moderately well sorted buff sandstone. The block contains numerous laminations defined by brown to dark brown staining. The thickness of these laminations varies from 0.04 in. (1 mm) to more than 2 cm (0.8 in.) over short distances. There are isolated patches of dark brown black material (probably organic matter) that is soft and loosens easily from the sample surface. Some laminae are truncated by minor faults, several of which can be identified in hand specimen. The faults are typically narrow (less than 1 cm (0.4 in.)), and have apparent dips ranging between 50 and 20 deg. There is no fault gouge and the sandstone character is only slightly altered to a lighter color in the deformed regions. The lack of intragranular deformation in these zones suggests that faulting occurred prior to cementation. It is therefore probable that these minor faults are related to the synsedimentary faults reported to control sediment accumulations in the Johnson Quarry area. Steep intralayer micro-faulting deforms some layers and local contortions of laminae are also evident.



Figure 86. Johnson Quarry Test Block J-1-WD sample locations (after Agar 1998)

- a. *Sample J-1A-WD.* This sample (Figure 87) was selected to include pretest fractures propagating in from the irregular block surface. One fracture has nucleated at a bend on the block surface and the other has formed close to an adjacent bend. Both fractures have relatively straight traces and are spatially associated with brown staining. Soft dark brown material in the sample block had already been plucked out of the fractures prior to cutting thin sections. Thin Section Sample TS-J-1A-1WD was cut to include the two fractures and the edge of the specimen surface including one fracture tip. The section was impregnated with blue epoxy to examine porosity variations by optical microscopy. Thin Section Sample TS-J-1A-2WD was cut on the vertical surface perpendicular to Thin Section Sample TS-J-1A-1WD to examine the fractured edge of the sample and a third, gently dipping fracture that trend subparallel to the open fracture surface. This second thin section was also impregnated with blue epoxy.
- b. *Sample J-1B-WD.* This sample (Figure 88) was cut in the center of the test block. The sample includes dark brown, elongate patches that are truncated by a fault with an apparent dip of 40 deg. The open fractures were deemed by the Corps to be more critical to the objectives of this study than the fault characteristics. Therefore Thin Section Sample TS-J-1B-1WD was placed to include two fractures that connected to the sample edge and a small portion of the fault. Thin Section Sample TS-J-1B-2WD was cut on a vertical surface perpendicular to that in Thin Section Sample TS-J-1B-1WD to compare structures in different orientations.

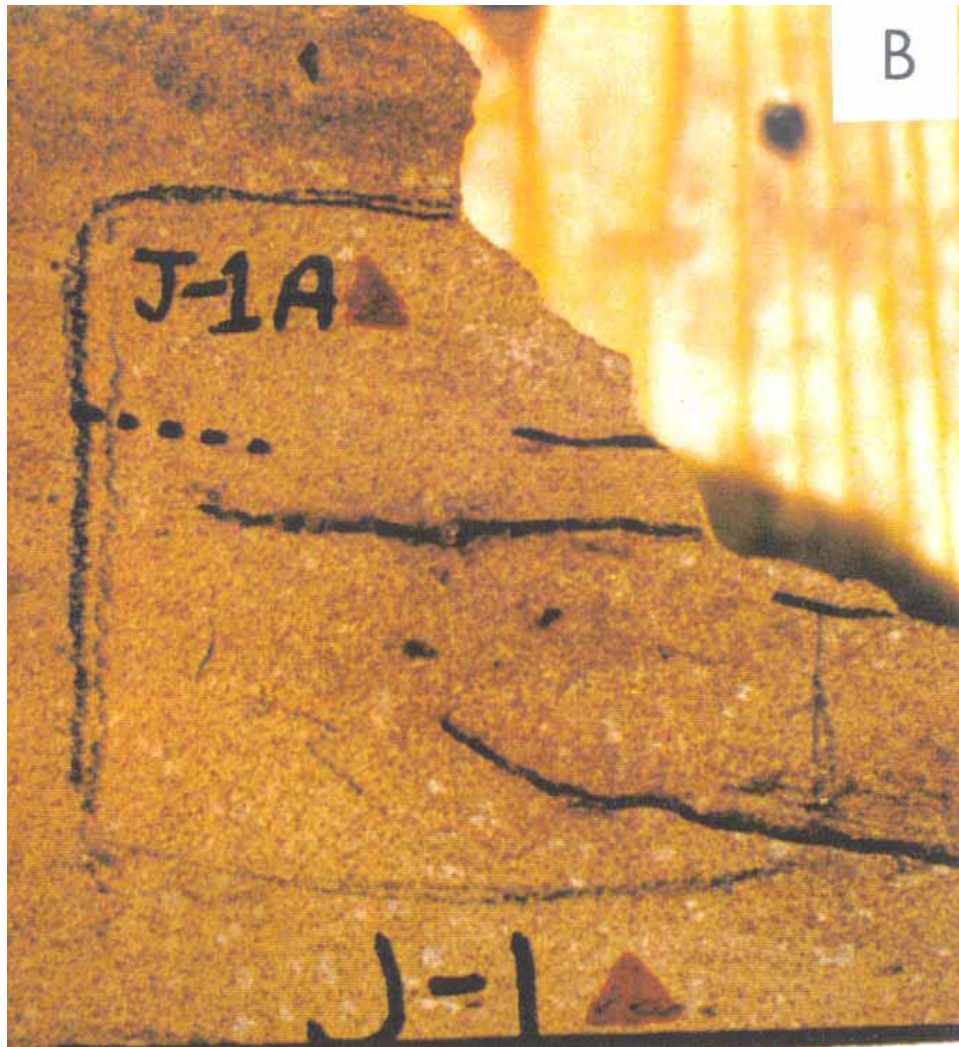


Figure 87. Johnson Quarry Sample J-1A-WD with pretest fractures penetrating from edge of sample (after Agar 1998)

- c. *Sample J-1C-WD*. This sample (Figure 89) was cut on the opposing side of the test block to Sample J-1A-WD. The sample includes several pretest fractures that appear to have nucleated on the edge of the block and propagated inwards. Thin Section Sample TS-J-1C-1WD was located to examine one major fracture penetrating the block in a region that was relatively free of brown laminations. Although there were several other fractures of interest in this sample, they were similar to those in Sample J-1A-WD. Given the budgetary limits for this study it was decided to examine the main fracture that had contrasting characteristics. The thin section was stained for two feldspars (combination Na-cobaltinitrite and K-rhodizonate).



Figure 88. Johnson Quarry Sample J-1B-WD (after Agar 1998)

Test Block J-2. Both Test Block J-2 and Test Block J-2-FT are medium-grained, buff, moderately well sorted sandstone. They do not contain the brown laminations evident in Test Block J-1-WD, and appear extremely homogeneous in hand sample. Representative areas were selected from the center of each block for thin sections to examine possible changes in the unfractured sandstone during testing. A double-headed arrow was used to indicate the direction perpendicular to the interpreted bedding orientation. Test Block J-2 is shown in Figure 90.

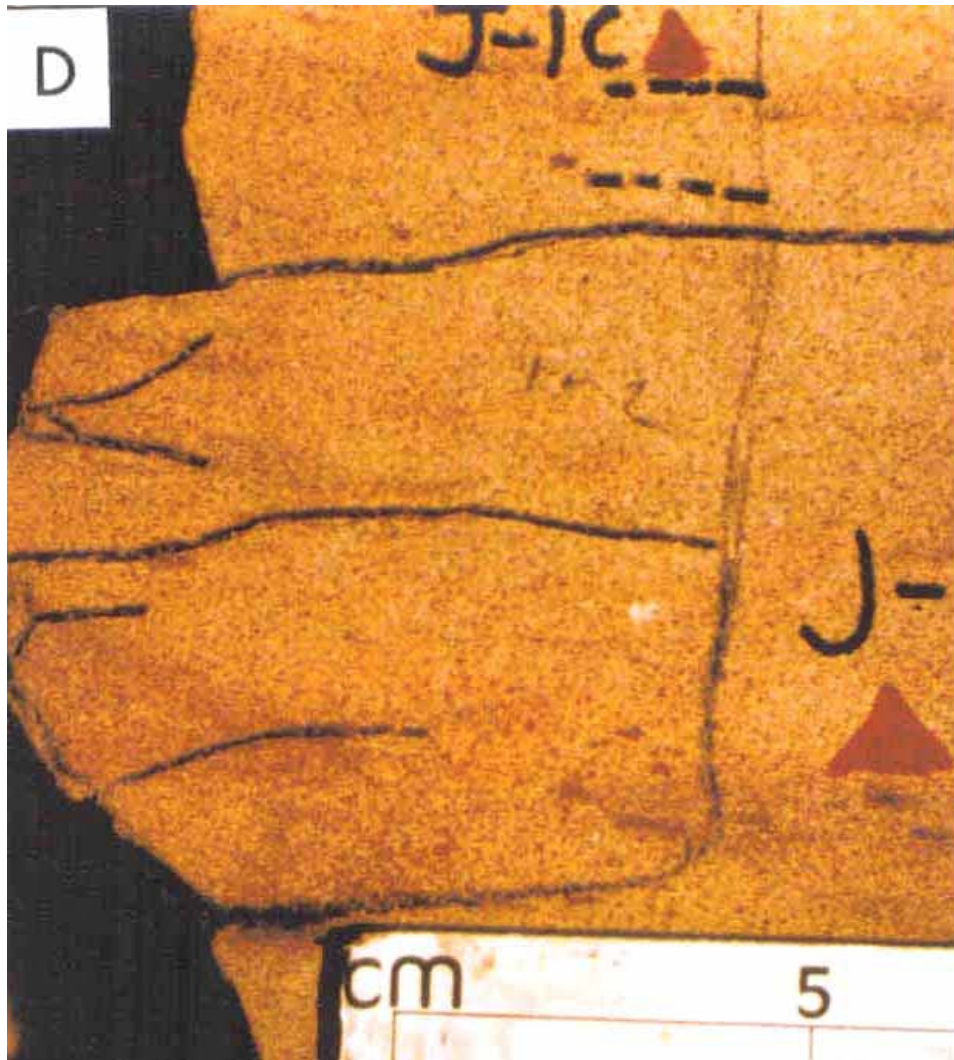


Figure 89. Johnson Quarry Sample J-1C-WD (after Agar 1998)

Sample J-2. This sample (Figure 91) was cut on one side of the test block away from the edges and included the tip of a pretest fracture. Thin Section Sample TS-J-2-1 was cut in a very homogeneous section away from the fracture tip. Thin Section Sample TS-J-2-2 was cut on a vertical, perpendicular section to that of Thin Section Sample TS-J-2-1. A third specimen was selected to study the open fracture surface in the corner of the block under secondary electron imaging but no thin section was made of this feature.

Test Block J-2-FT. This test block is shown in Figure 92.

Sample J-2-FT. This sample (Figure 93) exhibited no features related to potential **planes** of weakness or damage. Thin sections were therefore selected from two perpendicular sides of the block and located centrally within the specimen.

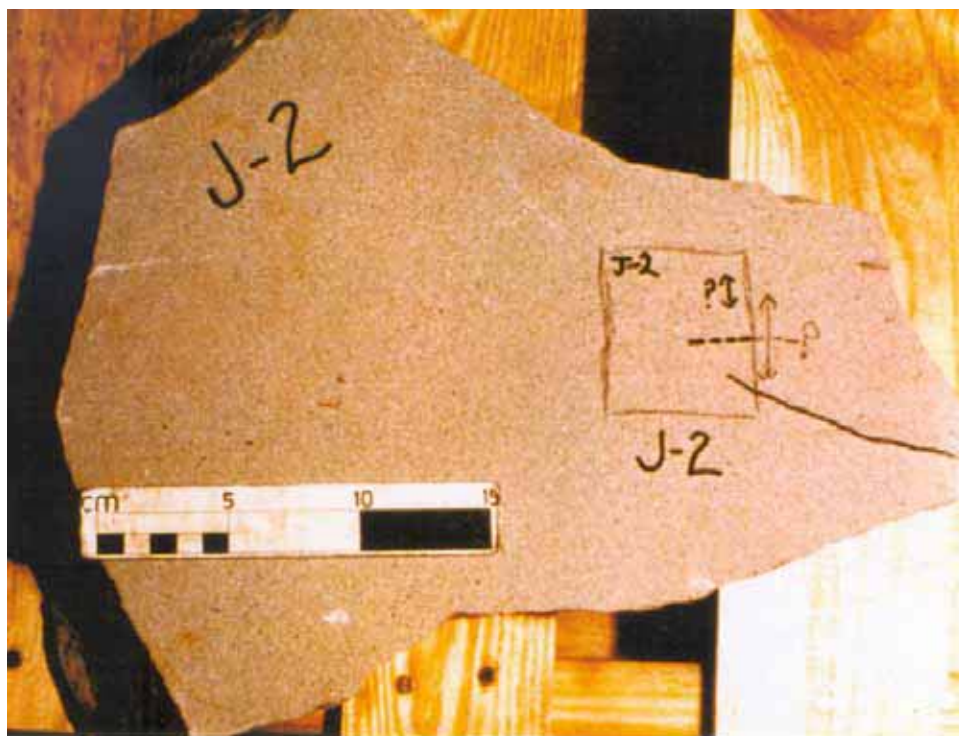


Figure 90. Johnson Quarry Test Block J-2 sample location prior to freeze-thaw exposure (after Agar 1998)

Composition, grain size, and porosity

The Berea sandstone in Test Blocks J-1-WD, J-2, and J-2-FT consists of a moderately well-sorted sandstone containing detrital quartz grains (some of metamorphic origin), lithic fragments whose relict textures suggest they are of volcanic origin, grains of potassium feldspar, chlorite, muscovite and amphiboles as well as detrital and authigenic Fe-Ti oxides, pyrite and clays (illite smectite), sparse glauconite and organic matter. Combination feldspar staining indicates potassium feldspar is at least 95 percent of the optically visible feldspars. Modal proportions are estimated from thin sections to be 10 to 15 percent potassium feldspar; 10 to 15 percent lithic fragments; 65 percent quartz; 5 percent clay minerals, detrital micas, and amphiboles; 3 percent calcite; and less than 2 percent opaques and glauconite. EDS spectral analyses were used to verify mineral phases. Quantitative analyses show that the potassium feldspar has a consistent orthoclase composition. Carbonate cement compositions range from calcite to ankerite and sideritic carbonate. Micaceous phases are commonly muscovites or partly altered chlorites. The mineral assemblage is common to all three test blocks, but Test Block J-1-WD contrasts with both Test Block J-2 and Test Block J-2-FT in its high content of hydrous magnesium-calcium-sulfate that is associated with dark brown laminations and lenses evident in hand sample.

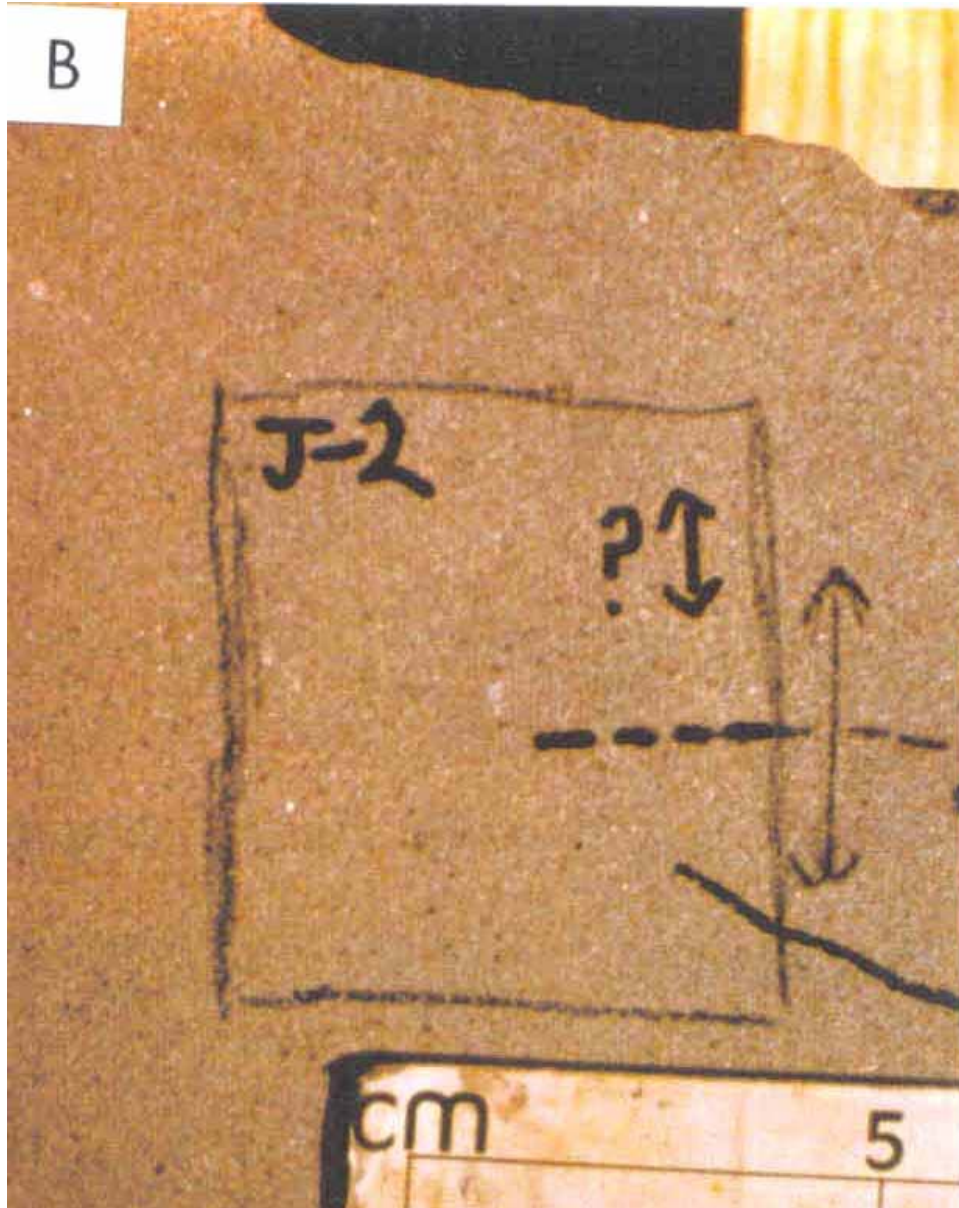


Figure 91. Johnson Quarry Sample J-2 prior to freeze/thaw exposure (after Agar 1998)

Grain size analyses from digital images gives a mean grain size from 150 to 200 microns (0.006 to 0.008 in.). Quartz grains typically have subrounded grain shapes, but their edges are flattened and commonly sutured by pressure solution that pervades all the samples. Lithic fragments have variable shapes from angular to rounded. They are commonly situated in the interstices of quartz grains. Platy muscovite and chlorite grains are commonly kinked or deflected around adjacent quartz grains.

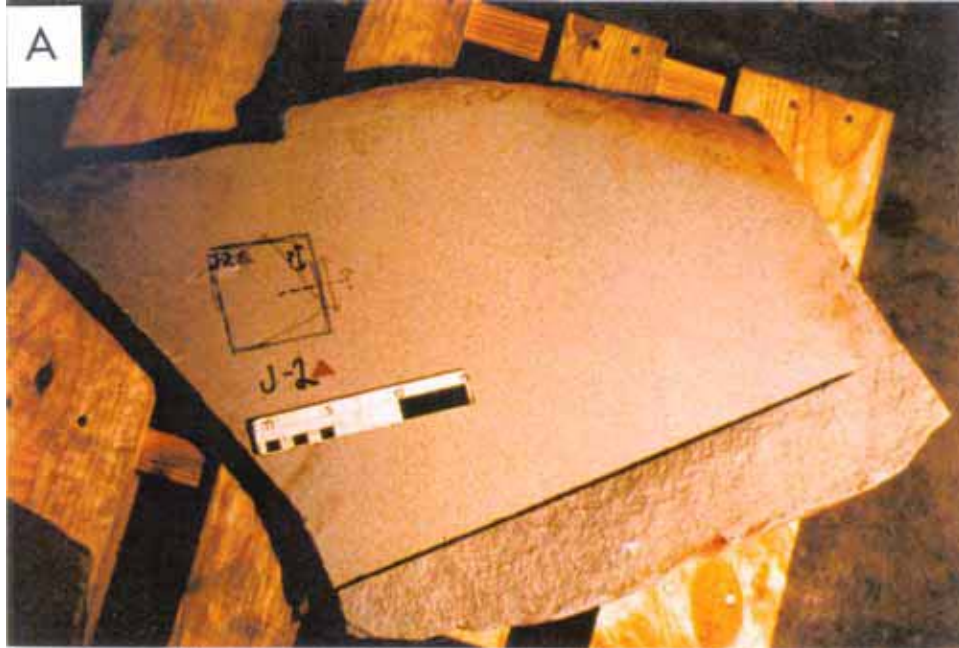


Figure 92. Johnson Quarry Test Block J-2-FT sample location (after Agar 1998)

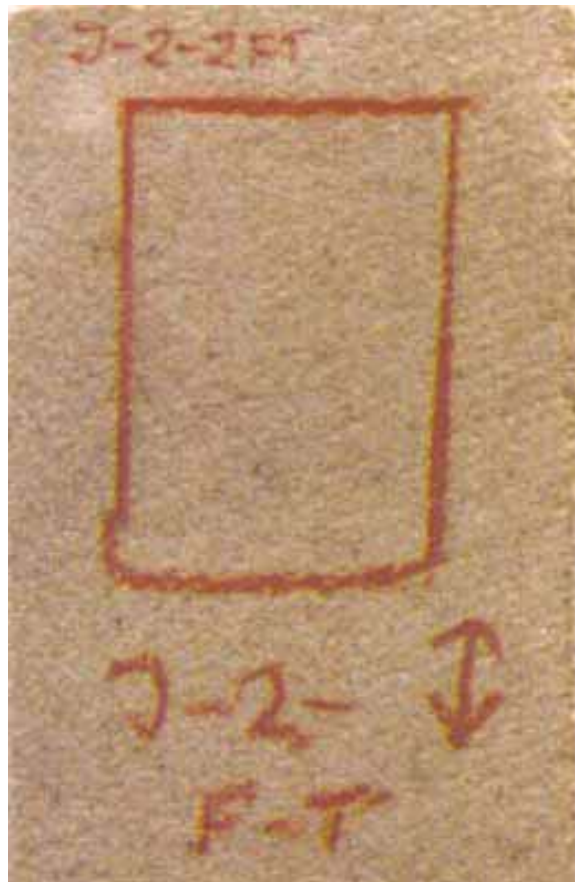


Figure 93. Johnson Quarry Sample J-2-FT (after Agar 1998)

Even though pressure solution is pervasive in the Johnson Quarry samples, the porosity is relatively high (estimates ranging from 17 to 23 percent for back-scatter image analysis, and 26 to 34 percent for optical estimates) and pore spaces have a variable morphology on thin section scale. In some areas the porosity is evenly distributed, but in other areas the disaggregation and plucking of material during thin section preparation forms large, irregular pores. Although the latter porosity is not a direct representation of the in situ porosity in the test blocks, it does give a useful indication of the locations and distributions of soft or disaggregated material that was easily dislodged. Qualitative differences observed in the extent of plucking between Test Block J-2 (less) and Test Block J-2-FT (more) thin sections may be caused by loosening of grains in the freeze/thaw testing.

Texture and diagenesis

Quartz, carbonate (calcite, ankerite and sideritic carbonate), fine-grained potassium feldspar, and clay minerals (illite/smectite) are the dominant cement phases in both Test Block J-2 and Test Block J-2-FT. A hydrous Mg-Ca sulfate forms a fifth cement phase in Test Block J-1-WD. The cement distribution in all the thin sections is patchy. Some cement was clearly dislodged during sample preparation, but even when impregnated with epoxy the cement distribution appears uneven. Quartz grains are commonly sutured by pressure solution seams, and secondary quartz overgrowths are evident under cathodoluminescence imaging. Although the pressure solution seams suture grains, they may also form future planes of weakness. Where pressure solution seams cross more than one grain, they tend to be oriented parallel to interpreted bedding planes but do not form a penetrative cleavage. In several places, the seams have opened preserving the flattened quartz grain boundaries on the margins of a microcrack. Apart from the local shape-preferred orientations of quartz and mica grains caused by compaction and pressure solution, there is no other evidence for either shape or crystallographic preferred orientations.

Patches of carbonate cement infill pores between quartz and lithic fragments. The calcite cement patches are typically zoned, comprising an inner, magnesium-rich core that is enveloped by weakly ferrous carbonate. Textural relations where calcite cement grains are flattened along their boundaries indicate that at least some of the pressure solution postdates the calcite phase of cementation. Quartz cement that predates the calcite cement is distributed as rims around quartz grains. Luminescence images indicate that some of the quartz cement may invade intragranular fractures in quartz, but in other cases fractures formed and sealed before the quartz overgrowths. Quartz luminosity under cathodoluminescence imaging is varied and probably reflects different sources of quartz grains, (e.g., vein quartz, volcanic, or metamorphic). The quartz grains commonly exhibit a substructure in which luminescent rims and healed intragranular fractures are apparent. These substructures may have formed prior to deposition as a consequence of thermal and mechanical stresses in volcanic or metamorphic source regions. They do not extend into quartz overgrowth rims and therefore predate them.

The hydrous Mg-Ca sulfate in the J-1-WD samples is distributed both as an interstitial cement that appears as a dark meshwork around grains and as a

microfracture fill. Crosscutting relations indicate that the sulfate cement post-dates some pressure solution and is younger than both the calcite, clay and quartz cements. An overall sequence of cementation is interpreted to be quartz \pm clay, calcite \pm clay pressure solution with additional minor quartz cementation, followed by sulfate cement.

Fractures, pressure solution seams, and local grain alignments

Sample J-1A-WD. The two pretest fractures in Thin Section Sample TS-J-1A-1WD are both associated with high proportions of the Ca-Mg sulfate although the locations of the open fracture surfaces do not directly coincide with seams of the sulfate cement. The fracture that extends from the sharp bend in the sample surface has the larger aperture. The aperture is variable (0.1 to 0.5 mm (0.004 to 0.02 in.)), and the fracture surfaces vary between approximately planar and an irregular morphology controlled by grains jutting out from the surface into the fracture cavity. The fracture surface locally coincides with the long axes of mica and chlorite grains. Matching morphologies on either side of the fracture indicate that there has been no lateral displacement. Porosity is elevated close to the fracture surface as a consequence of grain plucking. It is probable that most of this plucking occurred during thin section preparation, but grains are clearly less consolidated adjacent to the open fracture surface. At the specimen surface, the fracture aperture increases from 0.2 to 0.6 mm (0.008 to 0.02 in.), but there is no obvious increase in fracture damage or grain plucking along the edge of the section.

The second fracture in this section is represented by a thin (less than 1-mm) trace of sulfate cement that wraps around grains, giving it the appearance of a stylolite seam (although it is not). Some white mica flakes are aligned subparallel to this seam that is also subparallel to interpreted bedding orientation. There is no increase in intragranular fractures or pressure solution towards this feature. Backscatter imaging reveals minor intragranular fracturing along the thin section edge. The appearance of this feature as an open fracture prior to block testing may have been due to the sulfate material being easily dislodged. In the thin section there is a fine microfracturing but nothing that resembles the open fracture on the sample surface. The sulfate cement does not form a continuous vein fill. It thickens and thins following an approximately planar trace. There is no apparent compositional control on the location of these veins.

The gently dipping pretest fracture in Thin Section Sample TS-J-1A-2WD exhibits a similar close association with dark brown staining by sulfate cement. The sulfate has permeated microfracture arrays in quartz and potassium feldspar grains indicating that the cement precipitated synchronously with or after some of the microfracturing. The main microfracture, however, probably opened at a later (very recent) stage as the fracture surfaces are not weathered. Microfractures surrounding the main fracture surface accommodate only minor strains, and there is no evidence for frictional sliding along them. There is little evidence for disaggregation controlled by these fractures in this example although they may provide future planes of weakness. Locally dense arrays of microfractures are present adjacent to open fracture surfaces giving the rock a shattered appearance.

Sample J-1B-WD. This sample contains an open fracture surface with similar characteristics to those of the open fracture in Sample J-1A-WD. The fracture follows a curvilinear trace with an increase in porosity along parts of the microfracture walls due to grain plucking. Even though grain plucking is evident, relatively fragile hydrous sulfate cement is preserved in several regions close to the fracture. Mica flakes are aligned parallel to the fracture surface and may have guided the fracture propagation trace. The micas are kinked and folded around grains as a result of compaction, but locally they appear to control the orientation of the fracture surface.

The backscatter image of Sample J-1B-WD indicates that there is no evidence for chemical alteration along the fracture margin. If any fill was present, it was dislodged during sample preparation. As would be expected, quartz grains are relatively stable, but the feldspar rich cement and detrital volcanic clasts tend to break up and disaggregate. Elongate stringers of sulfate are typical of the dark stained regions in hand sample that are oriented subparallel to bedding. They are prone to weathering and tend to fall apart during specimen handling. The sulfate fills interconnected lenses and patches of porosity. Distribution of this cement appears to be commonly localized to stringers, but it is likely that some of the sulfate material was lost during sample preparation. Weakly aligned detrital muscovite and chlorite flakes commonly parallel stringers of sulfate. The feldspar and clay cement have a weakly foliated appearance that may have been caused by compaction. A zone of preferred shape orientation is oriented at about 30 deg to the margins of the open fracture surface showing that not all fracture orientations are controlled by detrital mica flakes or sulfate stringers.

Sample J-1C-WD. This sample displayed variable fracture damage along the edge of the specimen. A prominent triangular zone of fracture quartz grains is evident at the edge of the thin section above an open fracture surface. An apparent grain size reduction results from intense intragranular fracturing that creates numerous angular grains. The intense fracturing may be caused by local stress release during thin section preparation.

Sample J-2. The fracture tip region in Sample J-2 was opened along the fracture surface and examined in secondary mode. Minimal force was necessary to open the fracture and so it is unlikely that artifacts were induced during specimen preparation. The surfaces show the flattened shapes of quartz grains caused by pressure solution, but no evidence for enhanced dissolution processes along the fracture. Fresh conchoidal fractures with well-defined edges through some of the quartz grains indicate that the fracture is probably of recent origin.

Summary

The mechanical stability of samples from Test Block J-1-WD is clearly impacted by the presence of zones of sulfate cement and organic matter. Fractures tend to localize at irregularities on block margins, assisted by the presence of micas and/or sulfate cement parallel to bedding. The fractures appear relatively stable and do not cause significant damage in the surrounding material. There is no evidence for shear displacement along fractures nor is there any evidence of chemical alteration along open fracture surfaces. Most fractures are

interpreted to be of recent origin except where the sulfate cement seals some transgranular fractures. Locally intense, intragranular fracturing has occurred probably through stress release. Pressure solution has generated a weak-to-moderate anisotropy in all the samples. The secondary cement associated with this process may help to stabilize the quarystone. On the other hand, some of the straight pressure solved boundaries have tended to pull apart. Qualitative thin section observations suggest that the freeze/thaw samples from Test Block J-2-FT were more prone to grain scale plucking during sample preparation than the untested Sample J-2.

Recommendations

- a. It is important to map out the distribution of organic sulfate material within the quarry and determine how prevalent it is in existing break-water material. Blocks of quarystone rich in this material are likely to be highly unstable.
- b. Examine the blocks of Berea sandstone in breakwaters to see whether or not the fractures on the block margins examined in this study are the primary source of breakup.
- c. Review mechanical testing data for the Berea sandstone, and examine the distribution of fractures in blocks at different levels within the breakwaters to evaluate the effects of loading and stacking arrangements on breakup.
- d. Obtain orientation data for mesoscopic fractures in the quarry to evaluate whether layer parallel anisotropy formed by pressure solution controls fracture orientations by subsequent stress release along them.

Thornton Quarry

Test block, samples, and thin sections

Test Block MTC-3-FT/WD. Test Block MTC-3-FT/WD (Figure 94) was subjected to both freeze/thaw and wet/dry testing, and is extensively fractured. Samples MTC-3A-FT/WD and MTC-3B-FT/WD are vuggy, gray dolomite selected from the same test block. Layering in the test block is defined by horizons of bioclastic material and irregular brown clay laminations. Trails of vugs also trend parallel to these layers. A double-headed arrow was marked perpendicular to these layers to show the direction perpendicular to bedding.

Test Block MTC-3-FT/WD was one of the most fracture-damaged blocks in this study. In hand sample, the fractures are open and link into and through numerous vugs. Although there is no fracture fill phase evident in hand sample, parts of the fracture walls and the interiors of vugs weather to a yellow brown color. The test block surface displays several pre- and post-test fracture traces. Some of the post-test fractures link to pretest fractures, while others have formed adjacent to the margin of the test block. Both pre- and post-test fractures form roughly orthogonal sets, parallel and perpendicular to the bedding, but their

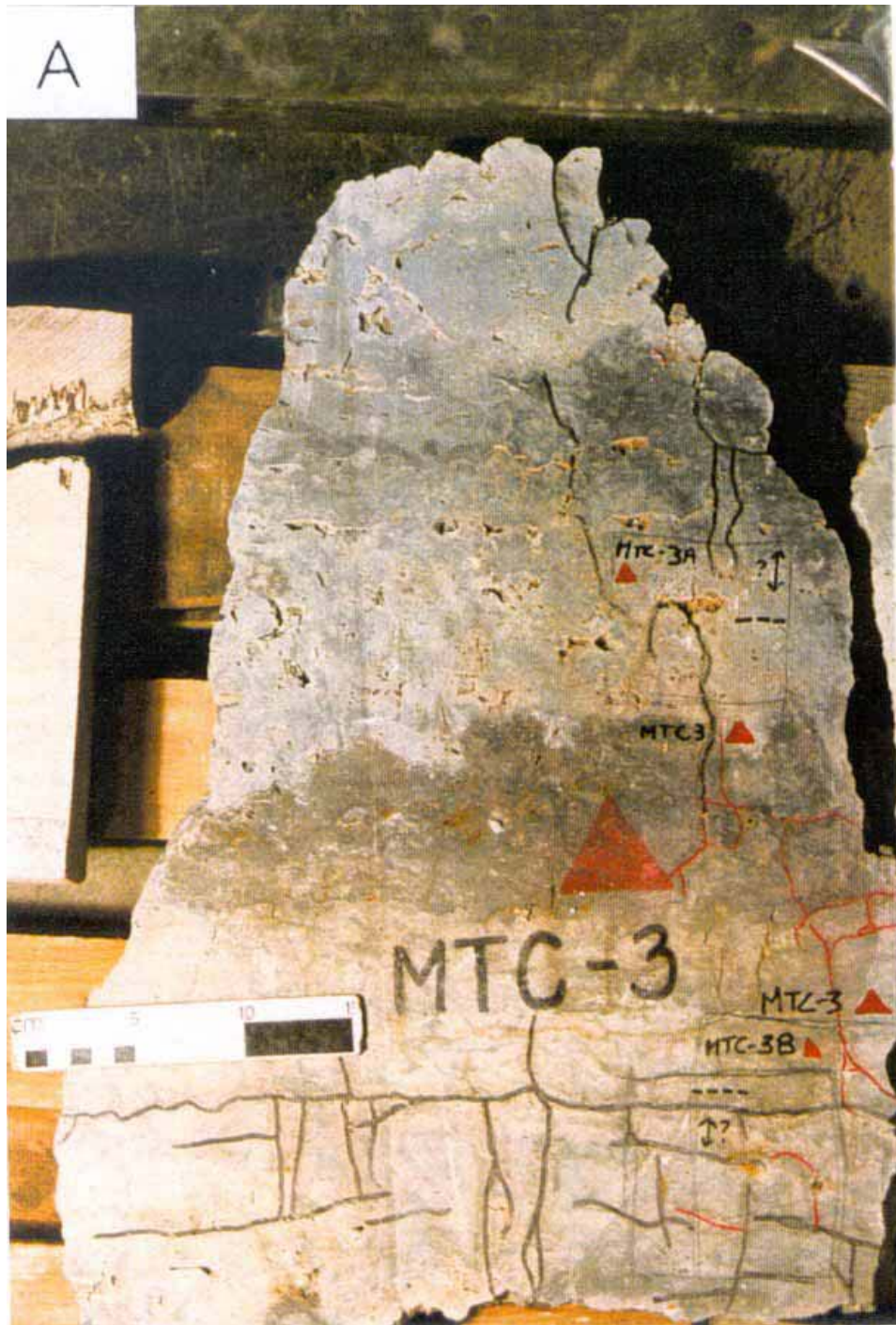


Figure 94. Thornton Quarry Test Block MTC-3-FT/WD sample locations. Arrows show direction perpendicular to interpreted bedding plane based on clay seam orientations (after Agar 1998)

traces are irregular. In hand sample, the character of the pre- and post-test fractures appears very similar. It would have been useful to have close-up photos of the block with no fracture markings before testing to compare with the pre- and post-test fracture delineations. The similarity and connectivity between pre- and

post-test fractures raises a question concerning the criteria used to define whether or not a fracture existed prior to testing.

- a. *Sample MTC-3A-FT/WD.* This sample (Figure 95) was selected to include several pretest (black lines) fractures in the interior part of the test block. Two thin sections were cut on the original marked surface of the block. Thin Section Sample TS-MTC-3A-1FT/WD includes three subvertical pretest fractures that taper into the center of the section. Several vugs are also present. Thin Section Sample TS-MTC-3A-2FT/WD was cut to include the open fracture surface of another steeply dipping pretest fracture that is deflected to a moderate dip into the sectioned area. Thin Section Sample TS-MTC-3A-1FT/WD was stained with Alizarin red to detect calcite.



Figure 95. Thornton Quarry Sample MTC-3A-FT/WD (after Agar 1998)

- b. *Sample MTC-3B-FT/WD.* This sample (Figure 96) was selected to include pre- and post-test fractures near the edge of the test block. Thin Section Sample TS-MTC-3B-1FT/WD includes one subvertical post-test fracture and one horizontal pretest fracture. The pretest fracture links into the post-test fracture. A vertical fracture extends below the post-test fracture, but it was not marked as either a pre- or post-test fracture. A splay from the post-test fracture veers toward the margin of the thin section. Thin Section Sample TS-MTC-3B-2FT/WD includes one subvertical and one subhorizontal example of pre- and post-test fractures. Both of the post-test fractures stop at the pretest fractures. Thin Section Sample TS-MTC-3B-2FT/WD was stained with K-Ferricyanide to detect ferrous carbonates.



Figure 96. Thornton Quarry Sample MTC-3B-FT/WD (after Agar 1998)

Composition, grain size, and porosity

The Thornton Quarry samples comprise mainly fine-grain dolomite with minor amounts of slightly magnesium calcite. Electron microprobe analyses show consistent dolomite compositions through both samples. In plane-polarized light, the dolomite appears cloudy, pale brown to white with numerous dark

brown inclusions. The dolomite grains typically appear pitted under backscatter imaging whereas calcite grains, that form late-stage overgrowths on vug rims, have a smoother appearance. Fine seams of green-brown clays form irregular, anastomosing laminations that trend roughly parallel to bedding. These seams contain magnesium and potassium bearing clays (probably smectite and illite) and fragments of potassium feldspar. In places the seams appear stylolitic. Minor Fe-oxides and Fe-sulfides are scattered throughout the matrix as well as within the clay seams (much less than 1 percent).

Grain size within the dolomite ranges from 40 to 80 microns (0.0015 to 0.003 in.) with clay and opaque phases generally less than 5 microns. Distinct changes in grain size across layer boundaries were not evident except between clay seams and dolomite. These probably represent primary compositional variations although pressure solution has contorted the clay seams. Grain boundaries in the dolomite are probably all secondary replacement features with some modification by pressure solution. The solution process along grain boundaries tends to obscure them under optical examination. Under secondary imaging, the smooth faces of randomly oriented dolomite rhombs are evident with micron-scale circular pits probably representing opened fluid inclusion cavities.

The character and quantity of porosity is spatially variable. Grain boundary porosity is typically low due to welding of grains by pressure solution. The most obvious porosity under optical examination is due to vugs that occur as linear trails subparallel to bedding as well as isolated, irregular shaped vugs. Fracture porosity forms apertures up to approximately 1 mm wide in thin section. Average porosity estimates from digital images are approximately 10 percent.

Texture and diagenesis

Backscatter electron imaging shows the dolomitization to be remarkably pervasive and homogeneous in Samples MTC-3A-FT/WD and MTC-3B-FT/WD. Cathodoluminescence signatures are also homogeneous except where calcite is present. Small patches of slightly magnesium calcite occur within dolomitic areas but most calcite is localized as overgrowth rims on the edges of crystals growing into vugs. The extensive dolomitization obscures any previous episodes of cementation in these samples but the morphology and structure of bioclasts is well preserved. Other work reports an earlier phase of silicification (Rock Products Consultants 1995), but it could not be identified in this study.

No shape or crystallographic-preferred orientation is evident in the dolomite. In the clay seams, however, there is a moderate-to-strong preferred orientation of micas with their long axes aligned parallel to the seam margins. The stylolitic form of the clay seams indicates that pressure solution has been operating but these microstructures are not strongly developed. Other centimeter-scale fabrics are formed by the perpendicular fracture arrays and the preferred alignment of vug trails.

The surface texture of the sample reflects the bimodal grain size of the dolomite, with large rhomb crystals protruding above a fine-grain matrix. Fluid inclusions have left behind pits in the finer-grain matrix.

Fractures and stylolites

Sample MTC-3A-FT/WD. The pretest fracture locations chosen for this section proved to penetrate only short distances into the sample, and their traces could not be located in thin sections. During cutting of the chip for Thin Section Sample TS-MTC-3A-1FT/WD, the sample developed a new fracture that cuts across the sample at about 60 deg. This fracture development is probably related to stored stress in the sample and therefore is considered as a post-test fracture. At one end of the fracture, an elongate fragment containing two microfractures has broken away from the fracture wall. Subsidiary hairline fractures trend sub-parallel to the main fracture walls, splaying out into the surrounding dolomite as well intersecting the main fracture surface. Grain boundaries in the surrounding dolomite have remained relatively tight.

Within the central region of this fracture, it has a relatively even aperture with only minor disaggregation along its margins. Subsidiary splays from the fracture isolate multigranular fragments that are potential regions of further disaggregation. Several dolomite grain fragments have disaggregated within one fracture that crosses the pretest fracture. The crosscutting relations between these fractures are ambiguous. The pretest fracture intersects and terminates in a vug and numerous minor fractures have developed around the vug walls. No chemical alteration is evident along the fracture margins except for minor variations in magnesium content.

The opposite open end of the same post-test fracture has a more irregular aperture than either of the two previous examples due to the fact that it passes through a vug. Adjacent vugs in the surrounding dolomite are undisturbed. Minor microfracture damage along the specimen edge has opened grain boundaries. Some microfracture damage is spatially associated with vugs. Microfractures in this sample tend to open along grain boundaries that form the narrow bridges between vugs. Narrow arrays of fine microfractures also develop parallel to the vug margin promoting disaggregation.

Pretest fractures in Thin Section Sample TS-MTC-3A-2FT/WD do not appear different from the post-test fracture in Thin Section Sample TS-MTC-3A-1FT/WD. The fractures have apertures locally exceeding 0.5 mm (0.02 in.) and do not display any indications of lateral displacements. The fracture walls are roughly parallel except where fractures have intersected vugs or where the fracture tips out. Grain plucking is evident around the edge of the thin section adjacent to fracture walls but the margins of the fractures appear relatively stable. Hairline fractures lined with fine brown clay minerals pervade both thin sections. These are not deflected by the open pretest fractures and are therefore interpreted as an earlier generation of microfractures. No chemical alteration is evident along either the pre- or post-test fracture surfaces in this sample.

Sample MTC-3B-FT/WD. Pretest fractures in this sample had similar characteristics to the fractures in Sample MTC-3A-FT/WD. In Thin Section Sample TS-MTC-3B-1FT/WD the pretest fracture had a wider aperture than the post-test fractures, but there is no evidence for lateral offset nor is there any evidence for chemical alteration either. Some of the pretest fracture walls in Thin Section Sample TS-MTC-3B-1FT/WD appear unstable due to branching microfractures, some of which are filled with clay seams. Some of these microfractures intersect at sharp turns in the open fracture margin. Fine hairline fractures trend along the fracture walls parallel to the main open fracture in Thin Section Sample TS-MTC-3A-1FT/WD. In Thin Section Sample TS-MTC-3B-2FT/WD, the pretest fractures were narrower than those in Thin Section Sample TS-MTC-3B-1FT/WD. The trace of the horizontal fracture roughly follows that of an array of clay seams but not exactly.

The fracture that was marked as a post-test fracture in Thin Section Sample TS-MTC-3B-2FT/WD extends perpendicular to the main pretest fracture. Overall the post-test fracture has a much narrower aperture than that of the pretest fractures and tapers away from their intersection. A fracture with an aperture of less than 5 mm (0.2 in.) extends from the opposite side of the pretest fracture and may be an extension of the post-test fracture that was not identified when the test block was originally marked.

Numerous microfractures cross this specimen at orientations predominantly subparallel and perpendicular to the interpreted bedding orientation. As these fractures were too fine to mark in the test block, it is not possible say at what point they formed relative to testing. These fractures typically have apertures of less than 5 microns (0.0002 in.). In Thin Section Sample TS-MTC-3A-1FT/WD some of these fractures are crossed by the post-test fracture, but crosscutting relations are ambiguous. The micro fracture traces are irregular on a grain scale. Sometimes they are deflected by vugs but not always. Vugs also form common points of intersection. Grain boundaries in the bridges between adjacent vugs tend to be more open than those in the surrounding dolomite and transgranular fracturing is evident in some bridges. Again, as in other fractures, there is no evidence of chemical alteration around the fracture margins.

The clay seam development in this sample is more extensive than those in Sample MTC-3A-FT/WD. In places, these seams appear stylolitic and coincide with parts of the pretest clay seams. In places, these seams are clearly a weakness in the Test Block MTC-3-FT/WD samples as open fractures have formed along them. However, they do not represent a penetrative anisotropy on thin section scale, nor do they always coincide with fracture orientations. Some seams have stylolitic traces, others follow anastomosing paths with several clusters of seams forming overlapping segments that are subparallel to bedding, and some have vug trails. The seams have preferred shaped alignment of detrital chlorite and clay minerals, but subgranular fragments of potassium feldspar have no preferred orientation. The dolomite grains in the margins of these clay seams appear to be corroded with undulatory or flattened grain boundaries. Fractures are locally deflected for 1 to 2 mm (0.04 to 0.08 in.) along clay seams.

Summary

The primary source of weakness in the Thornton Quarry samples are sub-perpendicular arrays of fractures that are interpreted primarily as unloading cracks formed by stress release before, during, or after quarrying. All the fractures are inferred to be of recent origin due to the lack of evidence for any chemical modification of the fracture surfaces by surface weathering or groundwater circulation. The propagation paths of these cracks often terminate in vugs that may serve to dampen the elastic response of the rock. Aligned trails of vugs, however, may promote fracture propagation. The open fracture walls exhibit varying degrees of stability, but they are common sites for grain-scale disaggregation and grain plucking.

Both samples have a homogeneous chemical composition resulting from the completeness of the dolomitization process. Remaining lithological contrasts are found at stylolite boundaries and provide a further source of weak anisotropy in the samples. The stylolite abundance and continuity does not appear to represent a major control on the breakup of the samples, but they maybe more abundant in other parts of the quarry.

Recommendations

- a.* Establish the relationship of microscale fracture orientation and distribution relative to mesoscale and macroscale fracture systems in the quarry and in situ stress conditions. This requires fully oriented samples.
- b.* It is critical to examine the behavior of this material in situ in breakwater settings and document the correlation between fracture system characteristics in the quarry and in the breakwaters.
- c.* Quantify the shapes and sizes of blocks during breakwater attrition may help to distinguish the different fracture systems contributing to any failure. Different fracture mechanisms may generate different populations of block shapes and sizes.
- d.* Determine the spatial variation in stylolites within the quarry and assessing their role in the breakwater setting in controlling block breakup.
- e.* Further investigations of the role of vugs and porosity distribution in failure locations are recommended. Are regions with high porosity more prone to failure than low porosity regions? If so, then a better understanding of the spatial distribution of porosity in the quarry would be valuable.
- f.* Seek out information on the distribution of dolomitization in the quarry. Is it always as homogeneous as in the samples used in this study? Are silicified regions more stable than dolomitized areas?
- g.* Seek out mechanical testing literature for the Thornton Quarry for information on documentation of specific failure mechanisms for loading conditions similar to those in the breakwater setting.

McCook Quarry

Samples from the McCook Quarry were unavailable for microstructural analysis.

Summary of Quarry Sample Microstructural Analyses

The following conclusions may be deduced from the microstructural analyses pertaining to the mechanical stability of samples studied in this evaluation.

- a.* Several different types of discontinuities and potential sources of weaknesses were recognized in the samples. These may act alone or together to promote disaggregation in breakwater stones, but their role cannot be fully evaluated without a better understanding of how breakup proceeds in the breakwater setting. From the microstructural analyses in these samples, the freeze/thaw and wet/dry testing did not provide conclusive evidence for the direct effects of these processes on rock stability. There was no real discernible difference between pre- and post-test open fractures except where the path of the fractures was controlled by a preexisting weakness.
- b.* The majority of open fractures in quarry samples appear to be very recent. There is little or no weathering on their surfaces. Fractures may have been generated as a direct result of quarrying or transport methods, but in several cases, stress release was probably a major contributing factor. A compilation of in situ stress data for the quarries and the relationship of principal stress orientations to existing discontinuities would help to understand the overall importance of stress release in the rock stability.
- c.* Although there are several open fractures in each sample set, most of the fracture walls appear relatively stable (but not all). Therefore, their existence may not necessarily be the primary cause of breakup. It is important to establish how fractures propagate through the samples by documenting the behavior of the quarriestones over several years.
- d.* Where planar, geological discontinuities exist, such as stylolites, they are obvious planes of weakness, and in several cases these parted during sample cutting. The overall impact of these features on rock stability may be influenced by the orientations of the blocks in the breakwater. Some loading configurations may keep these structures stable.
- e.* Grain scale preferred orientations do exist in some samples (e.g., Dempsey Quarry samples). Where platy minerals form part or all of the fabric, there exist significant weaknesses. Sample disintegration does not appear to be significantly impacted by crystallographic preferred orientations in quartz or calcite.

- f.* In Johnson Quarry the distinct sulfate vein filling and cement phases contribute to weakening the rock. Compositional variations in the Sandusky and Marblehead Quarry samples also control the locations of some fractures.
- g.* If such a study has not already been undertaken, it would be valuable to examine the loading patterns of blocks in breakwaters and evaluate whether there are consistent points of failure in this pattern that could be avoided by some different arrangement.
- h.* Analytical and computer modeling of the breakup of the blocks could place limits on the stresses that blocks could sustain in particular stacking configurations and would help to understand the overall breakup process.
- i.* A summary of the rock mechanics literature for each of these quarries should be made. Experimental deformation studies would be useful to test the role of vugs in the limestone and dolomite lithologies in localizing fractures.
- j.* This study was limited in scope to direct observations of microstructures with limited background information on the outcrop setting of the test blocks. It is crucial that any further studies construct detailed sketches of the geological features surrounding sampled areas, and that all samples are oriented. Information was lost in this study because the samples were not oriented at the outcrop, and features could not be related to meso-scale structures. This information could modify the interpretations.
- k.* A key objective of future studies should be linking the microstructures observed in the test blocks to microstructures and mesostructures, both in quarries and in existing breakwaters where the stones are already in use.
- l.* A detailed structural analysis of the quarries, including a structure map, is needed to establish the primary structural trends (joints, faults, flexures) and their relation to stratigraphy, in situ stress, and unloading histories.

5 Field Prototype Monitoring¹

Monitoring of specifically selected sections of four stone breakwaters and one stone revetment was accomplished according to the 3-year monitoring plan developed cooperatively among the U.S. Army Engineer Districts, Buffalo and Chicago, and the U.S. Army Engineer Research and Development Center. Prototype monitoring took place during the time period 1996 through 1998. Major findings of those investigations follow.

(Editor's note: There are various methodologies for extracting armor stone from quarries, including (a) mechanical cutting or sawing, (b) low-energy blasting, and (c) high-energy blasting. (These three extraction methodologies are discussed by the author in this chapter.) Once large stones are extracted from the working face, they may subsequently be resized by various methods, including (a) mechanically saw-cutting, (b) breaking with pneumatic chisels, and/or (c) drilling and splitting with wedges. These methods may be used exclusively or in combination. Armor stones originating from Valders Quarry, and evaluated as part of this MCNP monitoring study, are described and analyzed herein by the author as being cut dolomite. In actuality, the process for obtaining those armor stones involved exposing working faces at Valders Quarry and extracting large stone blocks by low-energy blasting, and then reducing those large blocks to the desired armor stone size by drilling and splitting with wedges. Subsequently, as many as two faces of some of those stones may have been cut (sawed) to produce a desired relatively uniform armor stone surface (Personal Communication, 20 August 2004, from Bill Gessel, Jr., owner, Valders Quarry, to Joseph A. Kissane, P.G., Geotechnical Engineer/District Geologist, U.S. Army Corps of Engineers, Chicago District, Chicago, IL). Based on additional information provided to Mr. Kissane by Mirza Baig, former District Geologist, Chicago District, (who participated in the inspection of the Chicago District's structures included in this study), most, if not all, armor stone from Valders Quarry described by the author in this chapter as being cut dolomite may also contain blast stresses and fractures not found in truly cut (sawed) limestone from Reed Quarry or sandstone from Johnson Quarry where stones are cut (sawed) from the quarry face with essentially no blasting utilized in the extraction process.)

¹ This section was written by David W. Marcus, formerly District geologist, U.S. Army Engineer District, Buffalo, Buffalo, NY.

Structures and Sections Monitored

Ten different sections of five Great Lakes harbor structures were selected for field prototype monitoring because these sections had experienced premature stone deterioration, and because these sections would provide a maximum variety of stone on the structures that had been produced from local quarries. Six different stone types existed on these 10 different structure sections, including (a) dolomite (cut and blasted), (b) limestone (cut and blasted), (c) quartzite (blasted), (d) taconite (blasted), (e) dolomitic limestone (blasted), and (f) sandstone (cut). The 10 different structure sections, the corresponding six different stone types with their method of extraction, the eight different quarry sources, and the number of individual stones evaluated in each section, are shown in the following:

- a. *Chicago Harbor breakwater, IL.*
 1. Sta 14+65 to sta 16+00

Cut dolomite—Valders Quarry	50 stones
Cut limestone—Reed Quarry	<u>81 stones</u>
Total	131 stones

- b. *Calumet Harbor breakwater, IL and IN.*
 2. Sta 117+55 to sta 118+90

Cut dolomite—Valders Quarry	3 stones
Cut limestone—Reed Quarry	132 stones
Blasted quartzite—Dempsey Quarry	<u>18 stones</u>
Total	153 stones

- c. *Calumet Harbor CDF revetment, IL.*
 3. Sta 33+00 to sta 33+40

Blasted dolomite—McCook Quarry	43 stones
Cut dolomite—Valders Quarry	3 stones
Cut limestone—Reed Quarry	1 stone
Blasted taconite—Iron Mountain Quarry	<u>2 stones</u>
Total	49 stones

- d. *Burns Harbor breakwater, IN.*
 4. Shore Arm section sta 53+60 to sta 54+55

Cut limestone—Reed Quarry	1 stone
Blasted quartzite—Dempsey Quarry	<u>60 stones</u>
Total	61 stones

 5. Big Burn section sta 03+30 to sta 04+10

Cut limestone—Reed Quarry	34 stones
Blasted dolomite—McCook Quarry	<u>103 stones</u>
Total	137 stones

- e. *Cleveland Harbor east breakwater, OH.*
 6. Sta 102+00 to sta 103+00

Cut sandstone—Johnson Quarry	94 stones
------------------------------	-----------

7. Sta 107+40 to sta 108+60
Blasted dolomitic limestone—Marblehead Quarry 73 stones
8. Sta 121+90 to sta 123+15
Blasted dolomitic limestone—Marblehead Quarry 73 stones
9. Sta 164+00 to sta 165+20
Blasted limestone—Sandusky Quarry 127 stones
10. Sta 197+50 to sta 198+75
Blasted dolomitic limestone—Marblehead Quarry 60 stones

Dolomite from the Thornton Quarry, Thornton, IL, and from the Cedarville Quarry, Cedarville, MI, has been used on structure sections not specifically identified already for monitoring. Laboratory samples were also obtained from stone on breakwaters structures that had originated from these two quarries, as well as samples from the eight quarries previously mentioned, for the purpose of providing details about rock composition, structural characteristics, and deterioration as part of the field prototype monitoring component of this MCNP study.

A total of 864 stones were evaluated in this field prototype monitoring study.

Typically representative photographs of the breakwater stone on the monitored structure sections are presented in Figures 97-107.



Figure 97. Chicago Harbor breakwater, Valders Quarry cut dolomite (low energy blasted, drilled and split, and then surfaces cut; see editor's note, p. 149). Dolomitic mudstone/reef-rock and dolomitic mudstone in one block. Although not presently fractured, there is excellent probability that this block will eventually fracture along the contact between the two rock types (Rock Products Consultants 1995)



Figure 98. Chicago Harbor breakwater, Reed Quarry cut limestone. These blocks have been in place about 75 years (Rock Products Consultants 1995)



Figure 99. Calumet Harbor breakwater, Reed Quarry cut limestone. Mechanical fractures both parallel and normal to bedding. This stone has been in place for about 30 years (Rock Products Consultants 1995)



Figure 100. Calumet Harbor breakwater, Dempsey Quarry low energy blasted quartzite (Rock Products Consultants 1995)



Figure 101. Calumet Harbor CDF, McCook Quarry high energy blasted dolomite. Dolomitic reef rock with somewhat brecciated appearance and a fracture normal to bedding. The fracture could either be blast-related or simply mechanical (Rock Products Consultants 1995)



Figure 102. Burns Harbor breakwater (Shore Arm section), Dempsey Quarry low energy blasted quartzite (Rock Products Consultants 1995)



Figure 103. Burns Harbor breakwater (Big Burn section), Reed Quarry cut limestone (photo by Robert R. Bottin, ERDC)



Figure 104. Burns Harbor breakwater (Big Burn section), McCook Quarry high energy blasted dolomite. Dolomitic mudstone exhibiting fracturing due to weathering processes (Rock Products Consultants 1995)



Figure 105. Cleveland Harbor east breakwater, Johnson Quarry cut sandstone (photo by Robert R. Bottin, ERDC)



Figure 106. Cleveland Harbor east breakwater, Marblehead Quarry low energy blasted dolomitic limestone. Note extensive fracturing (Rock Products Consultants 1995)



Figure 107. Cleveland Harbor east breakwater, Sandusky Quarry high energy blasted limestone (photo by Robert R. Bottin, ERDC)

Inspection of Breakwater Structure Sections

All visible and accessible sides of the above-water stones were inspected closely for any deterioration features, as described in the monitoring plan. An overt effort was made to only attribute a specific cause of a fracture based on unquestionably visible evidence that could be recorded by photography. The intent was to eliminate interpretations that could not be corroborated by another registered professional geologist. Examples of such evidence are (a) blast hole clearly visible with radiating fractures, (b) separation along a bedding plane with bedding plane features clearly visible, (c) fractures obviously radiating from chert nodules, and (d) fractures obviously radiating from vugs (voids). Recorded parameters included fracture orientation, magnitude, and type; progressive change in crack; and petrographic description, location, orientation, and photographs of each stone.

Fractures of all magnitudes, orientation, and types

Fractures were rated on a numerical scale based on the extent of penetration through the stone. Also recorded was the movement of stone. If a stone, or more than 20 percent of a stone, was dislocated, then the stone was considered lost. For the purposes of monitoring the geologic performance of the stone, only the progression of cracks was compared. Movement of the stone after it had broken up was considered a consequential effect, and not directly related to stone durability.

Qualitative terms were used to describe the condition of each stone. This was based on the presence and type of crack(s) the stone contains. Any crack(s) in a stone can be defined as (a) minor, (b) significant, or (c) failure based on the amount of stone it propagates along and/or penetrates through. A minor crack was defined as a nonopening crack on only one face of the stone. A significant crack was a nonopening continuous crack on two or more faces of the stone. A failure crack was a continuous throughgoing crack opening up 20 percent or more of the stone. A nonsignificant failure crack was a continuous throughgoing crack opening up less than 20 percent of the stone.

The condition of any stone was described as either (a) no cracks, (b) minor cracked, (c) multiply minor cracked, (d) significant cracked, (e) multiply significant cracked, (f) failed, (g) multiply failed, (h) fragmented, (i) multiply fragmented, (j) displaced, (k) multiply displaced, (l) lost1, (m) lost2 or (n) lost3. A stone was defined as **no cracks** if it was free of any cracks. A **minor cracked** stone contained a minor crack. A **multiply minor cracked** stone contained two or more minor cracks. A **significant cracked** stone contained a significant crack. A **multiply significant cracked** stone contained two or more significant cracks. A **failed** stone contained one failure crack with a separation thickness of hairline to 10 cm (4 in.) A **multiply failed** stone contained two or more failure cracks with a separation thickness of hairline to 10 cm (4 in.). A **fragmented** stone was one where two significant broken pieces (> 20 percent of the original volume) separate 10 cm (4 in.) to 0.6 m (2 ft) apart. A **multiply fragmented** stone was one where three or more significant broken pieces separate 10 cm (4 in.) to 0.6 m (2 ft) apart. A **displaced** stone was one where two significant broken pieces

move apart greater than 0.6 m (2 ft). A **multiply displaced** stone was one where three or more significant broken pieces move apart greater than 0.6 m (2 ft). A stone with 20 to 40 percent of its original volume missing was described as **lost1**. A stone with 40 to 80 percent of its original volume missing was described as **lost2**. A stone with 80 to 100 percent of its original volume missing was described as **lost3**.

Any stone that was failed, multiply failed, fragmented, multiply fragmented, displaced, multiply displaced, lost1, lost2, or lost3 was labeled a **rejected** stone. A rejected stone had lost its integrity and no longer functioned as one originally placed unit. The figures and photographs included show a representative example of no cracks, minor cracked, multiply minor cracked, significant cracked, failed, multiply failed, fragmented, multiply fragmented, displaced, multiply displaced, lost1, lost2 and lost3 stone.

The number of pieces the stone was in during the inspection period was noted. Displacement (movement or shifting) was recorded if the entire stone has moved more than a foot from its original location, or if pieces of the stone have moved apart greater than 10 cm (4 in.). Any noticeable change or progressive deterioration from the previous inspection was recorded. Stone changes such as extension of fractures, formation of new fractures, separation along fractures, seams and stylolites, spalling, volume loss, etc. were marked and again photographed each successive year. These photographs were from the same angle and distance from previous corresponding photos to clearly show all changes between inspection periods. The following scale of Table 2 was developed for comparison, and the photographs in Figures 108-121 illustrate the relative degrees of degradation.

Table 2 Relative Degree of Stone Degradation	
Nature of the Cracked Stone	Quality Rating, percent
No cracks (free of cracks)	100
Minor cracked (crack visible on one side of stone)	80
Multiply minor cracked	70
Significant cracked (crack visible on two sides of stone)	60
Multiply significant cracked	50
Failed (crack splits stone into two pieces)	40
Multiply failed	30
Fragmented	20
Multiply fragmented	10
Displaced	5
Multiply displaced	3
Lost1	2
Lost2	1
Lost3	0



Figure 108. No cracks, Cleveland Harbor east breakwater, Sandusky Quarry high energy blasted limestone, quality rating = 100 percent



Figure 109. Minor cracks, Cleveland Harbor east breakwater, Sandusky Quarry high energy blasted limestone, quality rating = 80 percent



Figure 110. Multiply minor cracked, Chicago Harbor breakwater, Valders Quarry cut dolomite (low energy blasted, drilled and split, and then surfaces cut), quality rating = 70 percent (courtesy of Rock Products Consultants 1995)



Figure 111. Significant cracks, Cleveland Harbor east breakwater, Marblehead Quarry low energy blasted dolomitic limestone, quality rating = 60 percent

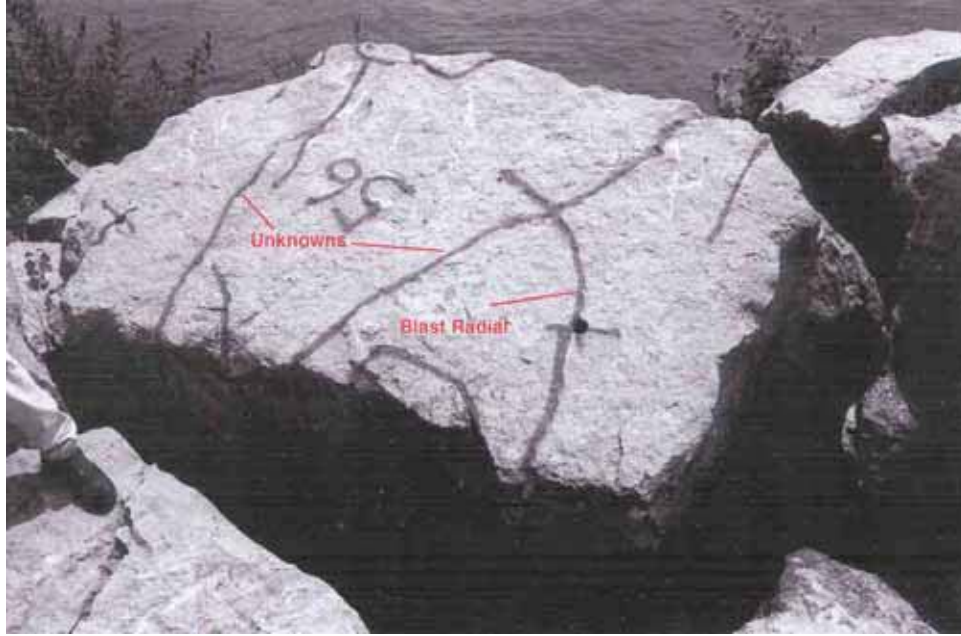


Figure 112. Multiply significant cracked, Cleveland Harbor east breakwater, Marblehead Quarry low energy blasted dolomitic limestone, quality rating = 50 percent

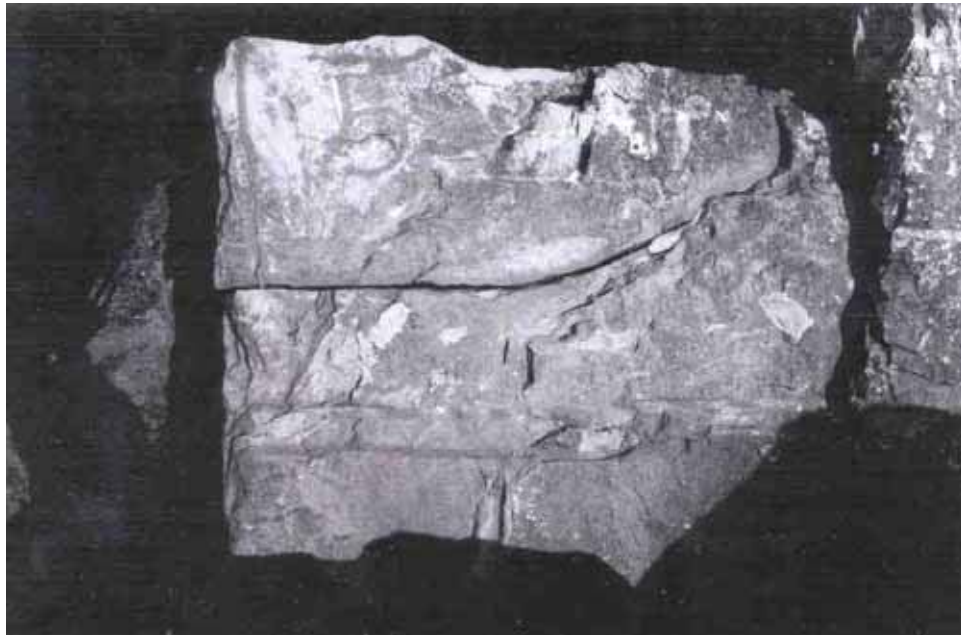


Figure 113. Failed, Cleveland Harbor east breakwater, Marblehead Quarry low energy blasted dolomitic limestone, quality rating = 40 percent



Figure 114. Multiply failed, Cleveland Harbor east breakwater, Marblehead Quarry low energy blasted dolomitic limestone, quality rating = 30 percent



Figure 115. Fragmented, Cleveland Harbor east breakwater, Marblehead Quarry low energy blasted dolomitic limestone, quality rating = 20 percent



Figure 116. Multiply fragmented, Cleveland Harbor east breakwater, Marblehead Quarry low energy blasted dolomitic limestone, quality rating = 10 percent



Figure 117. Displaced, Cleveland Harbor east breakwater, Marblehead Quarry low energy blasted dolomitic limestone, quality rating = 5 percent



Figure 118. Multiply displaced, Cleveland Harbor east breakwater, Marblehead Quarry low energy blasted dolomitic limestone, quality rating = 3 percent



Figure 119. Lost1, Cleveland Harbor east breakwater, Marblehead Quarry low energy blasted dolomitic limestone, quality rating = 2 percent



Figure 120. Lost2, Cleveland Harbor east breakwater, Sandusky Quarry high energy blasted limestone, quality rating = 1 percent



Figure 121. Lost3, Cleveland Harbor east breakwater, Marblehead Quarry low energy blasted dolomitic limestone, quality rating = 0 percent

Clearly visible evidence

Cracks were classified based on clearly visible evidence. The cracks were divided into the following types shown in Table 3.

Table 3 Relative Crack Classification Based on Nature of Crack	
Nature of the Crack	Type Classifications
No crack	0
Radiating from blast hole	1
Apparent radial (unknown cause)	2
Apparent blast fracture (concentric)	3
Dissolution at grout contact	4
Radiating or dissolution from vug	5
Radiating from chert nodule	6
Along a bedding plane	7
Along a stylolite	8
Along shale or clay seam	9
Mirror image	10
Hairline crack (unknown cause)	11
Angled to bedding plane (unknown cause)	12
Spall, edge, or corner (probable handling breakage)	13
Unidentified	14
Undifferentiated fabric	15
Perpendicular to bedding (stress or fabric related)	16
Undefined blast fracture	17

Progressive change in each crack

The progressive change in each crack was also recorded for the 3-year monitoring period. The sum of the changes to all cracks in a particular stone over the 3-year period yielded a change factor for that stone. The changes were numerically scored based on the following relative subjective point system of Table 4.

Table 4 Stone Crack Change Factor Relative Points	
Change Factor	Relative Points
No crack-to-minor cracked	+1
Minor cracked-to-multiply minor cracked	+1
Minor cracked-to-significant cracked	+1
Significant cracked-to-multiply significant cracked	+1
Significant cracked-to-failed	+1
Failed-to-multiply failed	+1

Petrographic description of each stone

Petrographic descriptions were also taken of each clearly visible stone. Only stones that were not covered in algae were described. This was necessary to insure an accurate description of the whole stone. A number of stones were not described in detail either because they were covered in algae or were not accessible due to high water. Only those stones that were accurately described were used in the comparisons.

Location of each stone

The location of each stone relative to the waterline was also recorded. The stones were described as being located either on the crest of the structure or at the waterline.

Orientation of each stone

The orientation of each stone relative to bedding was also recorded. The relative position of bedding was described as either horizontal, vertical, or angled. The relative proportion of orientations for each group of stone types were compared to evaluate whether the position affected the deterioration results.

Photographic documentation of each stone

The existing condition of each stone was photographed individually, and a videotape was made in 1995. The photographic documentation was used to track the progress of deterioration. A short description of any noticeable increase in deterioration and any change in the position of the stone on the structure were recorded. The changes in the stone such as an extension of an existing fracture, formation of a new fracture, or any other deterioration features, were marked with different colored paint prior to taking photographs in 1996. Similar procedures were followed in 1997. A detailed evaluation and photograph comparison was subsequently performed to document the observations recorded on the data sheets.

Breakwater Stone Deterioration

Stone quality classification was ascertained for each individual stone on each of the 10 breakwater structure sections monitored for three years (1995, 1996, and 1997). Figures 122 through 141 summarize the degradation conditions at the conclusion of monitoring (end of 1997), for each structure section. Additionally, these figures contain pertinent information regarding the degradation conditions for each stone type (a) cut sandstone, (b) cut limestone, (c) blasted limestone, (d) cut dolomite, (e) blasted dolomite, (f) blasted dolomitic limestone, and (g) blasted quartzite. That information is not displayed graphically although it is shown in Table 5 for subsequent presentation.

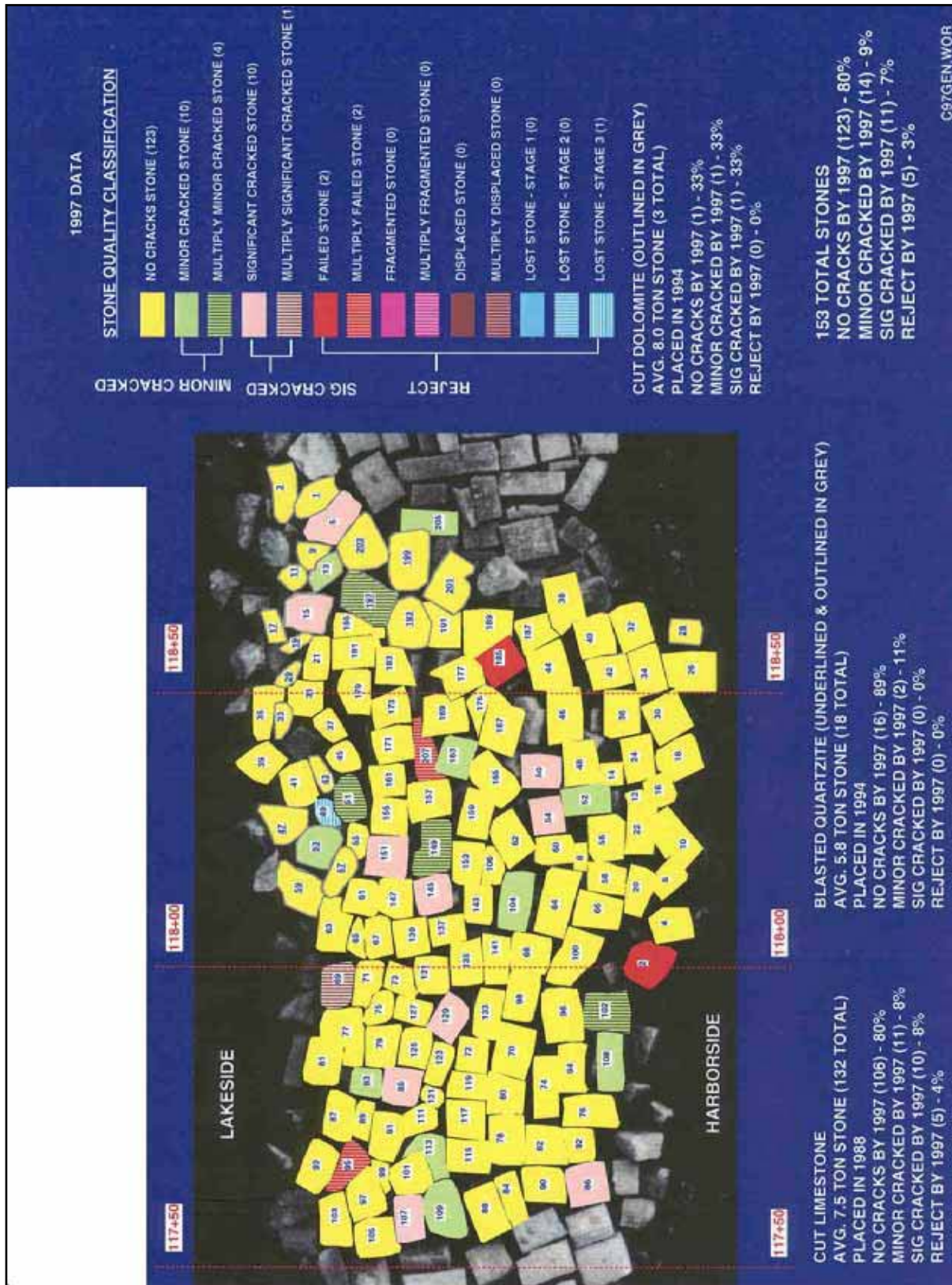


Figure 123. Calumet Harbor breakwater, sta 117+55 to sta 118+90, stone quality classification, end of 1997

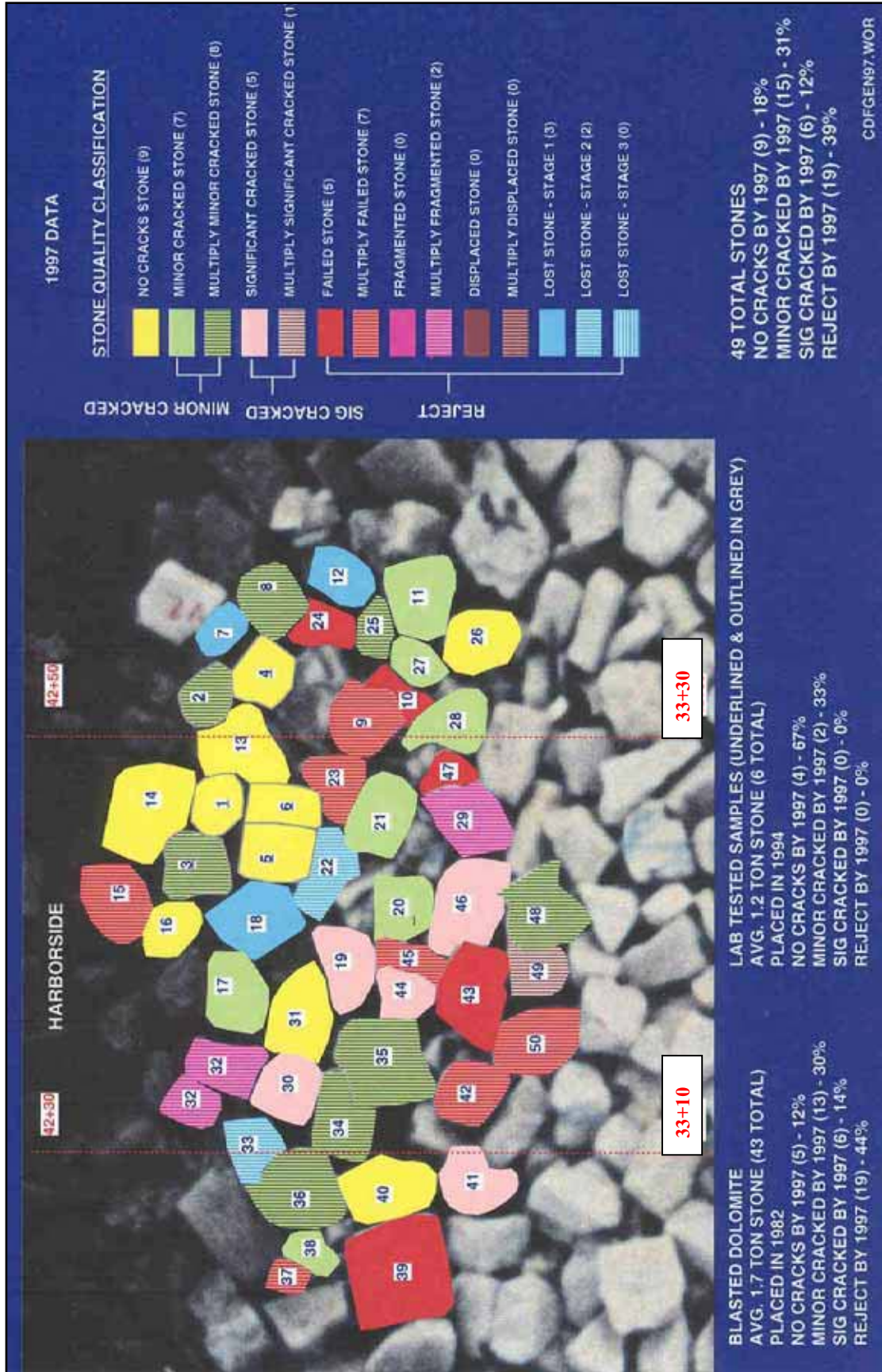
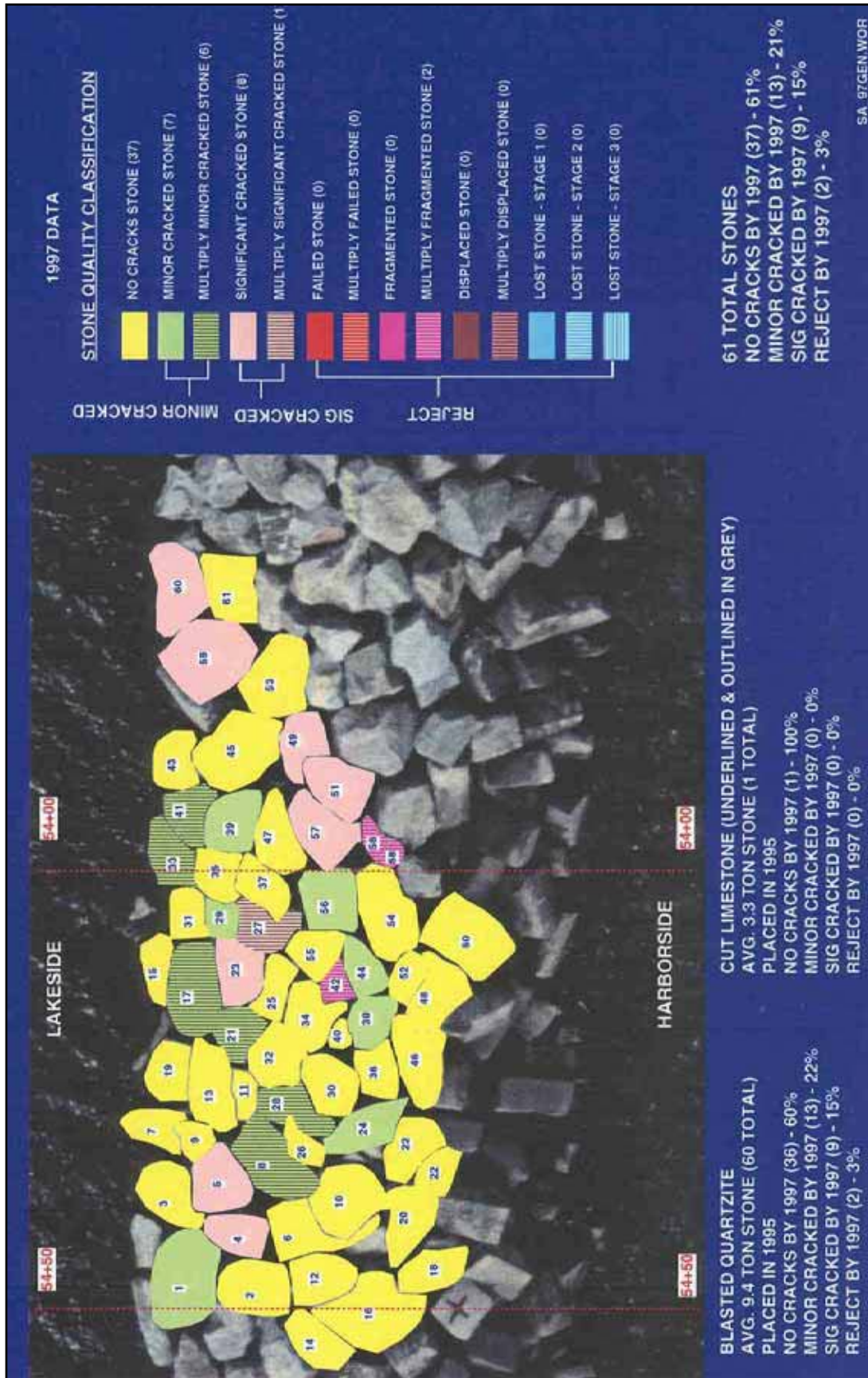


Figure 124. Calumet Harbor confined disposal facility, sta 33+00 to sta 33+40, stone quality classification, end of 1997



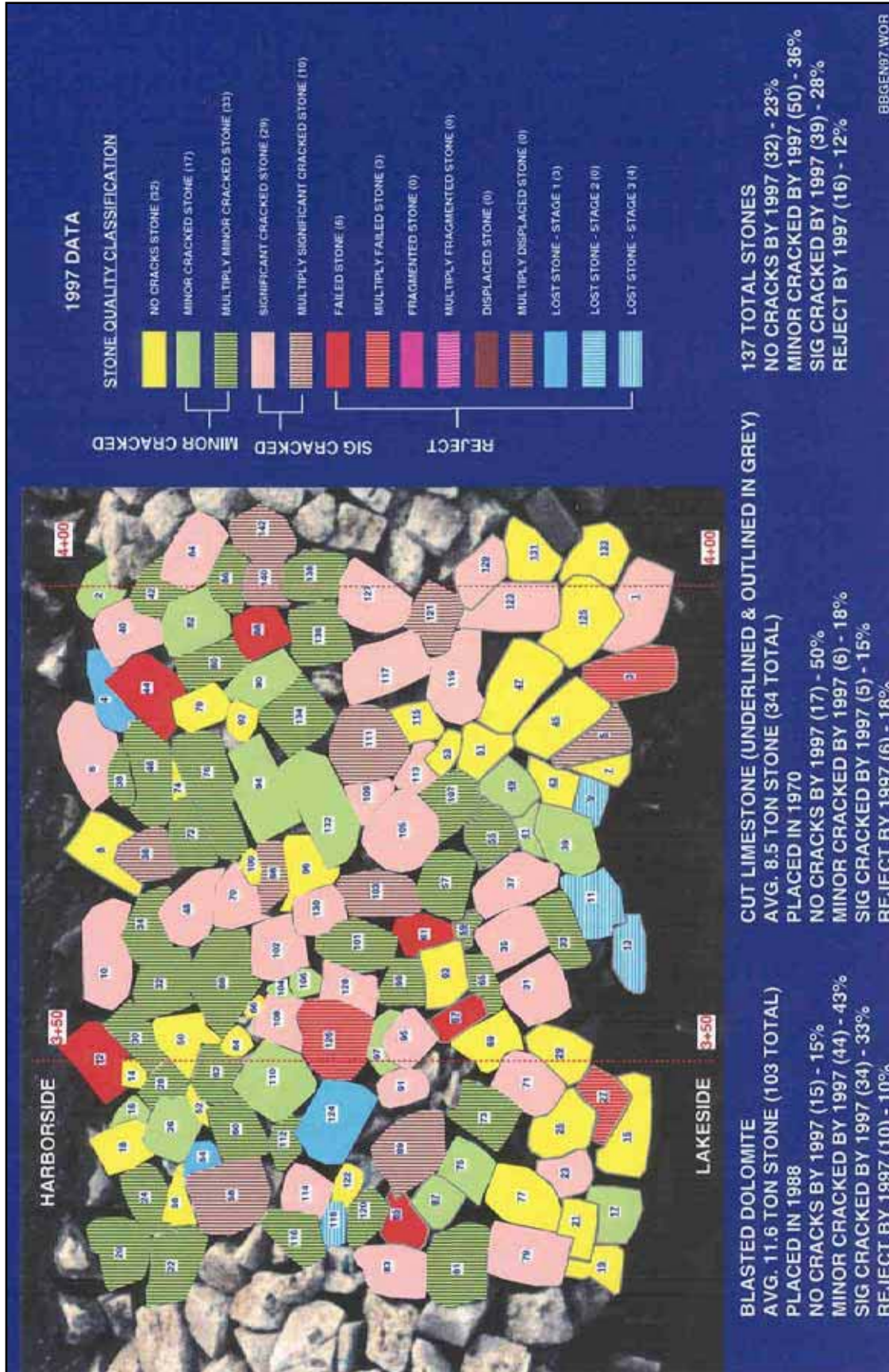


Figure 126. Burns Harbor breakwater (Big Burn section), sta 3+30 to sta 4+10, stone quality classification, end of 1997

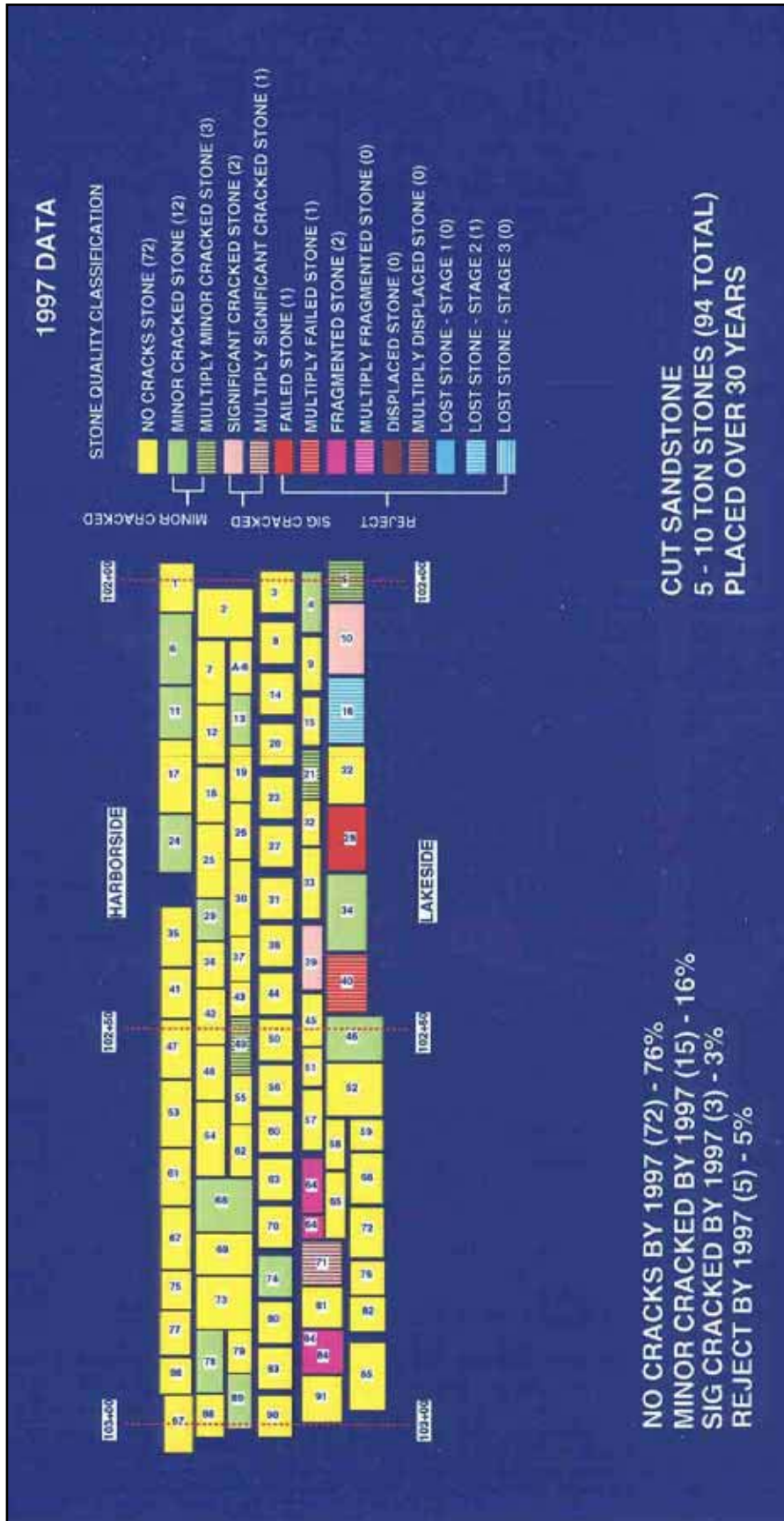


Figure 127. Cleveland Harbor east breakwater, sta 102+00 to sta 103+00, stone quality classification, end of 1997

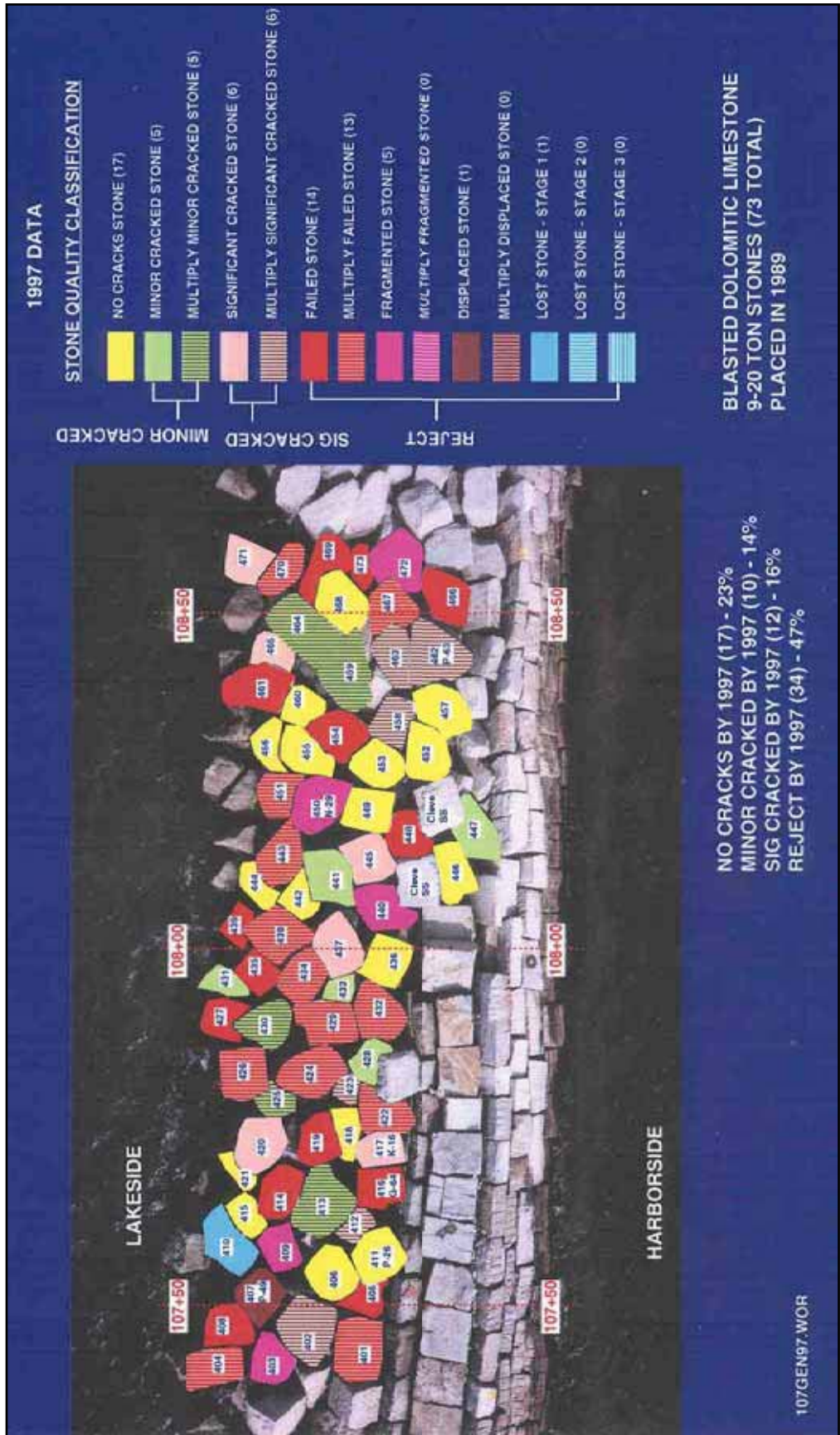


Figure 128. Cleveland Harbor east breakwater, sta 107+40 to sta 108+60, stone quality classification, end of 1997

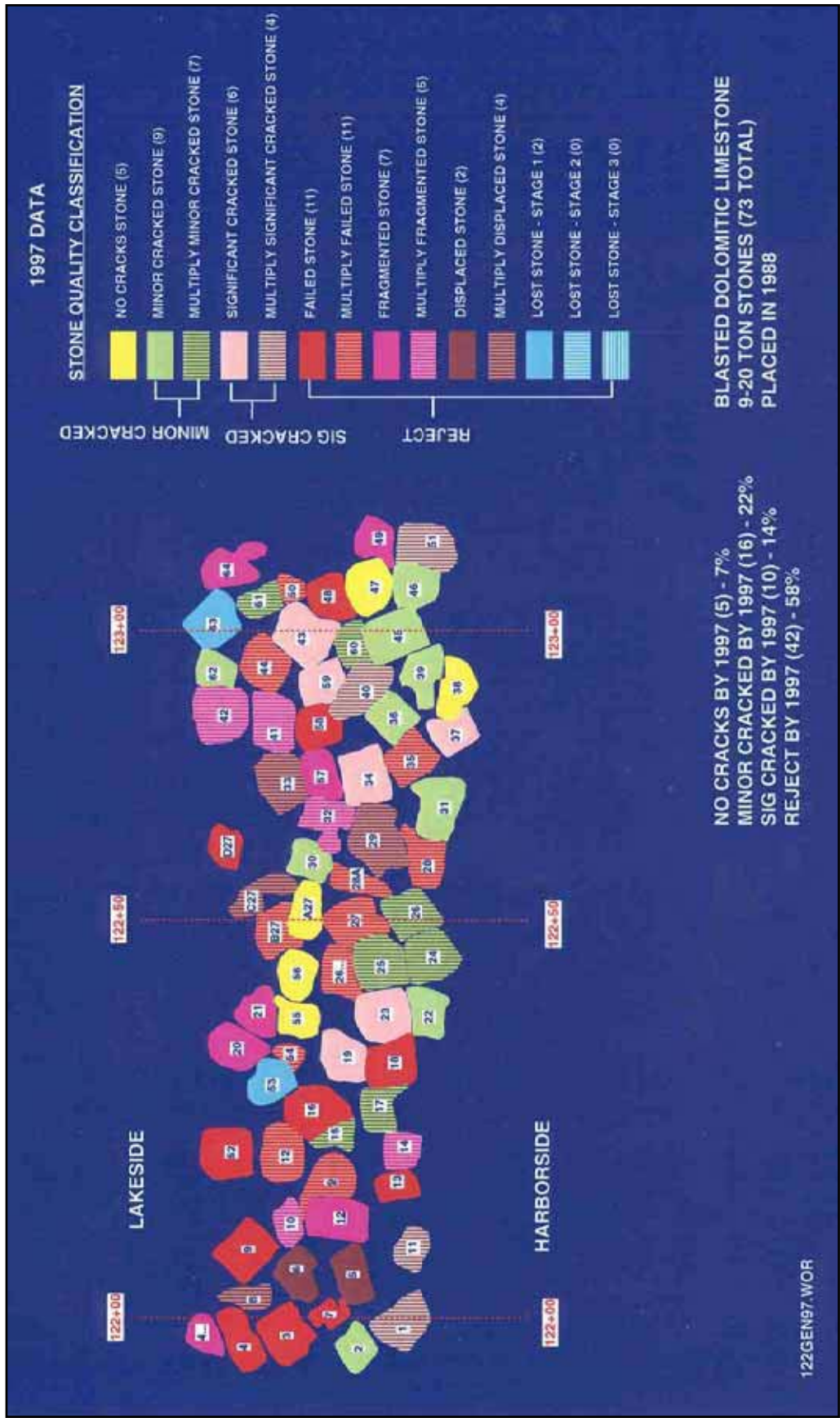


Figure 129. Cleveland Harbor east breakwater, sta 121+90 to sta 123+15, stone quality classification, end of 1997

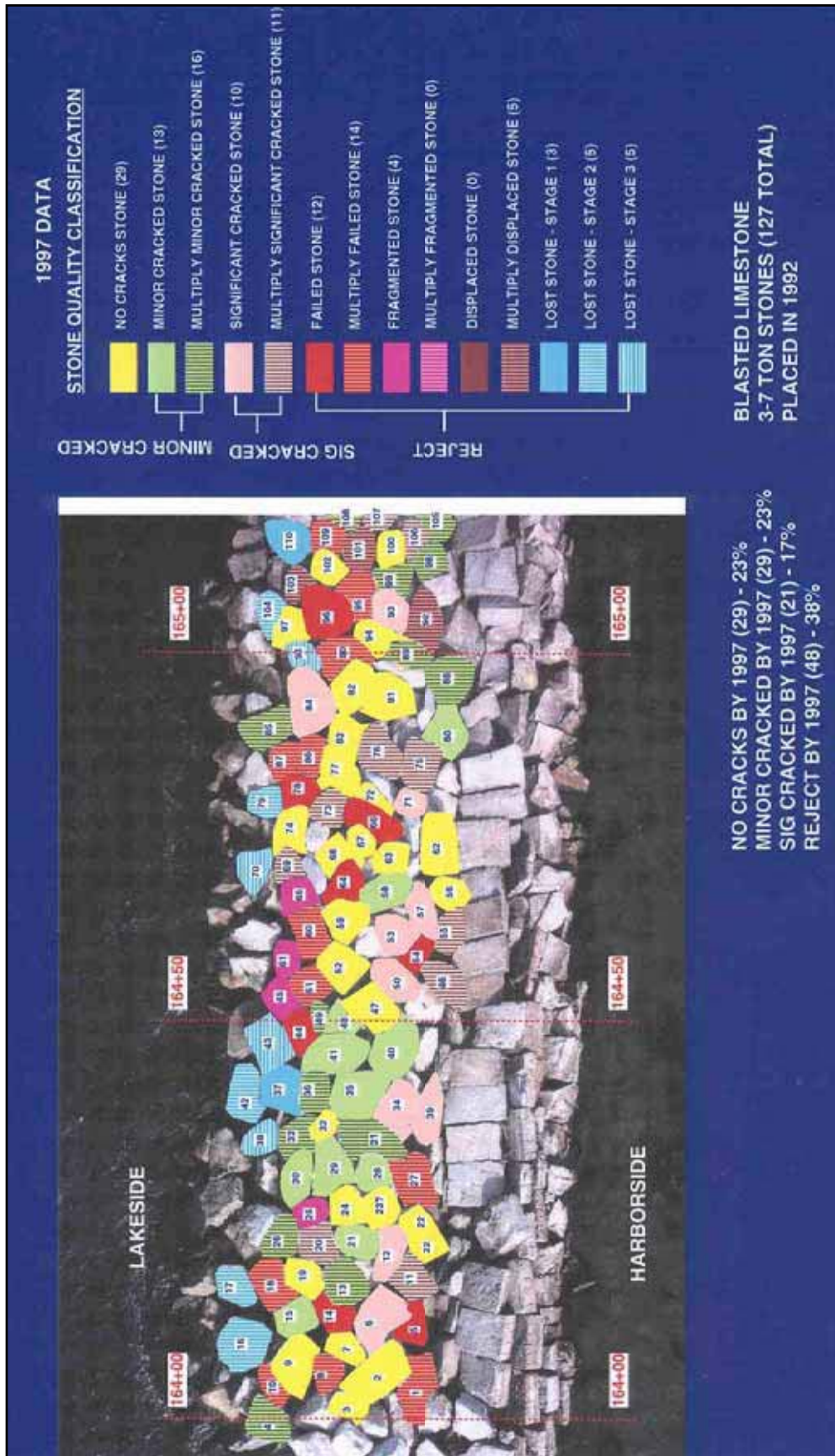


Figure 130. Cleveland Harbor east breakwater, sta 164+00 to sta 165+20, stone quality classification, end of 1997

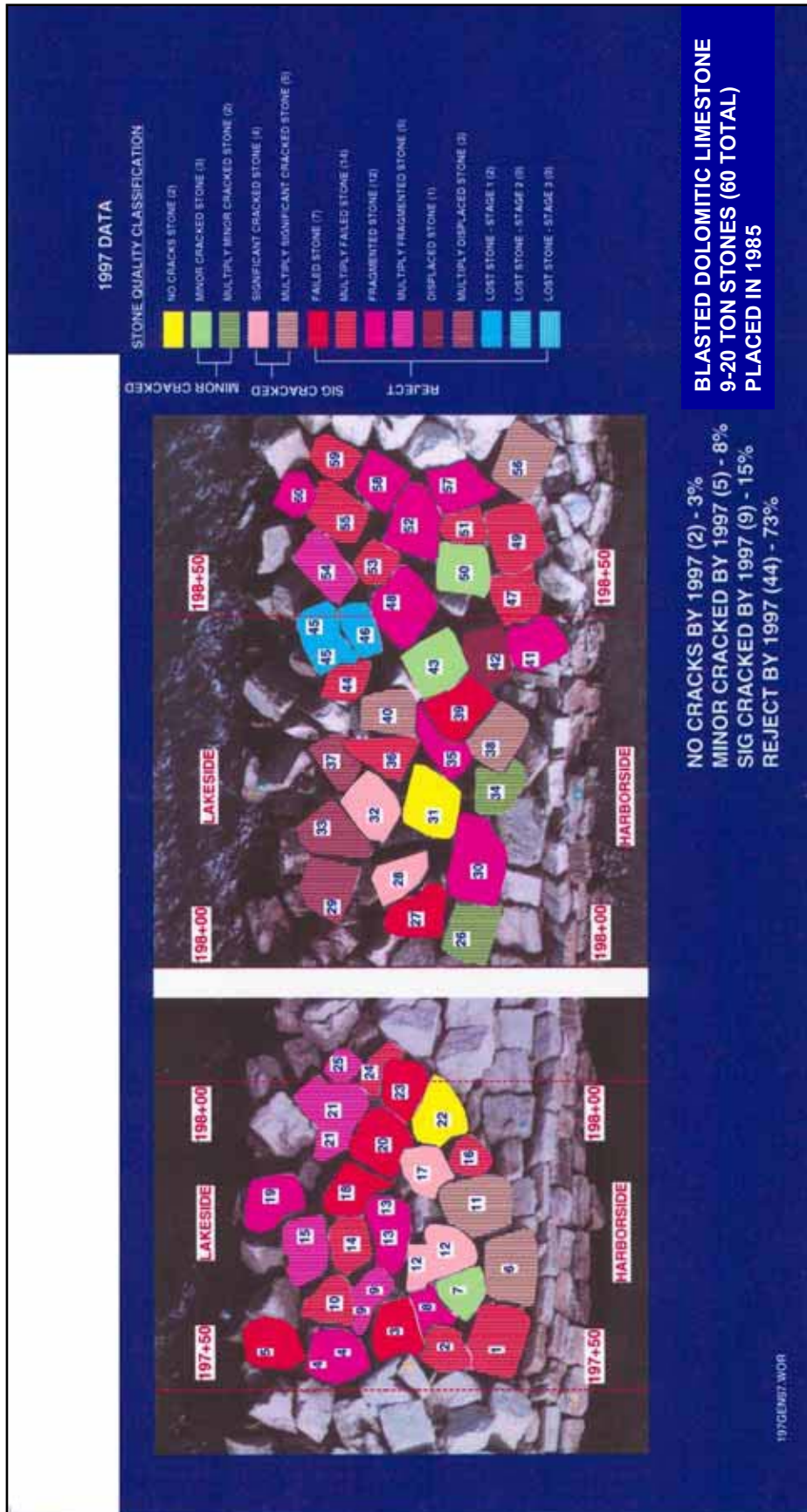


Figure 131. Cleveland Harbor east breakwater, sta 197+50 to sta 198+75, stone quality classification, end of 1997

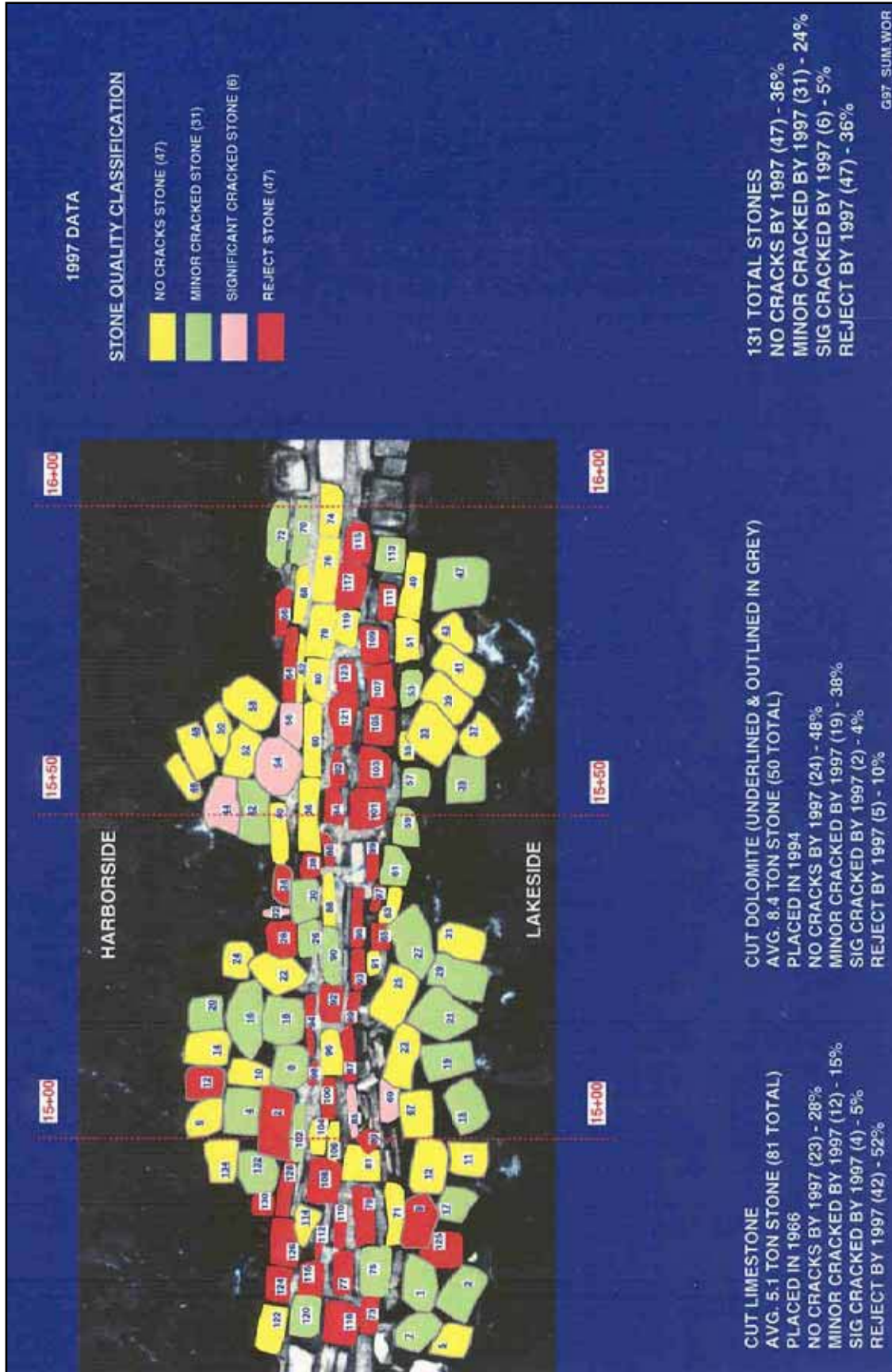


Figure 132. Chicago Harbor breakwater, sta 14+65 to sta 16+00, acceptable versus rejected stone, end of 1997

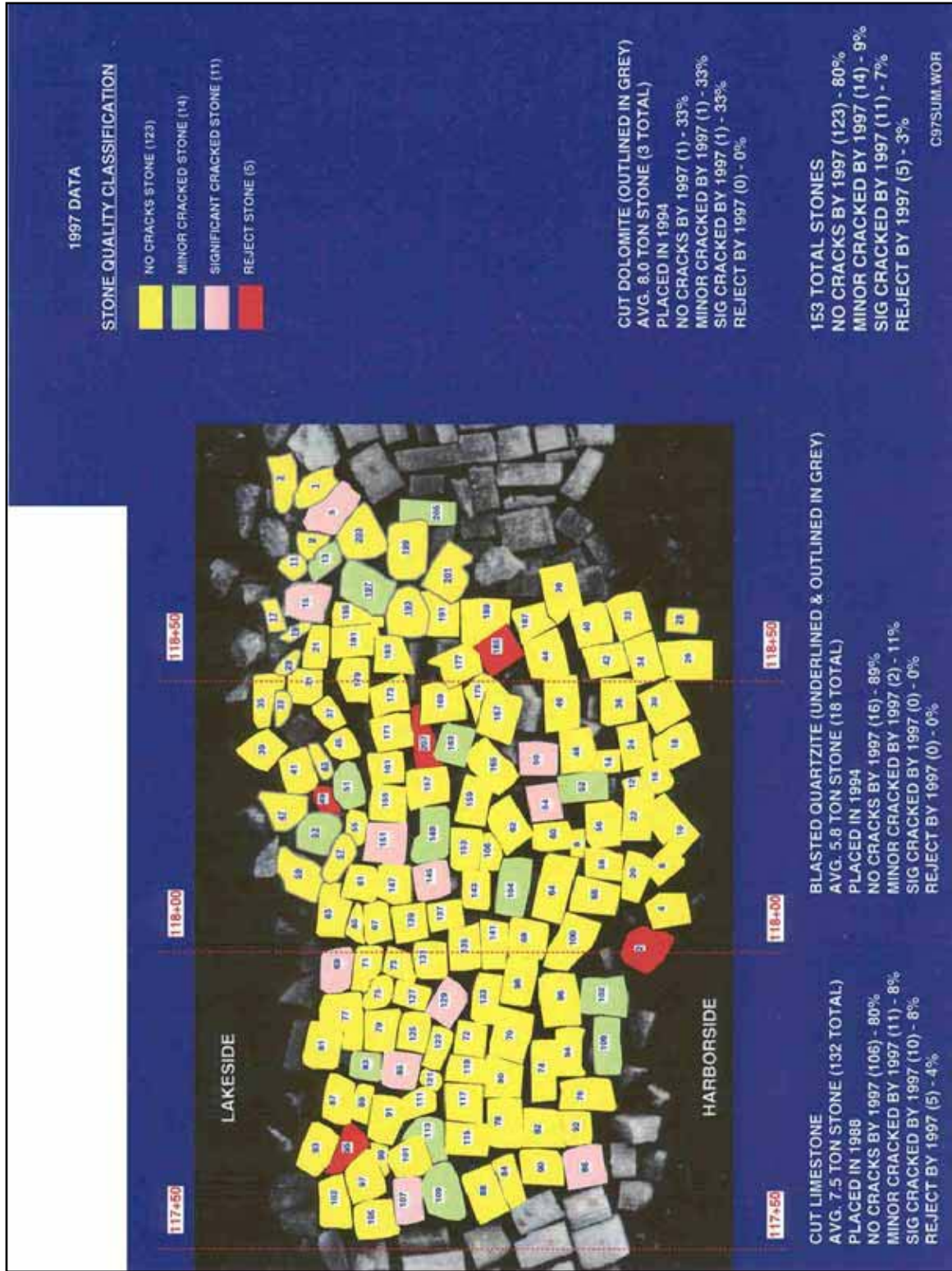


Figure 133. Calumet Harbor breakwater, sta 117+55 to sta 118+90, acceptable versus rejected stone, end of 1997

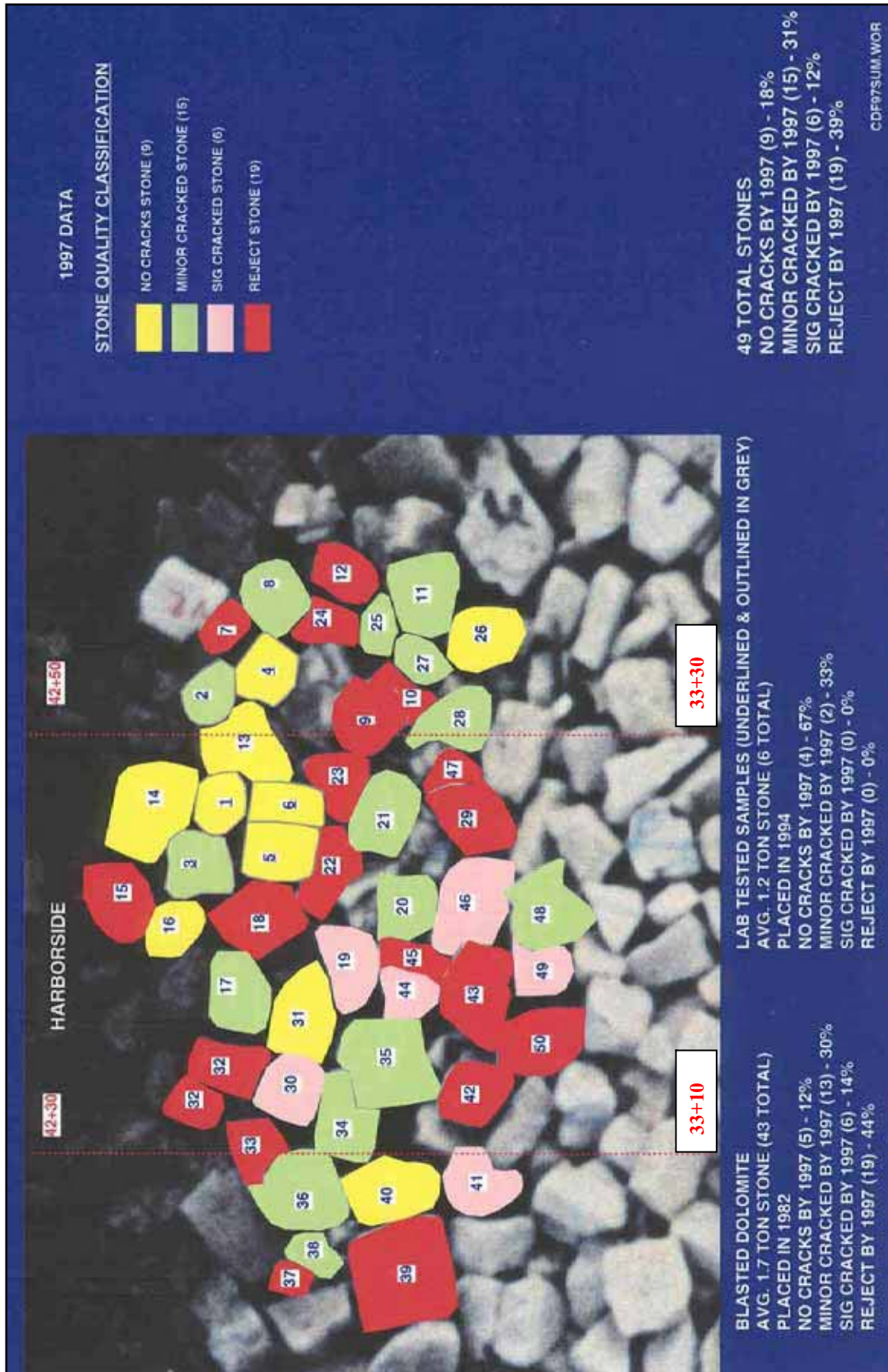


Figure 134. Calumet Harbor confined disposal facility, sta 33+00 to sta 33+40, acceptable versus rejected stone, end of 1997

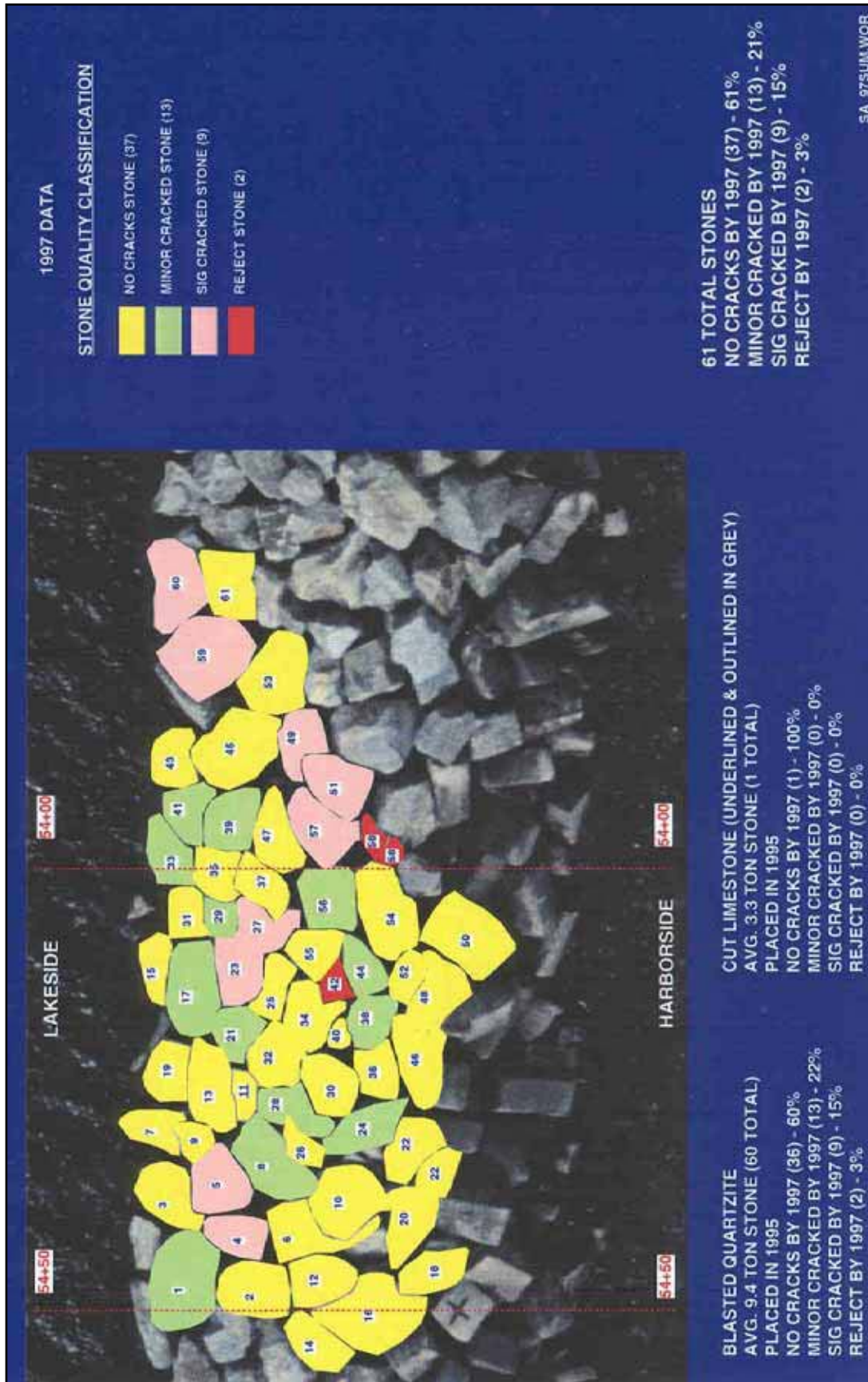


Figure 135. Burns Harbor breakwater (Shore Arm section), sta 53+60 to sta 54+55, acceptable versus rejected stone, end of 1997

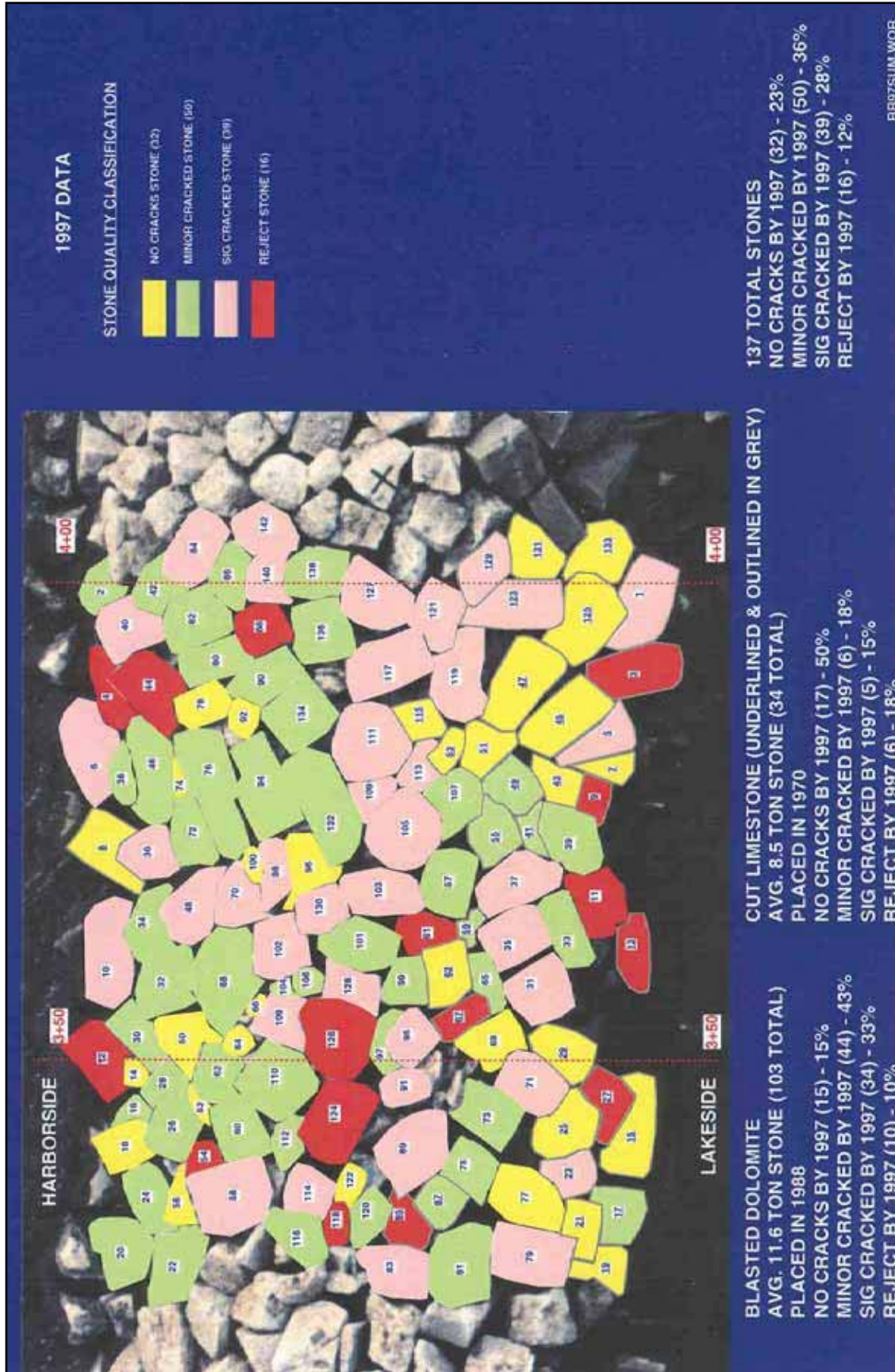


Figure 136. Burns Harbor breakwater (Big Burn section), sta 3+30 to sta 4+10, acceptable versus rejected stone, end of 1997

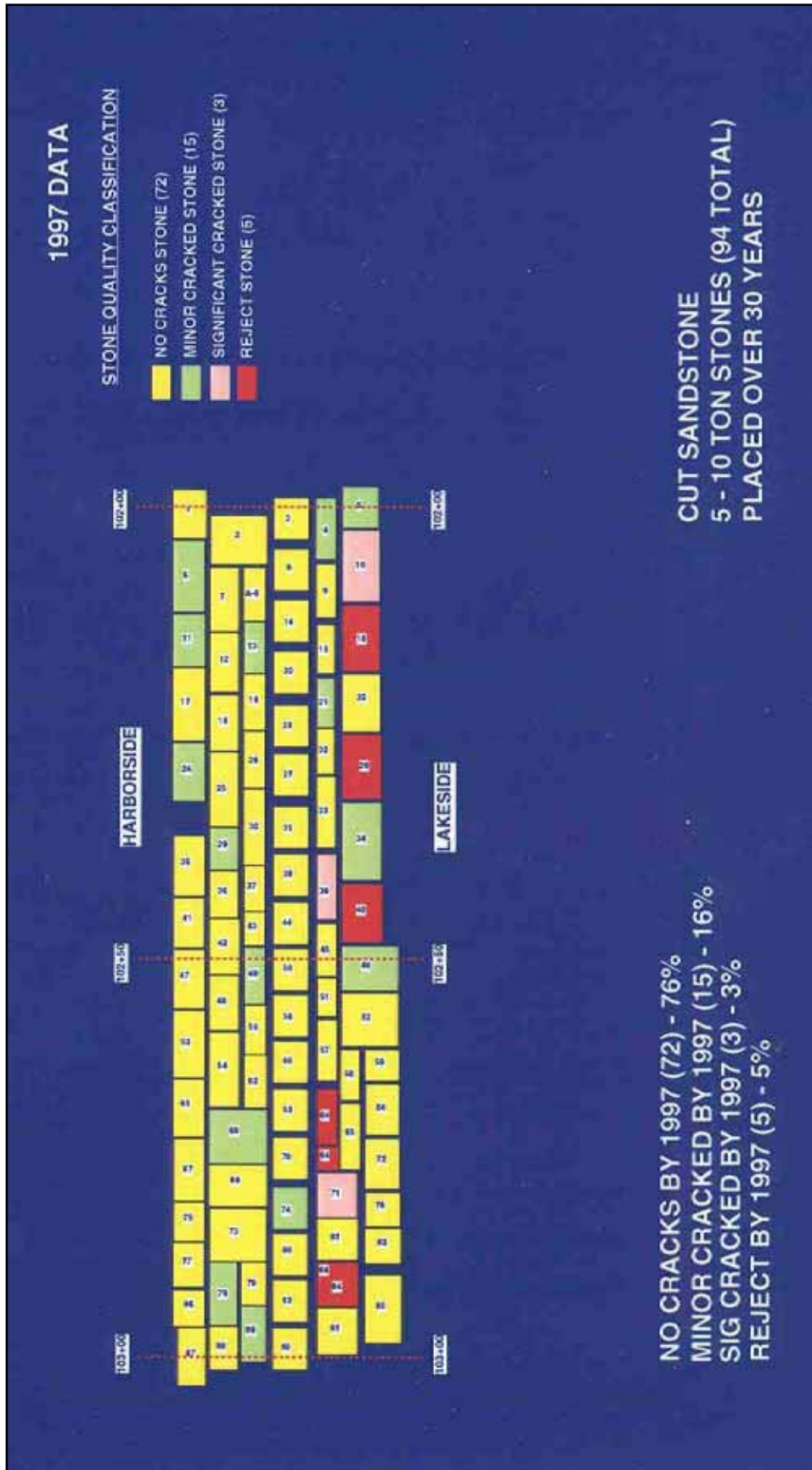


Figure 137. Cleveland Harbor east breakwater, sta 102+00 to sta 103+00, acceptable versus rejected stone, end of 1997

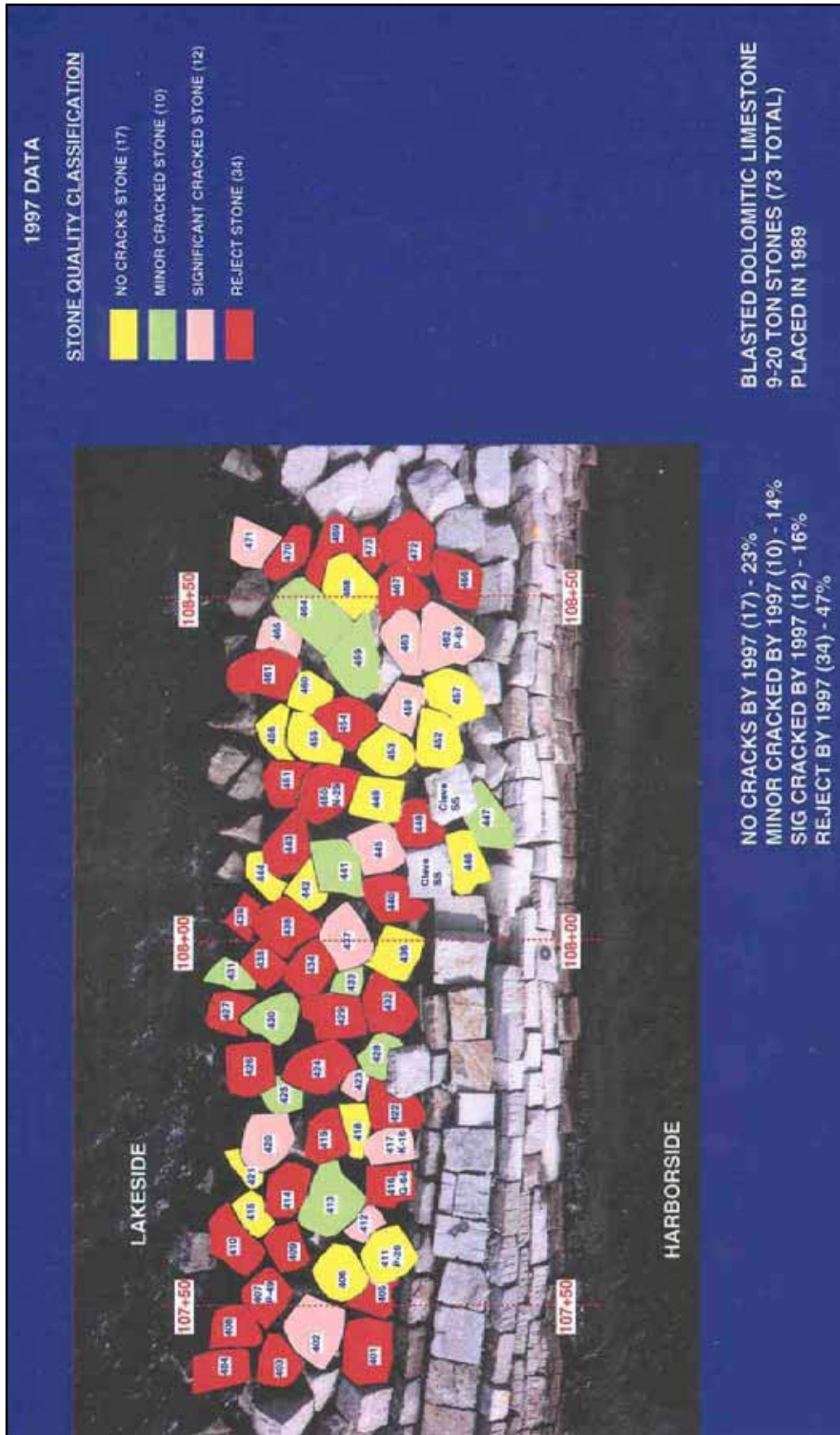


Figure 138. Cleveland Harbor east breakwater, sta 107+40 to sta 108+60, acceptable versus rejected stone, end of 1997

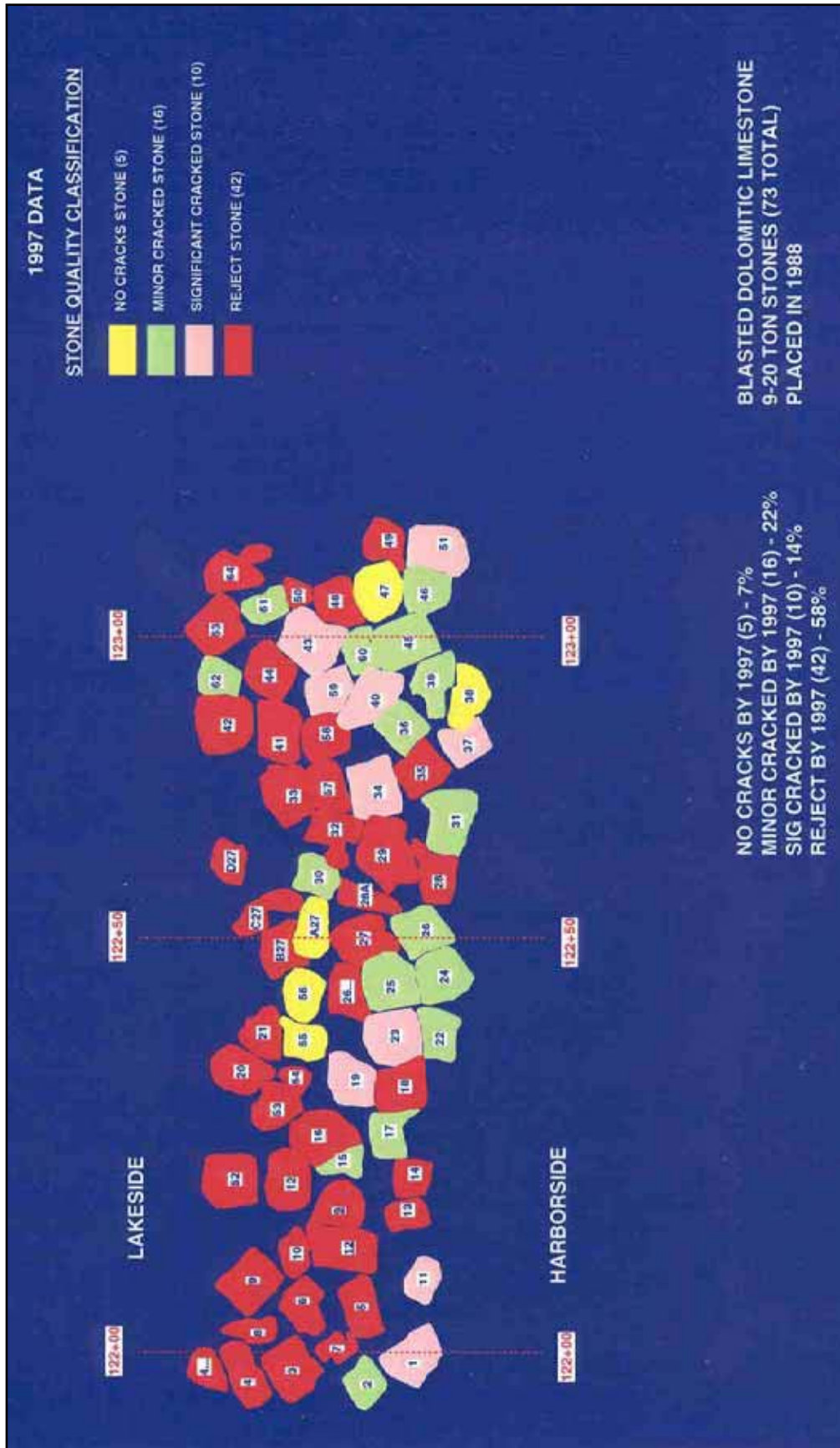


Figure 139. Cleveland Harbor east breakwater, sta 121+90 to sta 123+15, acceptable versus rejected stone, end of 1997

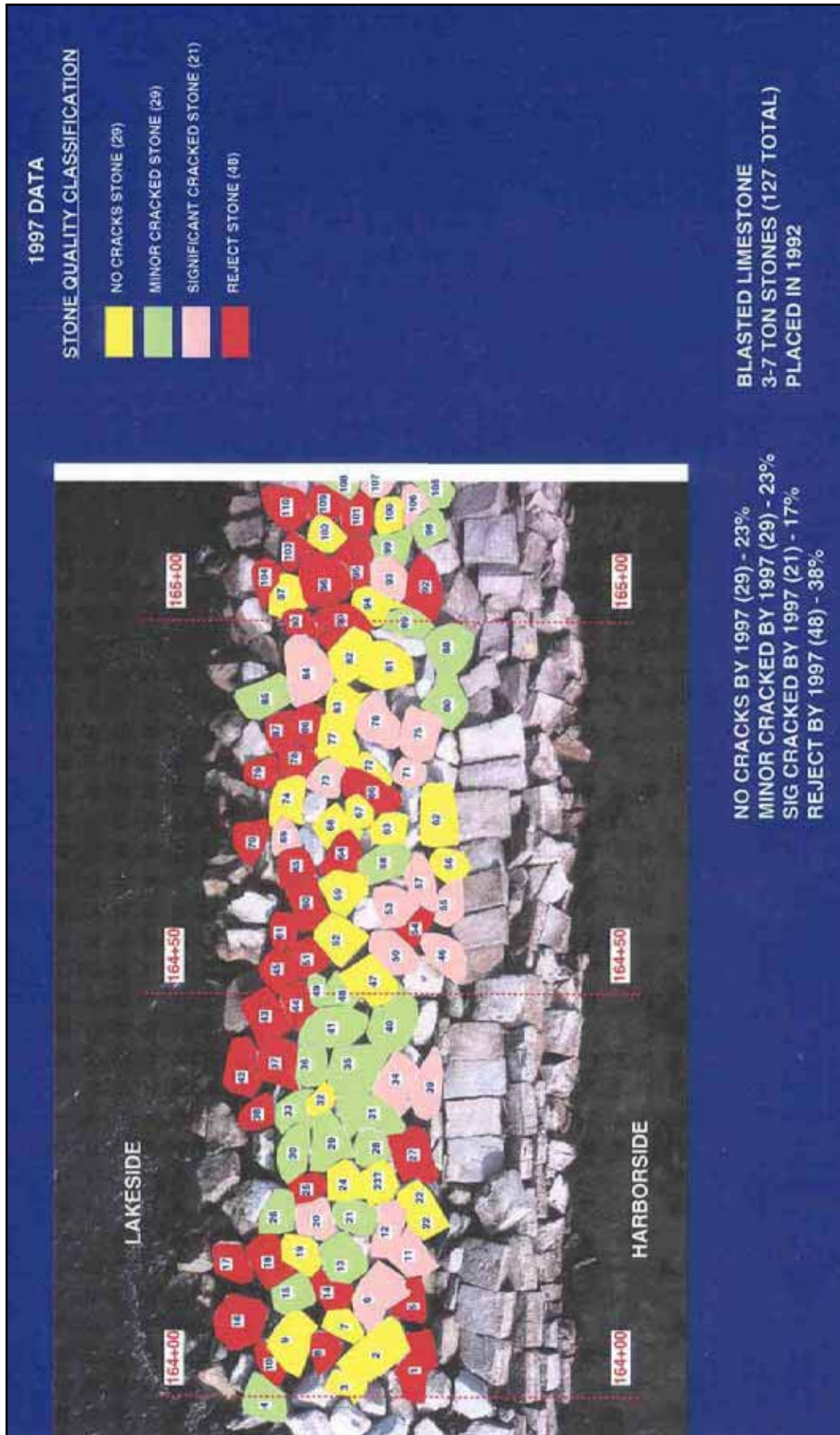


Figure 140. Cleveland Harbor east breakwater, sta 164+00 to sta 165+20, acceptable versus rejected stone, end of 1997

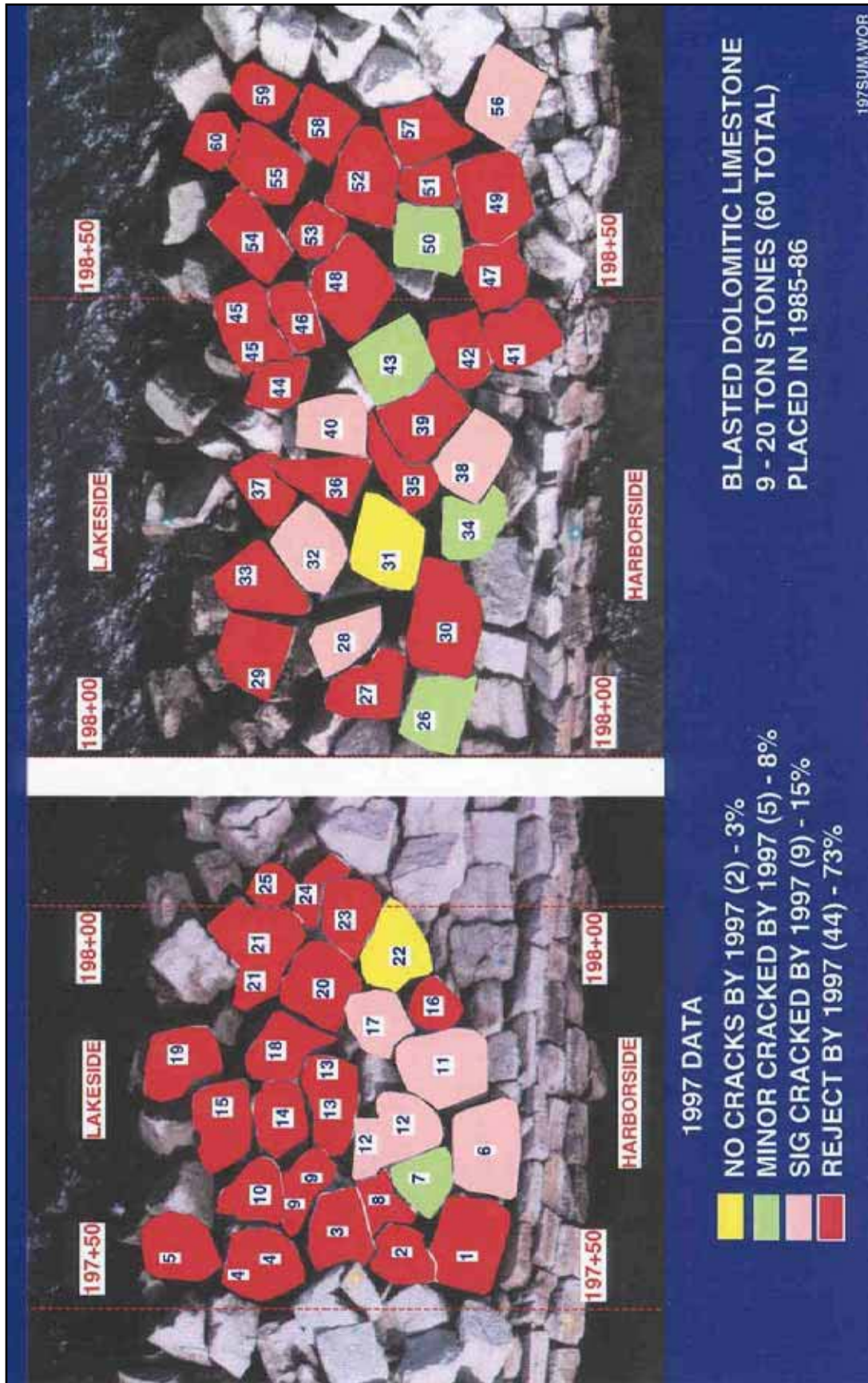


Figure 141. Cleveland Harbor east breakwater, sta 197+50 to sta 198+75, acceptable versus rejected stone, end of 1997

Table 5 Stone Deterioration, All MCNP Monitored Structure Sections (Continued)						
Stone Quality	No. Stones 1995	Percent Stones 1995	No. Stones 1996	Percent Stones 1996	No. Stones 1997	Percent Stones 1997
Chicago Harbor breakwater, sta 14+65 to sta 16+00						
Cut limestone placed in 1966, and cut dolomite placed in 1994						
No cracks	57	43.5	49	37.4	47	35.9
Minor cracks	26	19.9	30	22.9	31	23.7
Significant cracks	6	4.6	7	5.3	6	4.6
Rejected	42	32.1	45	34.4	47	35.9
Total stones	131	100.0	131	100.0	131	100.0
Calumet Harbor breakwater, sta 117+55 to sta 118+90						
Cut limestone placed in 1988, cut dolomite placed in 1994, and blasted quartzite placed in 1994						
No cracks	126	82.4	125	81.7	123	80.4
Minor cracks	13	8.5	13	8.5	14	9.2
Significant cracks	11	7.2	10	6.5	11	7.2
Rejected	3	2.0	5	3.3	5	3.3
Total stones	153	100.0	153	100.0	153	100.0
Calumet Harbor CDF revetment, sta 33+00 to sta 33+40						
Blasted dolomite placed in 1982, and laboratory samples placed in 1994						
No cracks	12	24.5	12	24.5	9	18.4
Minor cracks	12	24.5	12	24.5	15	30.6
Significant cracks	6	12.2	6	12.2	6	12.2
Rejected	19	38.8	19	38.8	19	38.8
Total stones	49	100.0	49	100.0	49	100.0
Burns Harbor breakwater (Shore Arm section), sta 53+60 to sta 54+55						
Cut limestone placed in 1995, and blasted quartzite placed in 1995						
No cracks	44	72.1	42	68.9	37	60.7
Minor cracks	11	18.0	11	18.0	13	21.3
Significant cracks	4	6.6	6	9.8	9	14.8
Rejected	2	3.3	2	3.3	2	3.3
Total stones	61	100.0	61	100.0	61	100.0
Burns Harbor breakwater (Big Burn section), sta 3+30 to sta 4+10						
Cut limestone placed in 1970, and blasted dolomite placed in 1988						
No cracks	41	29.9	36	26.3	32	23.4
Minor cracks	49	35.8	50	36.5	50	36.5
Significant cracks	37	27.0	38	27.7	39	28.5
Rejected	10	7.3	13	9.5	16	11.7
Total stones	137	100.0	137	100.0	137	100.0

(Continued)

Table 5 (Concluded)

Stone Quality	No. Stones 1995	Percent Stones 1995	No. Stones 1996	Percent Stones 1996	No. Stones 1997	Percent Stones 1997
Cleveland Harbor east breakwater, sta 102+00 to sta 103+00						
Cut sandstone placed over 30 years ago						
No cracks	72	76.6	71	75.5	71	75.5
Minor cracks	14	14.9	15	16.0	15	16.0
Significant cracks	3	3.2	3	3.2	3	3.2
Rejected	5	5.3	5	5.3	5	5.3
Total stones	94	100.0	94	100.0	94	100.0
Cleveland Harbor east breakwater, sta 107+40 to sta 108+60						
Blasted dolomitic limestone placed in 1989						
No cracks	37	50.7	21	28.8	17	23.3
Minor cracks	18	24.7	13	17.8	10	13.7
Significant cracks	3	4.1	11	15.1	12	16.4
Rejected	15	20.6	28	38.4	34	46.6
Total stones	73	100.0	73	100.0	73	100.0
Cleveland Harbor east breakwater, sta 121+90 to sta 123+15						
Blasted dolomitic limestone placed in 1988						
No cracks	13	17.8	7	9.6	5	6.9
Minor cracks	18	24.7	15	20.6	16	21.9
Significant cracks	13	17.8	12	16.4	10	13.7
Rejected	29	39.7	39	53.4	42	57.5
Total stones	73	100.0	73	100.0	73	100.0
Cleveland Harbor east breakwater, sta 164+00 to sta 165+20						
Blasted limestone placed in 1992						
No cracks	46	3602	34	2608	29	22.9
Minor cracks	24	18.9	28	22.1	29	22.9
Significant cracks	31	24.4	25	19.7	21	16.5
Rejected	26	20.5	40	31.5	48	37.8
Total stones	127	100.0	127	100.0	127	100.0
Cleveland Harbor east breakwater, sta 197+50 to sta 198+75						
Blasted dolomitic limestone placed in 1985						
No cracks	4	6.7	2	3.3	2	3.3
Minor cracks	6	10.0	6	10.0	5	8.3
Significant cracks	9	15.0	8	13.3	9	15.0
Rejected	41	68.3	44	73.3	44	73.3
Total stones	60	100.0	60	100.0	60	100.0

Figure 142 presents, by stone type at the 10 different breakwater structure sections, the percentage of rejected stones since those stones were originally placed on those sections, as determined by the three yearly monitoring events (1995, 1996, and 1997). The Cleveland Harbor east breakwater sections had previously undergone monitoring events as a part of other evaluations, and those data also are incorporated into this present MCNP study, and displayed in Figure 142. These data are separated by Corps Districts, and are displayed for the Chicago District in Figure 143, and for the Buffalo District (Cleveland Harbor east breakwater) in Figure 144.

The breakwater stone deterioration data for each year of the 3-year monitoring period by breakwater section for stone quality classifications of (a) no cracks, (b) minor cracks, (c) significant cracks, and (d) rejected stone, are presented in Figures 145 through 154. These data are a composite of all stone types for conditions at the conclusion of monitoring, and are presented in Table 5. These graphical displays again do not differentiate between stone types on the respective structure sections although pertinent notes regarding such are presented.

Figure 142 shows the percentage of rejected stones at all monitored breakwater structure sections by stone type since those stones were originally placed. Figure 143 shows that data for only those monitored structures in the Chicago District (Chicago Harbor breakwater, Calumet Harbor breakwater, Calumet Harbor CDF revetment, Burns Harbor breakwater (Big Burn section), and Burns Harbor breakwater (Shore Arm section)). Figure 144 shows that data for the monitored structure in the Buffalo District (Cleveland Harbor east breakwater). There exists a trend that most of the blasted sedimentary stones have a range of 40 to 72 percent failure within 15 years after placement. The cut sedimentary stones are showing much greater durability, with a trend of 5 to 52 percent failure after 30 to 78 years of placement. The cut sandstone in the Cleveland Harbor east breakwater is performing best, with only 5 percent failure after 30 years.

The data of Table 5 are further displayed in Figures 145 through 154 by stone quality classifications of (a) no cracks, (b) minor cracks, (c) significant cracks, and (d) rejected stone, versus number of stones in each classification, for each of the 10 monitored breakwater structure sections for the three monitored years (1995, 1996, and 1997).

The Cleveland Harbor east breakwater monitoring consisted of intensive surveys of five distinct sections of the structure. The five sections were composed of three different stone types; (a) cut sandstone (94 stones), (b) blasted limestone (127 stones), and (c) blasted dolomitic limestone (206 stones). The stone quality classifications for these three stone types for the total structure sections (427 stones), and a comparison of their degree of deterioration at the end of the monitoring period (1997), are presented in Table 6 and displayed graphically in Figure 155.

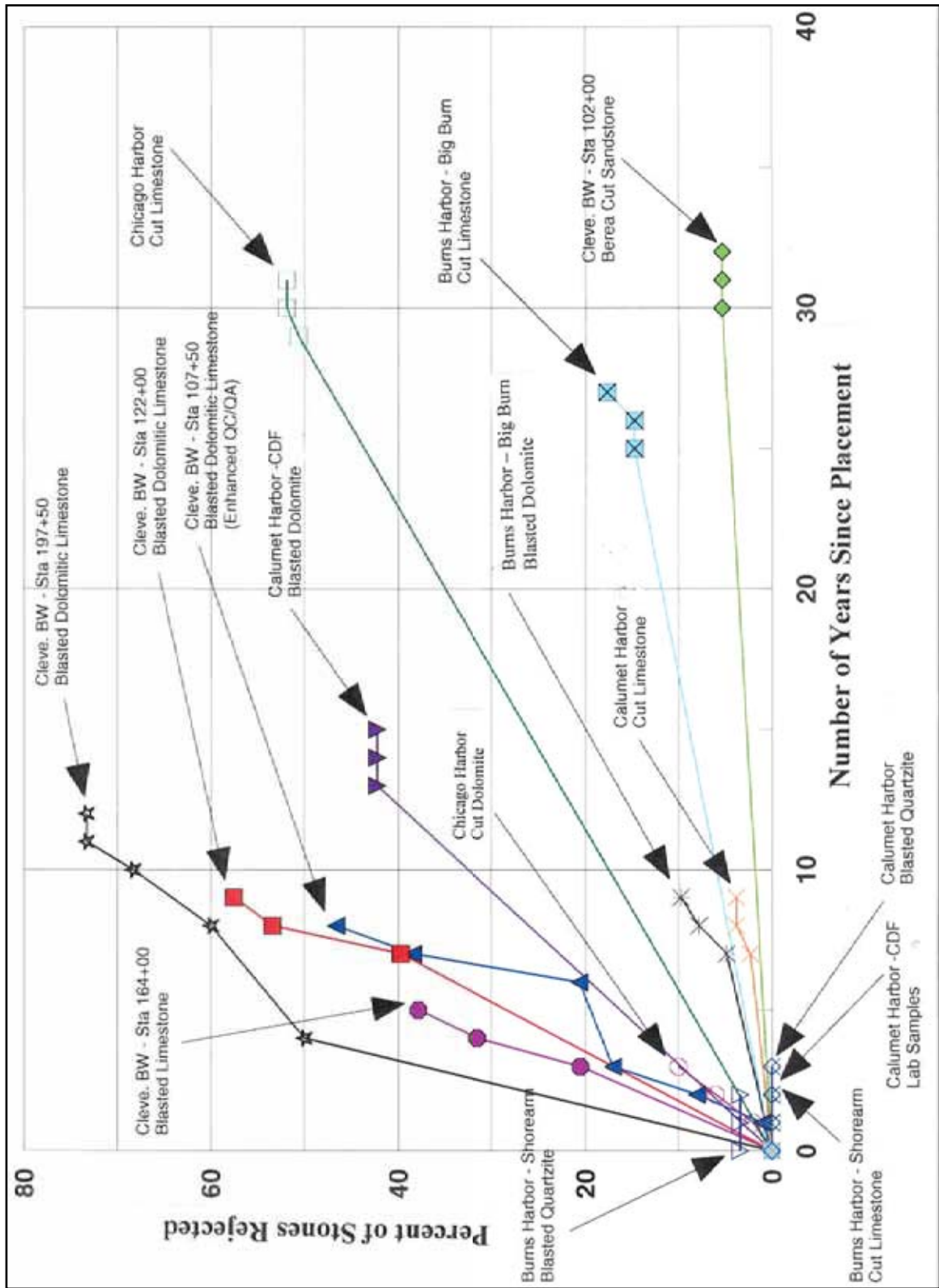


Figure 142. Percentage of rejected stones at monitored breakwater structure sections by stone type since those stones were originally placed

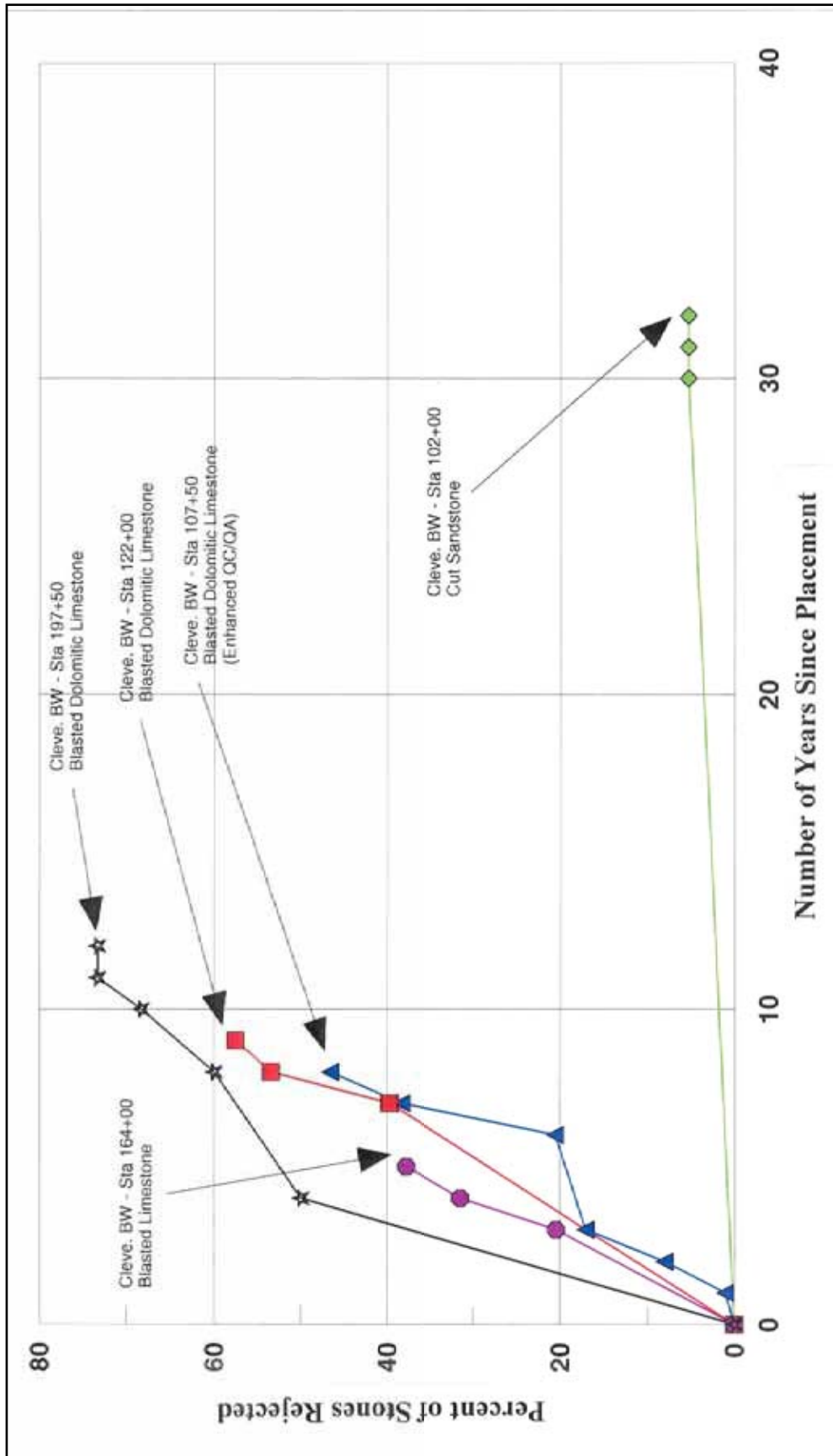


Figure 144. Percentage of rejected stones at monitored breakwater structure sections by stone type, within Buffalo District (Cleveland Harbor east breakwater), since those stones were originally placed

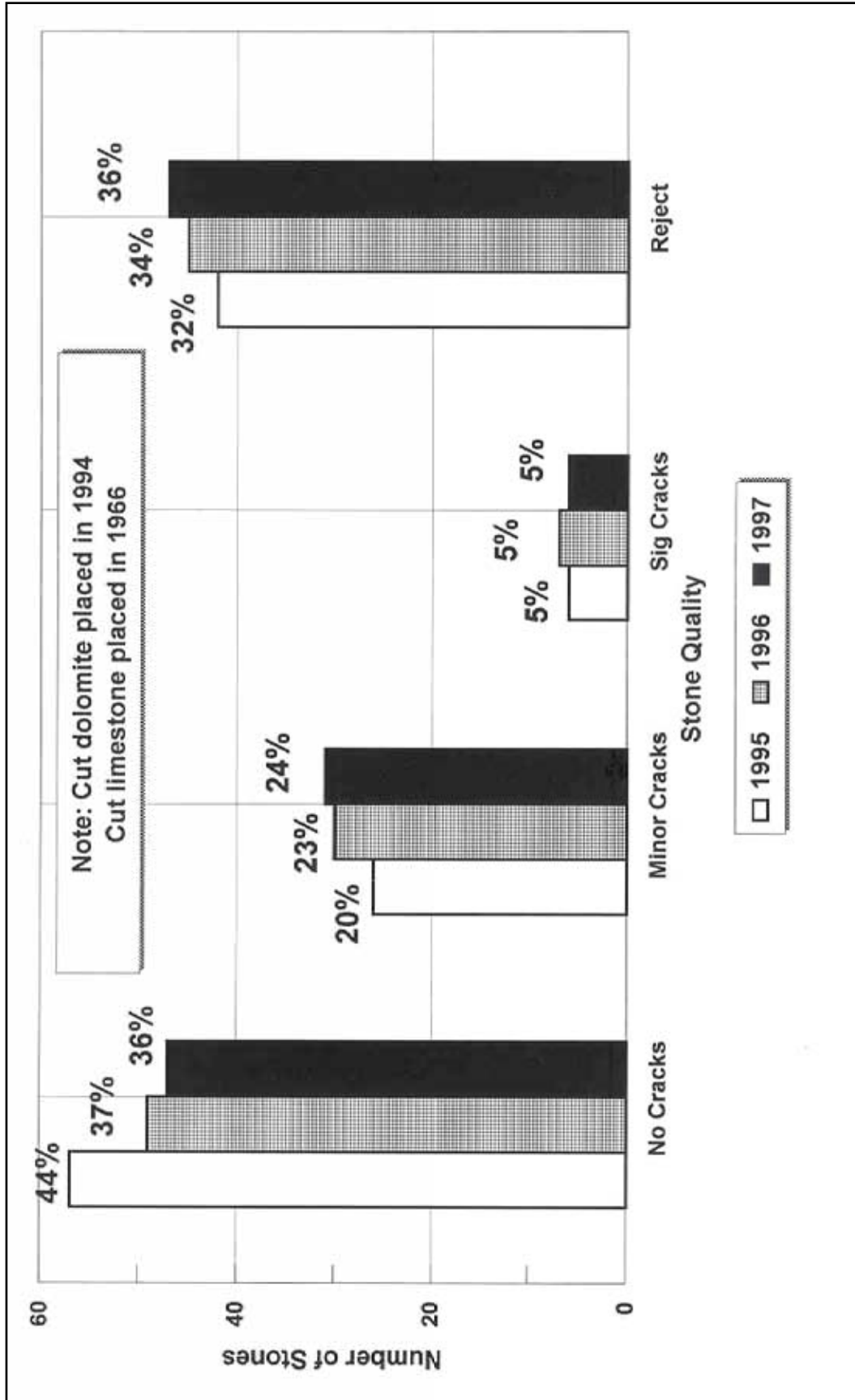


Figure 145. Stone quality comparison for monitored years at Chicago Harbor breakwater, sta 14+65 to sta 16+00, for total of 131 stones (composite of cut dolomite placed in 1994, and cut limestone placed in 1966)

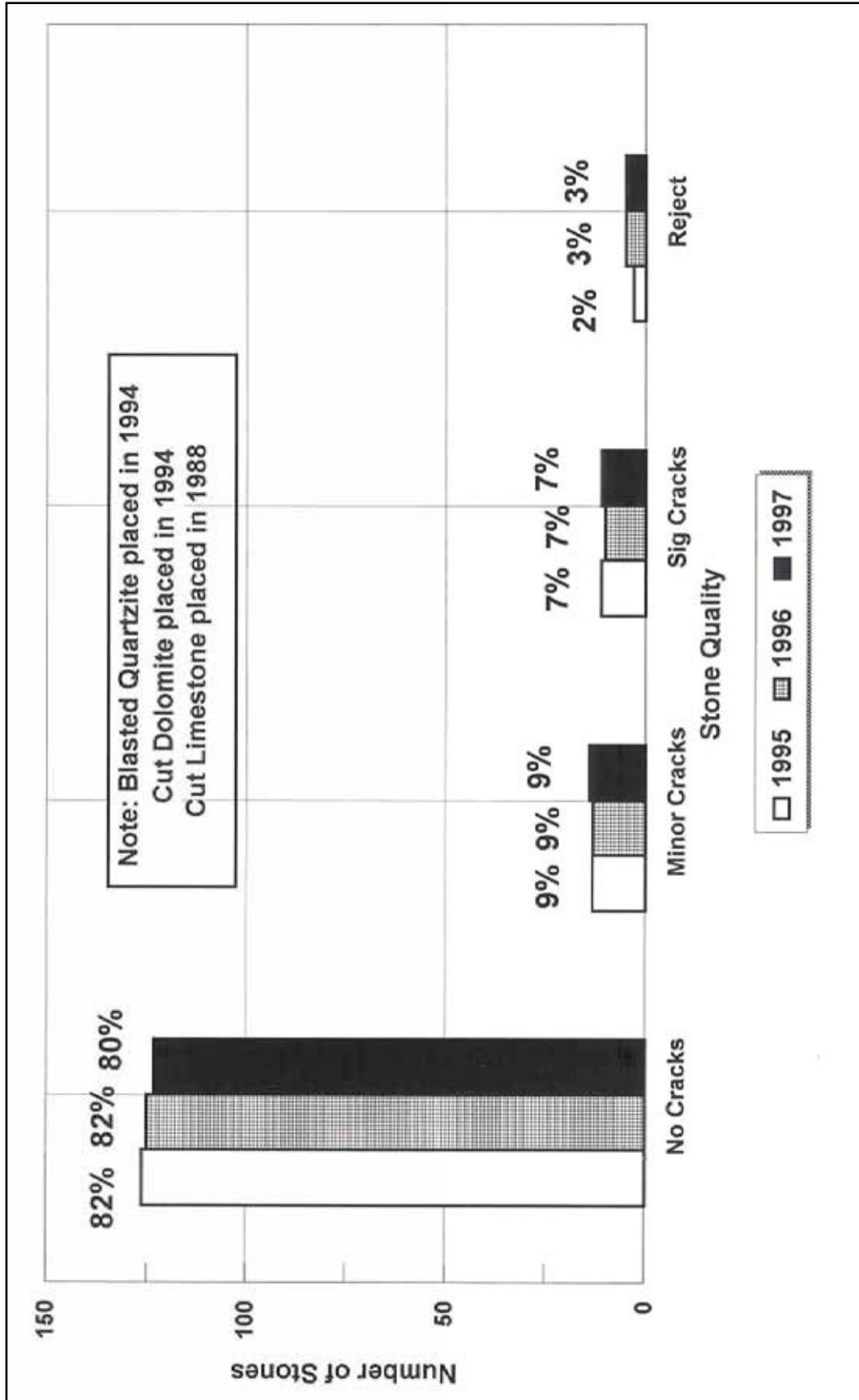


Figure 146. Stone quality comparison for monitored years at Calumet Harbor breakwater, sta 117+55 to sta 118+90, for total of 153 stones (composite of blasted quartzite placed in 1994, cut dolomite placed in 1994, and cut limestone placed in 1988)

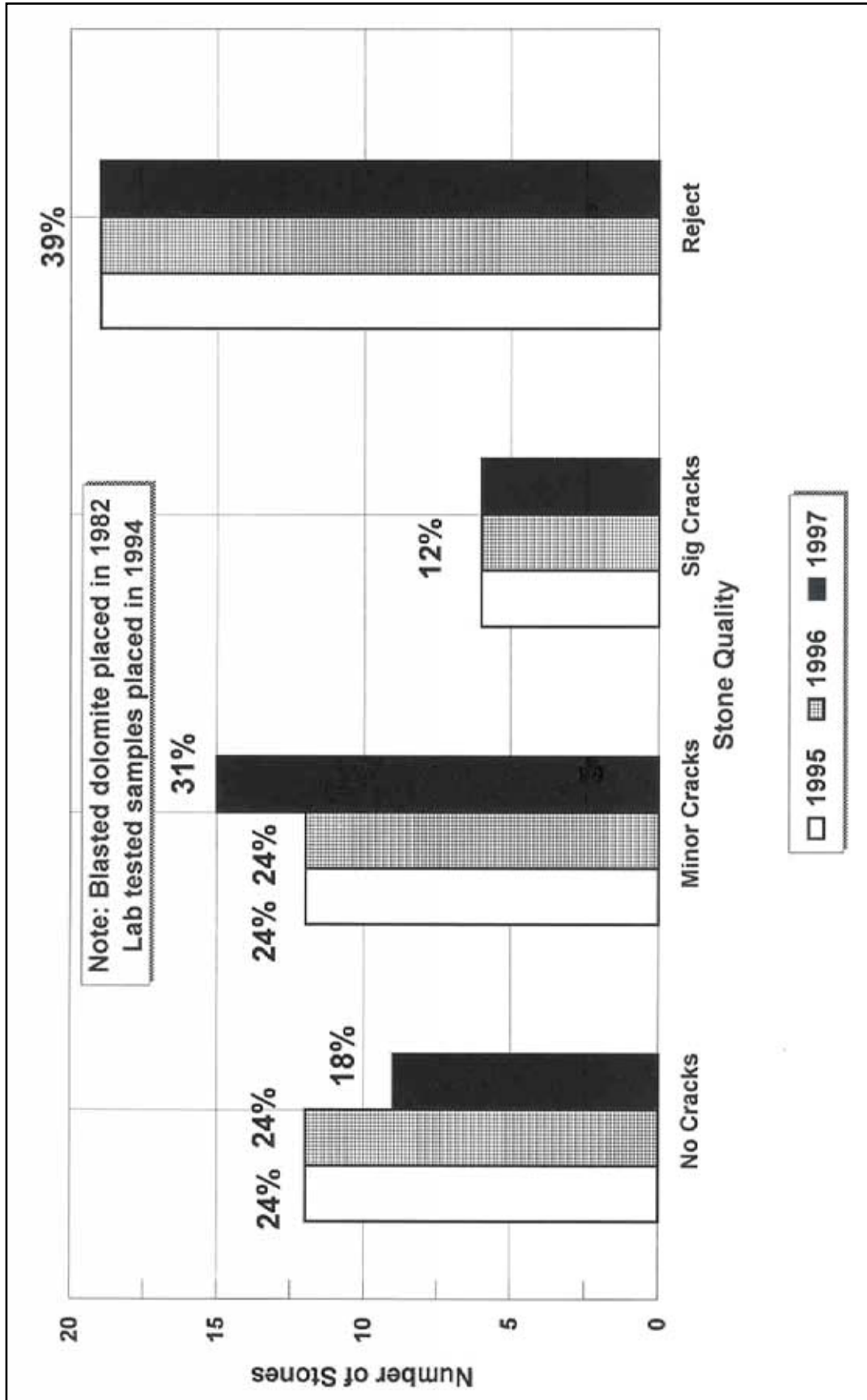


Figure 147. Stone quality comparison for monitored years at Calumet Harbor CDF, sta 33+00 to sta 33+40, for total of 49 stones (composite of blasted dolomite placed in 1982, and laboratory samples placed in 1994)

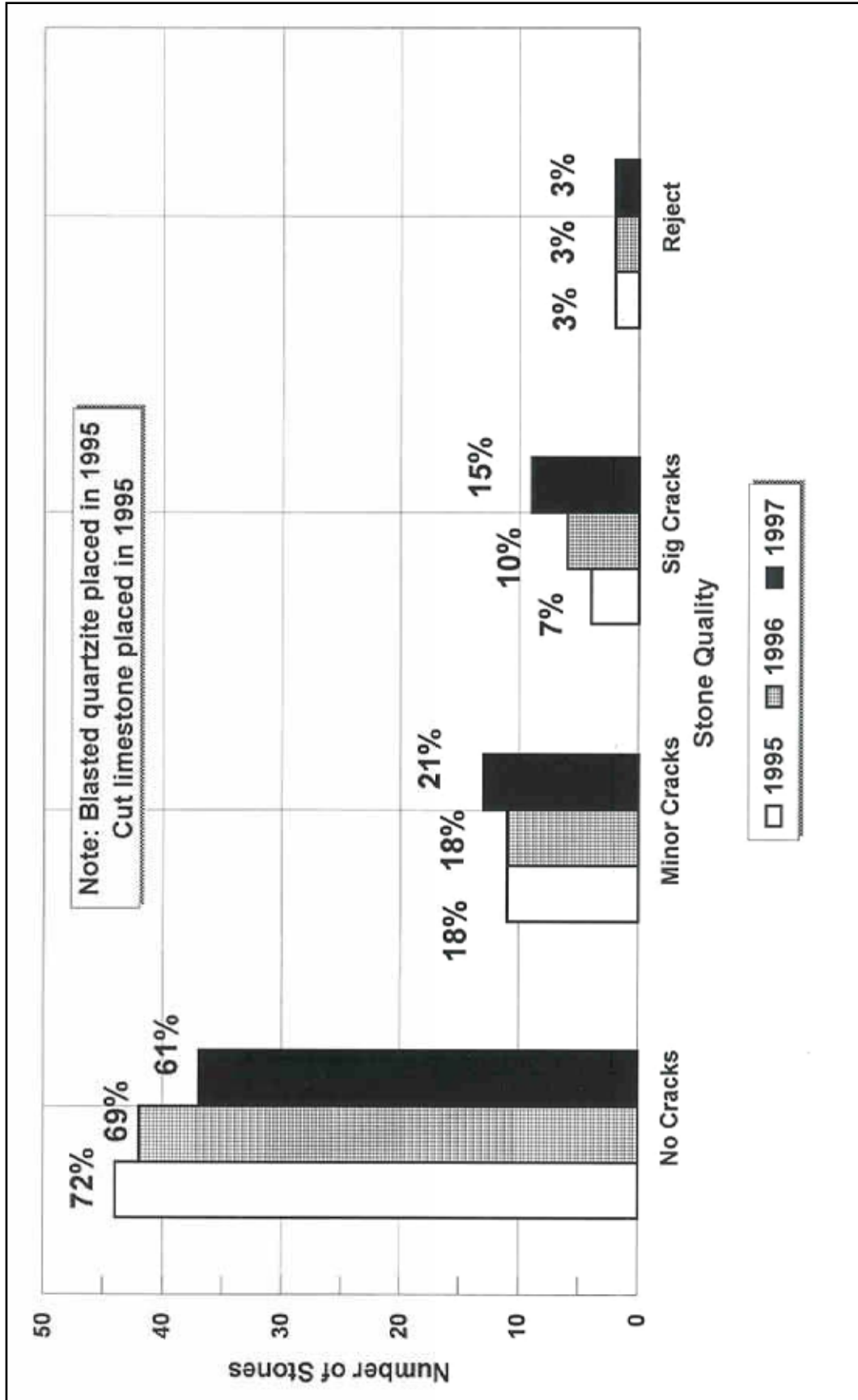


Figure 148. Stone quality comparison for monitored years at Burns Harbor breakwater (Shore Arm section), sta 53+60 to sta 54+55, for total of 61 stones (composite of blasted quartzite placed in 1995, and cut limestone placed in 1995)

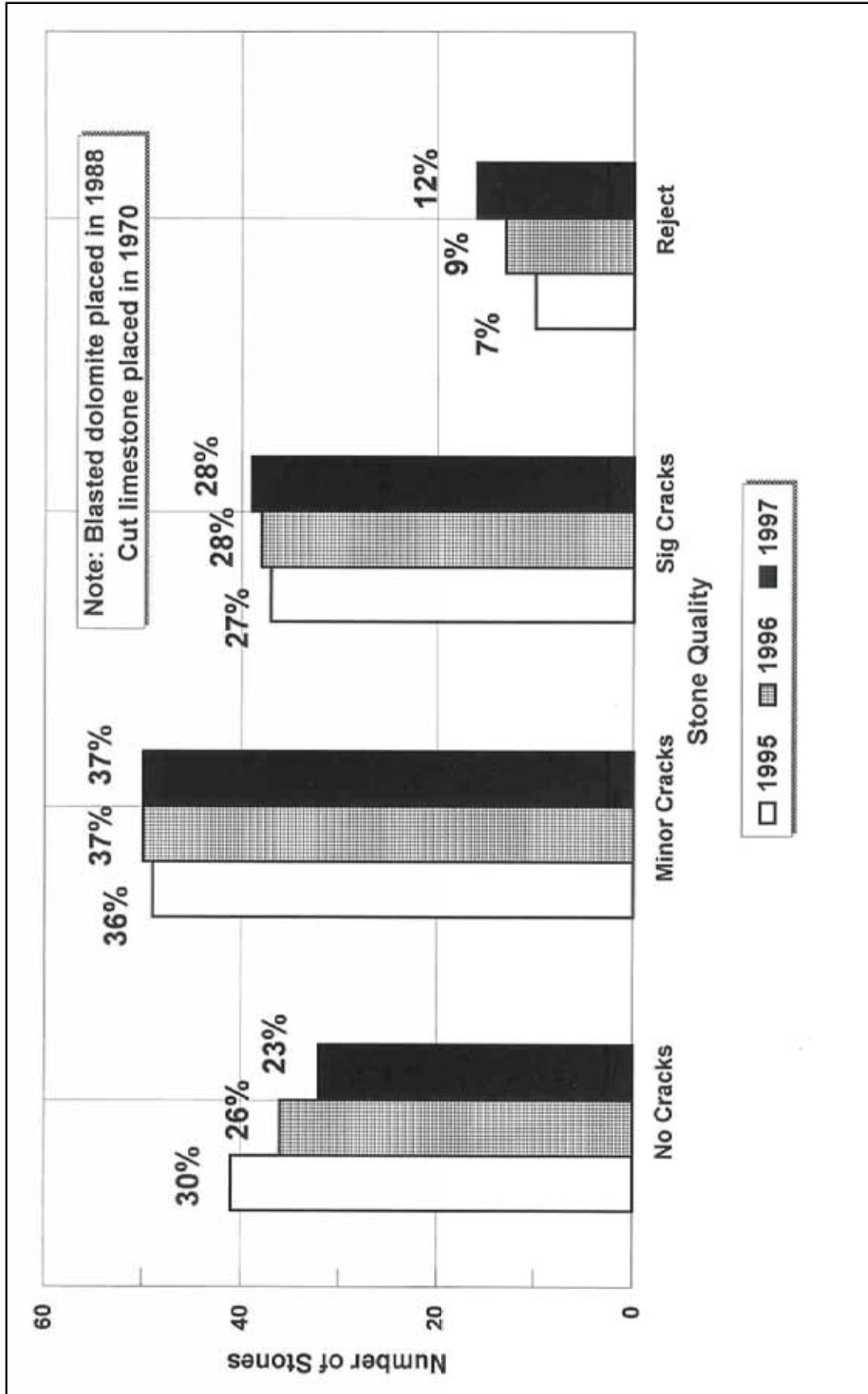


Figure 149. Stone quality comparison for monitored years at Burns Harbor breakwater (Big Burn section), sta 3+30 to sta 4+10, for total of 137 stones (composite of blasted dolomite placed in 1988, and cut limestone placed in 1970)

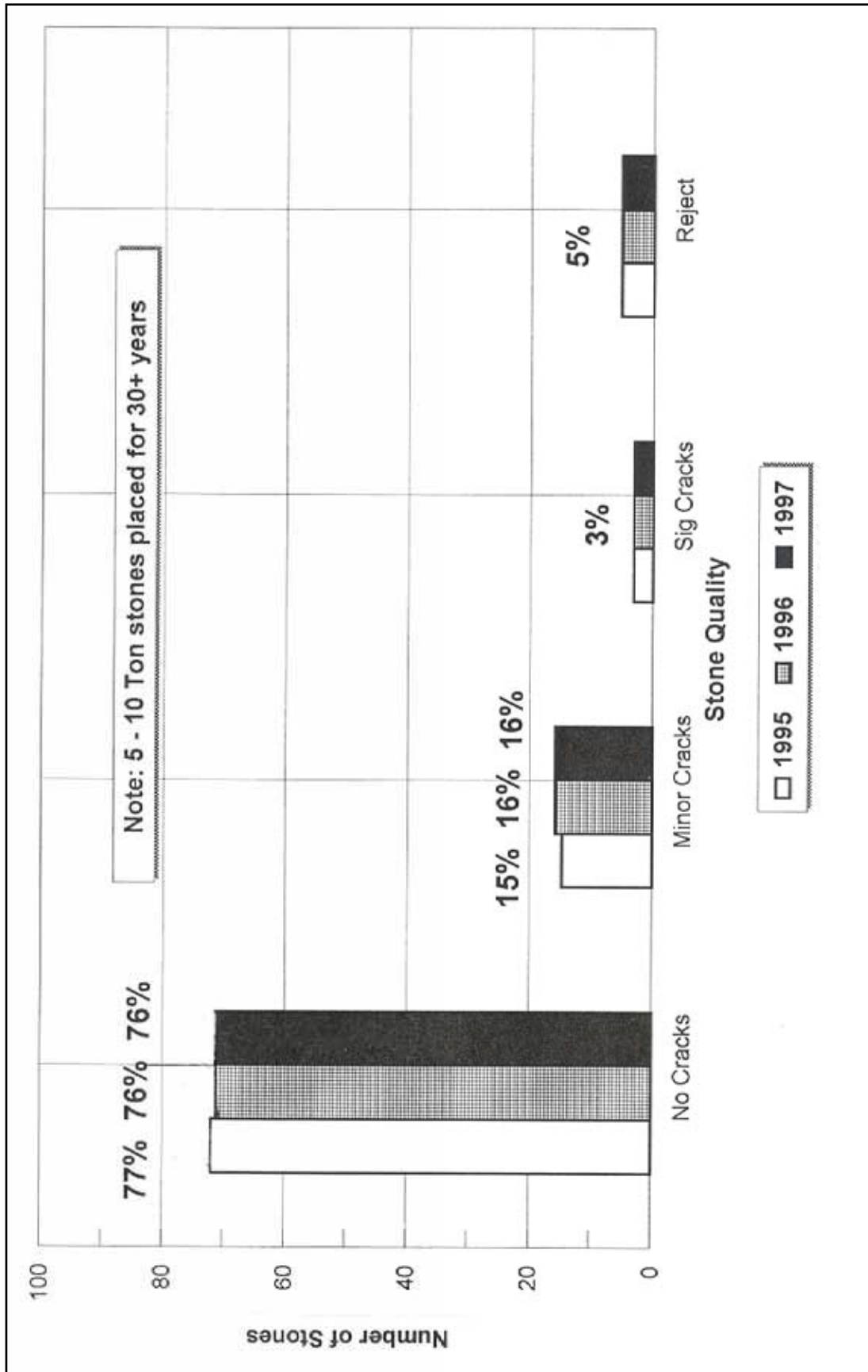


Figure 150. Stone quality comparison for monitored years at Cleveland Harbor east breakwater, sta 103+00 to sta 102+00, for total of 94 stones (cut sandstone placed over 30 years)

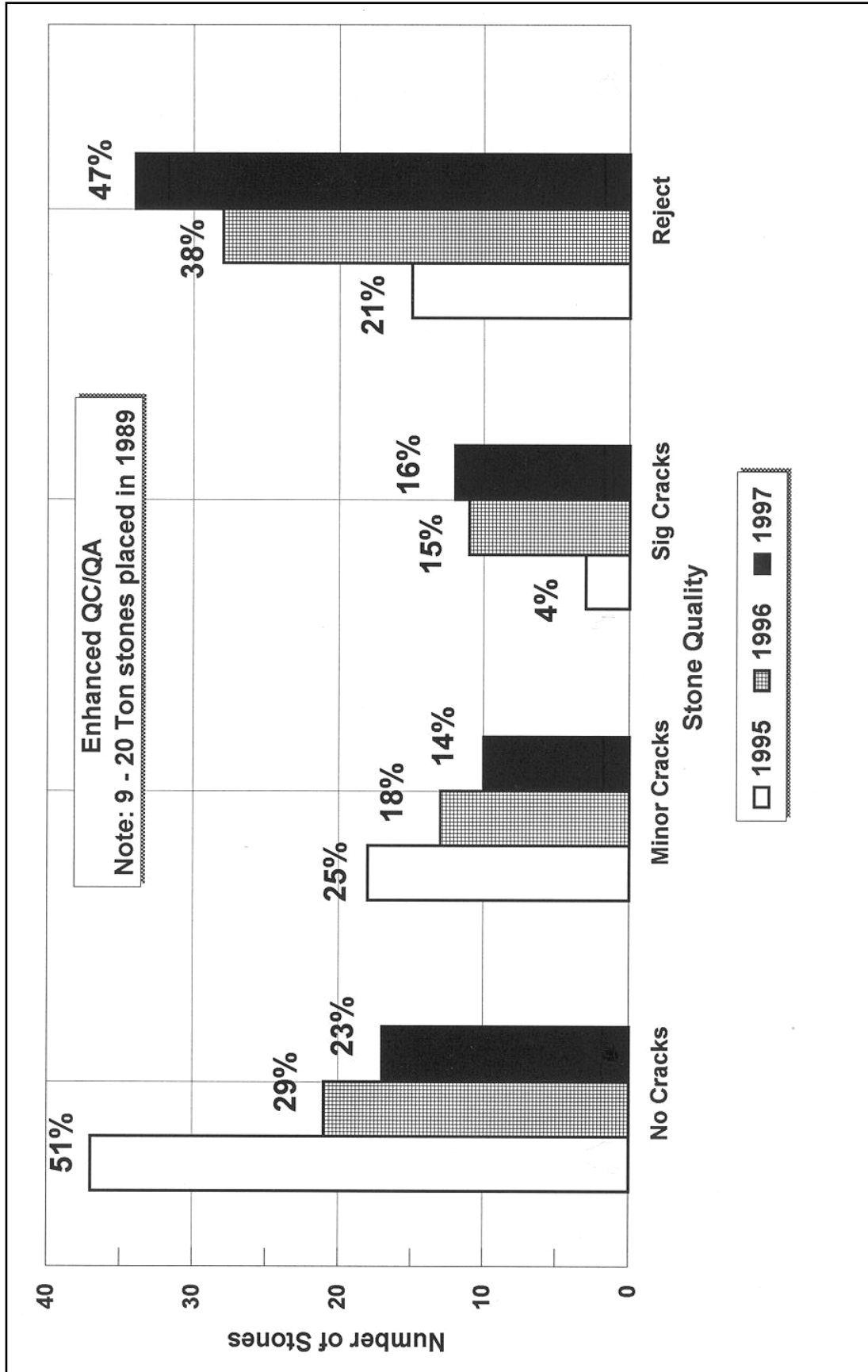


Figure 151. Stone quality comparison for monitored years at Cleveland Harbor east breakwater, sta 107+40 to sta 108+60, for total of 73 stones (blasted dolomitic limestone placed in 1989)

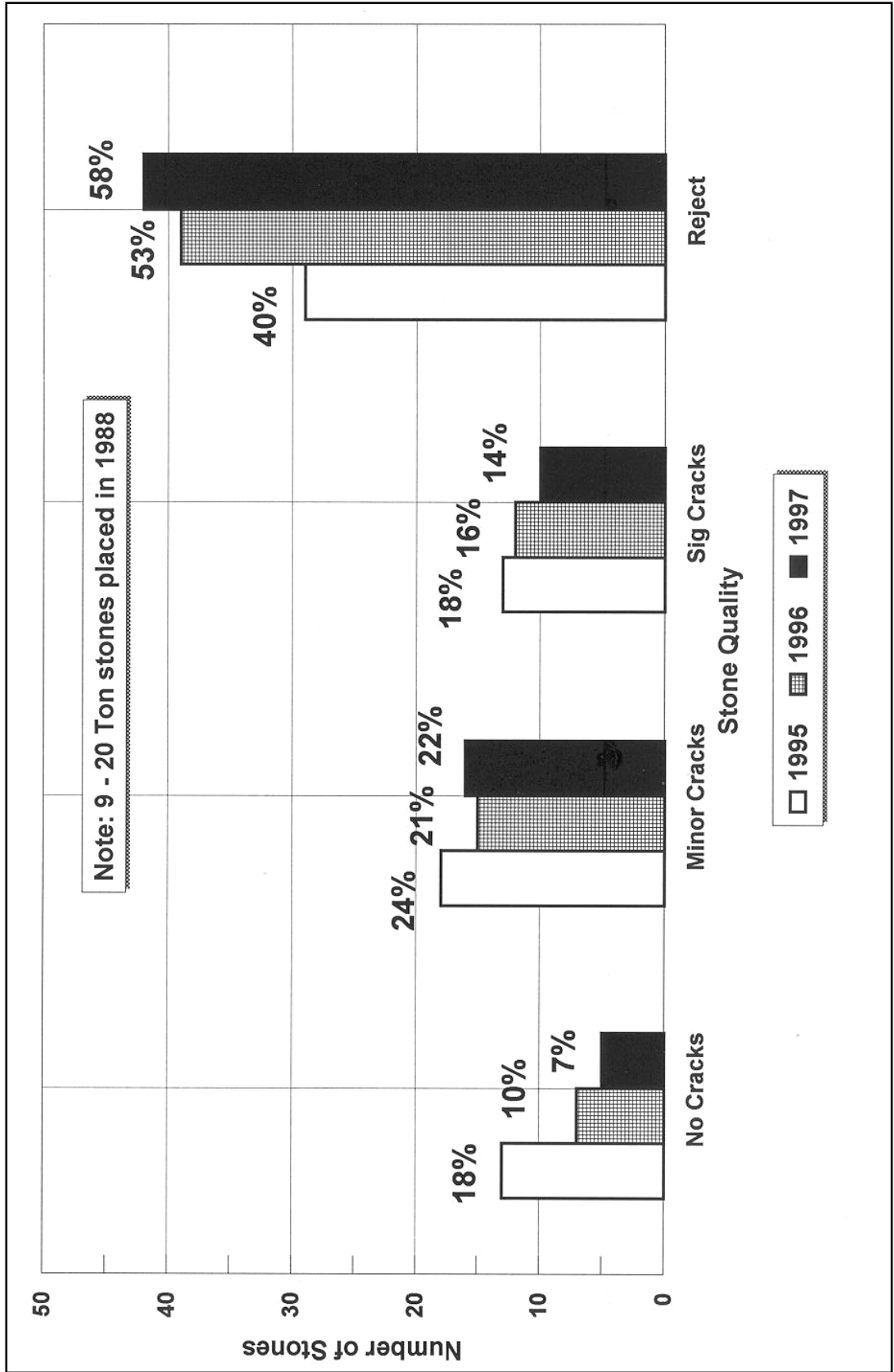


Figure 152. Stone quality comparison for monitored years at Cleveland Harbor east breakwater, sta 121+90 to sta 123+15, for total of 73 stones (blasted dolomitic limestone placed in 1988)

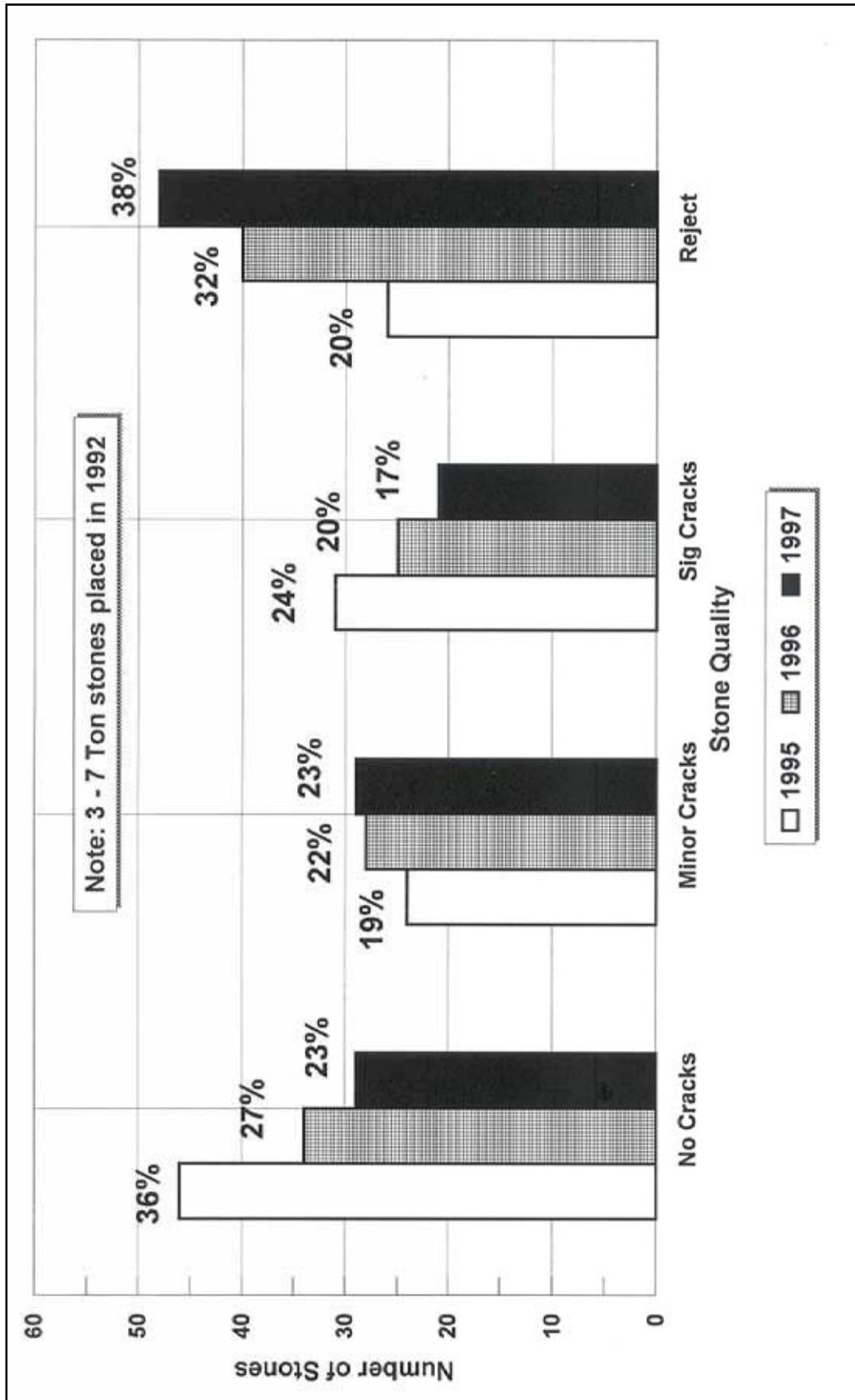


Figure 153. Stone quality comparison for monitored years at Cleveland Harbor east breakwater, sta 164+00 to sta 165+20, for total of 127 stones (blasted limestone placed in 1992)

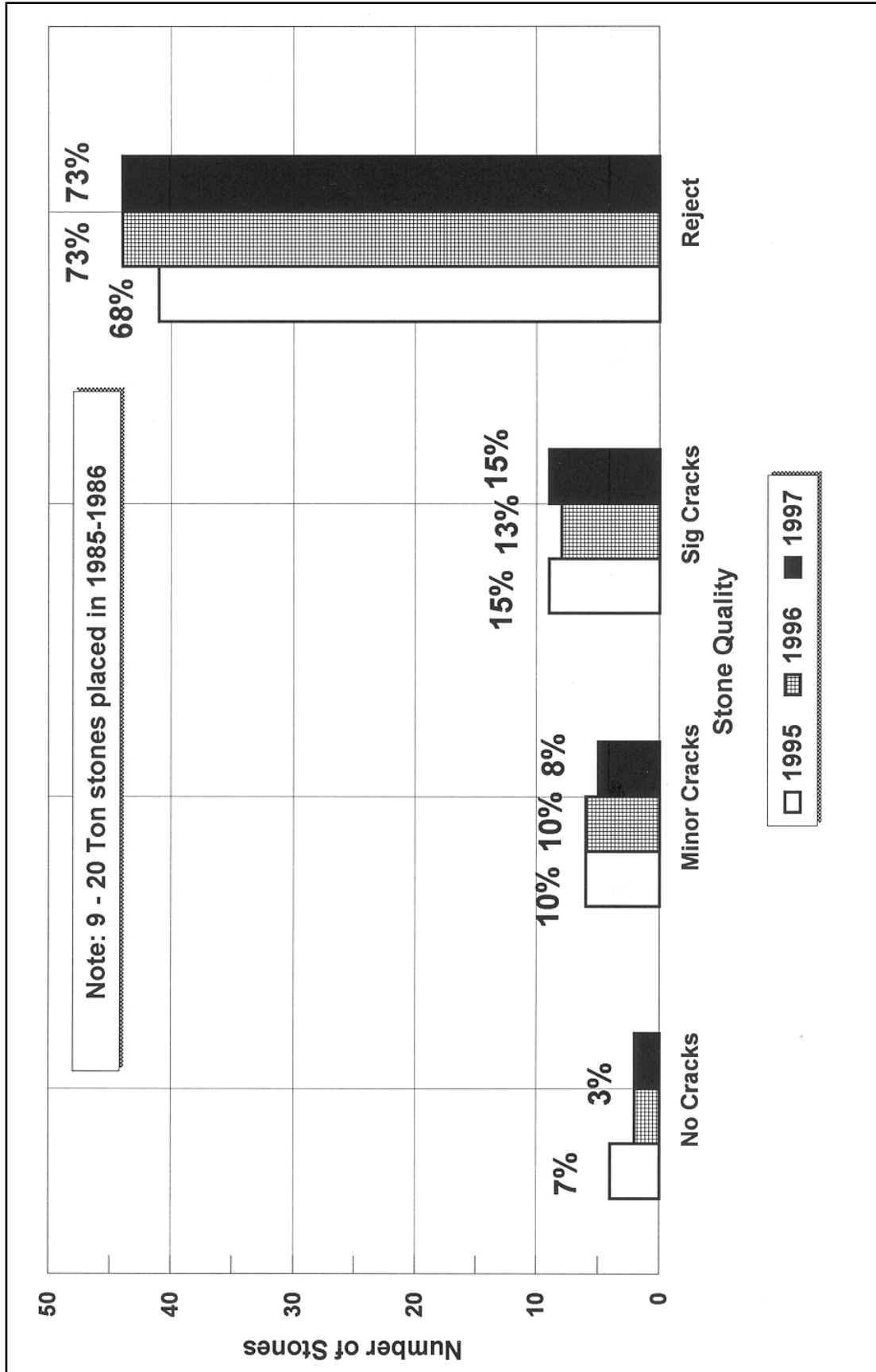


Figure 154. Stone quality comparison for monitored years at Cleveland Harbor east breakwater, sta 197+50 to sta 198+75, for total of 60 stones (blasted dolomitic limestone placed in 1989)

Table 6 Stone Deterioration, Cleveland Harbor East Breakwater Monitored Sections						
Stone Quality	No. Stones 1995	Percent Stones 1995	No. Stones 1996	Percent Stones 1996	No. Stones 1997	Percent Stones 1997
Sta 102+00 to sta 103+00, Cut sandstone placed over 30 years						
No cracks	72	76.6	71	75.5	71	75.5
Minor cracks	14	14.9	15	16.0	15	16.0
Significant cracks	3	3.2	3	3.2	3	3.2
Rejected	5	5.3	5	5.3	5	5.3
Total stones	94	100.0	94	100.0	94	100.0
Sta 164+00 to sta 165+20, Blasted limestone placed in 1992						
No cracks	46	36.2	34	26.8	29	22.9
Minor cracks	24	18.9	28	22.1	29	22.9
Significant cracks	31	24.4	25	19.7	21	16.5
Rejected	26	20.5	40	31.5	48	37.8
Total stones	127	100.0	127	100.0	127	100.0
Sta 107+40 to sta 108+60, Blasted dolomitic limestone placed in 1989						
Sta 121+90 to sta 123+15, Blasted dolomitic limestone placed in 1988						
Sta 197+50 to sta 198+75, Blasted dolomitic limestone placed in 1985						
No cracks	54	26.2	30	14.6	24	11.7
Minor cracks	42	20.4	34	16.5	31	15.0
Significant cracks	25	12.1	31	15.0	31	15.0
Rejected	85	41.3	111	53.9	120	58.3
Total stones	206	100.0	206	100.0	206	100.0
Total Sum of All Five Cleveland Harbor East Breakwater Sections Monitored						
No cracks	172	40.3	135	31.6	124	29.0
Minor cracks	80	18.7	77	18.0	75	17.6
Significant cracks	59	13.8	59	13.8	55	12.9
Rejected	116	27.2	156	36.6	173	40.5
Total stones	427	100.0	427	100.0	427	100.0

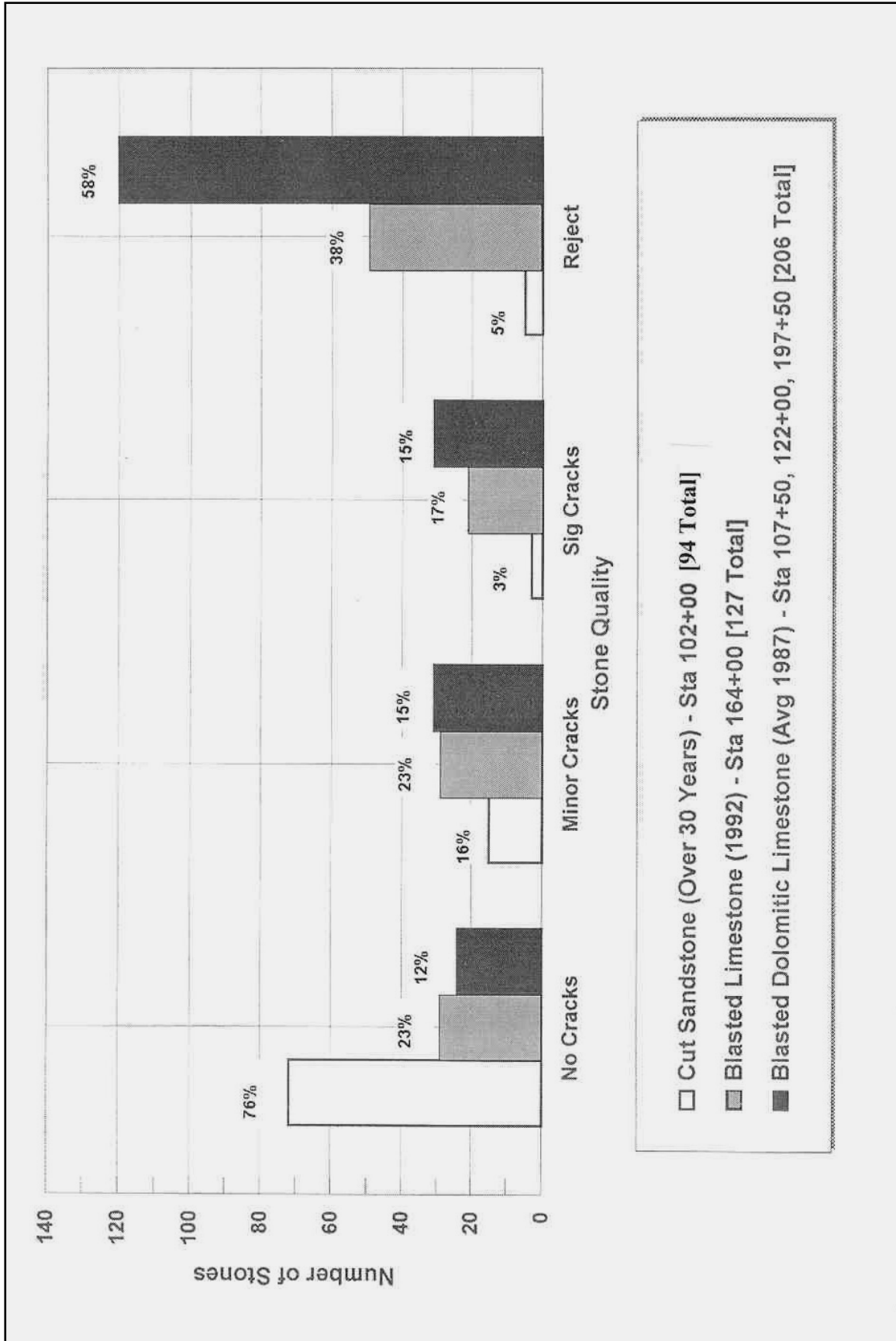


Figure 155. Cleveland Harbor east breakwater stone quality classification for three stone types on the monitored structure sections, for total of 427 stones, and a comparison of their degree of deterioration at end of monitoring period (1997)

Causes of Deterioration

The origin of fractures and hairline cracks in armor stone affecting rubble-mound structures was investigated by Livingston (1975). There are three significant external factors that contribute to stone deterioration:

- a. *Weathering environment*—(a) freeze/thaw cycles, and (b) wet/dry cycles.
- b. *Method of extraction*—(a) cutting (wire, cable, chain saw), (b) low-energy blasting; and (c) high-energy blasting.
- c. *Placement techniques*—cracks caused by mishandling which become progressively worse as the stone ages.

There are also three significant internal factors that affect the rate of deterioration:

- a. *Depositional facies*—environment of deposition directly influencing rock fabric and composition.
- b. *Diagenesis*—degree of interparticle suturing, cementation, and dolomitization; and extent of vugular porosity that affects overall induration and susceptibility to freeze/thaw action.
- c. *In situ stress*—nonisotropic relief of internal strain; and removal of confining stress, causing isotropic relief of internal strain and cracks to develop after the stone is removed from the rock formation.

Weathering Environment Deterioration

Normal weathering is a relatively slow process that can reveal what may appear to be an apparently clean, massive, fresh stone to actually be a thin, bedded, weak, and seamy stone within only a few years. Weathering can also change the mineralogical makeup of the rock. Through oxidation and dissolution, weathering alters the coloration of the rock, produces authigenic clay and iron oxides, and dissolves the mineral cements that hold a stone together.

The data in Table 7 show that the number of freeze/thaw cycles a stone in the Cleveland and Chicago area experience each year can be much greater than the 30 to 50 cycles conducted during durability testing. Therefore, the results drawn from lab tests may not be sufficient to accurately predict the performance under the harsh effects of the Great Lakes

Results from the summer 1996 inspection of Cleveland Harbor east break-water showed a significant increase in the number of new reject stones since the previous year. From a total of 427 stones, a total of 116 stones (27 percent) were failed stones in the beginning of the study (1995). In 1996 there were 40 more failed stones (156 total for 36 percent). Inspection results from 1997 revealed that 17 more stones had failed (173 total for 40 percent). From 1995-1996, 74 stones

Table 7 Freeze and Freeze/Thaw Cycles						
Month	1994-1995		1995-1996		1996-1997	
	Freeze	Freeze/Thaw	Freeze	Freeze/Thaw	Freeze	Freeze/Thaw
Chicago, IL (O'hara Airport)						
October	0	2	0	0	no data	no data
November	0	10	3	22	no data	no data
December	3	19	14	15	no data	no data
January	16	12	17	13	20	8
February	9	18	11	10	11	11
March	3	12	6	22	1	17
April	0	6	0	12	0	11
May	0	0	0	0	0	0
Total	31	79	51	94		
Cleveland, OH (Hopkins Airport)						
October	0	0	0	0	0	1
November	0	9	0	18	3	17
December	1	19	15	14	3	17
January	12	13	17	11	13	14
February	9	16	13	7	8	14
March	2	15	7	21	2	20
April	0	8	0	10	0	9
May	0	0	0	2	0	0
Total	24	80	52	83	29	92

developed additional or new failure changes compared to 43 stones that developed failure changes from 1996-1997 in the Cleveland sections. This finding coincides with a significant increase (almost double) in the number of freeze cycles the Cleveland area experienced. In the 12-month interval from the 1995 inspection to the 1996 inspection, a total of 52 freeze cycles and 83 freeze/thaw cycles were recorded. This is in sharp contrast to the 24 freeze cycles and 80 freeze/thaw cycles in 1994-1995, and 29 freeze cycles and 92 freeze/thaw cycles in 1996-1997.

Method of Extraction Deterioration

There are three general categories of extraction methods represented in the data; (a) cutting (wire, cable, chain saw), (b) low-energy blasting, and (c) high-energy blasting.

Cutting method

Stone extracted under this method is sawn from the rock formation by using a traveling wire coated with oil and abrasives, or by using a chain saw. Stones are split to size with hydraulic splitters and drills to minimize fragmentation. Drill holes and calyx holes are used to start a new lift. Production rates are tied to the building stone industry. Cut stones used for armor stone are taken from waste rock that is discolored or contains other defects that make it unacceptable for use

as architectural stone. Large quantities of waste rock were generated earlier in the twentieth century some of which are still available, but supplies are drastically diminished. Unit extraction costs are the highest of the methods discussed because this is a slow and labor-intensive process. However, the price of the waste rock does not reflect the true cost of extraction. It is usually sold at rates comparable to blasted stone to free up much needed space around the quarries. These stones tend to have very long cure periods as they have been stockpiled for over 10 years in some cases. The stone extracted by this method are the Berea sandstone and the Bedford limestone.

Blasting method

Blasting tends to open fractures primarily through gas pressure action. The initial compressional shock wave travels through the rock quickly, and may also cause some crack formation especially in the immediate vicinity of the blast hole. It is common to see cracks running parallel to blast holes, even in quarries practicing minimal blast energy extraction methods. A secondary set of concentric cracks also commonly forms around blast holes. It is the action of expanding gas that lifts the rock mass and separates it from the quarry wall.

The action from expanding gases creates a significant amount of tensional forces in the rock and results in the most damage. The expansion of gas is responsible for separation along bedding, and for generating fractures parallel to the principle stress axes in the rock mass. Any inherent weakness or anisotropy in the rock is susceptible to penetration by expanding blast gases.

An unexpected finding of this study is the divergent modes of deterioration between the breakwater reaches monitored at the Chicago Harbor breakwater and those monitored at the Cleveland Harbor east breakwater. Based on the data, the Columbus formation at the Cleveland Harbor east breakwater is significantly more prone to blast fracturing than any of the formations monitored at the Chicago Harbor breakwater. This cannot be explained, since the lithology, blasting methods and, presumably, the physical properties of the stones are similar. The largest difference in lithology is the fact that the Columbus formation is not as pure a dolomite as is the Silurian series and may therefore contain diagenetic inhomogeneities that are more prone to blast damage.

There may also be an observational bias in the data in that the inspectors may have prescribed causes to cracks that were not substantiated or may have overlooked associations with some cracks. It was noted during detailed geologic descriptions of the stones at the Cleveland Harbor east breakwater that there is a fair amount of stones prone to deterioration due to fabric related causes, but the Columbus formation in general is not as susceptible to this type of deterioration as is the Silurian series. The inspector responsible for description of the geology of the stones was not the same inspector recording the deterioration data. Hence, while the data appear to diverge, there are independent observations that confirm that there is a significant difference in the mode of deterioration between the Silurian series and the Columbus formation.

Low-energy blasting. Stone extracted by the low powder (low bench height) method is blasted from the rock formation using narrow (less than 7.6 cm (3 in.) in diameter), closely spaced (less than 1.5 m (5 ft) apart), shot holes from bench heights of less than 9.1 m (30 ft). These types of shot patterns are designed for extraction of armor stone. Although the details of shot hole spacing may vary from quarry to quarry, the overall energy imparted to the rock is relatively similar (low specific charge < 0.2 kg per cu m (0.34 lb per cu yd), one row of holes). Production rates for this type of stone extraction vary depending on bedding plane spacing and joint spacing naturally occurring in the quarries, as compared to the size of stone specified for the structure. The smaller sized armor stones are easier to obtain. Unit extraction costs are intermediate in price. Cure periods for these stones are variable depending on the armor stone market. Generally the cure period is the minimum specified, as extraction often follows award of a specific contract. The stone extracted by this method are the Niagaran series from the Valders Quarry near Valders, WI; the Waterloo quartzite from the Dempsey Quarry near Waterloo, WI; and the Columbus formation from the Marblehead Quarry of Marblehead, PA, near Sandusky, OH.

High-energy blasting. Stone extracted by the high powder (high bench height) method is blasted from the rock formation using large (greater than 11.4 cm (4.5 in.) in diameter) widely spaced (greater than 3 m (10 ft) apart) shot holes from bench heights greater than 9.1 m (30 ft). These types of shot patterns are designed for extraction and maximum fragmentation of aggregate. The aggregate may be used for construction or as a lime feed. Stones remaining from the blast, which are too large for the crusher, are often set aside, to be sold as armor stone. This is convenient for the quarry operator since they do not need to perform expensive manipulations to further break down the large pieces for aggregate. Hence, this stone tends to be economical as it is essentially waste rock left over from the more profitable aggregate production. Production rates for this type of armor stone can be low and may take a significant amount of time before the quarry has accumulated enough armor stone to market, depending on the annual quantity of aggregate produced from that source. Cure periods are generally 90 days. Some jobs may require quantities already stockpiled at the quarry. If the job requires more stone than is stockpiled, cure periods will be much shorter. The stone extracted by this method are the Niagaran series from a quarry near Cedarville, MI; the Niagaran series from the McCook Quarry near McCook, IL; and the Columbus formation from the Sandusky Quarry near Parkertown, OH.

Conclusions regarding method of extraction deterioration

The average quality of stone for the three methods of extraction (cutting, low-energy blasting, high-energy blasting) was determined for different stone types from various breakwaters that had come from different quarries. The average quality was determined by the quality rating scale previously discussed. Results are summarized in Table 8.

Table 8 Effect of Extraction Method on Average Quality of Sedimentary Stone		
Cutting Method of Extraction		
Stone Type	Age, years	Average Quality
Berea sandstone (Johnson Quarry)	31	92
Salem limestone (Reed Quarry)	10	94
Blasting Method of Extraction Columbus formation limestone and dolomitic limestone		
Type of Blasting	Age, years	Average Quality
High Energy Blasting (Sandusky Quarry)	6	63
Low Energy Blasting (Marblehead Quarry)	9	48
Blasting Method of Extraction Silurian series dolomite		
Type of Blasting	Age, years	Average Quality
High Energy Blasting (McCook Quarry)	16	61
High Energy Blasting (Cedarville Quarry)	10	67
Low Energy Blasting (Valders Quarry)	4	58

The most striking difference in durability is the difference between cut stone and blasted stone. Cut stone average quality varies from 92 to 94 after 31 and 10 years of use, respectively. This is in stark contrast to the average quality that ranges from a low of 48 for 9 years and a high of 67 for 10-year-old, high-energy extracted stone. It is clear from these results that the cut sedimentary stone is performing better than the blasted sedimentary stone, regardless of the blasting method employed.

These numbers also indicate that the average economic life for a cut stone is well over 40 years, whereas a blasted stone (regardless of blasting method) may last a minimum of 4 years or a maximum of 16 years without requiring some sort of rehabilitation. Intuitively, one would expect the high energy blasting methods to produce stone with a shorter economic life than stone extracted using a low energy extraction method. However, the only conclusion that can safely be reached from these data is that cut stone will tend to have fewer problems associated with it than blasted stone of the same type and general characteristics.

More research is required to determine exactly when rehabilitation is necessary. This conclusion assumes that rehabilitation would be recommended when the average quality is equivalent to a multiply significant cracked stone. In practice, a major rehabilitation may be recommended much sooner if an area of the structure has a higher concentration of stones showing more rapid rates of deterioration than the average over the whole structure.

Another surprising result is that the blasting methods do not appear to significantly alter the rate at which the stone deteriorates. For instance, the stone extracted from the Sandusky Quarry using high-energy extraction methods is approximately 15 points better than the stone from the Marblehead Quarry that uses low-energy extraction. Taking into account the relative ages, these two methods appear to be essentially performing equally. The same phenomena were observed for the Niagaran series dolomites. Both high-energy quarries appear to

be deteriorating at approximately the same rates as the low-energy quarry. The 95 percent confidence levels for these averages are approximately ± 10 points.

The number and percentage of rejected sedimentary stones on the monitored sections is presented in Table 9 and Figure 156, respectively, for the end of the 1997 survey for cut and blasted methods of extraction.

Table 9 Rejected Sedimentary Stones, Cut and Blasted Method of Extraction, 1997 Results						
Section	Stone Type	Age, years	Number of Blasted		Number of Cut	
			Rejected	Total	Rejected	Total
Chicago B/W	dolomite	3			5	50
Chicago B/W	limestone	31			42	81
Calcumet B/W	dolomite	3			0	3
Calcumet B/W	limestone	9			5	132
Calcumet CDF	dolomite	3			0	3
Calcumet CDF	limestone	3			0	1
Burns (Shore Arm)	limestone	2			0	1
Burns (Big Burn)	limestone	27			6	34
Cleveland B/W Sta 102+00	sandstone	32			5	94
Calcumet CDF	dolomite	1	19	43		
Burns (Big Burn)	dolomite	9	10	103		
Cleveland B/W Sta 107+40	dolomitic limestone	8	34	73		
Sta 121+90	dolomitic limestone	9	42	73		
Sta 164+00	limestone	5	48	127		
Sta 197+50	dolomitic limestone	12	44	60		
Total Number of Stones		197	479	64	399	
Total Percent of Stones Rejected			41.1		16.0	
Average Stone Age, years (weighted)			8.70		19.62	
Range of Stone Age, years			5 to 15		2 to 32	
Average Percent of Stones Rejected/Year			4.7		0.8	

Data from this MCNP study show that cut sedimentary stones are performing better than blasted sedimentary stones. From Table 9, approximately 16.0 percent of the 399 cut stones included in the survey were categorized as failed stones with a weighted average age of 19.6 years (average percent of rejected stones per year = 0.8 percent per year). This finding contrasts with 41.1 percent of the 479 blasted stones considered to have failed with a weighted average age of 8.7 years (average percent of rejected stones per year = 4.7 percent per year). (Subsequent data from the quartzite show that 2.6 percent of the 78 blasted stones considered to have failed had an average age of 2.2 years (average percent of rejected stones per year = 1.2 percent per year)).

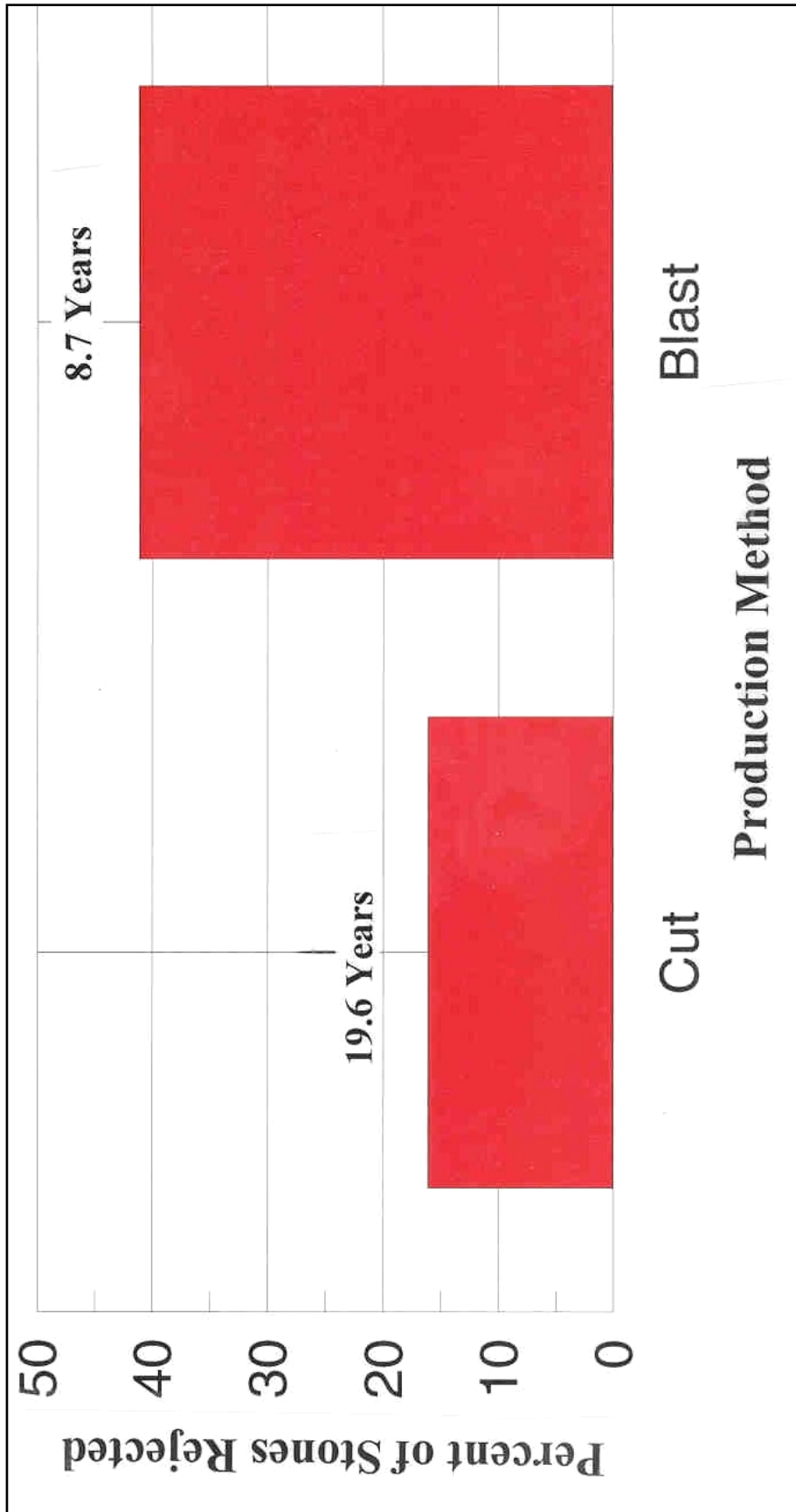


Figure 156. Cut versus blasted comparison of rejected sedimentary stones (limestone, sandstone, dolomite, and dolomitic limestone) on monitored structure sections, and weighted average number of years since placement of stone on structure

The data for six different stone geologies (dolomite, dolomitic limestone, limestone, quartzite, sandstone, and taconite) at the structure sections monitored in 1997 are shown in Table 10. This table presents, for each structure section, the stone geology type, the method of extraction, the number of years since placement, the total number of stones evaluated, the number of stones rejected, and the percent of each stone type rejected. A rejected stone has previously been defined as any monitored stone on the structure section that is either (a) failed, (b) multiply failed, (c) fragmented, (d) multiply fragmented, (e) displaced, (f) multiply displaced, (g) lost1, (h) lost2, or (i) lost3. Here, again, the terms failed, multiply failed, fragmented, multiply fragmented, displaced, multiply displaced, lost1, lost2, and lost3 have previously been defined with respect to stone cracks. A rejected stone had lost its integrity and no longer functioned as one originally placed unit.

The data of Table 10 are presented in Figure 157 to show the percent of stones rejected at each structure section in 1997 for each of the six different stone geologies under consideration, along with the weighted average stone age for each of the stone types. Without regard to the method of extraction (cut versus blasted), it appears that five of the six stone types have an average percent of stones rejected per year of 2.0 or less. Only the dolomitic limestone has a larger average percent of stones rejected per year of 6.1 stones rejected per year. However, these data must be further analyzed with regard to the method of extraction. The data from Table 10 are displayed in Figures 158 and 159 for cut versus blasted dolomite and cut versus blasted limestone, respectively, for each of the different structure sections where the specified stones had been placed.

Table 11 considers both the stone geology and the production methods (cut and blasted) for extracting the stones from the quarries. For limestone, where cut versus blasted methods of extraction are directly comparable within the same geology, these MCNP data show the cut method of extraction is significantly better than the blasted method, whereby 1.1 stones are rejected per year by cutting and 7.6 stones are rejected per year by blasting. For dolomite, the differences are not quite as readily apparent. It appears the blasting method of extraction may actually be superior to the cutting method; however, the cut dolomite stones had been on the structure only 3 years when the 1997 survey was conducted (see editor's note, p 149). Further studies may indicate a reversal of this trend. Only blasted dolomitic limestone was evaluated during the MCNP study; no cut dolomitic limestone was available for comparative analyses. From the data of Table 11, blasted dolomitic limestone appears to be comparable to blasted limestone, strictly from a consideration of the percent stones rejected per year. Figure 160 shows the relationship between the percent of stones rejected versus the stone geology and production method. The weighted average number of years since the stones were placed on the structure sections, for both cut and blasted methods of extraction, also are shown in Figure 160.

**Table 10
Rejected Stones for Six Stone Geologies Monitored, Cut and Blasted Methods of Extraction, 1997 Results**

Structure Section	Method	Age years	Number Rejected	Number Total	Percent of Stones Rejected				Sandstone	Taconite
					Dolomite	Dolomitic Limestone	Limestone	Quartzite		
Chicago B/W	Cut	3	5	50	10.0					
Chicago B/W	Cut	31	42	81		51.9				
Calumet B/W	Cut	3	1	3	33.3					
Calumet B/W	Cut	9	5	132		3.8				
Calumet B/W	Blast	3	0	18			0.0			
Calumet CDF	Blast	15	19	43	44.2					
Calumet CDF	Cut	3	0	3	0.0					
Calumet CDF	Cut	3	0	1		0.0				
Calumet CDF	Blast	3	0	2					0.00	
Burns (Shore Arm)	Cut	2	0	1		0.0				
Burns (Shore Arm)	Blast	2	2	60			3.3			
Burns (Big Burn)	Cut	27	6	34		17.7				
Burns (Big Burn)	Blast	9	10	103	9.7					
Cleveland B/W										
Sta 102+00	Cut	32	5	94				5.3		
Sta 107+40	Blast	8	34	73		46.6				
Sta 121+90	Blast	9	42	73		57.5				
Sta 164+00	Blast	5	48	127			37.8			
Sta 197+50	Blast	12	44	60		73.3				
Total Number of Stones					202	206	376	78	94	2
Total Number of Stones Rejected					35	120	101	2	5	0
Total Percent of Stones Rejected					17.3	58.3	26.9	2.6	5.3	0.0
Average Stone Age, years (weighted)					8.61	9.52	13.98	2.23	32.00	3.00
Range of Stone Age, years					3 to 15	8 to 12	2 to 31	2 to 3	32	3
Average Percent of Stones Rejected/Year					2.0	6.1	1.9	1.2	0.2	0.0

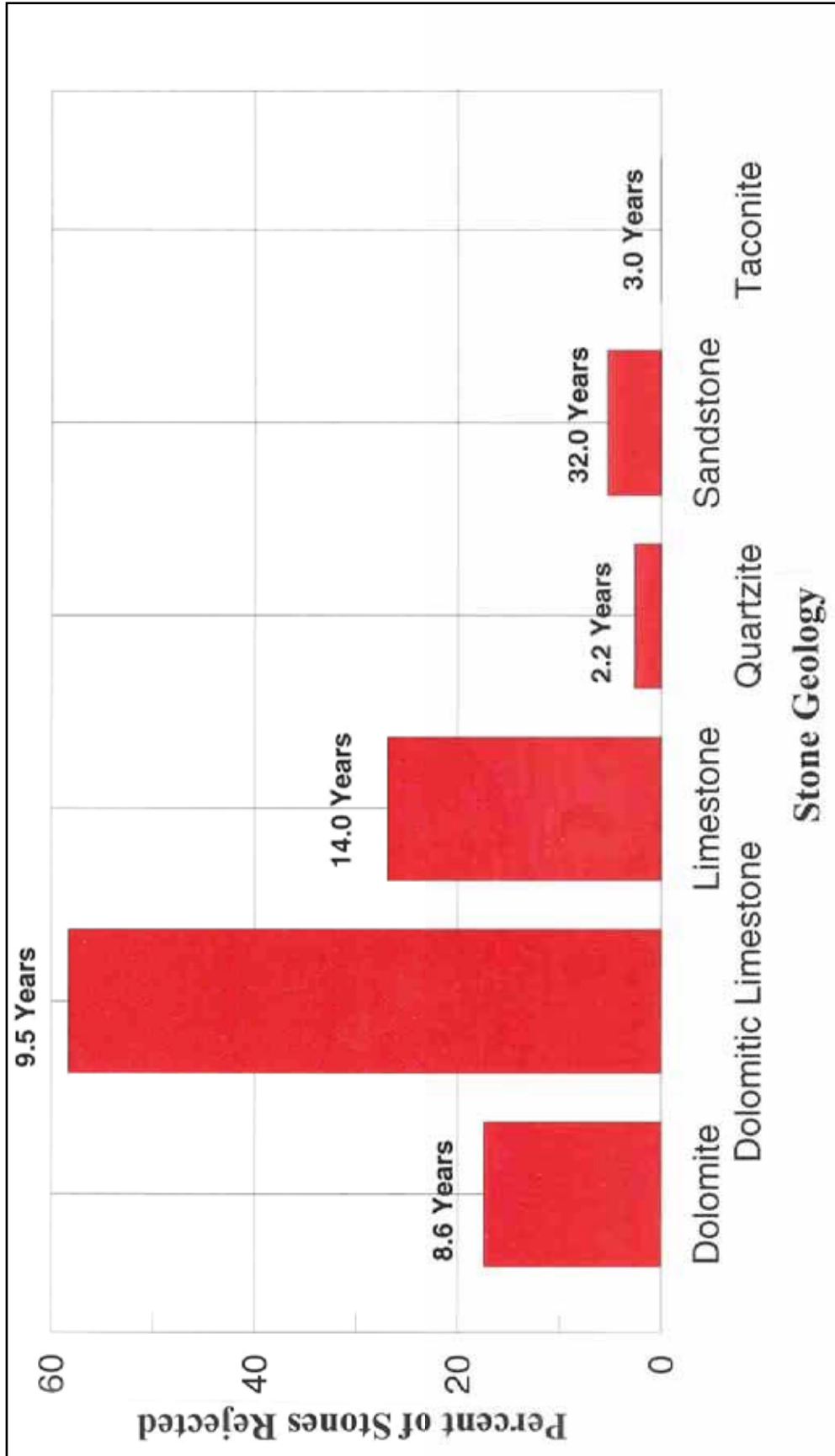


Figure 157. Percentage of stones rejected on monitored structure sections versus six stone geologies evaluated, and weighted average number of years since placement of stone on structure

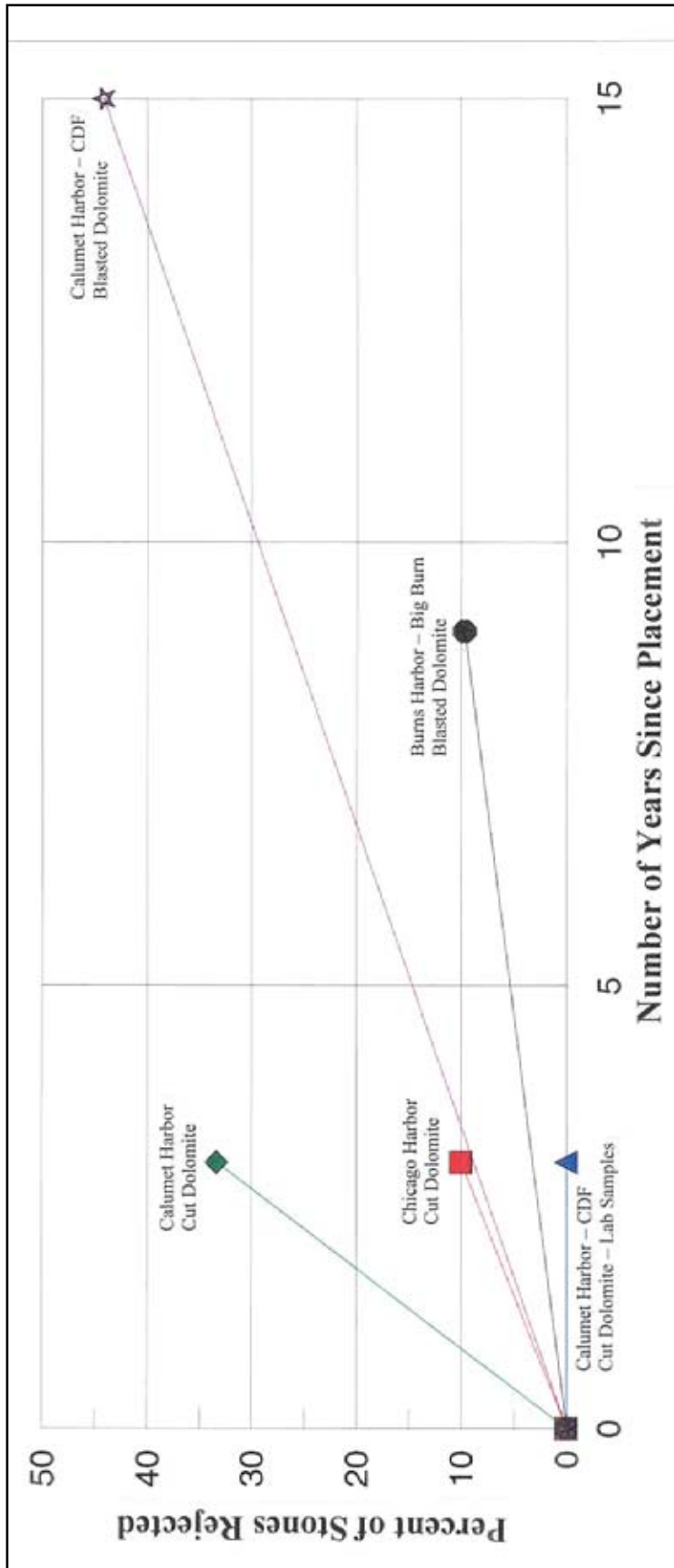


Figure 158. Percentage of stones rejected on monitored structure sections versus number of years since placement of stone on structure sections, for five monitored sections with cut and blasted dolomite

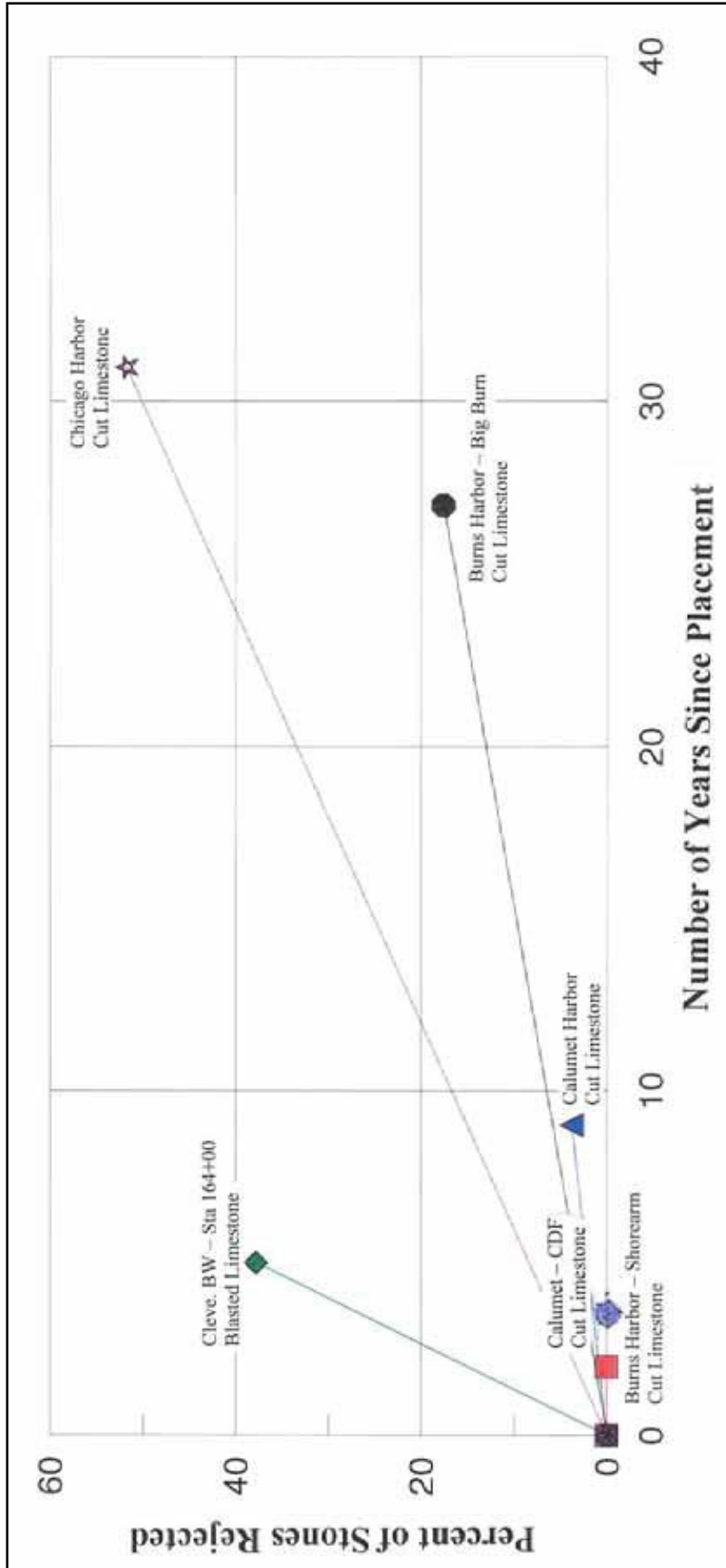


Figure 159. Percentage of stones rejected on monitored structure sections versus number of years since placement of stone on structure sections, for six monitored sections with cut and blasted limestone

**Table 11
Stone Geology and Production Method, Cut and Blasted Methods of Extraction, 1997 Results**

Structure Section	Method of Extraction	Dolomite		Dolomite Limestone Blasted	Limestone		Quartzite Blasted	Sandstone Cut	Taconite Blasted
		Cut	Blasted		Cut	Blasted			
Chicago B/W	Cut	50							
Chicago B/W	Cut				81				
Calumet B/W	Cut	3							
Calumet B/W	Cut				132				
Calumet B/W	Blast						18		
Calumet CDF	Blast		43						
Calumet CDF	Cut	3							
Calumet CDF	Cut				1				2
Calumet CDF	Blast								
Burns (Shore Arm)	Cut				1				
Burns (Shore Arm)	Blast						60		
Burns (Big Burn)	Cut				34				
Burns (Big Burn)	Blast		103						
Cleveland B/W									
Sta 102+00	Cut							94	
Sta 107+40	Blast			73					
Sta 121+90	Blast			73					
Sta 164+00	Blast						127		
Sta 197+50	Blast			60					
Total Number of Stones		56	146	206	249	127	78	94	2
Total Number of Stones Rejected		6	29	120	53	48	2	5	0
Total Percent of Stones Rejected		10.5	19.9	58.3	21.3	37.8	2.6	5.3	0.0
Average Stone Age, years (weighted)		3.00	10.76	9.52	18.63	5.00	2.23	32.00	3.00
Range of Stone Age, years		3	9 to 15	8 to 12	2 to 31	5	2 to 3	32	3
Average Percent of Stones Rejected/Year		3.5	1.8	601	1.1	7.6	1.2	0.2	0.0

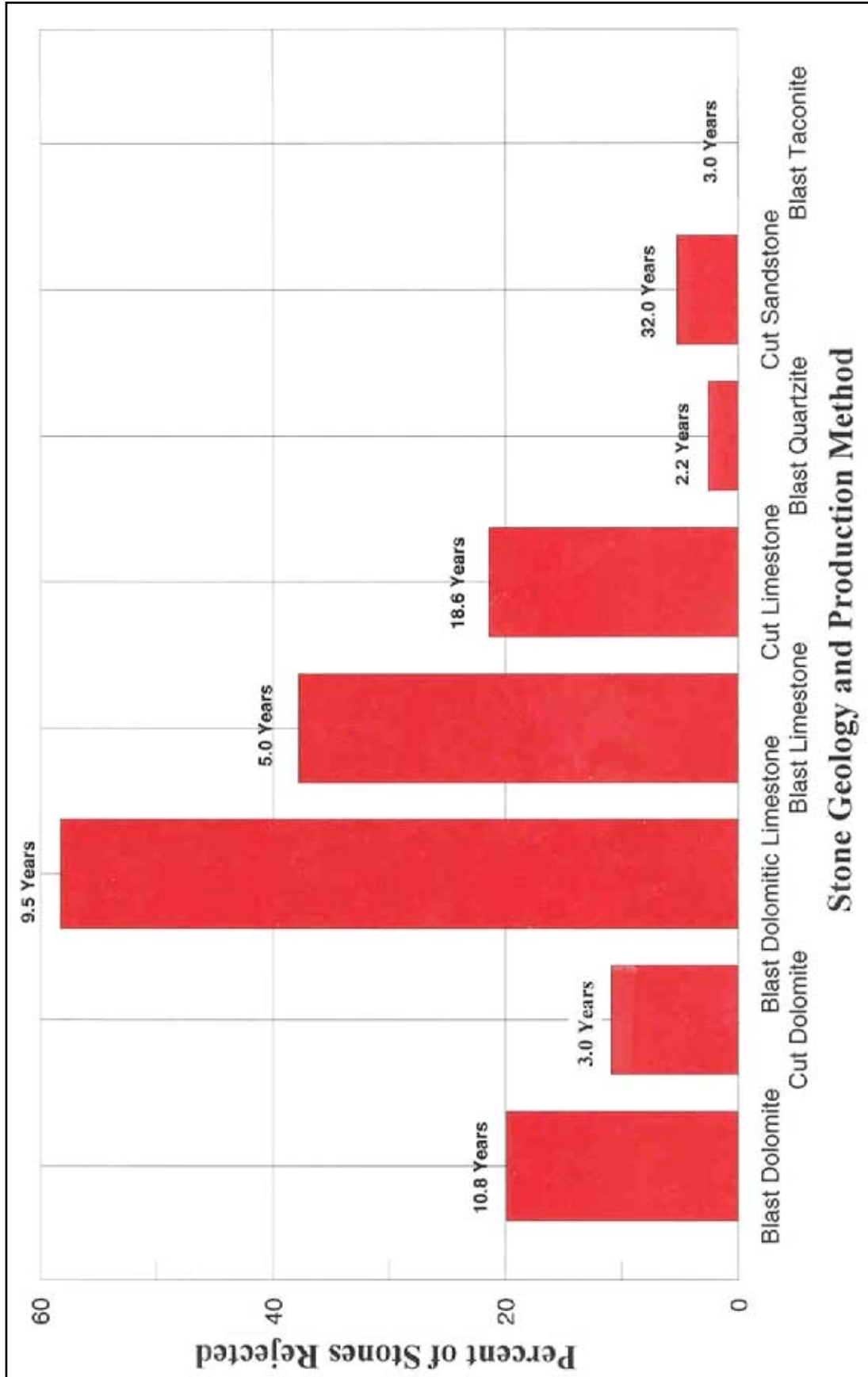


Figure 160. Percentage of stones rejected on the monitored structure sections versus stone geologies and production methods (cut and blasted methods of extraction), and weighted average number of years since placement of stone on structure

Placement Techniques Deterioration

Placement methods are a critical part of construction. Brittle stones such as the Silurian series and Columbus formation are prone to damage when dropped from a height of over 0.30 m (1 ft). Hard stones such as these and the Waterloo quartzite are difficult to grab with clamshell type buckets. For this reason, neither clamshell nor leaf-type buckets should be used. Only stone grabs can place stone without dropping or damaging it. Damage caused by improper handling is commonly evidenced by scrap marks on the sides of the in-place stones. Impact breakage at edges or corners and subsequent spalling is also indicative of poor or improper handling.

The stones placed on the Cleveland Harbor breakwater did not exhibit cracking attributed to corner edge or spalling. However, there were a large number of unknown cracks that might have occurred from handling.

The worst reach for spalling was found at Burns Harbor breakwater, which exhibited several corner-edge and spalling type cracking, but it was a small percentage (less than 8 percent) of all the stone placed. A small number of spalls were also recorded in the Silurian series from the Valders Quarry, WI, and from the McCook Quarry, IL, but these were an insignificant amount (only one stone in each case).

Depositional Facies Deterioration

Each of the stones from the selected sections of the monitored prototype breakwaters was closely inspected, and a geologic description was prepared using standard methods. Based on the lithologic characteristics, the stones were assigned to their respective facies. Facies were previously defined during quarry inspections by Rock Products Consultants (1995).

The durability of the various facies were measured by three parameters; (a) change factor, (b) quality rating, and (c) number of cracks. The data for each stone include more than one crack in a number of cases. For these stones, the total number of cracks was summed for that stone. All the durability parameters were taken from the final condition of the stone, as measured at the end of the field investigations. A number of facies identified in the quarries were not represented on the breakwaters, as should be expected. In particular, a number of facies described in the Dempsey Quarry were not represented in stones on the breakwater. The numbers of samples representing each facies varied from one (Dempsey Quarry facies e) to as many as 94 (Johnson Quarry facies a).

In addition to dividing the stones by facies, the stones were also divided into groups within each facies based on the age of the stone (age being defined as how long the stone had been on the breakwater). All facies and ages were generally well represented, with a few exceptions. A number of facies and ages are underrepresented in the sample groups, with only one or two stones representing the group. These small sample groups were not considered in the analysis as they were considered statistically unreliable. Also, some of the stones could not be

neatly categorized into one facies because they exhibited characteristics from more than one facies. This was especially true of the stones from the Marblehead Quarry, which had a large number of stones that exhibited a combination of two facies, and from the Sandusky Quarry, where the investigator could not differentiate between facies a and b (intershoal and shoal facies). For the Sandusky Quarry, facies a and b were grouped together as one group. In these cases, the stones were categorized as representing a combination of facies in one stone. The facies data that have more than one subscript represent stones exhibiting more than one facies.

An arithmetic mean was calculated for each of the three durability parameters for each age stone within each facies. Standard deviations were calculated by (a) finding the deviation of each value from the arithmetic mean, (b) squaring the deviation, (c) summing the squared values, (d) dividing by the number of samples, and (e) taking the square root of the quotient. A 95 percent level confidence limit was calculated for each of the durability parameters.

When two mean values were compared to one-another, a standard t- test was performed to determine whether the difference in values was statistically significant. If the results of the t-test fell between 100 and 95 percent probable, the differences were real. If the results of the t-test fell between 95 and 80 percent probable, the differences were considered significant and worthy of additional study. If the results of the t-test fell below 80 percent probable, the differences were not considered statistically valid.

Table 12 summarizes the results of the durability evaluations. Facies in Table 12 are identified by the following:

- a. R – Reed Quarry, Salem formation limestone.
- b. J – Johnson Quarry, Berea formation sandstone.
- c. D – Dempsey Quarry, Waterloo formation quartzite.
- d. V – Valders Quarry, Niagaran series dolomite.
- e. C – Cedarville Quarry, Niagaran series dolomite.
- f. MC – McCook Quarry, Niagaran series dolomite.
- g. M – Marblehead Quarry, Columbus formation dolomitic limestone.
- h. S – Sandusky Quarry, Columbus formation limestone.

A number of conclusions can be drawn from the preceding durability information. A systematic variation occurs in durability within the blasted stones with an apparent dependence on facies. By comparing quality ratings in the two carbonate groups (the Silurian series and the Columbus formation), it is observed that, in some cases, facies influences the durability of the stone. For example, within the McCook Quarry samples, facies MC_{b-16} has a quality rating of 68 (\pm 95 percent confidence range from 78.9 to 57.1) with an average number of cracks per stone of 2.7 (\pm 95 percent confidence range from 4.3 to 1.1). This is in contrast to MC_{d-16} which has a quality rating of 40 (\pm 95 percent confidence

Table 12 Quarry Facies Durability Evaluations							
Facies	Number of Samples	Change		Quality		Cracks	
		Factor	± 95 Percent	Rating	± 95 Percent	Number	± 95 Percent
Salem formation limestone							
Rb-10	6	0.0	0.00	93.0	15.3	0.3	0.5
Rb-78	2	0.0	n/a	30.0	n/a	3.0	n/a
Rb/c-10	1	0.0	n/a	60.0	n/a	4.0	n/a
Rb/c-78	2	0.0	n/a	40.0	n/a	2.5	n/a
Rc-28	1	0.0	n/a	100.0	n/a	0.0	n/a
Rc-10	39	0.2	0.16	95.6	5.0	0.3	0.2
Rc-78	16	0.1	0.10	51.9	17.7	1.9	0.6
Rd-28	21	0.1	0.20	80.5	10.8	0.7	0.4
Rd-4	2	0.0	n/a	100.0	n/a	0.0	n/a
Rd-10	52	0.0	0.00	94.4	3.9	0.2	0.1
Rd-78	22	0.2	0.20	60.0	15.1	1.2	0.5
Re-10	1	0.0	n/a	100.0	n/a	0.0	n/a
Berea formation sandstone							
J _a	94	0.0	0.04	91.5	3.5	0.4	0.1
Waterloo formation quartzite							
D _{a-3}	10	1.1	0.90	71.0	13.9	1.2	0.5
D _{b-3}	4	0.0	0.00	90.0	13.9	0.5	0.7
D _{d-3}	16	0.8	0.70	78.8	12.3	0.9	0.5
D _{e-3}	27	0.0	0.00	94.8	4.4	0.3	0.2
D _{e-4}	14	0.0	0.00	98.6	3.0	0.1	0.2
Niagaran series dolomite							
V _{b1-10}	1	0.0	n/a	60.0	n/a	4.0	n/a
V _{b1-4}	7	0.3	0.4	31.4	13.0	0.7	0.9
V _{b2-4}	2	2.0	n/a	70.0	0.0	7.7	1.4
V _{c-10}	2	2.0	n/a	70.0	n/a	1.0	n/a
V _{c-4}	9	1.1	1.7	71.1	19.8	1.3	1.2
C _{a-10}	14	0.4	0.6	62.9	10.6	3.7	1.1
C _{b-10}	30	0.4	0.3	73.0	7.5	1.8	0.4
C _{c-10}	17	0.4	0.5	66.5	7.5	2.7	0.6
C _{d-10}	35	0.5	0.3	67.1	4.1	3.1	0.4
Columbus formation dolomitic limestone							
MC _{a-16}	1	0.0	n/a	80.0	n/a	1.0	n/a
MC _{b-16}	15	0.8	1.0	68.0	10.9	2.7	1.6
MC _{c-16}	4	0.5	1.2	55.0	28.7	2.8	1.2
MC _{d-16}	8	0.6	0.8	40.0	8.2	2.4	0.8
M _{a-9}	1	2.0	n/a	60.0	n/a	4.0	n/a
M _{a-10}	7	3.0	3.7	47.1	17.1	4.3	1.5
M _{a-13}	6	7.8	8.0	33.3	7.6	5.2	2.4
M _{a/b1-9}	3	5.0	6.9	30.0	0.0	5.7	2.9
M _{a/b1-10}	5	9.0	10.2	38.0	13.8	6.0	2.1
M _{a/b2-10}	3	3.3	6.2	33.3	8.6	4.3	3.2
M _{a/b2-13}	4	6.5	9.5	35.0	12.0	5.5	2.7
M _{b1-9}	32	3.7	1.8	62.2	9.1	1.9	0.3
M _{b1-10}	15	3.5	2.9	58.7	12.4	3.2	2.0
M _{b1-13}	18	6.4	4.7	37.8	7.2	4.7	1.2
M _{b1/b2-10}	27	3.9	1.9	48.9	9.5	2.9	0.6
M _{b1/b2-13}	4	0.5	1.2	40.0	9.8	3.0	1.4
M _{b2-9}	20	4.8	3.1	51.5	11.7	2.9	0.9
M _{b2-10}	10	1.5	1.1	58.0	15.4	3.8	1.0
M _{b2-13}	28	2.4	1.6	45.4	8.4	3.3	0.7
Columbus formation limestone							
S _{a/b-6}	41	2.5	1.2	62.7	7.6	2.0	0.5
S _{c-6}	30	1.9	0.9	70.0	9.0	1.5	0.4
S _{d-6}	51	2.4	1.1	56.7	7.5	3.0	0.4

range from 48.2 to 31.8) with an average number of cracks per stone of 2.4 (\pm 95 percent confidence range from 3.2 to 1.6). The t-test indicates the relationship between the quality ratings of these two populations is better than 99 percent, and is therefore real (i.e., there exists 1 chance in 100 of it being random). Clearly, the degree of deterioration is much greater in facies MC_{d-16}. Also interesting is that the average number of cracks per stone are essentially the same for both of these facies.

From Table 12, it can be determined that the Marblehead Quarry facies M_{b1} of the Columbus formation dolomitic limestone performed the best after 9 and 10 years of service with a change in quality of -3.5 points per year. However, the rate doubled between the 10th and 13th years to a rate of -7 points per year. Facies M_a appears to have deteriorated at a fairly constant rate of -6.7 points per year. What is especially interesting to note is that the means from the Marblehead Quarry and the means of the younger stone from the Sandusky Quarry tend to fall linearly which supports an overall Columbus formation average deterioration rate of -3.6 points per year. There are some internal variations which could be due to either normal statistical variation or, possibly, due to facies dependent weathering effects. A less linear but average increasing trend in short-term change is observed for the Columbus formation as well. The short-term change is increasing at roughly +0.43 points per year. This is the equivalent of the addition of a minor crack every 2.5 years.

Reed Quarry facies R_d of the Salem formation limestone shows a smooth trend of increasing rate of quality deterioration with age. The change in quality is -0.5 points per year the first 78 years. This rate is seven times slower than the Columbus formation. The rate of short-term change increases slightly with age, from 0 at 10 years to 0.2 at 78 years. This is roughly 0.003 points per year or the addition of a minor crack every 390 years (based on mean values).

The Niagaran series dolomite rate of change in quality varied from -13.8 points per year for the Valders Quarry average (based on 4-year stone) to 6.8 points per year for the Cedarville Quarry average (based on 10-year stone), and to 3.8 points per year for the McCook Quarry average (based on 16-year stone). Grouping these together, the second derivative (deceleration) of the quality versus age rate for the Niagaran series dolomite as a whole is approximately +0.8 points per year per year. In other words, the initial rate is -13.8 points per year. However, this slows at a rate of 0.8 points per year until the rate of quality change versus age is -3.8 points per year after 16 years. This apparent reversal of rate is in contrast to the Columbus formation that exhibits increasing rates of deterioration with age. It is possible that the Niagaran series do not form a straight-line relationship comparable to that observed in the Sandusky and Marblehead Quarries for the Columbus formation. Hence, combining the Niagaran series stones from a number of sources may be providing a correct estimate of the temporal change in rate of deterioration. Supplemental studies would be required to track the long-term trends in deterioration for the Niagaran series stones to insure the trend is real.

Waterloo formation quartzite from the Dempsey Quarry does not have a long performance record. The rate of change in quality with age is approximately -0.75 points per year based on limited data. This rate is comparable to that of the

cut stones, but it is not known how the rate of change will increase (or decrease) with time.

Quarry facies have previously been defined in the field by Rock Products Consultants (1995). Table 13 is a key to the crack associations with these 26 different quarry facies that are shown in Figures 161 through 163. The 17 different crack natures have been previously defined in Table 3.

Facies Number	Quarry Facies	Facies Number	Quarry Facies
1	Rb – Reed Quarry	14	Ca – Cedarville Quarry
2	Rc – Reed Quarry	15	Cb – Cedarville Quarry
3	Rd – Reed Quarry	16	Cc – Cedarville Quarry
4	Re – Reed Quarry	17	Cd – Cedarville Quarry
5	Ja – Johnson Quarry	18	Vb1 – Valders Quarry
6	Da – Dempsey Quarry	19	Vb2 – Valders Quarry
7	Db – Dempsey Quarry	20	Vc – Valders Quarry
8	Dd – Dempsey Quarry	21	Ma – Marblehead Quarry
9	De – Dempsey Quarry	22	Mb1 – Marblehead Quarry
10	MCa – McCook Quarry	23	Mb2 – Marblehead Quarry
11	MCb – McCook Quarry	24	Sa/b – Sandusky Quarry
12	MCC – McCook Quarry	25	Sc – Sandusky Quarry
13	MCD – McCook Quarry	26	Sd – Sandusky Quarry

Examination of Figures 161 through 163, in conjunction with the key to these figures from Table 13, will show that for facies MC_c (facies 12) the predominant known cracks are parallel to bedding (50 percent of samples) and spall or corner cracks (25 percent of samples), whereas the predominant cracks in MC_b (facies 11) are no cracks (13 percent), cracks associated with stylolites (25 percent), and cracks associated with clay seams (26 percent). Both of these facies have a large amount of cracking unassociated with any defined cause (60 percent for MC_b (facies 11) and 73 percent for MC_c (facies 12)). Given that both of these facies were extracted using the same high-energy blasting, it is apparent that facies MC_b is more prone to containing stones with no cracks, and that facies MC_c has a greater propensity to separate parallel to bedding. The reason for this disparity is that MC_b is an interreef facies which characteristically has higher energy and contains less continuous thin bedding planes than facies MC_c which is a backreef facies and is deposited in quieter water and, therefore, more prone to continuous thin bedding surfaces marked by planolites. The reason the average number of cracks between these two facies are the same is that facies MC_b contains a wider variety of cracks, including cracks associated with stylolites.

A number of other comparisons were made, and are summarized in Table 14.

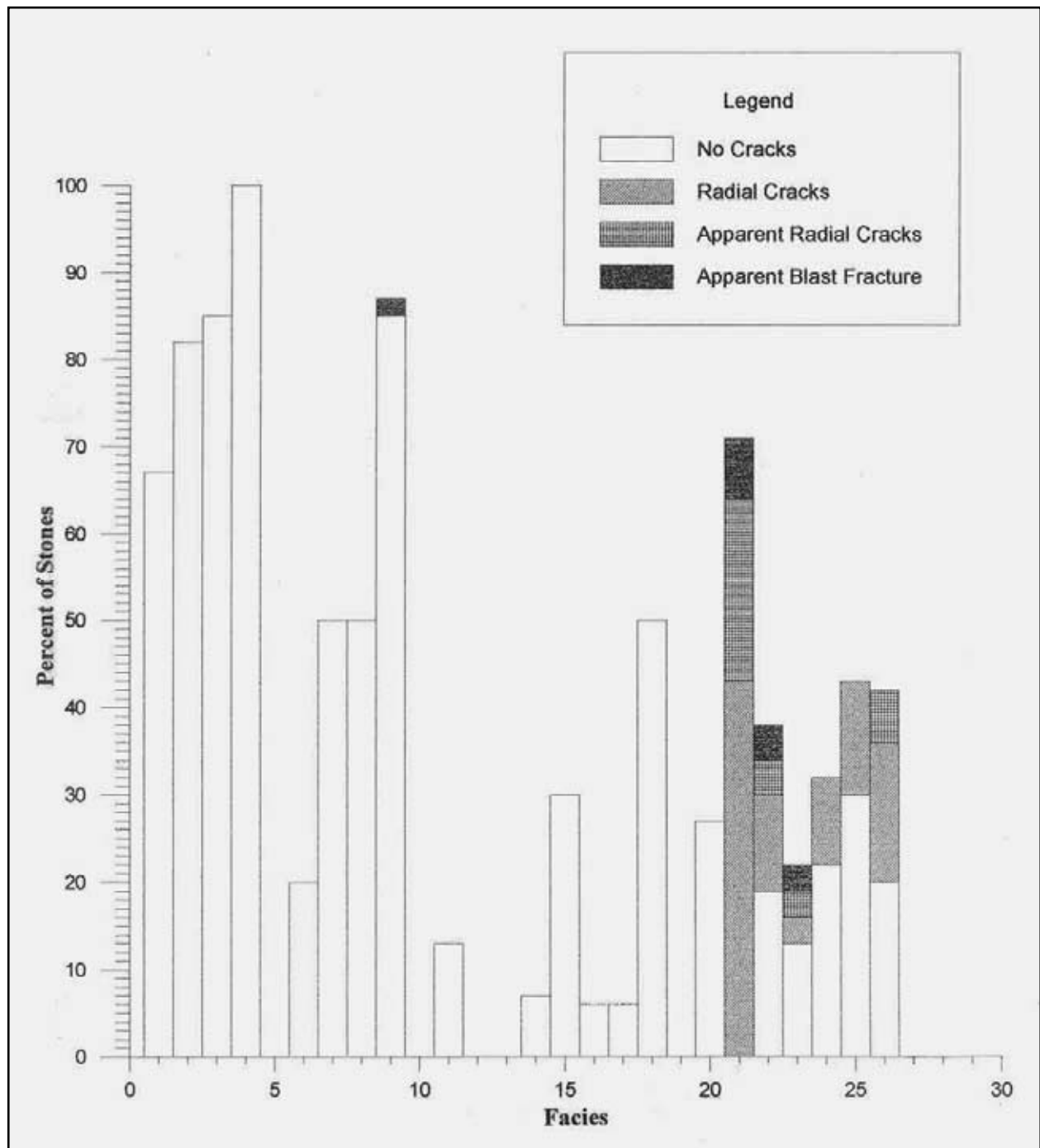


Figure 161. Crack association with quarry facies, 10 years or younger stones, for crack types 0 through 3

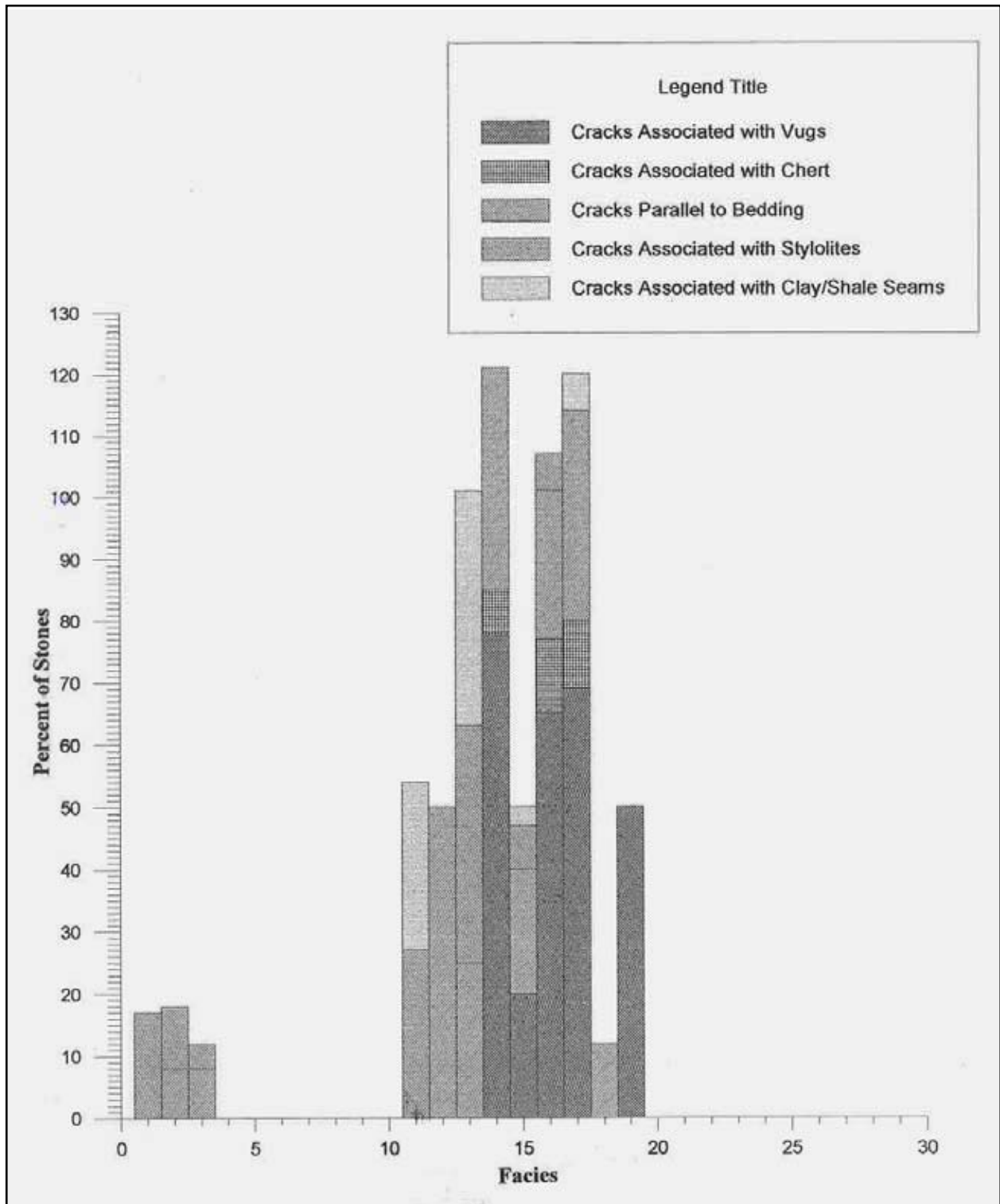


Figure 162. Crack association with quarry facies, 10 years or younger stones, for crack types 5 through 9

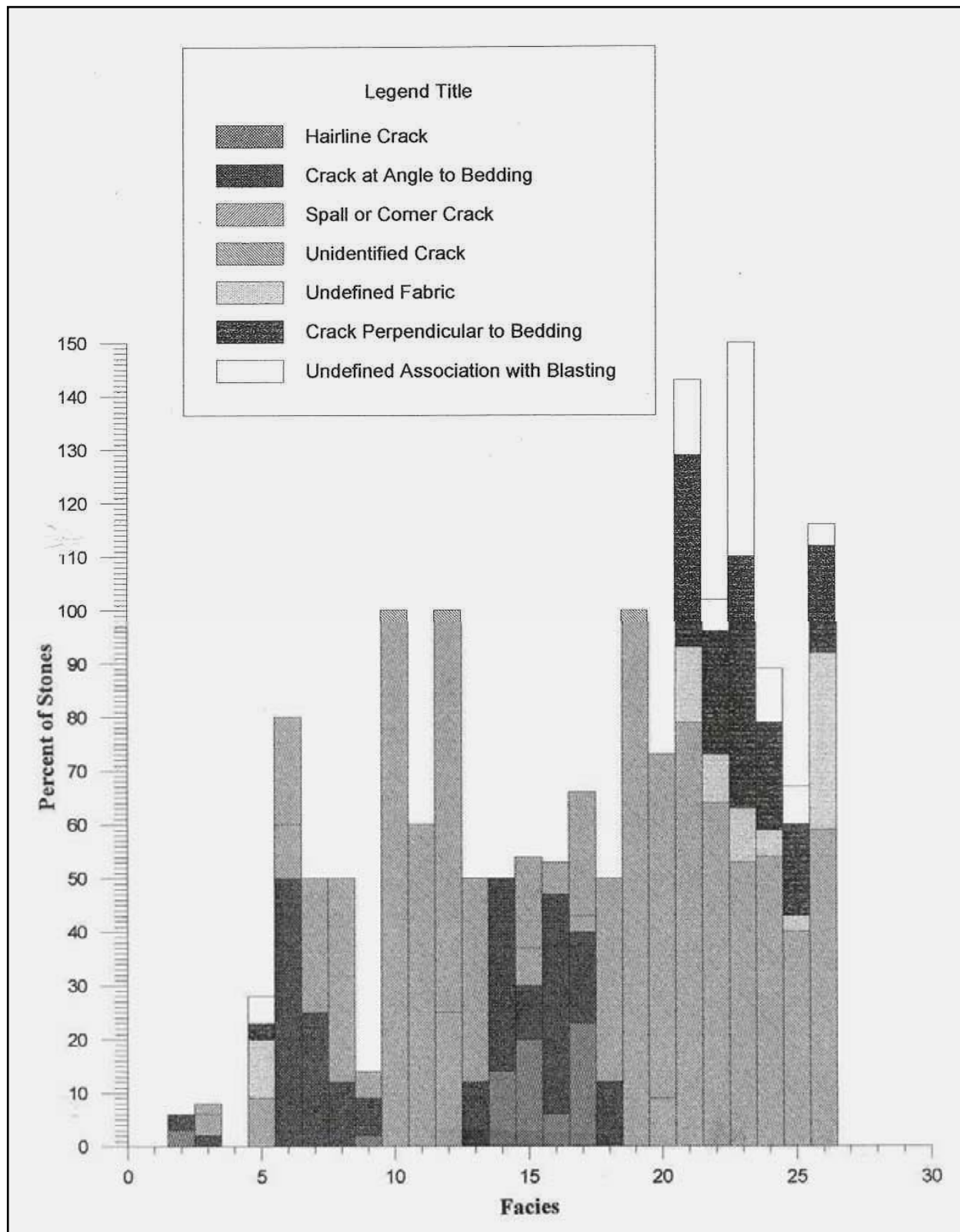


Figure 163. Crack association with quarry facies, 10 years or younger stones, for crack types 11 through 17

Facies Compared	Quality Rating	t-test Results (Percent)
MCb-16 vs. MCd-16	68.0 vs. 40.0	99.0
Da-3 vs. De-3	71.0 vs. 94.8	99.9
Sc-6 vs. Sd-6	70.5 vs. 56.7	96.5
Cb-10 vs. Cc-10	73.0 vs. 67.1	87.0
Vc-4 vs. Vb1-4	71.1 vs. 31.4	86.0
Mb1-9 vs. Mb2-9	62.2 vs. 51.5	84.0
Cb-10 vs. Cd-10	73.0 vs. 67.1	83.0
Ma-13 vs. Mb2-13	33.3 vs. 45.4	80.0
Mb1-13 vs. Mb2-13	37.8 vs. 45.4	79.0
Ma-10 vs. Mb1-10	47.1 vs. 58.7	< 79.0

As can be seen from Table 14, there were several other strong correlations between quality ratings and facies. Most notable are the Dempsey Quarry Waterloo quartzite facies D_a and D_e . These facies are banded gravel and massive quartzite respectively. The massive quartzite was performing in a superior fashion to the banded gravels. The banded gravel facies contained seams of pebbles that were absent in the massive quartzites, and were slightly more hematitic. Otherwise the compositions of the two were similar.

There is also an important contrast between the Sandusky Quarry S_c and S_d facies of the Columbus formation limestone. The S_d facies is a crinoid limestone with occasional chert, common planosites, and thin clay seams. The S_d facies was interpreted as shallow marine (euxinic type environment). The S_c facies is a low clastic content, massive, thick-bedded mudstone, and was interpreted as more open marine (outer shoal type environment). The low energy deposition and organic activity expressed in S_d results in a stone not as resistant to weathering as the more massive and clean limestone deposited in more open marine conditions.

Interpretation of the remaining Columbus formation facies is difficult. The Columbus formation Marblehead Quarry M-series stones were difficult to assign to a specific facies due to the fact that the lithology of these stones was variable within individual stones. Comparisons suggest possible relationships, but are contradictory in many cases. Overall, these stones performed in a relatively poor fashion. However, due to the variability in lithology and diagenetic features of these stones, it was difficult to draw any firm conclusions based on only facies interpretations.

Diagenesis Deterioration

General observations

Given a consistent method of extraction, gross lithology has always been recognized as a factor in stone durability. Weakly indurated (cemented) rocks such as sandstones and limestones are prone to relatively rapid deterioration. Strongly indurated rocks such as unweathered granites and quartzites are thought to generally last longer. However, not all areas of the country have the ability to

obtain granite or quartzite without incurring significant transportation costs. This study looked not only at the relative durability of gross lithologic characteristics, but also at the more subtle differences caused by depositional environments and diagenetic history. Prior to this study, there was little-to-no information on performance of breakwater stone. From a practical standpoint, unless justification can be made for incurring the greater cost of importing strongly indurated stone from greater distances or only allowing the use of cut stone, the geologist can only select stone from the most favorable lifts. Even if low-energy blasting is dictated in the stone specification, the geologist will still be responsible for accepting stone from the most favorable lift. Selection of the most favorable lift is based on geologic facies.

Influence of gross lithology

Lienhart et al. (1999) discussed the predicted service life of armor stone. Conclusions included the fact that laboratory testing for determination of true rock quality in terms of expected performance is not clear-cut, may be misleading, and requires extensive interpretation by an expert in the field of stone geology. A prediction of service life of armor stone is possible, but the process is extremely complex and cannot be determined merely through the measurement of one parameter or one characteristic such as unconfined compressive strength.

Lienhart (2003) developed a systems approach to evaluation of armor stone sources. Recommendations included a petrographic evaluation and consideration of all geologic properties including (a) specific gravity, (b) absorption, (c) adsorption, (d) unconfined strength, (e) Schmidt rebound, (f) sonic velocity, (g) point load, (h) Los Angeles abrasion resistance test (500 revolutions), (i) durability index, (j) Brazilian tensile strength (along potential plane of weakness), (k) fracture toughness, (l) accelerated weathering tests, (m) sulfate soundness, (n) and durability absorption rate. Conclusions by Lienhart (2003) included "...It is almost impossible to find one individual with experience and knowledge in all aspects of the systems approach analysis. A team of experts must be utilized, and the team must be carefully chosen to provide full coverage of all aspects of the analysis..."

The evaluated stones are placed into four general lithologic categories; (a) crystalline rock, (b) dolomite, (c) dolomitic limestone, and (d) clastic. Induration is qualitatively discussed based on the combination of unconfined compressive strengths, friability as estimated by manipulation of hand samples, and degree of suturing of grains in thin section. More sutured grain-to-grain contacts are interpreted to better transfer stresses to the individual grains, thereby mobilizing the inherent strength of the grain constituents.

Crystalline rock. Stone from the Dempsey Quarry Waterloo formation quartzite is the only crystalline rock monitored in this study. It is the most indurated of all the groups as evidenced by its relatively high unconfined compressive strengths (upwards to 2,110 kg per sq cm (30,000 lb per sq in.)) and suturing of grain-to-grain contacts in thin-section. The grain constituents are primarily quartz. Extraction of this stone is primarily influenced by natural joint planes in the rock, and by fractures generated by low-energy blasting.

Dolomite. The second lithologic type is dolomite, which includes all stone from the Niagaran series from the Valders, McCook, and Cedarville quarries. These dolomites have varying amounts of silicate impurities depending on depositional environments, but are generally pure dolomites. The Niagaran series is also well indurated where silicate impurities and vuggy porosity is absent. Evidence of the induration is high uncompressive strengths (upwards to 705 kg per sq cm (10,000 lb per sq in.)) and suturing of grain-to-grain contacts in thin-section. The grain constituents are primarily dolomite. Extraction of this stone is primarily influenced by natural bedding planes, joints, and fractures generated by blasting. The sample population includes stone from high- and low-energy blasting.

Dolomitic limestone. The third lithologic type is dolomitic limestone, which includes the Columbus formation from the Marblehead Quarry. These stones have varying amounts of silicate impurities similar to the Silurian series, but also have a varying diagenetic characteristic. The diagenetic character of the Columbus formation varied from pure limestone to pure dolomite, sometimes within a single stone. The suturing of grains is not as pronounced as in the Silurian series. The stone is moderately well indurated as evidenced by its unconfined compressive strength (upwards to 845 kg per sq cm (12,000 lb per sq in.)) and intermediate suturing of grains. The grain constituents are primarily either dolomite or calcite. The sample population includes stone extracted using either high- or low-energy blasting.

Clastic. The Bedford limestone and Berea sandstone make up the fourth lithologic type, which is clastic. Although these two stones are not the same lithology (the Bedford is limestone and the Berea is sandstone), they are included here as clastic deposits. The Berea sandstone is slightly better indurated than the Bedford limestone due to the fact that it contains silica cement. Evidence of the Berea sandstone's induration is its unconfined compressive strength (upwards to 705 kg per sq cm (10,000 lb per sq in.)), its relative friability, and its degree of suturing of grains in thin section. The Bedford limestone is a pure limestone with practically no silicilastic impurities, but was deposited as a clastic deposit made up of discrete carbonate fragments. The overall texture is clastic with carbonate cement. Bedford limestone is weakly indurated as evidenced by its slightly lower unconfined compressive strength than Berea sandstone, its friability, and its grain-to-grain contacts in thin section. Even though the unconfined compressive strength of the Bedford limestone is slightly lower than Berea sandstone, both these stones perform quite well because of the open pore structure which allows for free drainage of entrapped water during freezing. Bedford limestone contains clastic depositional features such as cross-bedding, and is graded in places. The grain constituents for these stones are calcite for the Bedford limestone, and quartz for the Berea sandstone. Both were extracted using traveling wire cutting methods.

Table 15 compares the average durability of the four lithologic categories previously discussed.

Table 15 Average Durability of Four Lithologic Categories	
Stone Type	Average Quality, percent
Crystalline	84 after 3 years
Dolomite	67 after 10 years
Dolomitic limestone	47 after 10 years
Cut clastic	94 after 10 years

Cut clastics (limestone and sandstone) are performing the best. Dolomitic limestones are deteriorating at roughly twice the rate as quartzite, and 30 percent faster than pure dolomite.

In Situ Stress Deterioration

Deterioration due to in situ stresses can be a major problem if proper cure periods are not followed. Relief of internal strain is usually observed during the first few months after a stone has been extracted. Cracks caused by this phenomenon may open enough to cause progressive failure by freeze/thaw action. A detailed study of this phenomenon was beyond the scope of this study, and would require extensive instrumentation. However, this area warrants additional study.

In a stone that has uniform physical properties such as pure dolomite with uniform composition and texture, isotropic stress relief is exhibited by relaxation perpendicular to the natural regional stress fields of the in situ rock. This is evidenced by the common occurrence of throughgoing planar cracks oriented in mutually perpendicular axis observed in stones shortly after extraction. This type of failure was observed from massive stones from the Silurian series.

Stress relief is a fairly common phenomenon that should be a concern for any deep quarry, such as the McCook Quarry, or in a quarry under active horizontal stresses such as those in Ohio. Seepage of water into a stone and subsequent frost pumping would be a problem where the in situ stress could cause strains of 0.15 mm (0.006 in.) or more.

In an anisotropic rock, the induced stress is a function of the orientation of the internal fabric of the stone. For instance, if part of the stone was composed of an argillaceous dolomite with a certain value of Young's Modulus and another part of the same stone was composed of a clean limestone with a different value of Young's Modulus, a shear force would develop along the boundary between the two lithologies. Cracking in an anisotropic stone will tend to follow the depositional or diagenetic fabric of the stone and not necessarily along mutually perpendicular planes. This type of cracking was observed in stone from Reef Talus facies and in stone from the Marblehead Quarry where dolomite was in contact with limestone.

Based on empirical evidence, stone can react quickly to the relief of stresses, or it can take months to years. The stress caused by quarry blasting releases quickly, but the release of stored stress resulting from the removal of overburden or unloading of the rock takes longer. The time required for release of unloading stress is a function of its homogeneity, compaction, and surrounding temperature conditions. Creep in crystalline rock such as quartzite, and in carbonate rocks such as dolomite or limestone is short lived. These rocks behave in a brittle fashion. More ductile rock such as argillaceous sandstone, argillaceous siltstone, or claystone may exhibit longer periods of creep and may therefore require longer cure periods. The minimum amount of time required for curing has not been well established and historically has been based on trial and error.

The Silurian (Niagaran) series dolomite from the McCook Quarry, IL, the Valders Quarry, WI, and the Cedarville Quarry, MI, exhibit planar fracturing perpendicular to bedding in the quarry shortly after excavation, but none was observed on the breakwater. Marblehead Quarry exhibited a significant amount of cracking perpendicular to bedding. Some of this may be due to homogenous stress relief, but some was obviously attributed to remnant desiccation cracks on bedding surfaces. Based on the results of this study, it is suspected that the cure periods for the Columbus formations of the Marblehead Quarry, OH, and the Sandusky Quarry, OH, were inadequate due to the large number of unknown cracks (which may be attributable to anisotropic stress relief) and cracks perpendicular to bedding, and due to the overall poor quality. Stress relief may take years.

Enhanced QC/QA Program

An enhanced Quality Control/Quality Assurance (QC/QA) program was initiated for the 1989 rehabilitation of the Cleveland Harbor east breakwater sta 107+40 to sta 108+60 to insure that no stones exhibiting blast-type fractures were placed on the breakwater. The enhanced QC/QA program was initially thought to be effective in improving the stone quality of the blasted dolomitic limestone used here. A 100 percent visual inspection of all stones were conducted at the quarry, and only stones without any significant or throughgoing cracks were accepted. Initial inspections conducted after placement showed only a small percentage of failure (less than 2 percent after one year). But the 1997 inspection showed that approximately 47 percent of the stones have failed (Table 5, Figure 142). The deterioration rate of this station is now consistent with other stations, and with the conventional QC/QA plan utilized during the 1985 rehabilitation from sta 197+50 to sta 198+75 (Figure 164)

The enhanced QC/QA program for Cleveland Harbor east breakwater sta 107+40 to sta 108+60 has 20 percent of its failed stones with greater than 10.16-cm (4-in.) displacement of the stone fragments, while the other Cleveland Harbor east breakwater stations have approximately 50 percent. This is most likely due to the shorter length of time the failed stones have had to be moved around by major storms. The majority of the failed stones at sta 107+40 to sta 108+60 are still in place, with relative movement between the pieces of less than 10.16 cm (4 in.).

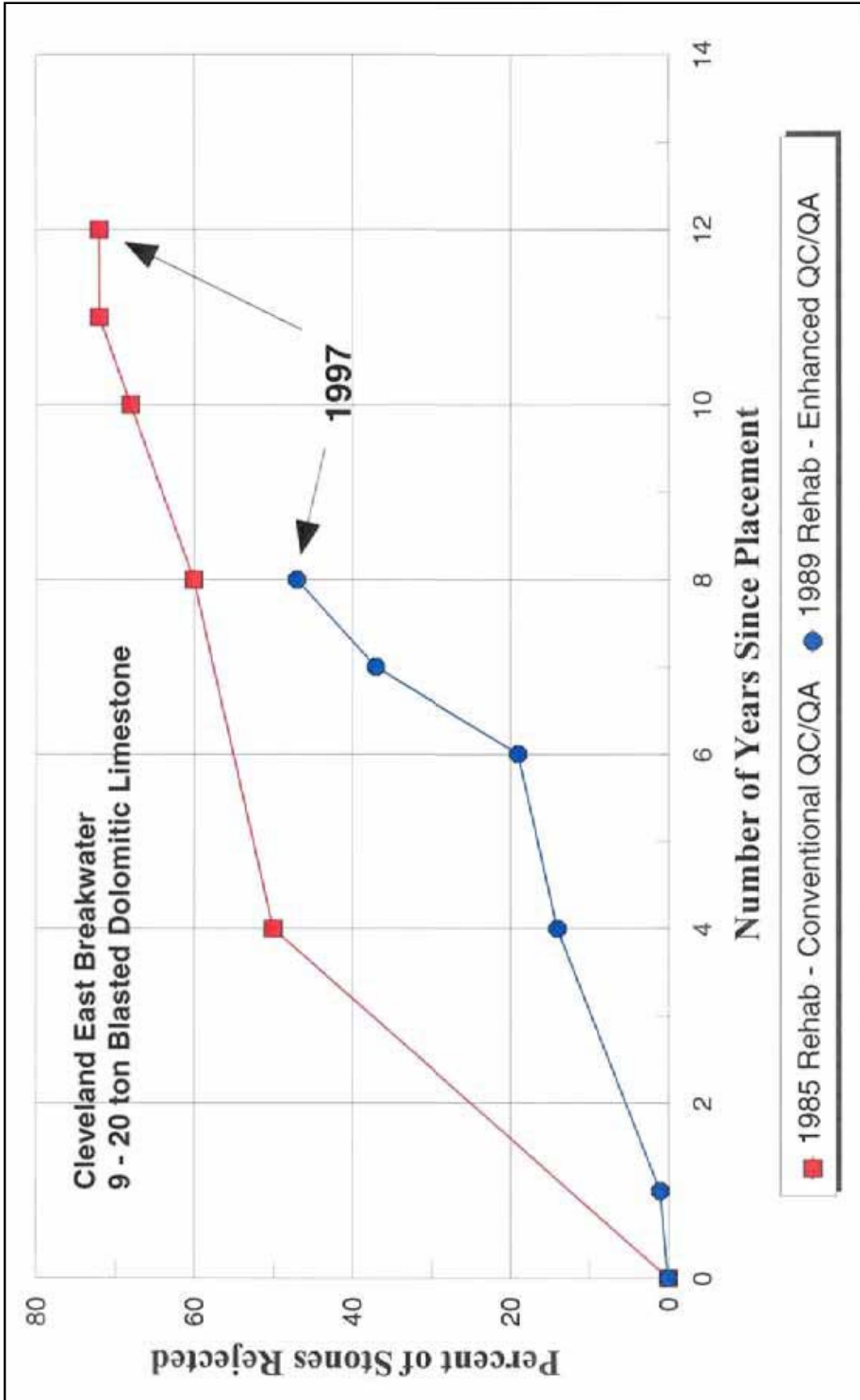


Figure 164. Conventional rehabilitation 1985 QC/QA versus enhanced rehabilitation 1989 QC/QA

The use of smaller blasted stones (2,720 to 6,350 kg (3 to 7 tons)) at sta 164+00 to sta 165+20 on the Cleveland Harbor east breakwater was initially thought as a possible method to increase the percentage of highly durable stones. The smaller size stone was thought to contain less blast-related cracks and would thus more likely avoid more inherent geologic discontinuities than would larger stones. The deterioration rate is similar to the other stations with larger blasted stones (8,165 to 18,145 kg (9 to 20 tons)). However, results from the 1997 inspection indicated that 13 stones from sta 164+00 to sta 165+20 were subsequently lost due to wave action (10.2 percent of the 127 stones, compared to a range of 1 to 3.3 percent from the other stations). The use of smaller stones did not perform as intended. The smaller stones are deteriorating at similar rates as the larger stones, and have a higher percentage of loss due wave action because to the resultant smaller size of the fragments.

6 Summary and Conclusions

Statement of Problem

Background

There are 107 coastal projects in the Great Lakes and Ohio River Division with breakwaters and/or jetties extending more than 146,304 m (480,000 lin ft) in length. For the greater part of the last century, the Great Lakes and Ohio River Division has experienced chronic and recurring problems with stone durability on these project breakwaters and jetties. Results of a Division-wide deterioration inventory by the Great Lakes and Ohio River Division in 1990 indicated significant premature deterioration of armor stone, most of which was Silurian and Devonian limestones and dolomites. Extensive maintenance and rehabilitation of existing structures is needed due to the premature deterioration, and tens of millions of dollars will be required for these repairs.

The mechanism fracturing the stone has not been positively identified. There indeed may be several contributors to susceptibility of stones to weathering and degradation. Each of several physical factors may result in fractures in the armor stone; however, and more importantly, they make it more likely that the environment present at the sites can more readily degrade the stone. So, it is a matter of conditions prior to the stone being placed at the structure (from its formation as a rock mass, through its geologic history and ultimately its being transformed from a natural rock mass, to a construction material transported and placed onsite) that determine how durable it is when faced with the stresses it is subjected to in the structure.

One hypothesis concerns quarrying techniques. Most quarries in the Great Lakes region operate primarily for the production of construction aggregate, and blasting procedures used in these quarries are designed to maximize fracture in the rock lift. These blast effects may produce stresses in the stone that, over time, create fractures and break the stone into smaller pieces that may be below design specifications. Using different quarrying techniques may reduce the blast effects but at a higher cost for the stone production.

Another mechanism that may be responsible for the observed stone degradation is the removal of overburden. In situ stresses are present in some rock units as a consequence of thousands of feet of ice overburden during the Pleistocene ice age (12,000 years before present). Removal of that ice has resulted in isostatic rebound and uplift stresses, with fracturing in some rock masses. Regional uplift

in the geologic past may also have resulted in stress in the rock fabric. When stone is blasted free, the overburden pressures of the surrounding stone are removed. In some cases, it is believed that these overburden stress releases can produce fractures that occur for some time after the rock is excavated.

Stone degradation investigations

The following investigations are essential for developing technology to reduce Great Lakes breakwater and jetty stone deterioration.

- a.* It must be determined if more durable stone types are available, or if the durability of locally produced stone could be increased even if only at a higher cost. It may be more cost-effective in terms of life-cycle costs to use the better quality stone at a higher initial construction cost than using lower quality stone with a higher maintenance cost. Answers to these questions will require information on deterioration rates for different stone types available from different quarries that use different quarrying procedures. This information can then be incorporated with the effects of more stringent QC/QA practices during construction or rehabilitation.
- b.* It may be possible to use stone of a lesser quality on portions of the structure, thus saving the best stone for the most critical and susceptible areas. Armor stone placed below the wave splash zone may deteriorate at a slower rate than armor stone placed above this zone. There may be significant differences in deterioration rates between stones exposed to wave action on the lake side versus the harbor side of a structure, and between stones above and below the splash zone. The worst degradation will be seen in this region where wet/dry and freeze/thaw cycles are at a maximum.
- c.* The length of time that stones should be stored (aged) before placement on a structure is critically important. This storage factor concerns the length of time that a stone needs to lie dormant to allow blast-induced fractures or fractures from release of tectonic stresses to become apparent. Waiting periods of 30 to 90 days are typically specified, but it is commonly believed that a longer waiting period would be beneficial. However, storage of the large amount of stone required for a breakwater or jetty is expensive, and is not practical without documentation data to prove the benefits, if any, of longer storage. Curing requirements will vary by stone type, porosity, and in situ percent water; therefore, the waiting period is not a standard number of days.

Study components

Stone deterioration on breakwaters and jetties arises from a combination of interactions pertaining to the quality of stone available, operational and handling practices at the quarry, and environmental weathering conditions after placement on the project structure. Four different and distinct components of the stone degradation investigation are essential to fully comprehend the mechanisms that give rise to chronic premature deterioration of armor stone on breakwaters and

jetties around the Great Lakes. These four investigation components include the following.

Quarry field geological observations. Seven different quarries that have historically provided material for Great Lakes breakwater and jetty construction and rehabilitation projects were investigated. These seven quarries were selected for evaluation because stone from these quarries has been used on sections of prototype structures to be monitored due to premature deterioration. The stone produced by these seven quarries included (a) Salem formation limestone from Reed Quarry, Bloomington, IN, (b) Niagaran series dolomite from Valders Quarry, Valders, WI, (c) Waterloo formation quartzite from Dempsey Quarry, Waterloo, WI, (d) Columbus formation limestone from Sandusky Quarry, Parkertown, OH, (e) Columbus formation dolomitic limestone from Marblehead Quarry, Marblehead, OH, (f) Berea formation sandstone from Johnson Quarry, Kipton, OH, and (g) Racine formation dolomite from Thornton Quarry, Thornton, IL. Field geological observations had previously been performed at an eighth quarry (McCook Quarry, McCook, IL). The McCook Quarry produces Niagaran series dolomite.

Laboratory durability testing. Laboratory durability testing of stone samples to accelerate weather exposure freeze/thaw and wet/dry effects, and to determine specific gravity and sample petrography, was performed. The laboratory durability testing samples came from the eight quarries where field geological observations had been performed, plus samples from a ninth quarry (Iron Mountain Quarry, Iron Mountain, MI). The Iron Mountain Quarry produces taconite.

Quarry sample microstructural analyses. Microstructural analyses of quarystone samples from seven different quarries to determine microscale features in the rock that affect stability, and their relations to compositional and textural variations, were conducted after laboratory durability testing. These were the same quarries for which quarry field geological observations had also been performed, except stone samples from McCook Quarry were not available for quarry microstructural analyses.

Field prototype monitoring. Field monitoring of 10 specific sections of five structures to document progressive deterioration rates among different stone types, different degrees of environmental exposure, and different levels of stone quality control, was conducted. The five structures were (a) Chicago Harbor, IL, breakwater, (b) Calumet Harbor, IL and IN, breakwater, (c) Calumet Harbor, IL, CDF revetment, (d) Burns Harbor, IN, breakwater, and (e) Cleveland Harbor, OH, east breakwater. The 10 sections of structures selected for evaluation contained deteriorated stone from the eight quarries previously discussed, plus stone from the Calumet Harbor CDF revetment that originally came from a ninth quarry, the Iron Mountain Quarry, Iron Mountain, MI. The Iron Mountain Quarry produces taconite. Also, stone from a tenth quarry (Cedarville Quarry, Cedarville, MI) was evaluated by this field prototype monitoring study because stone from this quarry has previously been placed on other stone structures around the Great Lakes. The Cedarville Quarry produces Niagaran series dolomite.

A total of six different stone types were evaluated, including (a) dolomite, (b) limestone, (c) quartzite, (d) sandstone, (e) taconite, and (f) dolomitic limestone. Ground inspections by registered professional geologists were made to catalogue, at the monitored sections, all stone fractures and offset measurements in armor stone above the high-water mark, between low water and high water on the harbor side, and between low water and high water on the lake side (annually for 3 years). Broken stones were marked to show in aerial photographs to insure repeatability, and to document progression of deterioration.

Quarry Field Geological Observations¹

Reed Quarry and Salem formation limestone

Reed Quarry, located slightly northwest of Bloomington, IN, excavates limestone from Mississippian age Salem formation. Salem formation limestone is primarily mined for architectural purposes and is relatively lithologically homogeneous, as evidenced by the small variation in lithology and physical properties throughout the area. This is one of the last wire cut or cable saw quarry operations left in the Indiana limestone region. Most of the other operations have gone to a chain saw device. Production at Reed Quarry involves wire sawing four sides of each block and then line drilling and wedging out each block. Production averages about 8 blocks per day. Each block is about 2.7 m (9 ft) high, 1.2 m (4 ft) wide, and 2.1 m (7 ft) long. At a specific gravity of 2.48, this amounts to 17,690 kg (19.5 tons) per block, and a production rate of approximately 141,520 kg (156 tons) per day. The stone is only produced during nonfreezing months.

The stone is handled with stone tongs and a crane. This is very soft rock and must be carefully handled to prevent breakage. A clamshell bucket (with either two or four leaves) will destroy or permanently damage stone cut from the soft Salem limestone. All quarried stone is set aside and cured for a minimum period of 60 days. Stone that is unevenly colored cannot be used for architectural purposes and is cast aside in muck piles. The majority of stone in the muck piles has been cured for more than 2 years. Stone from the muck piles is available for use as armor stone. Transportation is by truck only.

Valders Quarry and Niagaran series dolomite

Valders Quarry, located just north of the town of Valders, WI, excavates Niagaran series dolomite. Transportation from the stone dock is by barge. The Niagaran series is one of numerous reef complexes that formed around the fringes of the Michigan Basin and northeast of the Wisconsin arch. Several lithological units are identified, including dolomitic mudstone interpreted as a supratidal, backreef environment, and reef dolomite. The dolomitic mudstone intertongues with reef-like dolomite. Reef accumulations are more discontinuous, allocthonous, and thinner, as compared to the large pinnacle Niagaran reef structures found in Illinois.

¹ This section is extracted essentially verbatim from Rock Products Consultants (1995).

Production is through a single line of 7.6-cm- (3-in.-) diam drill holes with a burden of 0.9 to 1.2 m (3 to 4 ft) and a spacing of 0.9 m (3 ft), from a maximum bench height of approximately 21 ft (6.4 m). The blast program is designed to parallel the principal joint orientation. This blast pattern is specifically designed to minimize overbreak and maximize the production of large armor stone and architectural stone. Stone with excessive vugs or discoloration is considered unsuitable for architectural stone and is readily available for armor stone. Since the architectural stone is taken from the lowermost bench, there is a significant amount of overburden that is wasted.

Dempsey Quarry and Waterloo formation quartzite

Dempsey Quarry (now Michels Quarry), located northeast of Waterloo, WI, extracts Waterloo formation quartzite. The quarry is 97 km (60 miles) from the stone dock in Milwaukee. Stone must be trucked from the quarry to the stone dock, where it is loaded onto Lake Michigan barges for shipping.

Waterloo formation quartzite is mined from shallow inliers of Precambrian crystalline bedrock. This formation is believed to be equivalent to the late Early Proterozoic Baraboo quartzite. The Waterloo formation quartzite is a meta-quartzite composed of well-sorted coarse sand with low angle tabular cross-bedding, to poorly sorted gravel breccia. The gravels are well rounded and predominantly composed of siliciclastic materials. The quartz mica assemblage supports a greenschist facies metamorphism. The age of the rock is estimated to be 1,630 million years. The unit was mildly folded along with Precambrian basement rocks during the early Paleozoic.

Dempsey Quarry is an open-pit operation working out of two benches. The upper bench is 3.0 to 6.1 m (10 to 20 ft) in height and the lower bench is 4.6 to 9.1 m (15 to 30 ft) in height. Because the stone is a quartzite with dipping beds, the quarry must make an extra effort to produce a flat floor. Production costs are much higher than for dolomite or limestone. Drills, loaders, tires, crushers, etc. wear out at a much faster rate. Due to the lack of parting planes and dominance of separation along joint surfaces, a horizontal row of holes are necessary to maintain a level floor in the quarry.

Stone is blasted using a single row of 7.0-cm- (2.75-in.-) diam holes drilled to 7.6 m (25 ft) depth, and drilled horizontally from the quarry floor. After the blast, the rock tumbles into the quarry separating along joint surfaces and micaceous seams. Using this method, some blocks may weigh as much as 36,285 kg (40 tons) after the blast. Large stones are further broken down by diamond drilling 5.1-cm- (2-in.-) diam holes and splitting with hydraulic splitters. Finished stone is separated and stockpiled using stone tongs with special carbide teeth to facilitate gripping this very hard rock. Stockpiled stone is cured for 30 to 90 days.

Sandusky Quarry and Columbus formation limestone

Sandusky Quarry, located at Parkertown, OH, excavates Columbus formation limestone. Stone is trucked approximately 16 km (10 miles) to Lake Erie, where it is transported by barge. Within the quarry are sequences of fine-grained clastics, limestones, and dolomites. The primary breakwater unit is the limestone Marblehead Member of the Columbus formation. The Marblehead has been interpreted as a transgressive trend from intershoal to shoal to outershoal conditions. The overlying basal Delaware formation has been interpreted as a sudden submergence below wave base followed by continued transgression and deeper water sedimentation.

Sandusky Quarry primarily produces Columbus formation limestone aggregates with a production capacity of up to 1,814,370 kg (2,000 tons) per hour. Armor stone is currently taken from the west side top bench of the quarry. The spacing of blast holes as measured in the quarry face ranges from 2.1 to 2.7 m (7 to 9 ft), and the blast holes are 17 cm (6.75 in.) in diameter. The bench height is approximately 15.2 m (50 ft). As evidenced by the blasting fractures within the blast holes and the large block of the Venice Member, the blasting agent must be high energy, leading to possible overbreakage. Due to the large bench height, large diameter holes, and apparent overbreak, it would appear that aggregate production methods may be utilized. The groundwater table is thought to be 4.6 m (15 ft) below the floor of the west face.

Marblehead Quarry and Columbus formation dolomitic limestone

Marblehead Quarry, located at Marblehead, OH, excavates Columbus formation dolomitic limestone. Coastal structure armor stone from Marblehead Quarry comes from medium bedded dolomitic limestone in the basal Columbus formation of Middle Devonian age. Units of fossiliferous packstone/mudstone, a dark brown bioclastic zone, and a dolomitic burrowed limestone have been interpreted as indicative of near normal marine lagoonal depositional conditions.

Excavation is performed by open-pit quarry utilizing three benches. Only the middle bench is currently used for breakwater stone. The bench height of the middle bench is approximately 3.0 m (10 ft). Blast holes are 7.0 cm (2.75 in.) in diameter, and spacing between blast holes is 0.9 m (3 ft). Powder factors are not available.

Johnson Quarry and Berea formation sandstone

Johnson Quarry, located, north of Kipton, OH, excavates rock from the Berea formation sandstone. This rock unit is well documented in the literature as a homogeneous material well suited for experimental rock deformation studies. The Berea sandstone was deposited in a large deltaic complex that was expanding in a southwest direction as part of the Ontario paleofluvial system during Upper Devonian time. Sediment geometry includes large, linear sand bodies indicative of a constructive bird's foot-type delta similar to the Mississippi delta. It is reported that the Johnson Quarry comprises several fault-bound blocks that

formed thick growth fault deposits of the Berea sandstone. The complex contains shale units (Bedford shale) that have generated natural gas in some locations. The Berea sandstone forms economically viable hydrocarbon reservoirs that produced 222,600 kL (1.4 million barrels) of oil between 1980 and 1986.

The quarry has been worked for over 100 years. The quarry is filled with water and with previously sawn blocks of stone available. Production has been by wire saw. Blasting is currently being tried on this sandstone.

Thornton Quarry and Racine formation dolomite

Thornton Quarry, located in Thornton, IL, is situated in a monadnock of resistant Silurian (Niagaran) series dolomitized reef (the Thornton Reef) that rimmed the Illinois and Michigan Basins. This is an old quarry, having been opened in 1887.

Thornton reef complex is probably the best exposed and most widely known Silurian (Niagaran) series dolomite reef in the world. It has significant economic importance as the largest source of high quality aggregate in the Chicago metropolitan area. The reef is one of numerous exposures of Silurian reefs that developed in mid-to-late Silurian time on a broad platform surrounding shallow seas in the Great Lakes/Upper Mississippi River Valley area.

Thornton Quarry operation has grown over the years into a complex, open-pit operation consisting of four pits divided by roadways but interconnected by tunnels. The four pits are termed the north, the south, the middle, and the north-west quarries. Each quarry consists of two benches, the uppermost bench being approximately 50 m (165 ft) high and the middle bench being about 33 m (110 ft) high. The current operation is in a newly developed lower bench, approximately 24 m (80 ft) high in the middle quarry.

The south face of the middle bench would be the source of any large stone purchased from this quarry. The reef flank deposit is massive enough to produce large-size stone but, because bench height is so high, there is very little likelihood that a fracture-free stone could be produced. The bench height would have to be reduced to no more than 9 m (30 ft) and the blasting methods would have to be modified. Considering that the current production of aggregate at this quarry is 8,165 million kg (9 million tons) per year, there is no incentive for the quarry operators to go through such a change in production methodology in order to produce 9 to 18 million kg (10 to 20 thousand tons) of armor stone.

Another problem with this bench is the considerable lateral variation in stone quality because of the rapidly changing facies from reef flank to proximal fore-reef where large, poorly cemented, reef talus blocks up to 15 m (50 ft) across constantly appear. Also present are extensive glauconitic zones and seams. Toward the west end of the south middle bench the quality of the rock decreases significantly as blocks of reef talus become more frequent and the thin interreef beds appear.

McCook Quarry and Niagaran series dolomite

McCook Quarry, located near McCook, IL, excavates Niagaran series dolomite. Samples for durability testing and quarry description were taken from a previous quarry investigation. Stones from the McCook Quarry that had been placed on prototype breakwater structures were evaluated for deterioration by the field prototype monitoring phase of this MCNP study.

McCook Quarry is located on Silurian (Niagaran) dolomite bedrock high where there is little glacial overburden. The quarry has been in operation for approximately 70 years, and is a primary source of aggregate for the Chicago region. The Niagaran series formations exposed in the quarry consist of the Racine, the Sugar Run, and the Joliet formations. The Alexandrian is also exposed in the lowermost part of the quarry, but since the primary production is from the Niagaran, this discussion will not focus on the Alexandrian. The 60 m (200 ft) of exposed Niagaran is a shoaling upward sequence of dolomites that were deposited in a shallow marine environment. There is a pronounced discontinuity at the top of the Alexandrian.

Stone is mined for construction aggregate or as feed for the on-site lime plant. Blasting is from large diameter holes with 24-m- (80-ft-) high benches. The blasting is designed for high fragmentation. Large blocks of stone are set aside to sell as armor stone. There also was previously a riprap plant in the quarry that has been decommissioned.

Laboratory Durability Testing¹

Seventeen stone test blocks were subjected to accelerated environmental weathering freeze/thaw and wet/dry conditions in the Ohio River Division Laboratory as one part of this MCNP study. (Not all 17 test blocks were subjected to both freeze/thaw (FT) and wet/dry (WD) testing cycles.) The 17 test blocks were obtained from seven different quarries that have historically provided material for Great Lakes breakwater and jetty construction and rehabilitation. All samples were evaluated according to nationally accepted scientific testing standards.

Reed Quarry test block durability results

Test Block R-1-FT is sound, with no visible fracturing; however, the stylolitic seam can be deleterious to the soundness. The stylolite did part during freeze/thaw testing, and a 41 percent loss was the result. The sample is fairly tough, fairly hard, and very porous. The freeze/thaw percent loss was 41.8 percent, due to parting of the stylolitic seam. The specific gravity was 2.43. Absorption was 3.80, and adsorption was 0.11, resulting in an adsorption/absorption ratio of 0.03.

¹ This section was written by Kenneth E. Henn, III, former geologist, U.S. Army Corps of Engineers, Ohio River Division Laboratory, Cincinnati, OH; presently, geologist, U.S. Army Engineer District, Louisville.

Valders Quarry test block durability results

Test Block V-1-FT is dense, tough, and hard. The freeze/thaw percent loss was 0.28 percent, due to surficial spalling. The specific gravity was 2.78. Absorption was 1.00, and adsorption was 0.08, resulting in an adsorption/absorption ratio of 0.08.

Test Block V-2-FT is fairly dense, tough, and hard. The freeze/thaw percent loss was 0.25 percent, due to surficial spalling. The specific gravity was 2.76. Absorption was 1.04, and adsorption was 0.05, resulting in an adsorption/absorption ratio of 0.05.

Dempsey Quarry test block durability results

Test Block D-1-FT is tough, dense, and hard. The freeze/thaw percent loss was 0.83 percent, due to spalling of thin edges. The specific gravity was 2.69. Absorption was 0.08, and adsorption was 0.01, resulting in an adsorption/absorption ratio of 0.12.

Test Block D-3-FT is tough, dense, and hard. The freeze/thaw percent loss was 0.25 percent, due to spalling of thin edges. The specific gravity was 2.68. Absorption was 0.10, and adsorption was 0.01, resulting in an adsorption/absorption ratio of 0.10.

Sandusky Quarry test block durability results

Test Block S-1-FT/WD is dense, hard, and fairly tough, although the sample is prone to parting due to the high content of argillaceous laminations. The freeze/thaw percent loss was 4.10 percent, due to surficial spalling and parting of argillaceous laminations. The wet/dry percent loss was 0.17 percent, due to surficial spalling. The specific gravity was 2.63. Absorption was 2.87, and adsorption was 0.20, resulting in an adsorption/absorption ratio of 0.07.

Test Block S-2-FT is dense, hard, and fairly tough, although the sample is prone to parting, due to the high content of argillaceous laminations. The freeze/thaw percent loss was 0.51 percent, due to surficial spalling (23.60 percent loss was attained during sawing). The specific gravity was 2.55. Absorption was 3.27, and adsorption was 0.07, resulting in an adsorption/absorption ratio of 0.02.

Marblehead Quarry test block durability results

Test Block M-1-FT is hard, tough, and fairly porous. The freeze/thaw percent loss was 0.31 percent, due to surficial spalling. The specific gravity was 2.58. Absorption was 3.21, and adsorption was 0.05, resulting in an adsorption/absorption ratio of 0.02.

Test Block M-2-WD is hard, tough, and fairly porous. The wet/dry percent loss was 0.25 percent, due to surficial spalling. (48.5 percent loss was attained

during sawing.) The specific gravity was 2.63. Absorption was 2.11, and adsorption was 0.06, resulting in an adsorption/absorption ratio of 0.03.

Test Block M-3-FT/WD is hard, tough, and fairly porous. The freeze/thaw percent loss was 0.12 percent, due to surficial spalling. The wet/dry percent loss was 0.52 percent, due to surficial spalling. (50.0 percent loss was attained during sawing.) The specific gravity was 2.52. Absorption was 4.46, and adsorption was 0.06, resulting in an adsorption/absorption ratio of 0.01.

Johnson Quarry test block durability results

Test Block J-1-WD is porous, fairly hard, and fairly tough. The wet/dry percent loss was 0.17 percent, due to surficial spalling and disaggregation of surficial grains. The specific gravity was 2.23. Absorption was 8.86, and adsorption was 0.07, resulting in an adsorption/absorption ratio of 0.01.

Test Block J-2 was the pretest (prior to freeze/thaw exposure) equivalent of Test Block J-2-FT that was subjected to freeze/thaw testing only. The test block is porous, fairly hard, and fairly tough. The freeze/thaw percent loss was 0.56 percent, due to surficial spalling and disaggregation of surficial grains. The specific gravity was 2.22. Absorption was 7.36, and adsorption was 0.18, resulting in an adsorption/absorption ratio of 0.02.

Thornton Quarry test block durability results

Test Block MTC-1-FT/WD is fairly dense, tough, and hard. The freeze/thaw percent loss was 0.37 percent, due to surficial spalling. The wet/dry percent loss was 0.28 percent, due to surficial spalling. The specific gravity was 2.70. Absorption was 1.56, and adsorption was 0.21, resulting in an adsorption/absorption ratio of 0.13.

Test Block MTC-2-FT is fairly dense, tough, and hard. The freeze/thaw percent loss was 0.11 percent, due to minor surficial spalling. The specific gravity was 2.73. Absorption was 0.67, and adsorption was 0.25, resulting in an adsorption/absorption ratio of 0.37.

Test Block MTC-3-FT/WD is fairly dense, tough, and hard, but highly fractured. The freeze/thaw percent loss was 0.38 percent, due to surficial spalling. The wet/dry percent loss was 0.51 percent, due to surficial spalling. The specific gravity was 2.69. Absorption was 0.82, and adsorption was 0.07, resulting in an adsorption/absorption ratio of 0.09.

Test Block MTC-4-FT/WD is fairly porous, tough, and hard. The freeze/thaw percent loss was 1.41 percent, due to small surficial fracture partings. The wet/dry percent loss was 0.26 percent, due to surficial spalling. The specific gravity was 2.70. Absorption was 0.97, and adsorption was 0.06, resulting in an adsorption/absorption ratio of 0.0.

Test Block MTC-5-FT/WD is fairly dense, fairly tough, and hard. The freeze/thaw percent loss was 36.52 percent, due to open fracturing of bedding planes and of stylolitic seams. The wet/dry percent loss was 0.78 percent, due to surficial spalling. (53.2 percent loss was attained during sawing.) The specific gravity was 2.67. Absorption was 1.05, and adsorption was 0.18, resulting in an adsorption/absorption ratio of 0.17.

Conclusions

The number of freeze/thaw cycles a stone in the Cleveland and Chicago areas experiences each year can be much greater than the 30 to 50 cycles conducted during these accelerated weathering tests. Therefore, results drawn from these lab tests may not be sufficient to accurately predict the performance under the harsh effects of the Great Lakes.

Quarry Sample Microstructural Analyses¹

Reed Quarry and Salem formation limestone

The dominant features that affect failure in the Reed Quarry samples are clearly the stylolite seams. The stylolites are oriented subparallel to bedding; thus, any blocks used in breakwater construction would be better oriented with the bedding horizontal rather than vertical to avoid axial splitting. Of all the carbonate rocks examined in this study, the Reed samples have by far the most continuous and the highest amplitude stylolites. Although the process of pressure solution can help to cement the rock, the relatively high proportion of clay material left in the pressure solution seams can make the stylolites vulnerable to surface weathering and relatively weak.

Regions away from stylolite seams appear to be very stable. Once a block has separated along a stylolite seam it may be relatively stable within a breakwater construction. Other features such as micro-cracks and grain shape fabric appear to be relatively insignificant compared to the potential impact of any stylolite seam. Neither cementation nor weathering away from the stylolite seams appear to influence the location of weaknesses within the rock.

Valders Quarry and Niagaran series dolomite

The two Valders test blocks are markedly different in their textural characteristics (primarily due to presence or absence of vugs) although both are pervasively dolomitized. Relict sedimentary layers and some fossils, such as corals, can still be observed in both test blocks but predolomite cements cannot be distinguished. Both samples preserve evidence for two phases of dolomitization with subtle changes in the dolomite composition. Authigenic feldspar is the most abundant phase after dolomite and grew after dolomitization. Fractures examined from Test Block V-I-FT appear to be stable and cause minimal damage in the

¹ This section is extracted essentially verbatim from Agar (1998).

surrounding rock except towards the edge of the specimen. Silty horizons in Test Block V-2-FT have locally deflected fractures, but the fracture characteristics are otherwise similar to those of the Test Block V-I-FT samples.

Even though Test Block V-2-FT appeared much more unstable during sampling, the microstructures do not indicate extensive internal damage. All the fractures are fresh with unaltered surfaces, indicating that they are recent. Minor stylolite seams and local domains of crystallographic preferred orientation represent minor anisotropies in the samples but are unlikely to represent major sources of weakness.

Dempsey Quarry and Waterloo formation quartzite

The Dempsey quartzite fabric is dominated by muscovite seams that form an anastomosing spaced cleavage, and that are locally schistosity. Pressure solution along these cleavage planes has locally modified quartz grain shapes and redistributed chemical elements during metamorphism. Greenschist facies metamorphism has generated a mosaic texture within quartz with tight grain boundaries. Stress release in quartz grains surrounding fractures that have opened along the muscovite seams contributes to grain scale instabilities that promote disaggregation. A secondary anisotropy is controlled by changes in grain size but this does not appear to localize significant weaknesses in the samples used in this study. Quartz crystallographic preferred orientation is localized and is unlikely to generate planes of weakness. The samples appear chemically stable except where open fracture surfaces coated with muscovite have been partly illitized.

Sandusky Quarry and Columbus formation limestone

The Sandusky samples are compositionally and texturally heterogeneous. There is considerable evidence from microstructures that compositional boundaries within the samples are regions that can promote fracturing because of the mismatch of elastic properties between calcite and dolomite. Stylolite seams appear to have low cohesion, falling apart during sampling. However, there is minimal fracture damage around this type of parting. Grain boundaries around discrete open fractures are prone to opening and promote disaggregation. Local anisotropies are generated by clustering of stylolite seams parallel to bedding with some preferred alignment of bioclasts. A fissility develops along the edge of some samples, controlled by a combination of open fractures that may be generated through stress release, stylolite seams and veins. Porosity is spatially variable, changing with compositional variations.

Marblehead Quarry and Columbus formation dolomitic limestone

The Marblehead samples are characterized by incomplete dolomitization that may play an important role in weakening blocks. The calcite-rich matrix appears to be less mechanically stable than the dolomite-rich matrix, but more extensive observations, testing, and studies would be needed to test this hypothesis. The uneven distribution of porosity resulting from different fluid compositions

permeating the rock, and localized pressure solution may also influence the location of fractures. There do not appear to be any substantial differences in the fracture behavior of the wet/dry test samples to those of the freeze/thaw test samples. Nor does there appear to be any major chemical influence on the fracturing beyond that of the basic modal composition. The fractures in these samples represent some of the more complex fracture arrays examined in this study, with ambiguous cross-cutting relationships and numerous intersecting and splay fractures. There were, however, no indications of slip along the fractures.

Johnson Quarry and Berea formation sandstone

The mechanical stability of samples from Test Block J-1-WD is clearly impacted by the presence of zones of sulfate cement and organic matter. Fractures tend to localize at irregularities on block margins, assisted by the presence of micas and/or sulfate cement parallel to bedding. The fractures appear relatively stable and do not cause significant damage in the surrounding material. There is no evidence for shear displacement along fractures nor is there any evidence of chemical alteration along open fracture surfaces. Most fractures are interpreted to be of recent origin except where the sulfate cement seals some transgranular fractures. Locally intense, intragranular fracturing has occurred probably through stress release. Pressure solution has generated a weak-to-moderate anisotropy in all the samples. The secondary cement associated with this process may help to stabilize the quarystone. On the other hand, some of the straight pressure solved boundaries have tended to pull apart. Qualitative thin section observations suggest that the freeze/thaw samples from Test Block J-2-FT were more prone to grain scale plucking during sample preparation than the untested Sample J-2.

Thornton Quarry and Racine formation dolomite

The primary source of weakness in the Thornton Quarry samples are sub-perpendicular arrays of fractures that are interpreted primarily as unloading cracks formed by stress release, before, during, or after quarrying. All the fractures are inferred to be of recent origin due to the lack of evidence for any chemical modification of the fracture surfaces by surface weathering or groundwater circulation. The propagation paths of these cracks often terminate in vugs that may serve to dampen the elastic response of the rock. Aligned trails of vugs, however, may promote fracture propagation. The open fracture walls exhibit varying degrees of stability, but they are common sites for grain-scale disaggregation and grain plucking.

Both samples have a homogeneous chemical composition resulting from the completeness of the dolomitization process. Remaining lithological contrasts are found at stylolite boundaries and provide a further source of weak anisotropy in the samples. The stylolite abundance and continuity does not appear to represent a major control on the breakup of the samples, but they may be more abundant in other parts of the quarry.

McCook Quarry and Niagaran series dolomite

Samples from the McCook Quarry were unavailable for microstructural analysis.

Conclusions

The following summary conclusions were deduced by Agar (1998) from the microstructural analyses pertaining to the mechanical stability of samples from seven quarries studied in this evaluation.

- a.* Several different types of discontinuities and potential sources of weaknesses were recognized in the samples. These may act alone or together to promote disaggregation in breakwater stones, but their role cannot be fully evaluated without a better understanding of how breakup proceeds in the breakwater setting. From the microstructural analyses in these samples, the freeze/thaw and wet/dry testing did not provide conclusive evidence for the direct effects of these processes on rock stability. There was no real discernible difference between pre- and post-test open fractures except where the path of the fractures was controlled by a preexisting weakness.
- b.* The majority of open fractures in quarry samples appear to be recent. There is little or no weathering on their surfaces. Fractures may have been generated as a direct result of quarrying or transport methods, but in several cases stress release was probably a major contributing factor. A compilation of in situ stress data for the quarries and the relationship of principal stress orientations to existing discontinuities would help to understand the overall importance of stress release in the rock stability.
- c.* Although there are several open fractures in each sample set, most of the fracture walls appear relatively stable (but not all). Therefore, their existence may not necessarily be the primary cause of breakup. It is important to establish how fractures propagate through the samples by documenting the behavior of the quarriestones over several years.
- d.* Where planar, geological discontinuities exist, such as stylolites, they are obvious planes of weakness, and in several cases these parted during sample cutting. The overall impact of these features on rock stability may be influenced by the orientations of the blocks in the breakwater. Some loading configurations may keep these structures stable.
- e.* Grain scale preferred orientations do exist in some samples (e.g., Dempsey Quarry samples). Where platy minerals form part or all of the fabric, there exist significant weaknesses. Sample disintegration does not appear to be significantly impacted by crystallographic preferred orientations in quartz or calcite.
- f.* In Johnson Quarry the distinct sulfate vein filling and cement phases contribute to weakening the rock. Compositional variations in the Sandusky and Marblehead Quarry samples also control the locations of some fractures.

- g.* If such a study has not already been undertaken, it would be valuable to examine the loading patterns of blocks in breakwaters and evaluate whether there are consistent points of failure in this pattern that could be avoided by some different arrangement.
- h.* Analytical and computer modeling of the breakup of the blocks could place limits on the stresses that blocks could sustain in particular stacking configurations and would help to understand the overall breakup process.
- i.* A summary of the rock mechanics literature for each of these quarries should be made. Experimental deformation studies would be useful to test the role of vugs in the limestone and dolomite lithologies in localizing fractures.
- j.* This study was limited in scope to direct observations of microstructures with limited background information on the outcrop setting of the test blocks. It is crucial that any further studies construct detailed sketches of the geological features surrounding sampled areas and that all samples are oriented. Information was lost in this study because the samples were not oriented at the outcrop, and features could not be related to mesoscale structures. This information could modify the interpretations.
- k.* A key objective of future studies should be linking the microstructures observed in the test blocks to microstructures and mesostructures, both in quarries and in existing breakwaters where the stones are already in use.
- l.* A detailed structural analysis of the quarries, including a structure map, is needed to establish the primary structural trends (joints, faults, flexures) and their relation to stratigraphy, in situ stress, and unloading histories.

Field Prototype Monitoring¹

Stone quality classification was ascertained for each individual stone on each of the 10 breakwater structure sections monitored for three years (1995, 1996, and 1997). A total of 864 stones were evaluated in this field prototype monitoring study.

Causes of deterioration

There are three significant external factors that contribute to stone deterioration; (a) weathering environment (freeze/thaw cycles, and wet/dry cycles), (b) method of extraction (cutting (wire, cable, chain saw), low-energy blasting; and high-energy blasting), and (c) placement techniques (cracks caused by mishandling which become progressively worse as the stone ages).

There are also three significant internal factors characterizing stone that affect the rate of deterioration; (a) depositional facies (environment of deposition

¹ This section was written by David W. Marcus, former District geologist, U.S. Army Engineer District, Buffalo.

directly influencing rock fabric and composition), (b) diagenesis (degree of interparticle suturing, cementation, and dolomitization; and extent of vugular porosity that affects overall induration and susceptibility to freeze/thaw action), and (c) in situ stress (nonisotropic relief of internal strain; and removal of confining stress causing isotropic relief of internal strain, causing cracks to develop after the stone is removed from the rock formation).

Weathering environment deterioration

Normal weathering is a relatively slow process that can reveal what may appear to be an apparently clean, massive, fresh stone to actually be a thin, bedded, weak, and seamy stone within only a few years. Weathering can also change the mineralogical makeup of the rock. Through oxidation and dissolution, weathering alters the coloration of the rock, produces authigenic clay and iron oxides, and dissolves the mineral cements that hold a stone together.

Method of extraction deterioration

Based on the MCNP data, the Columbus formation at the Cleveland Harbor east breakwater is significantly more prone to blast fracturing than any of the formations monitored at the Chicago Harbor breakwater although the lithology, blasting methods, and presumably the physical properties of the stones are similar. The largest difference in lithology is the fact that the Columbus formation is not as pure a dolomite as is the Silurian series and may therefore contain diagenetic inhomogeneities that are more prone to blast damage.

The most striking difference in durability is the difference between cut stone and blasted stone. Cut stone average quality varies from 92 to 94 after 31 and 10 years of use, respectively. This is in stark contrast to the average quality that ranges from a low of 48 for 9 years and a high of 67 for 10-year-old, high-energy extracted stone. It is clear from these results that the cut sedimentary stone is performing better than the blasted sedimentary stone, regardless of the blasting method employed.

These numbers also indicate that the average economic life for a cut stone is well over 40 years, whereas a blasted stone (regardless of blasting method) may last a minimum of 4 years or a maximum of 16 years without requiring some sort of rehabilitation. It is intuitive to believe that high energy blasting produces stone with a shorter economic life than stone extracted using low energy blasting. However, another surprising result of this MCNP study is that the blasting methods do not appear to significantly alter the rate at which the stone deteriorates. Hence, the only conclusion that can safely be reached from these data is that cut stone will tend to have fewer problems associated with it than blasted stone of the same type and general character. More research is required to determine exactly when rehabilitation is necessary.

Six different stone geologies (dolomite, dolomitic limestone, limestone, quartzite, sandstone, and taconite) were evaluated. Without regard to the method of extraction (cut versus blasted), it appears that five of the six stone types have

an average percent of stones rejected per year of 2.0 or less. Only the dolomitic limestone has a larger average percent of stones rejected per year of 6.1 stones rejected per year. However, these data must be further analyzed with regard to the method of extraction (cut versus blasted).

For limestone, where cut versus blasted methods of extraction are directly comparable within the same geology, the MCNP data show that stone extracted by cut methods are performing better than stones extracted by blasted methods. For dolomite, the differences are not quite as readily apparent. It appears the blasting method of extraction may actually be superior to the cutting method; however, the cut dolomite stones had been on the structure only 3 years when the 1997 survey was conducted (see editor's note, p. 149). Later studies may indicate a reversal of this trend. Only blasted dolomitic limestone was evaluated during the MCNP study; no cut dolomitic limestone was available for comparative analyses. Blasted dolomitic limestone appears to be comparable to blasted limestone, strictly from a consideration of the percent stones rejected per year.

Placement technique deterioration

Placement methods are a critical part of construction. Brittle stones such as the Silurian series and Columbus formation are prone to damage when dropped from a height of over 0.30 m (1 ft). Hard stones such as these and the Waterloo quartzite are difficult to grab with clamshell type buckets. In no case should clamshell or leaf-type buckets be used for this reason. Only stone grabs can place stone without dropping or damaging it. Damage caused by improper handling is commonly evidenced by scrap marks on the sides of the in-place stones.

Impact breakage at edges or corners and subsequent spalling is also indicative of poor or improper handling. The stones placed on the Cleveland Harbor breakwater did not exhibit cracking attributed to corner edge or spalling. However, there were a large number of unknown cracks that might have occurred from handling. The worst reach for spalling was found at Burns Harbor breakwater (Big Burn section), which exhibited several corner-edge and spalling type cracking. But as a percentage of all the stones placed, it is a small number (less than 8 percent). A small number of spalls were also recorded in the Silurian series from the Valders Quarry, WI, and from the McCook Quarry, IL, but these were an insignificant amount.

Depositional facies deterioration

Each of the stones from the selected sections of the monitored prototype breakwaters was closely inspected, and a geologic description was prepared using standard methods. Based on the lithologic characteristics, the stones were assigned to their respective facies.

The durability of the various facies were measured by three parameters; (a) change factor, (b) quality rating, and (c) number of cracks. The data for each stone include more than one crack in a number of cases. For these stones, the total number of cracks was summed for that stone. All the durability parameters

were taken from the final condition of the stone, as measured at the end of the field investigations. A number of facies identified in the quarries were not represented on the breakwaters, as should be expected. In particular, a number of facies described in the Dempsey Quarry were not represented in stones on the breakwater. The numbers of samples representing each facies varied from one (Dempsey Quarry facies e) to as many as 94 (Johnson Quarry facies a).

In addition to dividing the stones by facies, the stones were also divided into groups within each facies based on the age of the stone (here age means how long the stone has been on the breakwater). All facies and ages were generally well represented, with a few exceptions. A number of facies and ages are under-represented in the sample groups, with only one or two stones representing the group. These small sample groups were not considered in the analysis as they were considered statistically unreliable. Also, some of the stones could not be neatly categorized into one facies because they exhibited characteristics from more than one facies. This was especially true of the stones from the Marblehead Quarry, which had a large number of stones that exhibited a combination of two facies, and from the Sandusky Quarry where the investigator could not differentiate between facies a and b (intershoal and shoal facies). For the Sandusky Quarry, facies a and b were grouped together as one group. In these cases the stones were categorized as representing a combination of facies in one stone.

Diagenesis deterioration

Given a consistent method of extraction, gross lithology has always been recognized as a factor in stone durability. Weakly indurated (cemented) rocks such as sandstones and limestones are prone to relatively rapid deterioration. Strongly indurated rocks such as unweathered granites and quartzites are thought to generally last longer. However, not all areas of the country have the ability to obtain granite or quartzite without incurring significant transportation costs. This study looked not only at the relative durability of gross lithologic characteristics, but also at the more subtle differences caused by depositional environments and diagenetic history. From a practical standpoint, unless justification can be made for incurring the greater cost of importing strongly indurated stone from greater distances or only allowing the use of cut stone, the geologist can only select stone from the most favorable lifts. Even if low-energy blasting is dictated in the stone specification, the geologist will still be responsible for accepting stone from the most favorable lift. Selection of the most favorable lift is based on geologic facies.

The evaluated stones are broken into four general lithologic categories; (a) crystalline rock, (b) dolomite, (c) dolomitic limestone, and (d) clastic. Cut clastics (limestone and sandstone) are performing the best. Dolomitic limestones are deteriorating at roughly twice the rate as quartzite, and 30 percent faster than pure dolomite.

In situ stress deterioration

Deterioration due to in situ stresses can be a major problem if proper cure periods are not followed. Relief of internal strain is usually observed during the first few months after a stone has been extracted. Cracks caused by this phenomenon may open enough to cause progressive failure by freeze/thaw action.

In a stone that has uniform physical properties such as pure dolomite with uniform composition and texture, isotropic stress relief is exhibited by relaxation perpendicular to the natural regional stress fields of the in situ rock. This is evidenced by the common occurrence of throughgoing planar cracks oriented in mutually perpendicular axis observed in stones shortly after extraction. This type of failure was observed from massive stones from the Silurian series.

Stress relief is a fairly common phenomenon that should be a concern for any deep quarry, such as the McCook Quarry, or in a quarry under active horizontal stresses such as those in Ohio. Seepage of water into a stone and subsequent frost pumping would be a problem where the in situ stress could cause strains of 0.15 cm (0.006 in.) or more.

The Silurian (Niagaran) series dolomite from the McCook Quarry, IL, the Valdars Quarry, WI, and the Cedarville Quarry, MI, exhibit planar fracturing perpendicular to bedding in the quarry shortly after excavation, but none was observed on the breakwater. Marblehead Quarry exhibited a significant amount of cracking perpendicular to bedding. Some of this may be due to homogenous stress relief, but some was obviously attributed to remnant desiccation cracks on bedding surfaces. Based on the results of this study, it is suspected that the cure periods for the Columbus formations of the Marblehead Quarry, OH, and the Sandusky Quarry, OH, were inadequate due to the large number of unknown cracks (which may be attributable to anisotropic stress relief) and cracks perpendicular to bedding, and due to the overall poor quality. Stress relief may take years.

Enhanced Quality Control/Quality Assurance (QC/QA) program

Even though QC/QA was routinely utilized in all projects, an enhanced QC/QA program was initiated for the 1989 rehabilitation of the Cleveland Harbor east breakwater sta 107+40 to sta 108+60 to ensure that no stones exhibiting blast-type fractures were placed on the breakwater. The enhanced QC/QA program was initially thought to be effective in improving the stone quality of the blasted dolomitic limestone used here. A 100 percent visual inspection of all stones were conducted at the quarry, and only stones without any significant or throughgoing cracks were accepted. Initial inspections conducted after placement showed only a small percentage of failure (less than 2 percent after 1 year). However, the 1997 inspection showed that approximately 47 percent of the stones have failed. The deterioration rate of this station is now consistent with other stations, and with the conventional QC/QA plan utilized during the 1985 rehabilitation from sta 197+50 to sta 198+75.

The use of smaller blasted 2,700- to 6,350-kg (3- to 7-ton) stones at sta 164+00 to sta 165+20 on the Cleveland Harbor east breakwater was initially thought as a possible method to increase the percentage of highly durable stones. The smaller size stone was thought to contain less blast-related cracks and would thus more likely avoid more inherent geologic discontinuities than would larger stones. The deterioration rate is similar to the other stations with larger blasted 8,165- to 18,145-kg (9- to 20-ton) stones. However, results from the 1997 inspection indicated that 13 stones from sta 164+00 to sta 165+20 were subsequently lost due to wave action (10.2 percent of the 127 stones, compared to a range of 1 to 3.3 percent from the other stations). The use of smaller stones did not perform as intended. The smaller stones are deteriorating at similar rates as the larger stones, and have a higher percentage of loss due wave action because of the resultant smaller size of the fragments.

Conclusions¹

There are essentially three methods presently available for extracting stone from quarries; (a) cutting, (b) low-energy blasting, and (c) high-energy blasting. Based on this MCNP study, there exists a trend that most of the blasted (low-energy and high-energy) sedimentary stones have a range of 40 to 72 percent failure within 15 years after placement. The cut sedimentary stones are showing much greater durability, with a trend of 5 to 52 percent failure after 30 to 78 years of placement. The cut sandstone in the Cleveland Harbor east breakwater is performing best, with only 5 percent failure after 30 years.

Factors impacting armor stone durability

Causes for stone deterioration include external factors (a) weathering environment, (b) method of extraction, and (c) placement techniques, and internal factors (a) depositional facies, (b) diagenesis, and (c) in situ stress. It is difficult to consider these factors independently in the field, as they act together. It is evident that the internal factors have significant effect on how readily the stone is impacted by the external factors. Of all the factors identified in this evaluation, weathering environment is the least controllable. The effects of freezing/thawing and wetting/drying are major role-players in armor stone durability. And the internal factors that determine hardness, strength, primary porosity, and rock fabric or texture, in turn, play a role in how susceptible the stone may be to weathering environment, stresses induced by the method of extraction, or placement techniques (i.e., the internal factors determine how significant the external factors are in the overall scheme of things). Effective QC/QA is critically important for armor stone durability.

The nonweather-related factors can be dealt with in various ways. Whether by specification of actual methods or enforcement of quality requirements, it is possible to control or influence the method of extraction and the placement techniques used in this type of construction. It is also possible to select sources

¹ This section was written by Joseph A. Kissane, geotechnical engineer/District geologist, U.S. Army Engineer District, Chicago.

having the best physical properties, thus reflecting the most desirable facies and having been formed by the diagenetic processes that result in the most durable stone with the least detrimental in situ stresses.

Curing time of freshly quarried stone

Once a block of stone is quarried, it is released from a state of equilibrium within the rock formation and placed in another environment within which it must reach stability prior to being used in construction. Stone freshly quarried and placed in a structure without proper seasoning may develop cracks months or years later. Ideally, blocks taken from a quarry should be permitted to cure through an entire season before acceptance. This will allow all seasonally exacerbated weaknesses to run their course so stone can be culled that does not hold up well enough. Practicality prevents this ideal from occurring. It would require large areas of real estate to store the stone in an easily inspected arrangement, and it would force quarry operators to take on huge risks pertaining to acceptability of stone without a guarantee of purchase.

The need for curing is based on two conditions that coexist and are inter-related in freshly quarried stone; (a) the existence of connate water within the freshly quarried stone, and (b) stress release or unloading. The time required for seasoning by air-drying of freshly quarried armor stone blocks will vary depending on porosity and pore size distribution, and on the degree of saturation. Recommendations of the Indiana Limestone Institute of America (undated) range from 60 to 90 days for stone quarried above the water table to at least 6 months for stone quarried from below the water table. For seasoning related to stress release and unloading, the time required will depend on the intensity of the stress field and on the rate of unloading, or to some combination of both. The duration will also depend on the degree of anisotropy of the geologic formation under consideration.

The matter of stone curing time is more important in some rock sources than in others. Some rock has the tendency to respond to in situ stresses immediately upon excavation, whereas other rock may take months or even years to show the effects of this factor. Generalizations as to which rock type takes how long are best not made when it comes to contracts and specifications, as the exceptions to generalizations will be cited and used as ammunition in claims. Project and contract schedules do not always make long curing times practical, and typical curing time requirements range from 60 to 90 days, with the understanding that these durations will allow most of the major stress-relief features to make themselves visible. However, smaller-scale fracturing often will not be visible in this time frame. Still, it is a matter of practicability that contract lengths are not able to include longer curing times, and quarries will not typically maintain large inventories of large stone in anticipation of upcoming contracts.

Curing time is also related to season. Winter quarrying is problematic, as water in the rock mass will behave differently to blasting energy as ice than it will as a liquid. Small fractures may grow during freeze-thaw cycles and the impact of this may only be known if a sufficient curing cycle is used. If a quarry is uncertain that they can maintain the quality of their production during winter

months, they will often scale back or shut down operations, rather than have multiple cycles of start-up and shut down when weather oscillates above and below freezing. Curing times are typically based on continuous days above freezing, and a period of 24 hr below freezing may restart the curing period. A reasonable approximation of required seasoning time, therefore, appears to be approximately 90 days minimum. Some stone may require more time.

Laid-up cut stone versus rubble-mound structures

Modern placement methods and project schedules now exceed the production capacities of cut sandstone and limestone quarries. As the costs associated with cutting, extracting, and placing cut stone blocks increased, subsequent construction and repair has consisted of rubble-mound structures of harder Silurian dolomite quarried by drill and blast methods. Compressively loaded cut stone has been augmented by or replaced with larger, irregularly shaped, supposedly interlocking, blasted angular stone. Stone with the integrity to bear significant compressive loads is indispensable. Rectilinear units are usually preferable to irregular, angular masonry units in a structure. Any placement that subjects stone to forces other than compression has an adverse effect. Stone fractured from movement (gentle rocking and rolling due to wave action) may be a significantly unrecognized and unreported problem.

The projects in this MCNP study include both purely rubble-mound and repaired laid-up structures. Stone in rubble-mound structures are not placed in any particular orientation, and the stability of the structures is based on the interlocking of the stones. Laid-up structures are constructed by stacking regularly shaped (typically rectangular) stones. The selection of design is often based (at least in part) on the availability of materials. Cut stone blocks are essential to the construction of laid-up structures, whereas rubble mounds can be constructed of either cut or blasted materials. The Great Lakes area is fortunate to have both cut stone and blasted rock quarries; however, the market fluctuations and availability of cut stone can be problematic, and cut stone cost may be as much as twice that of blasted stone.

Laid-up structures may deteriorate with age as much as rubble-mound structures (under certain conditions), and repairs can be more costly. (While some laid-up structures are over a century old, and are performing satisfactorily with only minor rehabilitation, others have deteriorated greatly. Not all laid-up structures have a timber crib core; some have a stone core.) Rubble mounds stabilize with time as they settle, and are not as prone to having their components sliding against each other because of the interlocking effect of the irregularly shaped pieces. Around the Great Lakes over the last 30 years, wooden timber cribs and wooden pilings used in association with many laid-up structures have rotted when exposed to air during low lake levels, causing the structures to collapse. Without the timber crib support, restoration of those laid-up structures is largely infeasible, and replacement or repair with rubble-mound arrangements has become necessary. Settlement of rubble mounds tends to be noncatastrophic, whereas settlement of laid-up structures either results in alignment problems or the formation of cavities in the structure between blocks or between blocks and the underlying foundation.

Burns Harbor breakwater is an example of a pure rubble-mound structure, constructed of variously shaped armor stone placed over underlying stone of progressively smaller size. Although the original stone included cut rectangular blocks of limestone, the blocks were not necessarily arranged in rows or placed to result in a flat-faced structure. The resulting structure partially reflects incoming waves, while significant part of the wave energy is dispersed randomly by the irregular surfaces, and part of the energy will be transmitted through the porous structure. Massive crystalline limestone or dolomite and crystalline metamorphic or igneous rocks are more often quarried by blasting and used in rubble-mound structures; however, cut limestone blocks were used in the early construction of Burns Harbor breakwater. These types of structures can be expeditiously constructed, requiring only that the stones be placed to maximize stability by interlocking with each other and the design is fairly uncomplicated; however, the interlocking may result in relatively high point loads occurring where blocks lock together. Where stresses exceed the rock strength, points of irregularly shaped stones may break off. Where settlement or damage occurs, it is relatively localized, and can be treated with supplemental placement of stone in the affected areas. The surfaces of these types of structures are not easily surveyed with a high degree of precision beyond an average grade line because of irregular shapes, and they are not easily navigated on foot, for the same reasons.

Cleveland Harbor east breakwater and Chicago Harbor breakwater are examples of structures that were originally constructed as laid-up structures with cut stone blocks. These types of structures rely more on the flat surface-to-surface friction to retain their stability compared to the interlocking or keyed-in relationship of the blocks in a rubble-mound structure, so the stresses on individual blocks are less than in a rubble mound. The relative smoothness of the blocks may make them more prone to sliding, and therefore be less stable in the long-term. Some laid-up structures are mortared or grouted together to address the issue of sliding, and this results in additional costs. The costs associated with cutting stone increase with hardness, so stone that is more readily cut tends to be relatively softer. Sandstone and oolitic limestone (limestone made up of cemented ooliths--spherical particles approximately sand-sized) are more common materials used in cut stone applications. Where settlement occurs, it is more likely to cause voids, as large parts of the structure hold shape because of the building-block nature of the stones. Repairs are more problematic because larger areas must be refitted to retain the overall alignment. Repair of damaged portions of these structures is often done with rubble mound construction in the interests of economy (availability of materials and economy of labor), and the resulting appearance is obviously contrasting. Construction and restorative maintenance of laid-up structures requires labor-intensive placement, and sizing is critical in achieving a tight block-to-block fit. These structures tend to be reflective of wave energy in comparison to rubble mound structures. Laid-up structures are easily surveyed and navigated on foot because of relatively uniform surfaces.

Service life of armor stone

Lienhart et al. (1999) discussed the predicted service life of armor stone. They believe present techniques of laboratory testing for determination of true rock quality in terms of expected performance are not clear-cut, may be

misleading, and requires extensive interpretation by an expert in the field of stone geology. Much of the testing performed on armor stone is based on protocols used to evaluate concrete aggregate and subgrade stone materials. These small-scale tests are clearly not appropriate for large armor stone evaluation. Enhanced laboratory techniques for testing and evaluation of armor stone should be developed and calibrated by long-term monitoring studies (at least 5 years duration). A prediction of service life of armor stone is exceedingly uncertain as the process is extremely complex. Service life cannot be determined merely through the measurement of one parameter or characteristic such as unconfined compressive strength.

It is clear that stone durability is a function of the rock type, the extraction methods used, the transportation methods, and the care in placement. These factors can be addressed independently both in the laboratory and hypothetically, but are not independent in the real world. The statement that granite is better than limestone for armor stone may be generally true, all other things being equal; however, such a statement can be used out of context to imply that whenever both are available, granite is preferable. This is not necessarily true. If a granite source is mined in a manner that makes it unsuitable or it contains weathered zones, it may be less acceptable than limestone. Likewise, if limestone sources are closer in a given locale, and costs are serious considerations for the construction of a project, the statement can be made that limestone is more economical as a material, and that same statement taken out of context may be false elsewhere. There are even disadvantages associated with rock types that are extremely hard, like metaquartzite. This material is so hard that it is more brittle than granite, limestone, or dolomite, and may be more prone to breakage during handling. It is also so hard that it wears out the steel buckets and teeth on loading equipment at a much higher rate than limestone or dolomite.

Design of armor stone structures

According to the *Coastal Engineering Manual* (2003), a rubble-mound structure is composed of random-shaped stones protected with a cover layer of selected armor units of either quarystone or specially shaped concrete units. An individual armor stone should be heavy enough to withstand the wave forces to which it will be subjected over its design life. The recommended design wave height (H_D) for a rubble-mound structure was considered by Hudson (1974) and the *Shore Protection Manual* (1977) to be the significant wave height (H_{33}) in front of the breakwater (where H_{33} is the average height of the largest 33 percent of the waves in the record at the project site). A later edition of the *Shore Protection Manual* (1984), and the *Coastal Engineering Manual*, recommends H_{10} as the design wave height, thus introducing a considerable safety factor over the 1977 recommendation. Due to the severe unique winter ice conditions around the Great Lakes, the Buffalo District uses an even more conservative H_{01} as the design wave height for armor stone (Chader 2001). Damage from waves higher than the design wave height is progressive, but the displacement of several individual armor units will not necessarily result in the complete loss of protection.

The weight (W) of an individual armor stone in the cover layer is directly proportional to the design wave height (H_D) and to the unit weight of the stone (ω_r). W is inversely proportional to the structure side slope (θ), specific gravity of the armor unit (S_r) relative to the water, and a stability coefficient (K_D). The stability coefficient (K_D) varies primarily with the shape of the armor units, roughness of the armor unit surface, sharpness of edges, and degree of interlocking obtained in placement of the individual armor stones. K_D is a comprehensive dimensionless stability coefficient that accounts for all variables other than structure slope, wave height, and the specific gravity of water at the site, and has been determined by extensive physical model wave/structure interaction stability tests over many years at ERDC/WES.

A rubble-mound breakwater or jetty cross section is determined by site-specific factors such as water depth, tide range, and wave height. When design dimensions of the structure permit the cover armor layer to be the recommended two quarystones in thickness, the stones comprising the cover layer can range from about $0.75 W$ to about $1.25 W$, with about 50 percent of the individual stones weighing more than W (*Coastal Engineering Manual* 2003). Again, because of the severe unique winter ice conditions around the Great Lakes, the Buffalo District adheres to even more conservative guidelines than recommended by the *Coastal Engineering Manual*. The Buffalo District allows the armor stone size to vary from about $0.9 W$ to about $2.0 W$. This provides the quarries slightly more leeway which translates into a slightly lower cost and an even more stable structure.

When structure elevations and grade lines are taken into consideration, the armor stone unit should not be of such a size as to extend an appreciable distance beyond the average level of the structure surfaces. Hence, design of a rubble-mound project requires consideration of the rock density, or the unit weight of the armor stone, ω_r . For example, it might be determined that an individual armor unit should have a weight for stability of $W = 13,605 \text{ kg}$ (30,000 lb). If Salem formation limestone with a specific gravity of $S_r = 2.34$ is used, the resulting volume would be approximately 5.8 cu m (205 cu ft). If Waterloo formation quartzite with a specific gravity of $S_r = 2.65$ is used, the resulting volume would be approximately 5.1 cu m (181 cu ft). Depending on the shape of these two stones, the space available might require the denser quartzite rather than the lighter oolitic limestone. At this point, availability of various stones and transportation costs enter design optimization considerations.

Stone source selection

Lienhart (2003) developed a systems approach to evaluation of armor stone sources. Recommendations included a petrographic evaluation and consideration of all geologic properties including (a) specific gravity, (b) absorption, (c) adsorption, (d) unconfined strength, (e) Schmidt rebound, (f) sonic velocity, (g) point load, (h) Los Angeles abrasion resistance test (500 revolutions), (i) durability index, (j) Brazilian tensile strength (along potential plane of weakness), (k) fracture toughness, (l) accelerated weathering tests, (m) sulfate soundness, (n) and durability absorption rate. Lienhart (2003) stated "...It is almost impossible to find one individual with experience and knowledge in all

aspects of the systems approach analysis. A team of experts must be utilized, and the team must be carefully chosen to provide full coverage of all aspects of the analysis...”

Internal factors are largely functions of natural processes well beyond direct control as they acted in the geologic past. The ultimate means of indirect control of most internal factors related to stone quality is through the process of source selection. Contract specifications for stone can be written to influence the source and type of stone, within limitations. In the past, specifications included lists of preapproved sources for such materials. This designation was found to be problematic, as it implied that the preapproved sources always provided acceptable material, and it transferred liability for the quality of the material to the agency rather than the contractor or his supplier. This made it difficult to reject unsatisfactory stone that might come from such sources. Acceptability during one contract with one size gradation and set of selection criteria did not always translate into the ability to produce acceptable stone for subsequent projects with potentially different needs.

An evolution of this preapproval approach has been to include listings in specifications of known sources that have been evaluated in some fashion in the past, and that have shown the potential to produce the appropriate quality and quantity of stone for such projects. Wording describing such lists must reflect that they are not guarantees of suitability, nor do they imply the sources' intent or desire to be available for the contract in question. Careful caveats are essential in such listing. It is also necessary to allow alternative sources, as it is not feasible for the contracting agency to list all potential sources, or have knowledge of their existence. Specifications should be written to include allowing alternative sources, provided the contractors verify their suitability, submit samples for laboratory testing, and coordinate appropriate inspections at the alternative source with the agency for its ultimate evaluation. It is best not to permit additional time for such evaluation, as this can prolong contract duration beyond the requirements of the project schedule. Also, if a contractor submits an alternative source that does not prove to be adequate or meet the specific criteria of the project, the contractor should be required to make a subsequent selection from the list of known sources as a means of preventing the process from delaying the project, even though there may be no time extensions granted.

Design of projects for the required project life (e.g., 50 years) may make it necessary to restrict the armor stone used in a contract to certain proven-durable rock types or, conversely, to exclude rock types proven to be less durable than the demands of the project environment. For example, in anticipation of Burns Harbor breakwater rehabilitation, the Chicago District prepared Memorandum for Record (MFR) (“Selection of rock type for large armor stone in shoreline construction and repair near or above lake elevation,” 13 February 2003) (Appendix A). The summary of that MFR states “The solicitation for Burns Harbor north breakwater repair work to be performed over a 3-year period will include a stipulation that the stone material source for armor stone shall not be limestone or dolomite. This decision is based on the need for material that has proven itself to be exceptionally durable in above-water construction in hostile physical elements such as those at Burns Harbor. Limestone and dolomite are being excluded from consideration for technical and economic reasons.

Limestone and dolomite quarries have shown greater variability in quality compared to the allowable materials, and the record indicates dolomite and limestone quality and durability is less likely to meet the project lifespan requirements for this project. This investigation has indicated proven availability of reasonably competitive sources of the allowable types of materials within the region, and the recognition that the use of limestone or dolomite would require a greater and more costly level of QA/QC, follow-up monitoring, and maintenance and repair over the lifetime of the project...”

It is necessary to evaluate such a restriction or inclusion in a document that justifies this design decision. Such a limitation might otherwise be seen by contractors or quarry operators as an arbitrary restriction on their ability to compete in the industry. Geography plays a role as well, as the transportation costs are usually the determining factor in the total cost of the stone at the site. Projects located within close proximity to marginal quality stone may have a difficult time justifying the additional cost of using stone from greater distances and a cost-benefit evaluation may be necessary. Unfortunately, politics may also play in the matter, as local stone sources that may be less durable are possibly within the same political constituency that provided the motivation for the projects approval and funding.

In the final source selection, it is still essential that an appropriately experienced geologist be involved in approval. Unlike many construction materials such as concrete or steel, stone is a natural material, and as such includes natural sometimes randomly occurring variability. It is virtually impossible to select a source based on laboratory test results and maintain a high degree of confidence in the stone’s consistency or whether the test results are representative of the overall character of the rock mass without first-hand inspection of the source. Because of the inherent nature of rock to vary within formation, from quarry lift to lift, or even within a quarry ledge, it is also necessary to have a high degree of confidence in the personnel making stone selection at the quarry after the source is approved. In the past, the onsite stone selection was often performed or overseen on a frequent basis by the contract representative. Now it is more often a contractor or subcontractor that performs selection, subject to final approval of the Contracting Officer’s Representative.

Performance-based specifications

There has been a trend in construction contracts toward allowing contractors to utilize their expertise and knowledge to determine the best and most appropriate methods to accomplish various aspects of the work, including excavation. Rather than prescriptively directing means and methods, construction contracts now tend to be more end-result oriented (i.e., performance-based). Only in exceptional cases is it acceptable to include specification of such details as blast-hole spacing, depth, velocity, delay time, and type of explosives used in quarrying. Rather, protocol dictates that contracts specify the end result such as the size, shape, and quality of the resulting stone. The exceptions to this are where rehabilitation and repairs are made that must conform to similar existing materials, or where local sponsors impose a preference (that may result in

additional costs that they must bear.) Examples include repairs to structures initially constructed of regularly sized or shaped cut stone blocks.

The same emphasis on performance-based specifications applies to transportation, handling and placement. These matters, although they have a potential impact of stone durability, are typically left to the contractors' choice. Project and quarry location may dictate the most economic transportation methods, at least in the immediate vicinity of the quarry and project. The size of stone may also dictate transportation method, in cases where large stone approaches the load limits of trucks, roads, and bridges. Other logistical considerations may also determine whether placement from onshore or offshore is appropriate, including such things as urban traffic patterns and project space constraints. The size of armor stone can also determine the most appropriate method of placement, particularly because some stone is so large that the equipment available to handle it is limited. But these considerations are seldom included in specifications, as they are determined to be "means and methods" left to the contractors' expertise.

Stone placement drop height

In spite of the tendency not to interfere with contractors' means and methods, it is considered appropriate to limit the permissible drop height in placement. This is a key element of assuring armor stone durability and controlling impacts on the underlying materials. This is appropriate in terms of protecting both the armor stone and the foundation or underlying bedding. It is important also since the effects of uncontrolled dropping of such large stone cannot be easily verified, especially underwater. The results of excessive dropping heights is often hidden from view and, even when placement is above water, the resulting fractures may occur out of sight or may not be evident until the stone is subjected to a season of weathering. Specifications often limit the free-fall from 0.61 to 1.52 m (2 to 5 ft) vertical, often depending upon the size of the stone since the energy of impact is a function of both the velocity and the mass of the stone (i.e., momentum.). For this type of construction, free-fall can be defined as the uncontrolled or unrestrained dropping, including unrestrained sliding down a surface. Regardless, it is essential that the contractor submit a detailed description of his equipment, means, and methods in detail in a work plan, and that the construction representatives monitor placement as well as quality of material as the project proceeds.

Use of lesser quality stone underwater

The effects of freezing/thawing and wetting/drying are significant in armor stone durability. Efforts to utilize stone of possibly lesser durability below the waterline in the interest of economy have met with variable success. The major issues that work against this approach are variable water level in some instances (e.g., the Great Lakes), and the practicality of mixing stone on barges used for transportation. Although quality criteria can conceivably be less restrictive for stone placed below water, the quality cannot be greatly lessened or the stone will not last even in that less-hostile environment. Lesser-quality stone, if used, would probably include shale, clay, or bedding planes that could be problems. If this

lesser-quality stone placed below better-quality stone deteriorated, then the better-quality stone would collapse into the voids.

It is also problematic to have stone that is acceptable for below-water placement separate from that for above-water placement, even when each are visibly marked. The difference in overall rock character is often not obvious to the contractor's personnel. If the shift's work requires that more than the above-water stone be on-hand and there appears to be plenty of below-water stone, there may be a temptation to use the material on-hand, regardless. It is unlikely that contractors will offer below-water stone at a cheaper rate than above-water stone if the gradation and source are the same, since the work required to excavate, inspect, transport, and place the stone is essentially the same. There also is a reluctance by the Contracting Officer to pay the same price for lesser-quality stone as better-quality stone. Thus, there is no real economic benefit in relaxing stone quality criteria for below-water stone.

Stone bedding plane orientation

Previous analysis of stone durability in these structures indicates sedimentary rock types perform best when they are placed with bedding in the horizontal direction, and recommendations to that effect appear in the literature. Sedimentary rock layers are deposited and lithified in a horizontal orientation, typically with the greatest principal stresses oriented vertically (the cumulative overburden forces of overlying rock through the period of rock formation). It is reasonable to assume that once quarried, the rock will continue to be at its most stable state with respect to the elements when it is oriented with the bedding planes horizontal. Although the relative durability may be improved by such a stipulation, the reality of construction is that it is not practicable in rubble mounds because the orientation of individual stones is fairly random to begin with. Preferential orientation would have to be marked on each stone and then placement would have to be carefully monitored. Bedding is not always obvious in massive or thick-bedded sedimentary rock once it is blasted, and the level of inspection necessary from the quarry to placement in the structure would be increased drastically by such a requirement. Inspection and handling are already more intense for cut stone, and marking the bedding orientation at the quarry would not be much of an additional step in the production of cut stone; however, requiring that stone be placed with bedding in the horizontal would still add to the inspection needed for cut stone used in laid-up structures.

Photographic documentation of stone showing deterioration in instances of stone in place with bedding not in the horizontal may be cited as proof of the advantages of horizontal orientation. However, it is not certain that these examples are merely conspicuous because the bedding itself is more conspicuous, a condition that is usually indicative of bedding planes that are inherently weaker to begin with. Rock with less apparent bedding, or massive rock, may be oriented with the bedding vertical but, because the bedding planes are not so conspicuous, these examples may not have been considered in evaluations of bedding plane orientation.

Crystalline metamorphic and igneous rock types (granite and quartzite in particular) are not as prone to exhibiting the same type or level of anisotropy with respect to strength, because of crystalline intergrowth and the overall strength of these rock types. Exceptions certainly exist, and the presence of even small amounts of clay, mica minerals, schistose, or phyllitic zones (zones of preferentially friable foliated mineral alignments) in these rock types can result in zones of weakness or susceptibility to weathering.

Because it is likely to pose such major difficulties in placement, it is not usually practical to specify orientation of stones in a structure, particularly a rubble mound. It is, therefore, more appropriate to select or specify stone that is relatively isotropic and free of prominent bedding planes or weak zones preferentially susceptible to weathering, especially when these contain significant amounts of clay. The emphasis should be on source selection and onsite quality control, as these areas represent the points in the process where scrutiny is most readily applied, rather than after the material has been transported great distances and placed at large effort in a breakwater.

Quality versus cost

Determining the relationship between short-term and long-term cost is not simple by any means. The long-term costs of using a less expensive material source is not as easily calculated as the initial savings. Data are being generated every year that prove the need for improved design and materials in navigational structures, and every year thousands of tons of stone are placed as part of O&M throughout the Corps.

There is a real “pay now or pay later” relationship in projects involving large stone. Stone is a natural resource that is nonrenewable within the time frame of civil works projects’ lifetime. And as urban areas sprawl, the demands on real estate and the perception of quarries as less than aesthetic features for residential neighborhoods may also have an impact on material availability. More durable and higher quality stone generally has greater costs associated with it at the time of construction, with the exceptions of projects located close to granite, quartzite or similar deposits. The initial costs of using more expensive materials in construction of a project must be weighed against the projected costs of routine maintenance and major repairs that may be necessary within the project life. The maintenance and repair costs are something that a district may consider in its O&M budget; however, local sponsors of projects the Corps builds may not have the same resources to cope with these costs. And there is always uncertainty as to the availability of O&M funds within the Corps as well. So the design of some structures may be skewed toward an acceptable level of O&M costs that might be different depending upon who is responsible for the project in operation and what the expectations are of O&M budgets.

Quality Control and Quality Assurance (QC/QA)

There has been a major trend in the past 25-30 years in public civil works to shift the responsibility of the quality of construction from the agencies

overseeing the work to the contractors performing the work. The immediate result has been the reduction of government QA staff and time spent overseeing things such as quality of stone used, parts of the quarry from where stone will be obtained, and care used in its extraction, transportation, and placement. Contractors have been tasked by the changing nature of contract specifications with increasing their diligence and thus, adding emphasis to these issues. Some contractors and quarry operators have adjusted to this new business environment while others have not. It is unlikely that the trend toward transferring responsibility to the contractors will be reversed in the near future. It is, therefore, important that the government QA personnel be increasingly diligent, and the specifications should be written to provide them with the authority necessary to enforce quality criteria. It is also necessary that the qualifications of the contractor's QC staff be a matter of record, as their responsibility is increased. And it is also necessary that quality criteria be as objective as possible, to avoid dispute and conflict over these costly items.

There can be no substitute for sound judgment when it comes to selection and approval of stone. Unlike steel or even concrete, natural materials such as stone require greater experience in inspection because they are prone to natural variability. Specifications should contain criteria for selection and approval; however, contractors' QC personnel should also be qualified to judge whether individual stones or portions of quarries are not acceptable. Specifications often include the qualifications for QC personnel, at least at the supervisory level. Whenever possible, government QA personnel should be familiar enough with the critical aspects of a particular source of stone to know what characteristics may be of particular concern. Source files within Corps District Offices, if not elsewhere within the Corps, should include reports identifying the strengths and weaknesses of known sources of stone, thus making it easier for the QA staff to address these potential concerns. It is also important that QA personnel know where to look and who to contact when questions arise on stone issues. It will not be possible for all districts to maintain expertise in all areas, and so it is essential that Corps-wide resources (literature, files, and personnel) be readily accessible to ensure maximum efficiency in the future. Effective QC/QA is critically important for armor stone durability.

References

- Adams, J. (1982). "Stress-relief buckles in the McFarland quarry, Ottawa," *Canadian Journal of Earth Sciences* 19(10), 1883-1887, National Research Council of Canada, Ottawa, Ontario, Canada.
- Agar, S. M. (1998). "Microstructural analysis of deterioration in breakwater rocks," Report prepared for U.S. Army Corps of Engineers, Chicago District, Chicago, IL, by Susan M. Agar, Northwestern University, Evanston, IL.
- American Society for Testing and Materials. (1988). "Standard test method for density, relative density (specific gravity), and absorption of coarse aggregate," International Standard ASTM C127, Books of Standards, Vol. 04.02, American Society for Testing and Materials, West Conshohocken, PA.
- _____. (1992). "Standard test method for evaluation of durability of rock for erosion control under wetting and drying conditions," International Standard ASTM D5313, Book of Standards, Vol. 04.08, American Society for Testing and Materials, West Conshohocken, PA.
- _____. (1994). "Standard practice for evaluation of rock to be used for erosion control," International Standard ASTM 4992, Book of Standards, Vol. 04.08, American Society for Testing and Materials, West Conshohocken, PA.
- Bates, R. L., and Jackson, J. A. (1987). *Glossary of geology*, Third Edition, American Geological Institute, Alexandria, VA.
- Bottin, R. R., Jr. (1993). "Broken/cracked armor unit survey of St. Paul Harbor, Alaska, outer breakwater," Memorandum for Record, Coastal Engineering Research Center, U.S. Army Engineer Waterways Experiment Station, Vicksburg, MS.
- _____. (1994). "Broken/cracked armor unit survey of St. Paul Harbor, Alaska, outer breakwater," Memorandum for Record, Coastal Engineering Research Center, U.S. Army Engineer Waterways Experiment Station, Vicksburg, MS.
- Bretz, J. H. (1939). "Geology of the Chicago region, Part 1, general," Bulletin No. 65, 69-81, Illinois State Geological Survey, Champaign, IL.

- Chader, S. A. (2001). "Relationship between coastal waves and Lake Erie water levels," *Proceedings, Ocean Wave Measurement and Analysis*, B. L. Edge and J. M. Hemsley, eds., San Francisco, CA, 620-629, American Society of Civil Engineers, Reston VA.
- Chiapetta, F. R. (1989). "Damaged armor stone on the Cleveland breakwater," U.S. Army Corps of Engineers, Buffalo District, Buffalo, NY.
- Coastal Engineering Manual*. (2003). Part VI, Design of Coastal Project Elements; Chapter 5, "Fundamentals of Design," H. F. Burcharth and S. A. Hughes, eds., Engineer Manual 1110-2-1100, Washington DC.
- Collinson, C., Sargent, M. L., and Jennings, I. R. (1988). "Sedimentary cover-- North American Craton: U.S.; Decade of North America," *The Geology of North America*, Vol. D-2, Chapter 14, "Illinois Basin Region," 383-426, The Geological Society of America, Boulder, CO.
- Droste, J. B., and Shaver, R. H. (1977). "Synchronization of deposition of Silurian reef-bearing rocks on Wabash platform with cyclic evaporites of Michigan basin reefs and evaporites: Concepts and depositional models," 93-109, American Association of Petroleum Geologists, Tulsa, OK.
- _____. (1983). "Atlas of Early and Middle Paleozoic Paleogeography of the southern Great Lakes area," Geological Survey Special Report 32, Indiana Department of Natural Resources, Indianapolis, IN.
- Dunham, R. J. (1962). "Classification of carbonate rocks according to depositional texture," Memorandum No.1, 108-121, American Association of Petroleum Geologists, Tulsa, OK.
- Embry, A. F., and Klovan, J. E. (1971). "A Late Devonian reef tract on Northeastern Banks Island, Northwest Territories," Canadian Petroleum Geology Bulletin 19; 730-781, Canadian Society of Petroleum Geologists, Calgary, Alberta, Canada.
- Feldmann, R. M., and Bjerstedt, T. W. (1987). "Kelleys Island: Giant glacial grooves and Devonian shelf carbonates in north-central Ohio," *Centennial field guide, North-Central section*, The Geological Society of America, Boulder, CO, 395-398.
- Flint, R. F. (1957). *Glacial and pleistocene geology*. John Wiley & Sons, London, England.
- Fookes, P. G., and Poole, A. B. (1981). "Some preliminary consideration on the selection and durability of rock and concrete materials for breakwaters and coastal protection works," *Quarterly Journal of Engineering Geology* 14(2), 97-128, The Geological Society, London, England.
- Gunn, G. R. (1986). "Stratigraphy and petroleum potential of Berea sandstone in Larkin and Williams fields, Midland and Bay Counties, Michigan," Bulletin No. 70, 1066, American Association of Petroleum Geologists, Tulsa, OK.

- Haimson, B. C. (1978). "Engineering geology, stress regime and mechanical properties of some Precambrian rocks in south central Wisconsin," *Geoscience Wisconsin* 2, 25-42, Wisconsin Geological and Natural History Survey, Madison, WI.
- Harrell, J. A., Hatfield, C. B., and Gunn, G. R. (1991). "Mississippian system of the Michigan basin; Stratigraphy, sedimentology, and economic geology," Special Paper No. 256, 203-219, The Geological Society of America, Boulder, CO.
- Headquarters, U.S. Army Corps of Engineers. (1997). "Engineering and design: Monitoring completed navigation projects," Engineer Regulation ER 1110-2-8151, Washington, DC.
- Hill, M. L. (1992). "Some case histories of armor stone production," *Durability of stone for rubble mound breakwaters*. American Society of Civil Engineers, New York, NY, 212-221.
- Hobbs, B. E., Means, W. D., and Williams, P. F. (1976). *An outline of structural geology*. John Wiley and Sons, New York, NY.
- Hudson, R. Y. (editor). (1974). "Concrete armor units for protection against wave attack," Miscellaneous Paper H-74-2, U.S. Army Engineer Waterways Experiment Station, Vicksburg, MS.
- Indiana Limestone Institute of America Inc. (undated). *Indiana limestone handbook*. 21st edition, Indiana Limestone Institute of America Inc., Bedford, IN.
- Ingels, J. J. C. (1963). "Geometry, paleontology, and petrography of Thornton reef complex, Silurian of northeastern Illinois," 47, 405-440, American Association of Petroleum Geologists, Tulsa, OK.
- Jumikis, A. R. (1983). *Rock mechanics*. 2nd edition, Trans Tech Publications Ltd., Aedermannsdorf, Switzerland.
- Kissane, J. A., Ott, M. A., and Schmidt, J. J. (2003). "Selection of rock type for large armor stone in shoreline construction and repair near or above lake elevation," Memorandum for Record, U.S. Army Corps of Engineers, Chicago District, Chicago, IL.
- Krynine, D. P., and Judd, W. R. (1957). *Principles of engineering geology and geotechnics*. McGraw-Hill Book Company, New York, NY.
- Lamar, J. E. (1967). *Handbook on limestone and dolomite for Illinois Quarry operators*. Bulletin 91, Illinois State Geological Survey, Champaign, IL.
- Latham, J. P., Poole, A. B., and Laan, G. J. (1990). "Geological constraints on quarried rock for use in coastal structures," *Proceedings, 61st International Association of Engineering Geology*, Amsterdam, Netherlands, D. G. Price, ed., A. A. Balkema Publishing Co., Rotterdam, Netherlands.

- Latham, J. P., Wang, H., and Poole, A. B. (1994). *Rock for maritime engineering: Coastal, estuarial and harbour engineers' reference book*. Chapman and Hall Publishing Co., London, England.
- Legget, R. F. (1973). *Cities and geology*. McGraw-Hill Book Company, New York.
- Lienhart, D. A. (1975). "Special study on the effect of curing on the durability of the Berea sandstone," Open-File Report #103/75.618B, U.S. Army Corps of Engineers, Ohio River Division Laboratory, Cincinnati, OH.
- _____. (1998). "Rock engineering rating system for assessing the suitability of armourstone sources," *Advances in aggregates and armourstone evaluation*. J. P. Latham, ed., Engineering Geology Special Publication No. 13, 91-106, The Geological Society, London, England.
- _____. (2003). "A systems approach to evaluation of riprap and armor stone sources," *Environmental and Engineering Geoscience IX(2)*, 131-149, The Geological Society of America, Boulder, CO.
- Lienhart, D. A., and Stransky, T. E. (1981). "Evaluation of potential sources of riprap and armor stone: Methods and considerations," *Bulletin* 18(3), 323-332, Association of Engineering Geologists, Denver, CO.
- Lienhart, D. A., Gerdson, A. H., and Sayao, O. J. (1999). "Predicted service life of armor stone: A case history," *Proceeding: Breakwaters '99; First International Symposium on Monitoring of Breakwaters*, 145-159, American Society of Civil Engineers, New York.
- Lilienthal, R. T. (1974). "Subsurface geology of Barry County, Michigan," Report of Investigation 15, U.S. Geological Survey, Michigan Division, Department of Natural Resources, Lansing, MI.
- _____. (1978). "Stratigraphic cross-sections of the Michigan basin," Report of Investigation 15, U.S. Geological Survey, Michigan Division, Department of Natural Resources, Lansing, MI.
- Livingston, C. W. (1975). "The origin of fractures and hairline cracks in armor stone affecting rubble dike design, confined dike dredge disposal projects, Cleveland and Huron Harbors, Lake Erie," Consultant's Report to Barodynamics, Inc., Grand Junction, CO.
- Lowenstam, H. A. (1950). "Niagaran reefs of the Great Lakes area, I," *The Journal of Geology* 58(4), 430-487, University of Chicago, Chicago, IL.
- _____. (1957). "Niagaran reefs in the Great Lakes area," Memorandum No. 67, 215-248, *Treatise on marine ecology and paleoecology*, H. S. Ladd, ed., The Geological Society of America, Boulder, CO.

- Lutton, R. J. (1982). "U.S. experience with armor-stone quality and performance," *Proceedings, Durability of stone for rubble for rubble mound breakwaters*, 40-55, American Society of Civil Engineers, New York.
- Lutton, R. J., Houston, B. J., and Wariner, J. B. (1981). "Evaluation of quality and performance of stone as riprap and armor," Technical Report GL-81-8, U.S. Army Engineer Waterways Experiment Station, Vicksburg, MS.
- Marcus, D. W. (1992). "Recent experience with armor stone cracking in the Buffalo District," *Proceedings, Durability of Stone for Rubble Mound Breakwaters*, 222-237, American Society of Civil Engineers, New York.
- _____. (1994). "Cracked breakwater stone investigation, Cleveland east breakwater, Cleveland, Ohio," U.S. Army Corps of Engineers, Buffalo District, Buffalo, NY.
- Markle, D. G., and Dubose, W. G. (1985). "Wave stability tests of dolos and stone rehabilitation designs for the east breakwater, Cleveland, Ohio," Technical Report CERC-85-10, U.S. Army Engineer Waterways Experiment Station, Vicksburg, MS.
- Mikulic, D. G. (1987). "The Silurian reef at Thornton, Illinois," *Centennial field guide, north central section*. The Geological Society of America, Boulder, CO, 209-212.
- Mikulic, D. G., and Kluessendorf, I. (1985). "Classic Silurian reefs of the Chicago area; 49th annual tri-state geological field conference, trip 2," University of Northern Iowa, Cedar Falls, IA.
- Morgan, M. H. (translator). (1960). *Vitruvius: The ten books on architecture*. Dover Publications Inc., New York.
- Nichols, T. C., Jr. (1980). "Rebound: Its nature and effect on engineering works," *Quarterly Journal of Engineering Geology* 13(2), 133-152, The Geological Society, London, England.
- Pashin, J. C., and Ettensohn, F. R. (1987). "An epeiric shelf-to-basin transition; Bedford-Berea sequence, northeastern Kentucky and south-central Ohio," *American Journal of Science* 287, 893-926, Yale University, New Haven, CN.
- Patton, J. B. (1974). "Glossary of building stone and masonry terms," Occasional Paper No. 6, Indiana Geological Survey, Bloomington, IN.
- Pray, L. C., and Mikulic, D. G. (1976). "The Thornton reef (Silurian), northeastern Illinois; 1976 revisitation," *Guidebook for a field trip on Silurian reefs, interreef facies, and faunal zones of northern Indiana and northeastern Illinois*." The Geological Society of America, Boulder, CO.

- Pope, J., Bottin, R. R., Jr., and Rowen, D. (1993). "Monitoring of east breakwater rehabilitation at Cleveland Harbor, Ohio," Miscellaneous Paper CERC-93-5, U.S. Army Engineer Waterways Experiment Station, Vicksburg, MS.
- Richey, H. G. (1951). *Richey's reference handbook for builders, architects, and construction engineers*. Simmons-Boardman Publishing Corporation, New York.
- Rock Product Consultants. (1995). "Quarry and breakwater investigation of stone deterioration," Report prepared for U.S. Army Corps of Engineers, Chicago District, Chicago, IL, by Rock Products Consultants (David A. Lienhart and Albert W. Gerdson, authors), Cincinnati, OH.
- Sbar, M. L., and Sykes, L. R. (1973). "Contemporary compressive stress and seismicity in eastern North America: An example of intra-plate tectonics," *Bulletin* 84(6), 1861-1882, The Geological Society of America, Boulder, CO.
- Shaver, R. H. (1977). "Silurian reef geometry; new dimensions to explore," *Journal of Sedimentary Petrology* 47, 1409-1424, University of Colorado, Boulder, CO.
- _____. (1978). "The search for a Silurian reef model, Great Lakes area," Special Report No. 15, U.S. Geological Survey, Washington, DC.
- Shore Protection Manual*. (1977). 4th ed., 2 Vol, U.S. Army Engineer Waterways Experiment Station, U.S. Government Printing Office, Washington DC.
- _____. (1984). 4th ed., 2 Vol, U.S. Army Engineer Waterways Experiment Station, U.S. Government Printing Office, Washington DC.
- Shrock, R. R. (1939). "Wisconsin Silurian Bioherms (organic reefs)," *Bulletin* 50, 529-562, The Geological Society of America, Boulder, CO.
- Smith, E. I. (1978). "Introduction to Precambrian rocks of south-central Wisconsin," *Geoscience Wisconsin* 2, 1-17, Wisconsin Geological and Natural History Survey, Madison, WI.
- STS Consultants Ltd. (1992). "McCook Quarry investigations," Report prepared for U.S. Army Corps of Engineers, Chicago District, Chicago, IL, by STS Consultants Ltd, Northbrook, IL.
- Swann, D. H. (1963). "Classification of Genevievian and Chesterian (Late Mississippian) rocks of Illinois," Report of Investigation, No. 216, Illinois State Geological Survey, Champaign, IL.
- Toksoz, M. N., Thomson, K. C., and Ahrens, T. J. (1971). "Generation of seismic waves by explosions in prestressed media," *Bulletin* 61(6), 1589-1623, Seismological Society of America, El Cerrito, CA.

- Tullis, J., Christie, I. M., and Griggs, D. T. (1973). "Microstructures and preferred orientations of experimentally deformed quartzites," *Bulletin* No. 84, 297-314, The Geological Society of America, Boulder, CO.
- U.S. Army Corps of Engineers. (1992). "Standard test method for resistance of rock to freezing and thawing," Standard CRD C144, U.S. Army Engineer Waterways Experiment Station, Concrete Research Division, Vicksburg, MS.
- Vernon, R. H. (1970). "Comparative grain-boundary studies of some basic and ultrabasic granulites, nodules, and cumulates," *Scottish Geological Journal* 6, 337-351, The Geological Society, London, England.
- Vutukuri, V. S., Lama, R. D., and Saluja, S. S. (1974). *Handbook on mechanical properties of rocks*. Vol. 1, Trans Tech Publications, Aedermannsdorf, Switzerland.

Appendix A

Memorandum for Record¹

SUBJECT: Selection of Rock Type for Large Armor Stone in Shoreline Construction and Repair Near or Above Lake Elevation, Burns Harbor North Breakwater Repair, Indiana

13 February 2003

Joseph A. Kissane, PG, Geotechnical Engineer/District Geologist
Monica A. Ott, PE, Project Manager
Joseph J. Schmidt, SE, Chief, Design Branch

U.S. Army Engineer District, Chicago
111 North Canal Street
Suite 600
Chicago, IL 60606

¹ This document appears in its entirety in this appendix, and is cited in the References section as Kissane et al. (2003).

MEMORANDUM THRU:

CELRC-TS-DG _____

CELRC-TS-DC _____

CELRC-TS-DE _____

CELRC-TS-HH _____

CELRC-TS-C-T _____

FOR RECORD

SUBJECT: Selection of Rock Type for Large Armor Stone in Shoreline Construction and Repair Near or Above Lake Elevation

1. RECOMMENDATION: The specifications for Stone Materials for Burns Harbor Breakwater Repair contracts shall stipulate that limestone and dolomite (carbonate rock types) will not be acceptable for armor stone (Type A-Stone), based on inferior durability exhibited by these materials compared to alternatives (notably granite, quartzite, gabbro, diabase, or basalt.)
2. REFERENCES:
 - a. Accelerated Weathering of Armorstone and Riprap – U.S. Army Corps of Engineers, Ohio River Division Laboratory Workshop, January 1996.
 - b. CELRC Inspection Reports, Inspection of Completed Works, Chicago Water Treatment Plant/Reach 5 Breakwater August 2001 and September 2002.
3. BACKGROUND: Burns Harbor, Porter County, IN, (see Figure A1) is a deepwater harbor at the southern end of Lake Michigan that receives significantly greater wave heights than the other navigational harbors in the U.S. Army Engineer District, Chicago. The north breakwater protecting the Burns Harbor Waterway is undergoing a series of repairs. Initial construction was completed in 1964. Subsequent surveys indicated the need for major repairs by the early 1970s. Repairs have included addition of substantial quantities of stone to the structure to protect the harbor. The Burns Waterway Harbor, Indiana Breakwater Major Rehabilitation Evaluation Report was prepared and approved in 1993, identifying opportunities to stabilize and improve the structure and reduce maintenance costs. Included in the study was the design of an underwater reef, in addition to repair and limited redesign of the breakwater, itself. The breakwater was surveyed in 1995 to assess its condition

SUBJECT: Selection of Rock Type for Large Armor Stone in Shoreline Construction and Repair Near or Above Lake Elevation

relative to design elevations and grades, and assess overall performance. Areas where repairs were necessary were prioritized and scheduled for detailed evaluation and subsequent repairs as funding and authorization became available.



Figure A1. Burns Harbor, IN, breakwater looking west

4. ISSUES: Observations from inspections of projects where limestone and dolomite were used in shoreline and harbor protection have raised concern for the long-term durability of these (carbonate) rock types where armor stones are exposed to wetting and drying and freeze-thaw cycles. Among the factors that have been considered partially responsible for the observed problems with carbonate rock as armor stone are the presence of deleterious materials (clay, chert, altered minerals, etc.), preexisting weathered zones, natural discontinuities (fractures, bedding planes,

SUBJECT: Selection of Rock Type for Large Armor Stone in Shoreline Construction and Repair Near or Above Lake Elevation

stylolites, joints, etc.), blast-induced fractures, fractures resulting from elastic rebound following excavation, and vugs. Quality control and quality assurance procedures have been cited as playing a role in selection of armor stone that will provide long-term performance; however, detailed and time-consuming examination by a qualified individual of each stone at the quarry and before placement has been necessary to ensure that only those stones free of compromising characteristics are used. This level of scrutiny is costly, and is contrary to the trend of decreased funding for Government inspections.

5. **ALTERNATIVES:** The alternatives to the previous contracting and construction specifications and procedures include the following:
 - a. Intensify the level of inspection by qualified Government technical elements, including geologist(s) at the quarry and construction site to approve only those stones meeting strict selection criteria. This alternative will require additional resources and costs, and may result in exceeding guidelines for level of inspection and oversight for construction contracts. It will also result in rejection of a majority of armor stones produced at limestone and dolomite quarries using drill and blast methods.
 - b. Additional monitoring and subsequent maintenance and repairs may be necessary if deterioration of armor stone results in significant changes in the performance of structures. Monitoring should be performed periodically, and additional unscheduled inspections may be considered following unusually intense storms, fluctuating lake levels or severe temperature variations, particularly involving greater numbers of freezing and thawing cycles. The costs of the inspections and repairs may be significant, especially weighed against the costs of construction alternatives that may reduce these out-year costs.
 - c. Stone sources may be used that have a greater resistance to weathering and other factors that cause premature deterioration of armor stone. There is a potential increase in material costs for the construction. This cost would be partially offset during construction by the cost of greater QA/QC costs required for less resistant (dolomite and limestone) materials. The costs would also be offset by significant reduction of maintenance and repair during the normal project life. The use of more resistant stone is likely to reduce the need for frequent intensive inspections during the project life.
6. **DISCUSSION:** Repair and restoration of shoreline protection has been undertaken throughout the Great Lakes region since the initial structures were placed in service nearly 100 years ago. Repairs and additions to the shoreline protection in place were made in response to additional development, and the determination that the original protection was insufficient, deteriorating, or both. The considerations in design

SUBJECT: Selection of Rock Type for Large Armor Stone in Shoreline Construction and Repair Near or Above Lake Elevation

include the relative durability of materials used, the construction costs associated with those materials, and the consideration of monitoring and maintenance costs, which may vary, depending on the materials selected. Burns Harbor north breakwater was constructed to protect the deep-water harbor located at the southern extreme of Lake Michigan. This location is subjected to climatic extremes and severe wave action, requiring the design of the breakwater to account for these factors. Durability of the material is a key element of the design.

- a. Historical Use of Limestone and Dolomite. Historically, the shoreline of Lake Michigan in the Chicago area has been protected by limestone and dolomite armor stone, much of which was quarried in the first half of the twentieth century from the Bedford limestone and similar formations of oolitic limestone in central Indiana. The largely rectangular stones were mechanically cut or manufactured from the relatively soft, moderately friable limestone material that is still quarried today for use as building stone. Parts of the Chicago shoreline were stabilized in the years before World War II using these cut limestone blocks placed in large stair-step fashioned revetment supplemented with offshore breakwaters (see Figure A2). The production rates for this type of stone were adequate when the construction was performed using the technology of the day; however, modern placement methods and project schedules now exceed the production capacities of these types of quarries. As the costs associated with the manufacturing and placement of cut limestone blocks increased, subsequent construction and repair has consisted of rubble-mound structures of harder Silurian dolomite quarried by drill and blast methods from deposits in Illinois and Wisconsin. Limestone and dolomite are closely related rock types. Both are sedimentary rocks deposited primarily in marine environments, with the significant difference being that in addition to calcium carbonate being the major component, dolomite consists of carbonate of magnesium and calcium. The structures and characteristics of the two rock types are so similar that the formations in which dolomites occur are often called limestones in the geologic literature. Because of the similar nature of the two rock types, and, consequently, the similarity of issues related to them in terms of use for armor stone production, they are treated the same in this discussion.
- b. Stone Material Characteristics. Shoreline project inspections typically include observations of the condition of armor stones as a criteria for the evaluation of the overall structure's condition. Overall quality and stone type, in combination with the structures' design, and appropriate maintenance and repair, are important in determining the long-term performance of shoreline protection. Quality and rock property issues include, but are not limited to hardness, presence of cracks, fissures, weathering features, bedding planes, and inclusion of weaker materials in the rock mass. For this discussion, stone type refers to the mineral composition and genesis of the rock being used. In combination with the structure's design,

SUBJECT: Selection of Rock Type for Large Armor Stone in Shoreline Construction and Repair Near or Above Lake Elevation



Figure A2. Limestone blocks in place along Chicago shoreline – Belmont to Diversey

stone quality and stone type determine the structure's resistance to weathering and mechanical deterioration from ice and wave action. The preferential selection of rock type can contribute to the longevity of structures by providing materials that will resist the elements for the duration of the project design life.

- c. Cut Versus Blasted Carbonate Rock. Observations and detailed inspection of the earliest of the limestone block structures has led some to question the concern for the durability of carbonate armor stone, as a high percentage of the so called Indiana limestone blocks are intact and in good condition more than 50 years after placement (see Figure A2). The comparison of cut limestone blocks to dolomite or limestone quarried by drill and blast techniques is not necessarily appropriate. Blasting results in both large and small-scale cracking of stone, not all of which may result in immediate separation, and not all of which is evident upon visual inspection. The shock waves generated by blasting are prone to reflection and refraction when they encounter even microscopic invisible natural variations in the rock mass. These shock waves begin to separate the rock along the natural variations in the material.

SUBJECT: Selection of Rock Type for Large Armor Stone in Shoreline Construction and Repair Near or Above Lake Elevation

- d. Planar Features as Zones of Weakness in Carbonate Rock. If abrupt variations in carbonate rock mass are linear or planar (in three dimensions) in nature; as bedding planes (whether intact or parted), stylolites and inherent joint patterns; the energy of the blast vibrations will exploit these planar features, and the potential for separation along the plane is greatly increased (see Figure A3). Physical separation may occur at the time of blasting or at some later date, whether as a result of vibration during handling and placement, or as a consequence of wave action or freezing and thawing. Minute fractures that develop along these planes of weakness may not be visibly evident after blasting or curing, and may only become evident after water has entered the rock mass to some depth from the surface of the stone – and in instances where the separation is extremely minute, this may take months, or years. If the water penetrates sufficiently and freezes, the rock may split. If the bedding plane contains even minute quantities of clay minerals, which are prone to absorption of water, the effect of alternating cycles of wetting and drying will result in separation growing as the clay mineral grains expand as water is absorbed.



Figure A3. Dolomite armorstones showing stylolites in various degrees of separation

SUBJECT: Selection of Rock Type for Large Armor Stone in Shoreline Construction and Repair Near or Above Lake Elevation

- e. Tensile Strength and Bedding Planes. The planar features in sedimentary rock types are also often characterized as having lower tensile strength than the overall rock mass. Some bedding planes, although physically tight (not separated) have little or no tensile strength. Over time, for various reasons, weak bedding planes will separate (see Figure A4). Most bedding planes represent prolonged periods of nondeposition or erosion in the geologic record, and so there is little bonding between newly deposited material and the underlying material which may have begun to solidify (lithify, or become rock.). Even massive thick-bedded highly-cemented or precipitated sedimentary rock types, including many limestone and dolomites, have large-scale planar weaknesses at bedding planes representing the boundaries between periods of their deposition. Although larger scale bedding planes, or those representing relatively obvious changes in the composition of the rock mass are often cemented, the cementation along these boundaries is typically a precipitate that adheres to the adjacent materials rather than the case of growth between individual adjacent grains or crystals.



Figure A4. Bedding planes in limestone armor stone on Chicago shoreline showing separation

- f. Planar and Boundary Features in Nonsedimentary Crystalline Rock. Igneous and metamorphic crystalline rock types, including granite, quartzite, gabbro, basalt, and diabase, may also exhibit planar zones of weakness at boundaries between

SUBJECT: Selection of Rock Type for Large Armor Stone in Shoreline Construction and Repair Near or Above Lake Elevation

materials of somewhat contrasting mineral composition; however, these boundaries are often more visible than the most subtle bedding planes in sedimentary rock. Where the boundaries are abrupt, they are typically characterized by marked changes in mineral composition and physical separation may be quite obvious. These boundaries may often be less abrupt and more transitional because the physical environment in which these rock types are formed. Igneous and metamorphic rocks form as a result of crystal growth and rock mass solidification in conditions of intense heat and or pressure, as opposed to the accumulation of granular sediments or the precipitation of soluble minerals under low pressures (as occurs in the formation of carbonate rocks in marine environments). The boundaries or zones in igneous and metamorphic rock masses form as a result of temperature distribution from the variation in the cooling/solidification with respect to the distance from the heat source, or pressure distribution during formation of the rock mass, rather than the passage of time between periods of deposition of sedimentary materials. In contrast to the bedding planes of sedimentary rocks, the bonding between mineral grains in igneous and metamorphic rocks may actually be the result of intergrowth of mineral crystals. Igneous and metamorphic rocks form at greater depths in the earth, under significant pressure and heat conditions, further strengthening the bonding between mineral crystals. Rock formed by the intergrowth of mineral crystals has a greater tensile strength and resistance to separation than sedimentary rock bonded by precipitated cementitious material because the mineral crystals of the crystalline rock are stronger than the cementitious material. In general, the unbroken or unseparated planar zones of concern to durability in igneous and metamorphic rocks occur where the minerals present are dominated by mica minerals, which are much weaker than the surrounding rock. Linear seams of contrasting color in granite are frequently quartz, and are not only harder than the surrounding rock, but bonded by intercrystalline growth and do not pose durability concerns (see Figure A5). These areas are conspicuous because of the visibly obvious differences between the minerals and the other crystalline minerals of the rock, and stones exhibiting these zones can readily be identified and screened out at the quarry if appropriate.

- g. Cracking in Igneous and Metamorphic Rock. Igneous and metamorphic rock types will also contain natural cracks and joints and develop cracks that may or may not result in immediate splitting of the rock into smaller pieces following blasting. As with carbonate rock, both natural discontinuities and blasting fractures may in some instances be small enough to be difficult or impossible to identify by the naked eye. Cracks resulting from blasting in sedimentary rocks are more likely to exploit pre-existing planes of weakness that are either parallel to or are actual bedding planes, because these rock types are anisotropic with respect to their strength properties. Igneous and metamorphic rocks are more likely to be isotropic in their strength properties, and have no bedding planes.

SUBJECT: Selection of Rock Type for Large Armor Stone in Shoreline Construction and Repair Near or Above Lake Elevation



Figure A5. Granite armor stone during sorting process – note absence of discontinuities

Aside from inherent orthogonal jointing patterns that are obvious to the quarry operator and inspectors because they are clearly visible, these rocks are more prone to random fractures resulting from blasting. Fractures in sedimentary rocks (including limestone and dolomite) that exploit and follow preexisting planes of weakness are likely to extend farther, compared to those in isotropic rocks – just as it is easier to split wood with the grain than it is to split composition materials without grain.

- h. Laboratory Properties. The specifications used for armor stone include laboratory test criteria. Misconceptions have arisen in interpreting the laboratory criteria as the determining factors in acceptance of stone. Most of the laboratory tests specified in contracts for armor stone have been developed for aggregate and road stone, as opposed to large pieces of rock. The sample size specified for these standardized tests is often several orders of magnitude smaller than individual armor stones, requiring armor stones to be cut to provide laboratory samples for testing. Selection of the portion of an armor stone for testing can be the determining factor in its passing or failing the test, rather than the bulk character of the rock. Aside from specific gravity, which is an essential variable in design of structures, other laboratory test results are appropriately used as preliminary screening tools in combination with the observations of an experienced geologist in evaluating the material sources. If materials fail to meet the laboratory test

SUBJECT: Selection of Rock Type for Large Armor Stone in Shoreline Construction and Repair Near or Above Lake Elevation

criteria, it is assumed they are not likely to perform adequately in the field; however, if they meet the laboratory test criteria, it cannot be assumed that the materials will perform adequately without corroborating information in the form of performance records and the visual evaluation of an experienced geologist. Physical properties identified as relevant to the durability of armor stone specified in the Burns Harbor repair contract are summarized in Table A1.

Table A1. Criteria for Stone Quality

Test	Test Method	Acceptance Criteria
Specific Gravity	ASTM C 127	2.6 - 3.0
Absorption	ASTM C 127	< 1 percent <u>or</u> > 3 percent
Los Angeles Abrasion	ASTM C 535	< 20 percent loss after 500 revolutions
Freeze-Thaw	ASTM D 5312	<2 percent loss after 35 cycles
Wetting-Drying	ASTM D 5313	<2 percent loss after 80 cycles
Petrographic Examination	ASTM C 295	No deleterious materials allowed
Field Examination	ASTM D 4992	No deleterious materials allowed
Compressive Strength	ASTM C-42	Minimum 3,000 psi

- i. Comparison of Physical Properties. Structures are designed and quantities estimated based on specific gravity generally in the range of 2.6 to 3.0. Limestone, dolomite, granite, quartzite, and gabbro are all within this range. Structures may be designed and quantities revised or adjusted with stone outside the range specified without impacting the performance of the structure, all other factors being equal. The other laboratory-based criteria are not major factors in design, but are used as relative indicators of stone durability, as they pertain to the ability of the stone to resist mechanisms of deterioration. Comparison of laboratory test results from limestone, dolomite, granite, gabbro, and quartzite from quarries in the northern Midwest is inconclusive with respect to decisively indicating the superiority of one material over the other; however, any comparison using laboratory tests is biased by the sample size required for testing. Limestone and dolomite typically do not perform as well in Los Angeles abrasion tests

SUBJECT: Selection of Rock Type for Large Armor Stone in Shoreline Construction and Repair Near or Above Lake Elevation

compared to granite, quartzite, or gabbro. It was noted in the course of investigating the laboratory characteristics of dolomite and limestone samples, numerous laboratory test results include the notation that tests were run on the intact portion of the sample, after the sample broke in transit or sample preparation. Such an occurrence further illustrates the danger of relying too heavily on laboratory results alone.

- j. Chemical Weathering Resistance. Although not a major consideration in the short-term, resistance to chemical weathering may become a long-term consideration for stone structures exposed to acid rain over long periods. Carbonate rocks, such as dolomite and limestone, are particularly susceptible to chemical weathering by weak carbonic acid, which is formed by the dissolving of carbon dioxide in rain. Igneous and metamorphic rocks such as quartzite, granite, gabbro, and diorite, are inert to acid rain, because the silica-based minerals in their makeup are insoluble in weak carbonic acid. While it is not possible that acid rain will dissolve whole blocks of dolomite or limestone within the project life, the susceptibility of these rock types to chemical weathering by acid rain; particularly where fractures, bedding planes, or openings already increase the likelihood of separation; adds to the potential for blocks to break up into pieces smaller than necessary to perform their function.
- k. Quality Control and Quality Assurance Issues. The Chicago District has been involved in shoreline protection contracts involving toe stone and armor stone from dolomite quarries in Illinois and Wisconsin for decades. The proper implementation of Quality Control (QC) at the quarry, and throughout the handling and placement of armor stone has been an essential part of construction. Quality Assurance (QA) has been hand-in-hand with Quality Control in the process. Because of budget constraints and agency policy, quality assurance and Corps oversight in the past 10 years has been limited to a small percentage of armor stone, often less than 20 percent. Contractors may or may not be aware that the Corps and local sponsors are relying more on contractors' QC than in years past. The reduction of QA is intended to place additional responsibility for the final product on the contractor, while reducing administration cost to the Government. However, because the Government is reducing its presence during certain activities, contractors may mistakenly interpret the reduced presence as an expression of a diminished level of concern by the Government for a particular aspect of the project. If the diligence of the contractor's QC does not meet this increased burden of responsibility, the overall quality of the construction is likely to suffer, and with diminished QA presence, and lessened oversight, the results will not be apparent until several seasons of stress. By that time it is difficult, if not impossible, to establish responsibility for any problems that develop. This is far more critical when using designs or materials that have less inherent capacity or tolerance for this potential diminished quality. It is also far more important to

SUBJECT: Selection of Rock Type for Large Armor Stone in Shoreline Construction and Repair Near or Above Lake Elevation

structures, like Burns Harbor breakwater, where the environmental stresses are great. Because limestone and dolomite require greater diligence in terms of QC to screen out unsuitable stones at the quarry and throughout construction, the repercussions of using these materials is greater than it is with materials that are inherently more durable, such as quartzite, granite, diorite, and gabbro.

1. Maintenance Case Histories. The Chicago and Detroit Districts have a long history of construction and maintenance of armor-stone structures. Until recent years, the Chicago District's record has been predominantly with dolomite and limestone materials. The Calumet Harbor Confined Disposal Facility (CDF) was constructed in 1984 using dolomite armor stone that rapidly deteriorated and has required major repairs in the years since. In response to the need for durable long-term repairs with a minimum of follow-up maintenance, the most recent repairs were performed using quartzite. Burns Harbor breakwater was constructed with cut limestone blocks in the early to mid 1960s and has subsequently been repaired using recycled cut limestone blocks, drill and blast dolomite and quartzite armor stone. In direct contrast to structures built and repaired with dolomite from quarries where the stone was excavated by drill and blast methods, the repairs using quartzite and granite at Burns Harbor and the Calumet CDF are virtually indistinguishable from the day they were completed in terms of the durability of the armor stone, even as much as 8 years later. The Reach 5 breakwater in south Chicago was reconstructed in 1998-99 using dolomite from Wisconsin. Inspection records for the 3 years following completion of the Reach 5 breakwater have included references to deterioration in the newly-placed armorstone ranging from fracturing associated with stylolites and blast fractures to ongoing and progressive surface spalling and flaking (see Figure A6). The U.S. Army Engineer District, Detroit, has used both dolomite and gabbro for construction and repair of breakwater structures, depending on the proximity to various source rocks and the specifications developed in accordance with Local Sponsors' restrictions. These structures have required maintenance by the Detroit District's labor crews, using materials that are similar or identical to the original structure, based solely on the sources proposed by the contract suppliers of stone to LRE. Based on the observations of Ron Erickson, the Detroit District Design Branch, who is responsible for the material selection for these projects, those projects constructed using dolomite have required nearly twice the amount of stone for repairs as those constructed of the more resistant gabbro stone.
- m. Monitoring Considerations. The degree of long-term durability is a factor in determining the need for long-term monitoring. Although the frequency of inspection of completed structures is primarily determined by regulations, structures with histories of suspect or less-than-designed performance are likely to be more closely monitored throughout their project life. Structures built with more durable materials will require less diligent and less costly monitoring over

SUBJECT: Selection of Rock Type for Large Armor Stone in Shoreline Construction and Repair Near or Above Lake Elevation



Figure A6. Even with QA/QC practices, this armor stone and others like it appear in Reach 5 breakwater. Note separations occurring at planar weaknesses

their project life. Structures that exhibit premature wear or diminished performance will require additional or supplemental investigations in the form of surveys and possibly design reevaluation to determine the causes of premature problems. The use of more durable materials in construction will reduce the potential need for supplemental investigations and surveys by reducing the potential for material failure as a factor in performance of the project.

- n. Cost Considerations. Two factors appear to have the greatest impact on the costs associated with armor stone: 1) transportation costs and 2) market conditions.

(1) Transportation costs are significant contributors to the overall costs of large-sized stones. Transportation is not independent of source stone type (limestone/dolomite versus quartzite/granite/gabbro) because the Chicago District and Burns Harbor are geographically located relatively close to sources of dolomite and limestone, compared to the other rock types. Unfortunately, the dolomite quarries located within the Greater Chicago area do not have a history of producing even marginally acceptable

SUBJECT: Selection of Rock Type for Large Armor Stone in Shoreline Construction and Repair Near or Above Lake Elevation

large-sized armor stone because of the bedding, chert components, and fracture pattern in these quarries. Limestone quarries in southern and south-central Indiana that provided cut limestone blocks for the early shoreline projects in Chicago cannot produce the quantity of stone required for the Chicago District's projects at an economical production rate. Dolomite quarries in Wisconsin have provided armor stone and toe stone for shoreline projects in Chicago; however, QC issues related to stylolites, vugs, bedding planes and weathering products (glauconite clay along bedding planes) have been raised on many projects using dolomite from the various quarries in Wisconsin. Quartzite deposits in south-central Wisconsin were exploited for armor stone in the early 1990s near the town of Waterloo, and one quarry in this area has supplied high quality durable armor stone under both construction contracts and supply contracts in the years since. The quarry near Waterloo is located closer to Chicago than the dolomite quarries near Manitowoc, WI, that have provided most of the large stone used for the repair and redesigned Chicago Shoreline projects. Granite quarries in the Wausau, WI, area have been in production for over 100 years, and have produced large-size stones associated with the production of architectural and building dimension stone. Granite quarries in the Wausau area have supplied high quality durable armor stone for U.S. Army Corps of Engineers projects for the Chicago and Detroit Districts. Gabbro deposits in northern Wisconsin and Minnesota have been mined for various purposes, and have supplied high quality durable armorstone for Detroit District projects along Lakes Michigan and Superior. Transportation as a cost factor is not purely related to geographical distance, but rather, may reflect the methods used – i.e., trucks, barges and/or rail. If a supplier or contractor has easy access to a particularly advantageous transportation method, this may be reflected in a lower bid.

- (2) Market conditions determine the price quarries charge contractors at the source of the stone, and to a lesser extent, determine the transportation costs associated with delivery. If the economy is such that the market for any of the products a quarry produces; whether these are aggregate, riprap, building dimension stone, or architectural stone; is depressed, quarries may be willing to price stone products at a lower price to stay in business. Conversely, if a quarry is maximizing his output with higher profit products, it may charge a higher price to produce large stone, or may choose not to even make a bid for large-sized stone. These considerations are independent of the rock type. An earlier repair contract at Burns Harbor was successfully bid by a contractor using quartzite from Waterloo, WI, competing against dolomite quarries with comparable transportation costs. The most recent Burns Harbor repair contract also reflects the impact of the market on stone prices. There was no restriction as to rock type for that

SUBJECT: Selection of Rock Type for Large Armor Stone in Shoreline Construction and Repair Near or Above Lake Elevation

contract, and the successful bidder chose to use granite from the Wausau, WI, area, because the price offered to the successful bidder by the granite supplier was competitive with the dolomite suppliers in the Manitowoc area. It is not always possible to identify the material sources of unsuccessful bidders on previous contracts, so it is not possible to compare dolomite/limestone bids to nondolomite/limestone bids. The price for armor stone in the bids for construction contracts for the 2002 Burns Harbor repair contract ranged from \$48 to \$58 per ton, and it can be reasonably assumed that these bids included dolomite as potential sources. By comparison, the 2002 Montrose North Chicago Shoreline project, which was also unrestricted, included an item for stone in the 1.5- to 4.5-ton range (smaller, and normally a lower cost per ton item). Bids for the Montrose North contract included unit prices from \$32.40 to \$46.00. The contractor has not indicated his stone source yet for this contract. And the unrestricted 41st to 43rd St. Chicago Shoreline contract had only two bidders for stone in the 1.5 to 4 ton size, at \$41 per ton and \$40 per ton. The selected contractor for that contract chose to use granite from Wausau for this size range in this contract. Based on these examples, indicating a wide price range for both dolomite and nondolomite sources, it is evident that the market price can determine the cost of stone in such a way as to make granite or quartzite competitive with limestone and dolomite.

- o. Available Sources of Stone. Quarries producing large armor stone are located throughout the upper Midwest and Great Lakes area. Limestone and dolomite are the dominant rock types at or close enough to the ground surface to be economically quarried in the region extending from the northern limits of the Ozark uplift in Missouri to southern Wisconsin. Along with dolomite quarries, quartzite, granite, and gabbro quarries are located in the area from south central to northern Wisconsin, Minnesota, and Northern Michigan. Natural variation in the host rock, quarrying expertise with large stone, and economic factors all play a role in whether these quarries can or will produce acceptable quality and quantity of armor stone for projects such as the Burns Harbor repair contract. It is an unfortunate reality that as the quality requirements for any material are increased, the number of potential sources decreases. Such is the case with armor stone, as it is with any commodity.
7. **SUMMARY:** The solicitation for Burns Harbor north breakwater repair work to be performed over a 3-year period will include a stipulation that the stone material source for armor stone shall not be limestone or dolomite. This decision is based on the need for material that has proven itself to be exceptionally durable in above-water construction in hostile physical elements such as those at Burns Harbor. Limestone and dolomite are being excluded from consideration for technical and economic reasons. Limestone and dolomite quarries have shown greater variability in quality compared to the allowable materials, and the record indicates dolomite and limestone

SUBJECT: Selection of Rock Type for Large Armor Stone in Shoreline Construction and Repair Near or Above Lake Elevation

quality and durability is less likely to meet the project lifespan requirements for this project. This investigation has indicated proven availability of reasonably competitive sources of the allowable types of materials within the region, and the recognition that the use of limestone or dolomite would require a greater and more costly level of QA/QC, follow-up monitoring and maintenance and repair over the lifetime of the project. Table A2 summarizes the comparisons used to reach this decision.

8. POC: Joseph A. Kissane, P.G. at (312) 846-5453

Approved by:

MONICA OTT, P.E.
Project Manager

JOSEPH SCHMIDT, S.E.
Chief, Design Branch

cf:
CELRC-TS-DG
CELRC-TS-HH
CELRC-TS-DE
CELRC-TS-C-T
CELRC-PM-PM

SUBJECT: Selection of Rock Type for Large Armor Stone in Shoreline Construction and Repair Near or Above Lake Elevation

Table A2. Summary of Issues

Issue	Quartzite, Granite Gabbro, Diorite	Limestone Dolomite	Comments
Past Performance	High	Low to High	Performance of dolomite ranged from structural failure to satisfactory performance
Frequency of Repair	Low	Low to High	
Scale of Required Repairs	None to Small	Small to Large-Scale	
QC/QA Requirements during construction	Low	High to Moderate	Selection of individual stones requires detailed inspection.
Monitoring Requirements after Construction	Low	Moderate to High	Level of monitoring dependent on observed performance in years immediately following construction.
Resistance to Breakage after Placement	High	Low to High	Limestone and dolomite resistance is variable depending on discontinuities. Limestone and dolomite durability is extremely variable even for stone within individual quarries
Potential for undetected discontinuities to cause large-scale deterioration	Low	Moderate to High	
Overall Durability	High	Low to High	
Specific Gravity	2.55 to 2.85	2.6 to 2.7	Not a deciding factor
Los Angeles Abrasion Loss	Less than 5 %	Less than 10%	Some samples of dolomite noted that testing performed on portion of sample that remained intact after breakage during handling.
Freeze Thaw Loss	Less than 2%	Less than 2%	
Wet-Dry Loss	Less than 2%	Less than 2%	
Cost	\$40-\$56	\$32-\$56	Data not available as to rock type proposed by unsuccessful bidders on past solicitations.
Availability	Moderately available	Readily Available	Availability excusive of quality issues.

REPORT DOCUMENTATION PAGE

Form Approved
OMB No. 0704-0188

Public reporting burden for this collection of information is estimated to average 1 hour per response, including the time for reviewing instructions, searching existing data sources, gathering and maintaining the data needed, and completing and reviewing this collection of information. Send comments regarding this burden estimate or any other aspect of this collection of information, including suggestions for reducing this burden to Department of Defense, Washington Headquarters Services, Directorate for Information Operations and Reports (0704-0188), 1215 Jefferson Davis Highway, Suite 1204, Arlington, VA 22202-4302. Respondents should be aware that notwithstanding any other provision of law, no person shall be subject to any penalty for failing to comply with a collection of information if it does not display a currently valid OMB control number. **PLEASE DO NOT RETURN YOUR FORM TO THE ABOVE ADDRESS.**

1. REPORT DATE (DD-MM-YYYY) June 2005		2. REPORT TYPE Final report		3. DATES COVERED (From - To)	
4. TITLE AND SUBTITLE Monitoring Stone Degradation on Coastal Structures in the Great Lakes – Summary Report				5a. CONTRACT NUMBER	
				5b. GRANT NUMBER	
				5c. PROGRAM ELEMENT NUMBER	
6. AUTHOR(S) David W. Marcus, Joseph A. Kissane, David A. Leinhart, Kenneth E. Henn III, Susan M. Agar				5d. PROJECT NUMBER	
				5e. TASK NUMBER	
				5f. WORK UNIT NUMBER MCMP 11M13	
7. PERFORMING ORGANIZATION NAME(S) AND ADDRESS(ES) See reverse.				8. PERFORMING ORGANIZATION REPORT NUMBER ERDC/CHL TR-05-1	
9. SPONSORING / MONITORING AGENCY NAME(S) AND ADDRESS(ES) U.S. Army Corps of Engineers Washington, DC 20314-1000; U.S. Army Engineer Research and Development Center Coastal and Hydraulics Laboratory 3909 Halls Ferry Road Vicksburg, MS 39180-6199				10. SPONSOR/MONITOR'S ACRONYM(S)	
				11. SPONSOR/MONITOR'S REPORT NUMBER(S)	
12. DISTRIBUTION / AVAILABILITY STATEMENT Approved for public release; distribution is unlimited.					
13. SUPPLEMENTARY NOTES					
14. ABSTRACT Stone deterioration on breakwaters and jetties arises from a combination of interactions pertaining to the quality of stone available, operational and handling practices at the quarry, and environmental weathering conditions after placement on the project structure. Four different and distinct investigations were essential to fully comprehend the mechanisms that give rise to chronic premature deterioration of armor stone on breakwaters and jetties around the Great Lakes, including: a. Quarry field geological observations. Seven different quarries that have historically provided material for Great Lakes break-water and jetty construction and rehabilitation projects were investigated. The stone produced by these seven quarries included (a) Salem formation limestone from Reed Quarry, Bloomington, IN, (b) Niagaran series dolomite from Valders Quarry, Valders, WI, (c) Waterloo formation quartzite from Dempsey Quarry, Waterloo, WI, (d) Columbus formation limestone from Sandusky Quarry, Parkertown, OH, (e) Columbus Formation dolomitic limestone from Marblehead Quarry, Marblehead, OH, (f) Berea formation sandstone from Johnson Quarry, Kipton, OH, and (g) Racine Formation dolomite from Thornton Quarry, Thornton, IL. Field geological observations had previously been performed at an eighth quarry (McCook Quarry, McCook, IL). The McCook Quarry produces Niagaran series dolomite. (Continued)					
15. SUBJECT TERMS		Dolomite	Limestone	Stone quarries	
Armor stone deterioration		Dolomitic limestone	Quartzite	Taconite	
Breakwaters		Jetties	Sandstone		
16. SECURITY CLASSIFICATION OF:			17. LIMITATION OF ABSTRACT	18. NUMBER OF PAGES	19a. NAME OF RESPONSIBLE PERSON
a. REPORT	b. ABSTRACT	c. THIS PAGE			19b. TELEPHONE NUMBER (include area code)
UNCLASSIFIED	UNCLASSIFIED	UNCLASSIFIED		312	

7. (Concluded)

U.S. Army Engineer District, Buffalo
1776 Niagara Street, Buffalo, NY 14207;
U.S. Army Engineer District, Chicago
111 North Canal Street, Chicago, IL 60606;
Rock Products Consultants
7229 Longfield Drive, Cincinnati, OH 45243-2209;
U.S. Army Engineer District, Louisville
P.O. Box 59, Louisville, KY 40201-0059;
Northwestern University
Department of Geology, Evanston, IL 60201

14. (Concluded)

b. Laboratory durability testing. Laboratory durability testing of stone samples to accelerate weather exposure freeze/thaw and wet/dry effects, and to determine specific gravity and sample petrography, was performed. The laboratory durability testing samples came from the eight quarries where field geological observations had been performed, plus samples from a ninth quarry (Iron Mountain Quarry, Iron Mountain, MI). The Iron Mountain Quarry produces taconite.

c. Quarry sample microstructural analyses. Microstructural analyses of quarry stone samples from seven different quarries to determine microscale features in the rock that affect stability, and their relations to compositional and textural variations, were conducted after laboratory durability testing. These were the same quarries for which quarry field geological observations had also been performed, except stone samples from McCook Quarry were not available for quarry microstructural analyses.

d. Field prototype monitoring. Field monitoring of 10 specific sections of five structures to document progressive deterioration rates among different stone types, different degrees of environmental exposure, and different levels of stone quality control was conducted. The five structures were (a) Chicago Harbor, IL, breakwater, (b) Calumet Harbor, IL and IN, breakwater, (c) Calumet Harbor, IL, confined disposal facility (CDF) revetment, (d) Burns Harbor, IN, breakwater, and (e) Cleveland Harbor, OH, east breakwater. The 10 sections of structures selected for evaluation contained deteriorated stone from the eight quarries previously discussed, plus stone from the Calumet Harbor CDF revetment that originally came from a ninth quarry, the Iron Mountain Quarry, Iron Mountain, MI. The Iron Mountain Quarry produces taconite. Also, stone from a tenth quarry (Cedarville Quarry, Cedarville, MI) was evaluated by this field prototype monitoring study because stone from this quarry has previously been placed on other stone structures around the Great Lakes. The Cedarville Quarry produces Niagaran series dolomite.

Ground inspections by registered professional geologists were made to catalogue, at the monitored sections, all stone fractures and offset measurements in armor stone above the high-water mark, between low water and high water on the harbor side, and between low water and high water on the lake side (annually for 3 years). Broken stones were marked to show in aerial photographs to insure repeatability, and to document progression of deterioration.